2011

HIV Protease Inhibitors Trigger Lipid Metabolism Dysregulation Through Endoplasmic Reticulum Stress and Autophagy

Beth Shoshana Zha
Virginia Commonwealth University

HIV PROTEASE INHIBITORS TRIGGER LIPID METABOLISM DYSREGULATION THROUGH ENDOPLASMIC RETICULUM STRESS AND AUTOPHAGY

A dissertation submitted in partial fulfillment of the requirements for the degree of Doctor of Philosophy at Virginia Commonwealth University.

by

BETH SHOSHANA ZHA
B.S., The College of William and Mary, 2006

Director: Huiping Zhou
Assistant Professor, Department of Microbiology and Immunology

Virginia Commonwealth University
Richmond, Virginia
December, 2011

Acknowledgments

There are very few people, if any, in this world who can state they received a PhD on their own. I would not have gone very far without both mentorship and friendship. The list of people I would like to thank for aiding in my endeavours is lengthy, and therefore this acknolwedgment page is not truly complete. For this, I apologize.

However, there are number of individuals I would like to thank for aiding my research. Pat Bohdan taught me almost all I know about cell culture technique. Without her, I am certain the Hylemon and Zhou laboratories would have floundered. In the same regard, Emily Gurley is the center of these laboratories, spending hours keeping us all straight, and ordering materials at whim which we forget to order ourselves. To complete the trio, I would also like to thank Elaine Studer - now Kennedy. I wish you many years of happiness with your new husband!

The mentorship I have received is far and deep. First, I would like to thank Dr. Jason Ridlon. Not only does he teach me about quality research, but also the latest political happenings. Thank you for always keeping your door open for my random and sometimes odd questions. These following individuals not only taught me a lot, but were all the greatest friends: Xudong Wu taught me many basic techniques of which this project began. Lixin Sun taught me careful experimental techniques, essential for clear results. Risheng Cao taught me how to laugh even at stressful times. Bokai Lei taught me a lot about pharmacodynamics. Jian Xiao never failed to make us smile and helped wherever needed. Xiqiaou Zhou was our personal cancer expert! Yi Huang and Yun Wang aided in my times of need (both experimentally and mentally). Most recently, Renping Zhao and Xiaouxuan Zhang have supported me greatly in my last (and most important) experiments and writings. Nǐmen shí wǒ zui hǎo de péngyǒu.

The individuals who owe my greatest dept of gratitude: My committee and professors for their words of inspiration and wisdom. Xuan Wang, for her tireless effort to keep our laboratories clean, for completing almost all the real time RT-PCR plates, slicing tissue to perfection, and being the greatest help inside and outside of laboratory. Wǒmen hui yizhī ji de nǐn de fuchu. My advisor, Dr. Huiping Zhou, has taught me how to work hard and be persistent. Thank you for even allowing me the honor to work with you. Wǒ yongyuan buhui wang jì nǐn. Lastly, to my intelligent, handsome, hardworking, and wonderful husband. You are a teacher, a leader, and a best-friend. Nǐ shí wǒ de wei yī. Wǒ ai nǐ.

Table of Contents

Acknowledgments ii

Table of Contents iii

List of Tables vi

List of Figures vii

List of Abbreviations x

Abstract xiv

CHAPTER I: Background 1

I. HIV and Consequential Difficulties 1

A. Human Immunodeficiency Virus 1

B. FDA Approved Antiretrovirals in Sequence of Viral Cycle 3

C. History Leading to Current Drug Class Recommendations 4

D. Consequences of Mutations 6

II. HIV Protease 7

III. Side Effects of HIV Protease Inhibitors 11

A. Metabolic Syndrome 11

B. HIV PI-Induced Dyslipidemia 13

IV. Endoplasmic Reticulum Stress 15

A. HIV PI-induced Metabolic Diseases and NAFLD Connection 15

B. Endoplasmic Reticulum Stress and the Unfolded Protein Response 16

1. IRE1 ····· 17
2. PERK ····· 18
3. ATF-6 ····· 20
C. ER Stress and Induction of Apoptosis ····· 21

D. ER Stress and Activation of the Inflammatory Cascade ····· 21

V. Autophagy ····· 23

A. Autophagy Pathways ····· 23

1. Formation of Autophagosomes ····· 24
2. Few Key Proteins ····· 25
3. LC3 and Importance in Autophagy Detection ····· 26
B. Autophagy and ER Stress ····· 28

VI. Adipocytes ····· 29

A. Cellular Properties ····· 29

B. Adipose Tissue ····· 35

C. ER Stress in the Adipocyte ····· 37

D. Autophagy and Lipid Metabolism in the Adipocyte ····· 42

VII. Liver ····· 44

CHAPTER II: Materials and Methods ····· 47

Materials ····· 47

Cell Culture Techniques ····· 48

In Vitro Studies ····· 50

In Vivo Studies ····· 61

Statistical analysis ····· 63

CHAPTER III: HIV Protease Inhibitors Dysregulate Adipogenesis through Endoplasmic Reticulum Stress Activation and Alteration of PPARγ mRNA Stability ····· 64

STUDY RATIONALE ····· 64

RESULTS ····· 66

SIGNIFICANCE ····· 93

CHAPTER IV: HIV Protease Inhibitors LOPV and RITV Induce Autophagosome Accumulations in Adipocytes ····· 97

STUDY RATIONALE ····· 97

RESULTS ····· 98

SIGNIFICANCE ····· 111

CHAPTER V: Raltegravir Inhibits LOPV/RITV-Induced Autophagosome Accumulation in Hepatocytes ····· 114

STUDY RATIONALE ····· 114

RESULTS ····· 116

SIGNFICANCE ····· 132

CHAPTER VI: Final Discussion ····· 134

HIV PIs in Adipocytes ····· 135

HIV PIs in Adipocytes - Autophagy Induction ····· 142

HIV PIs in Hepatocytes ····· 147

HIV PI-Induced UPR and Induction of Autophagy ····· 149

Targeting HIV PI-Induced Metabolic Side Effects ····· 150

Conclusion ····· 153

Vita ····· 204

List of Tables

Table 1. Real-time RT-PCR primers specific for mouse mRNA 52

Table 2. Real-time PCR primers specific to Rat and Human mRNA, respectively. 53

List of Figures

Figure 1. Diagram of HIV subtypes. 2

Figure 2. Targeting HIV Lifecycle. 5

Figure 3. Molecular structure of HIV PIs 10

Figure 4. Depiction of the UPR.. 19

Figure 5. Potential pathways between ER stress activation and cellular apoptosis. 22

Figure 6. Simplification of Autophagy. 27

Figure 7. Maturation of adipocytes. 36

Figure 8. HIV PIs time-dependently activate the UPR in differentiated 3T3-L1s 68

Figure 9. HIV PIs dose-dependently activate the UPR in non-differentiated 3T3-L1s. 69

Figure 10. HIV PIs activate the UPR in differentiated murine and human adipocytes 70

Figure 11. HIV PIs induce transcriptional increase of UPR genes in adipocytes. 71

Figure 12. LOPV/RITV induces ER stress *in vivo*. 72

Figure 13. HIV PIs deplete ER calcium stores in 3T3-L1s. 74

Figure 14. HIV PIs induce cell death in differentiated 3T3-L1s. 75

Figure 15. HIV PIs induce cell death in SGBS cells. 76

Figure 16. HIV PIs increase inflammatory cytokines in differentiated 3T3-L1s. 78

Figure 17. LOPV/RITV slightly increases inflammation *in vivo*. 79

Figure 18. HIV PIs differentially affect adipocyte maturation. 82

Figure 19. HIV PIs differentially affect LD number and size in differentiating 3T3-L1s.... 83

Figure 20. HIV PIs inhibit activity of the PPARγ promoter. 84

Figure 21. HIV PIs differentially alter PPARγ mRNA levels. 85

Figure 22. *In vivo* pulldown of PPARγ mRNA after treatment with HIV PIs in 3T3-L1 cells. 86

Figure 23. HuR and CUGBP-1 bind to PPARγ. 87

Figure 24. 3'UTR PPARγ activity is increased with HuR and CUGBP-1 overexpression. 88

Figure 25. RITV increases HuR and CUGBP-1 translocation in 3T3-L1s..... 89

Figure 26. HIV PI-induced alteration of adipogenesis is abrogated in absence of CHOP. .. 91

Figure 27. CHOP knockout may abrograte HIV PI-induced lipid metabolism dysregulation and inflammation in AT. 92

Figure 28. HIV PIs activate LC3B conversion. 99

Figure 29. HIV PIs Activate LC3B conversion in human ASCs..... 100

Figure 30. HIV PIs quantifiably increase autophagosomes in 3T3-L1 cells. 101

Figure 31. Darunavir does not significantly activate autophagy in 3T3-L1s. 103

Figure 32. HIV PIs increase late autophagosome accumulation without dose-dependence. 104

Figure 33. Effect of HIV PIs on p62 degradation. 105

Figure 34. Effect of HIV PIs on GFP-LC3B cleavage. 107

Figure 35. CHOP and HIV PI-induced LC3B. 108

Figure 36. ATF-4 and HIV PI-induced LC3B. 110

Figure 37. Raltegravir abrogates LOPV/RITV-induced lipid accumulation in rat primary hepatocytes. 117

Figure 38. LOPV/RITV 4:1 activates LC3B conversion in rat and mouse primary hepatocytes. 118

Figure 39. Raltegravir abrogrates LOPV/RITV-induced LC3B conversion in hepatocytes. 119

Figure 40. Raltegravir abrogrates HIV PI-induced autophagy at the mRNA level. 121

Figure 41. Raltegravir abrogrates LOPV/RITV-induced late autophagosome accumalation in rat primary hepatocytes..... 122

Figure 42. Raltegravir abrogates HIV PI-induced autophagy induction in hepatocytes. ... 123

Figure 43. CHOP plays a central role in raltegravir inhibition of LOPV/RITV-induced LC3B activation. 125

Figure 44. Raltegravir inhibits LOPV/RITV-induced LC3B. 126

Figure 45. Raltegravir lack of autophagy induction relies on CHOP 127

Figure 46. p62 accumulates with high concentrations of LOPV/RITV treatment 129

Figure 47. Affect of HIV PIs and raltegravir on GFP-LC3 cleavage in HepG2 cells 130

Figure 48. LOPV/RITV and raltegravir do not increase LC3B conversion. 131

Figure 49: HIV PI-Induced ER stress activates autophagy and dysregulates cellular lipid metabolism. 152

List of Abbreviations

ADD1	adipocyte determination and differentiation-dependent factor
AIDS	Acquired Immuno Deficiency Syndrome
AMPV	amprenavir
ASCs	adipose-derived stem cells
AT	adipose tissue
ATF	activating transcription factor
Atg	autophagy related genes
ATGL	adipose triglyceride lipase
ATZV	atazanavir
Autophagy	macroautophagy
AV	autophagic vacuole
BP	blood pressure
C/EBP	CCAAT enhancer binding proteins
CHOP	C/EBP homologous protein
CGI-58	Comparative Gene Identificant-58
CREBP	cAMP response element binding protein
CRFs	circulating recombinant forms
CTT	CTP:phosphocholine cytidylyltransferse

CUGBP	CUG-binding protein
DAD	Data Collection on Adverse Events of Anti-HIV Drugs
DMII	Diabetes Mellitus II
DMSO	dimethyl sulfoxide molecular biology grade
DNL	*de novo* lipogenesis
DRV	darunavir
eIF2α	eukaryotic translation initiation factor 2α
ER	endoplasmic reticulum
ERK	extracellular signal-regulated kinases
FA	fatty acids
FRIL	freeze-fracture replica immunolabeling
HAART	Highly Active Antiretroviral Therapy
HDL	high density lipoprotein
HIV	Human Immunodeficiency Virus
HSL	hormone sensitive lipase
HTN	hypertension
IBMX	3-Isobutyl-1-methylxanthine
IDL	intermediate density lipoproteins
IDV	indinavir
Insig	insulin-induced gene
JNK	c-Jun NH(2)-terminal protein kinases
LDL	low density lipoproteins
LIR	LC3-interacting region
LOPV	lopinavir
MAPKs	mitogen-activated protein kinases

MAP-LC3	microtubule associated protein light chain 3
MPH	mouse primary hepatocyte
MSCs	mesenchymal stem cells
NAFLD	nonalcoholic fatty liver disease
NASH	nonalcoholic steatohepatitis
NEFA	non-esterified fatty acids
NFV	nelfinavir
NHLBI	National Heart Lung and Blood Institute
NNRTI	non-nucleoside reverse-transcriptase inhibitors
NRTI	nucleotide/nucleoside reverse-transcriptase inhibitors
PAS	pre-autophagosomal nucleation site
PAT	Perilipin/ADRP/TIP47
PE	phosphatidylethanolamine
PERK	protein kinase-like ER kinase
PKA	protein kinase A
PPARγ	peroxisome proliferator activated receptor γ
PPRE	PPARγ responsive element
PtdCho	phosphatidylcholine
RITV	ritonavir
ROS	reactive oxygen species
RPH	rat primary hepatocytes
RT	reverse transcriptase
RXR	retinoid X receptor
SCAP	SREBP cleavage activating protein
SE	standard error

SGBS	Human Simpson-Golbai-Behmel Syndrome
SREBP	sterol regulatory element binding proteins
SQV	saquinavir
TGs	triglycerides
TORC1	serine/threonine protein kinase target of rapamycin complex 1
TRV	tipranavir
UPR	unfolded protein response
VLDL	very low density lipoproteins
XBP	X-box-binding protein

Abstract

HIV PROTEASE INHIBITORS TRIGGER LIPID METABOLISM DYSREGULATION THROUGH ENDOPLASMIC RETICULUM STRESS AND AUTOPHAGY

Beth Shoshana Zha

A dissertation submitted in partial fulfillment of the requirements for the degree of Doctor of Philosophy at Virginia Commonwealth University

Virginia Commonwealth University, 2011

Major Director: Huiping Zhou
Assistant Professor, Department of Microbiology and Immunology

HIV protease inhibitors (PI) are core components of Highly Active Antiretroviral Therapy (HAART). HIV PIs are extremely effective at suppressing viral load, but have been linked to lipodystrophy and dyslipidemia, which are major risk factors for cardiovascular disease. Recent studies indicate that activation of endoplasmic reticulum (ER) stress is an important cellular mechanism underlying HIV PI-induced dysregulation of lipid metabolism.

However, the exact role of ER stress in HIV PI-associated lipodystrophy and dyslipidemia remains to be identified.

Hepatocytes and adipocytes are important players in regulating lipid metabolism and the inflammatory state. Dysfunction of these two cell types is closely linked to various metabolic diseases. In this dissertation research, we aimed to define the role of activation of ER stress in HIV PI-induced dysregulation of lipid metabolism in adipocytes and hepatocytes and further identifty the potential molecular mechanisms. Both cultured and primary mouse adipocytes and hepatocytes were used to examine the effect of individual HIV PIs on ER stress activation and lipid metabolism. The results indicated that HIV PIs differentially activate ER stress through depletion of ER calcium stores, activating the unfolded protein response (UPR). UPR activation further lead to an alteration of cellular differentiation through downstream transcription factor CHOP. At the same time, HIV PIs also altered adipogenesis via differential regulation of the adipogenic transcription factor PPARγ. HIV PI-induced ER stress was closely linked to dysregulation of autophagy activation through CHOP, and upstream ATF-4, signaling pathways. In hepatocytes, the integrase inhibitor raltegravir abrogated HIV PI-induced lipid accumulation by inhibiting ER stress activation and dysregulation of autophagy pathway.

Our studies suggest that both ER stress and autophagy are involved in HIV PI-induced dysregulation of lipid metabolism in adipocytes and hepatocytes. The key components of ER stress and autophagy signaling pathways are potential therapeutic targets for HIV PI-induced metabolic side effects in HIV HAART-treated patients.

CHAPTER I: Background

I. HIV and Consequential Difficulties

A. Human Immunodeficiency Virus

The overwhelming impact the Human Immunodeficiency Virus (**HIV**) has on the world is undeniable – by the end of 2009 there were 33.3 million people living with HIV in the world, with 1.8 million deaths in that year alone (*1*). The first identification of Acquired Immuno Deficiency Syndrome (**AIDS**) in the United States was in 1980, and since then, more than 27 million people have died from complications of infection. In addition, the high rate of deaths can be directly attributed to the lack of available medications – only 36% of the infected population received adequate antiretroviral therapy (*2*).

Besides the known political and monetary issues at hand, there are multiple HIV viral subtypes and sub-subtypes that have been described and overwhelm pharmaceutical availability. In fact, most research completed on HIV therapies has occurred, and continues to occur, in Europe and America, targeting the HIV-1 strain, although much of the world population is also afflicted by HIV-2. In addition, HIV-1 has 3 clades (M, O, and N), of which M is most common in the United States. M has 9 subtypes, and under these, there exist sub-subtypes which recombine to form circulating recombinant forms (CRFs) in multiply-infected individuals (Figure 1). Differences even within the strain related CRFs can be the basis seen in differences of cellular tropisms, viral fitness, and effect in each individual's therapy.

The ability of HIV to rapidly mutate due to the imperfect enzyme used for genome replication has resulted in a multitude of strains resistant to therapies on the market. To combat viral strain mutations, Highly Active Antiretroviral Therapy (**HAART**) has increased in

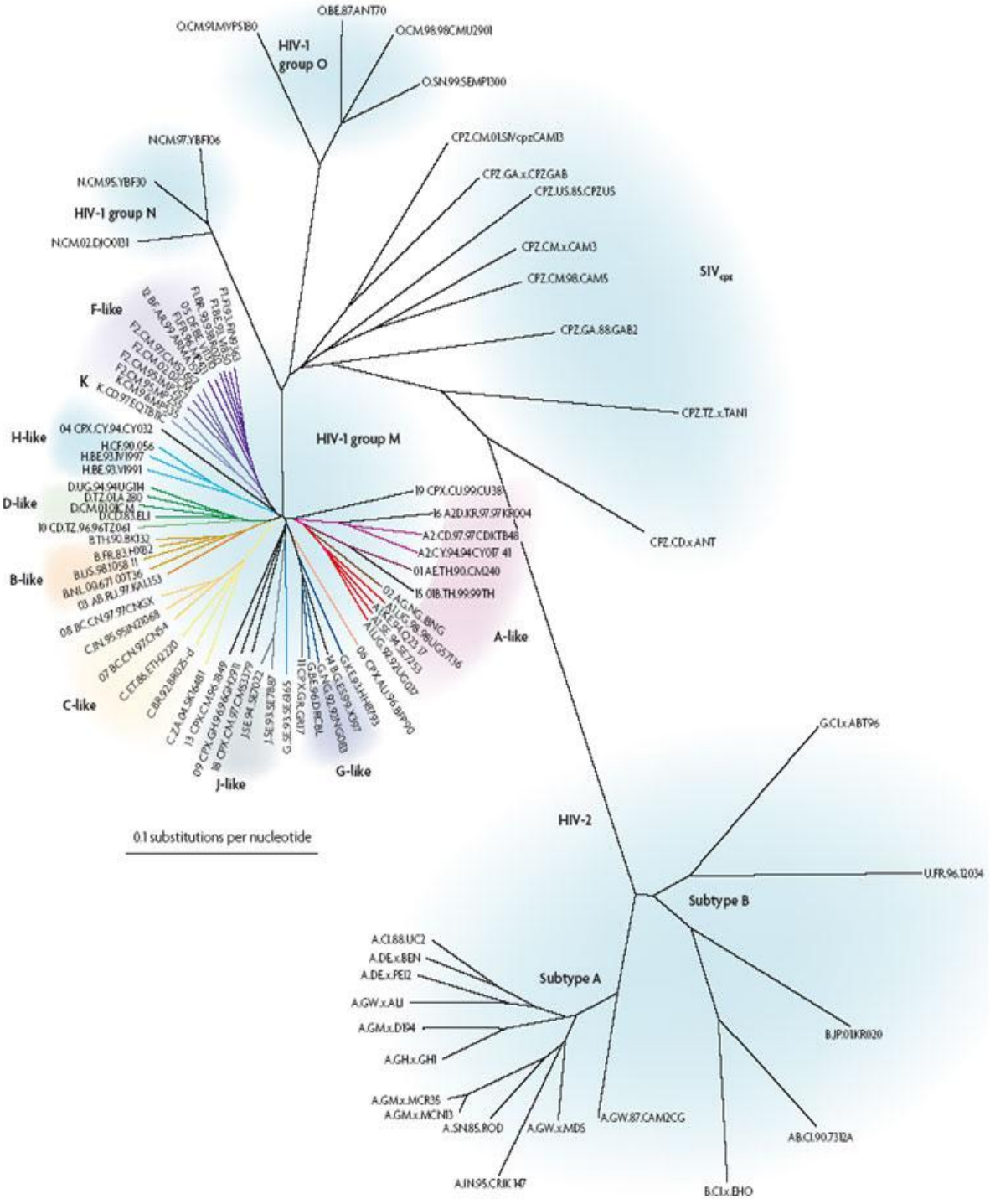

Figure 1. Diagram of HIV subtypes. Depiction of HIV-1 and -2 subtypes and clades. Reprinted by permission from Macmillan Publishers Ltd: [Nature Reviews Microbiology] (*3*), copyright (2007).

complexity and effectively decreased deaths from opportunistic infections in those that are candidates for this treatment. This century has seen the ability of HAART to turn a deadly virus into a chronic infection. Due to polymorphic differences in individual strain enzymes, that some individuals are infected with less common strains, and diverse side effect profiles, physicians must seriously consider which drugs to prescribe to each individual in their clinic.

B. FDA Approved Antiretrovirals in Sequence of Viral Cycle

The first essential step in HIV infection of immune cells (T cells or macrophages) is fusion of the viral and cellular membranes. This process occurs through interaction of the viral glycoprotein, gp120, and the CD4 molecule on the cell surface. After the initial interaction between these two proteins, viral proteins utilize a secondary receptor interaction through CXCR4 (T-tropic) or CCR5 (M-tropic). **Maraviroc** is a relatively recently approved antiretroviral that inhibits fusion *via* binding to, and therefore preventing interactions, to CCR5. Another, less commonly prescribed, is **Fuzeon** (enfuvirtide), which binds to the viral gp41.

After entry into the cellular cytoplasm, the viral genome (two copies of a single-stranded RNA) is reverse-transcribed into DNA by the viral enzyme, reverse transcriptase (RT). The first anti-HIV drugs to come on the market inhibited this enzyme. There are currently three classes of inhibitor, **nucleotide and nucleoside analogs (NRTI)**, as well as **non-analogues (NNRTI)**, and those drugs that can act as both. NRTIs are analogues to deoxynucleotides which are incorporated into the growing DNA chain. NRTIs lack one significant motif of deoxynucleotides, a 3'-hydroxyl group, which is essential in linking each deoxy in the chain. Without this hydroxyl group, NRTIs cause a halt in synthesis, terminating the chain. NNRTIs, on the other hand, bind directly to the RT itself, inhibiting the function of an essential enzyme.

The next step is integration of the newly synthesized viral DNA strand and the host genome by the viral integrase enzyme. In 2007, the FDA approved **Raltegravir**, which directly inhibits this enzyme, thereby preventing viral genome integration and latency of HIV in the host cell.

Upon host cell activation, often in times of stress such as infection and inflammation, the integrated virus cuts itself from the host genome, and begins the viral replication cycle. Here, the virus utilizes the host enzyme RNA polymerase to produce multiple copies of packagable RNA strands from the viral DNA sequence. At the same time, the host cell machinery is recruited to synthesize viral proteins that will be necessary for virion production and release. After protein production and the beginning of packaging, the viral enzyme protease cleaves long HIV proteins into functional segments (see Section II). Mature virions are subsequently released when immature particles bud from the membrane and form mature infectious virions with the help of protease. **HIV protease inhibitors (PI)** essentially inhibit viable virion production by inhibiting the action of this essential viral enzyme.

Please see Figure 2 for a depiction of HIV life cycle and how each class of anti-HIV drugs inhibits replication of the virus in a host cell.

C. History Leading to Current Drug Class Recommendations

Zidovudine, an NRTI, was the first drug approved in 1987. As is the case of the following approvals of zalcitabine, stavudine, and didanosine, the NRTIs seemed effective, yet the development of resistant strains caused a rebound in opportunistic infections in patients.In 1995, a major turning point occurred with the approval of HIV PIs ritonavir, saquinavir, and indinavir. Not only did these drugs work independently to help reduce viral load, but

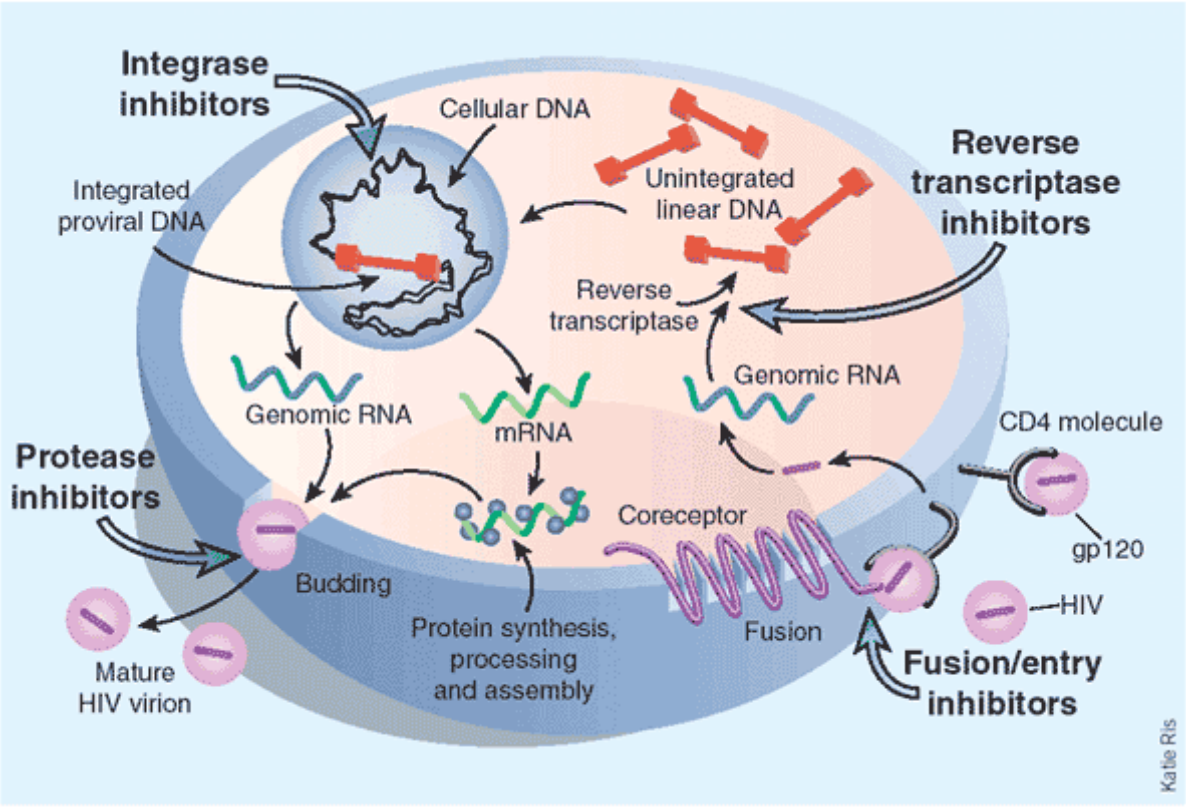

Figure 2. Targeting HIV Lifecycle. Current marketed anti-HIV therapies target different stages of HIV life cycle, from fusion, reverse transcription, integration, and viable virion budding. Drug classes are labeled to the targets they inhibit. Reprinted by permission from Macmillan Publishers Ltd: [Nature Medicine] (*4*), copyright (2003).

combination therapy with NRTIs drastically decreased opportunistic infections. This regimen is now known as HAART, and most frequently includes two NRTIs with one PI, though 2 NRTIs

combination therapy with NRTIs drastically decreased opportunistic infections. This regimen is now known as HAART, and most frequently includes two NRTIs with one PI, though 2 NRTIs with 1 NNRTI, or 3 NRTIs are also used. With the constant battle of resistant strains in the current HIV-infected population, addition of integrase or fusion inhibitors can increase efficacy of these regimens.

D. Consequences of Mutations

The continuous development of drugs has allowed successful combat towards resistant strains. Resistance in individual strains is not rare due to an inherently high mutation rate of HIV resulting from the imperfect reverse transcriptase enzyme. Yet, the probability of mutation leading to resistance to a given antiretroviral increases when patients are inconsistent in the taking the prescribed drug.

The variety of mutations seen in individual infectious viruses can be divided into subclasses, primary (major) or secondary (minor). The most significant mutation in the case of HIV drug resistance is that of secondary mutations. In this instance, a point change occurs, confirring resistance to a drug. These mutations are dependent on the background genetics of the particular viral strain and the resulting fitness of that virion after such a mutation. For instance, a single amino acid change in subtype F1 will be needed for resistance to a PI. This point mutation differs from the one needed for subtype G2 to confer resistance. Genetic diversity must be taken into account to understand mutations resulting in drug resistance. One significant example – non B type HIV will not mutate as much as B type HIV at specific amino acids needed for resistance to PI because efficiency of replication drops more than half compared to the respective wild type.

These genetic barriers allow a clinician to use a patients viral genotype to determine which HAART regimen will be most effective in decreasing viral load. In addition, genotyping can be repeated after a few years of treatment to determine what drugs to add or switch to decrease selction of mutated strains. Unfortunately, this process can inevitably end as the physician uses all available drugs due to mutating strains and/or individual non-compliance.

II. HIV Protease

The HIV genome is a single-stranded mRNA, of which each virion carries two copies. There are 9 genes that encode 15 proteins, 3 of which are essential. The nonessential genes include *vif*, or viral infectivity factor which aids in stable reverse transcription; *vpr*, or encoding viral protein R which arrests cells in G2; *vpu*, or viral protein U which promotes virion release; *rev*, or regulator of viral gene expression which inhibits splicing of transcripts; and *tat*, or transcriptional activator which enhances RNA polymerase II. The essential genes are – *gag*, *pol*, and *env* which encode for structural proteins, essential enzymes, and envelope proteins respectively. During translation, gag is translated as a long 55 kDa precursor, and pol as a 160-kDa Gag-Pol fusion protein. These polypeptides must be cleaved at specific moments in the HIV life cycle in order to produce functional proteins and viable virions.

This essential activity is handled by HIV protease, which cleaves the polypeptides during virion budding. Protease recognizes substrates that have multi-folded domains, containing linking regions with non-homologous and asymmetric sequences. The crystal structure of protease was first shown in 1989 by Merck Sharp and Dohme Research Laboratories (*5*), giving both interesting knowledge about HIV and a structure-based drug design for inhibition of virion production.

Protease is an aspartic protease within the peptidase family A2 (retropepsin endopeptidase). It cleaves between either a tyrosine-phenylalanine or tyrosine-proline, which no human host cell enzyme accomplishes. Despite high sequence mutation, the catalytic triad (Asp-Thr-Gly) is well conserved, though other regions may change due to both genetic variation and drug resistance.

Protease contains a quartenary structure, and is a dimer by which each monomer consists of 99 amino acids (*6*), and the N- and C-termini of the dimers interdigitate to form a four-stranded interface. Together, there are three domains – a terminal (or dimerization) domain, core, and flap. While the terminal and core domains are essential for stabilization and interface for the active site, the flaps are exposed loops that enclose the active site for ligand interactions. Despite the multi-domains of this enzyme, protease is quite stable due to a hydrophobic core, packing of side chains, and the Fireman's grip (a conserved aspartyl protease scaffold of H-bonds involving the catalytic residues).

As protease is essential for the production of viable, infectious virions, it became the second target of inhibition for anti-HIV therapy. When PIs were introduced to the market, their effectiveness with NRTIs was almost immediately noted, and thus initiated the term of HAART. There are currently two generations of drugs, peptidic and non-peptidic (Figure 3). The peptidomimetic class, though quite large and inherently diverse in structure, are related by a peptide bond present in each molecule, with a non-hydrolysable amino acid at the scissile bond. These molecules mimic the tetrahedral transition-state intermediate formed during the catalysis event, but become stuck due to inability of cleavage, inhibiting the entry of viral proteins (*7, 8*). Within this class, some (i.e. ritonavir) are less peptidic in nature, but exploit the symmetry of protease, enhancing stability while decreasing effectiveness. The non-peptidic class has moieties

to displace water in the active site cleft. This H_2O molecule is thought to play a role in opening and closing the flap domains, thereby affecting substrate interaction and stability (*7*).

Saquinavir (**SQV**) was the first PI approved by the FDA in 1995 (now as Invirase when boosted with Ritonavir). Indinavir (**IDV**) reached the market in 1996 (Crixivan), and due to a great outcome with NRTIs, set the bar for HAART. Ritonavir (**RITV**) was marketed that same year, but now is only given as a booster as it inhibits cytochrome P450 (the enzyme that metabolizes most PIs and subsequently decreases their bioavalability). Nelfinavir (**NFV**) was marketed in 1997, and subsequently became the first PI to be recommended for pediatric patients. In 1999, Amprenavir (**AMPV** – now prescribed as prodrug fosamprenavir) was introduced (Lexiva).

Lopinavir (**LOPV**) entered the prescription option in 2000. It was structurally designed for mutated PIs seen often with a mutation of protease at Val82. It is similar to RITV (same core), but due to low bioavailability, it was prescribed only with a RITV combination. Now, the only form of LOPV available on the market is as a co-formulation pill, Kaletra (the first drug not available in single formulation). Kaletra was so successful in both drug-naïve and drug-experienced patients, it became first-line therapy in 2006, and now has only been surpassed by Darunavir-RITV. Atazanavir (**ATZV**) was approved in 2003, and is now marketed under Reyataz. It was the first PI approved for once-daily dosing, increasing the pressure in development of more convenient PIs.

Non-peptidic PIs, Tipranavir (**TRV**) and Darunavir (**DRV**), have relatively recently reached the market – 2005 and 2006 respectively. TRV (Aptivus) development utilized coumarin as a template, and is now used in multiple resistant strains, but not in patients with little resistance due to a high side effect profile. DRV (Prezista) is now the first-line HIV PI. DRV

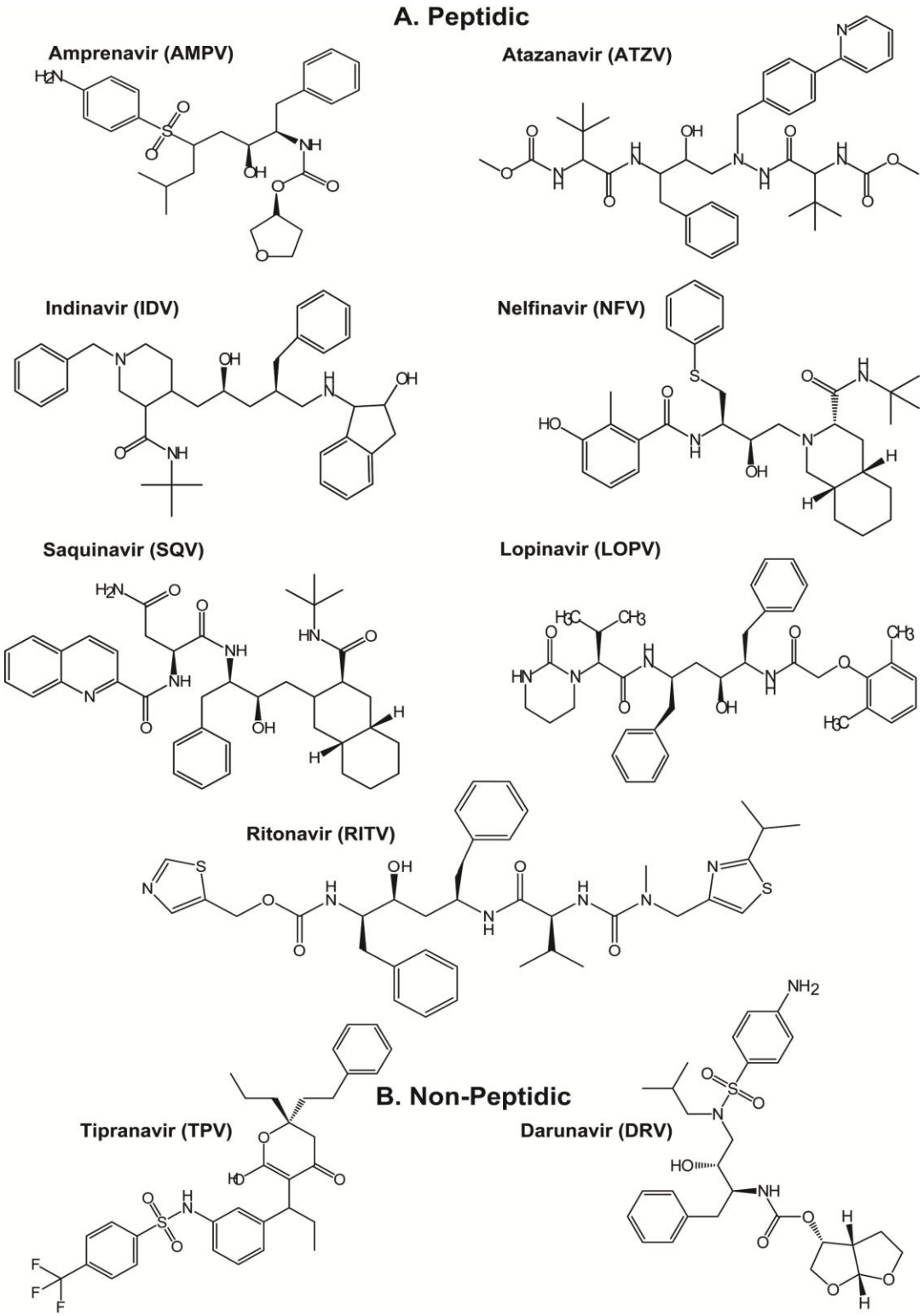

Figure 3. Planar structure of current HIV PIs. A) Peptidic and **B)** non-peptidic HIV PI subclasses were drawn in ChemDraw. Abbreviations are used in this dissertation. Figure revised with permission from Sage Publications: [Toxicologic Pathology] (9), copyright (2009).

design is based on AMPV (with a few stereochemistry changes to increase binding in resistant strains), and as such, the side effect list is low and effectiveness increased. However, both these second generation PIs must be taken in conjunction with RITV, whose lipid side effect is high. Despite this, the effectiveness of DRV combined with lowered long term side effects has resulted in surpassing prescription numbers of Kaletra in the past year.

III. Side Effects of HIV Protease Inhibitors

A. Metabolic Syndrome

As the list of FDA approved antiretrovirals is long, so is the inventory of side effects. Even though the life expectancy of HIV-infected patients under HAART has been extended, the various HAART-induced side effects significantly affect quality of life. However, it is difficult to concretely determine if these effects are secondary to the therapies or the virus itself.

In some cases, it may actually be both. One example of this is diminished bone density, observed in a large proportion of HIV infected individuals. It is already known that treatment-naïve patients often have low bone mass, with as high as a 50% prevalence of osteopenia (*10*). There has even been proposed mechanisms of this phenomenon such as the induction of differentiation of bone absorbing cells (osteoclasts) (*11, 12*). To make matters worse, HAART treatment can further the reduction of bone density in a yet unknown manner (*13*). As in other side effects discussed, HIV itself can induce major pathology in individuals with no prevention, or even an exacerbation, by the drugs used to stop its replication.

Despite these apparent complexities, there is still a large list of drug-attributable side effects. Most commonly, these include general side effects with the NRTI/NNRTIs, ranging from rash, anemia, nausea, vomiting, diarrhea, and sleep disturbances. More severely, it is not

uncommon to observe liver toxicities, pancreatitis and neuropathy in certain patients, often with underlying risk factors. Further, in the past decade, there has been increasing concern over long-term HAART patients experiencing early-onset cardiovascular risk factors such as hypertension (HTN) and insulin resistance. With parallel observations in the American population, some attributed these to environmental factors not due to the drugs.

Some large clinical trials, especially the Data Collection on Adverse Events of Anti-HIV Drugs (DAD), have elucidated many particulars of HAART side effects. One specific phenomenon noticed in the '90s of lipodystrophy (change of body lipid composition) and dyslipidemia (changes in blood lipid levels) were better explained. Now peripheral wasting is no longer attributed to viral wasting but to NRTIs (especially stavudine and zidovudine) (*14-17*); and fat accumulation is not just a physiological phenomenon but due to PI treatment (*13, 18*). Together, this HAART side effects has been termed HIV-associated lipodystrophy (*19*). This has pathophysiologically been defined as selective damage of adipose tissue with subcutaneous fat loss and/or central fat accumulation.

Additional PI-specific side effects include dyslipidemia, glucose alterations, and insulin resistance, which can lead to diabetes (DMII), HTN, and cardiovascular dysfunctions (*20-22*). A bottom line through these multiple investigations is that myocardial infarction is directly correlated with PIs, and not other components of HAART (*20, 23*). Interestingly, these side effects are also components of the clinically defined Metabolic Syndrome.

The Metabolic Syndrome is a diagnosable syndrome, and a high risk factor for myocardial infarctions and strokes. To be diagnosed, according to the National Heart Lung and Blood Institute (NHLBI) criteria (*24*), a patient must have 3 out of the 5 diagnosis:

1) >35" central circumference in woman, or >40" in men.

2) A triglyceride level >150mg/dL (or on treatment).

3) A high density lipoprotein (HDL) <50mg/dL in women or <40 in men (or on treatment).

4) A blood pressure (BP) >130/85 (or on treatment).

5) High fasting blood glucose level, or insulin resistance (or on treatment).

Importantly, each component above is an individual risk factor for atherosclerosis.

HIV PI-induced atherosclerotic cardiovascular complications are leading to an increased cause of mortality in HIV-1 infected persons in developed countries (*25*). During the last decade, an extensive effort has been put forth to study HIV PI-induced side effects. Both *in vitro* and *in vivo* animal studies from our laboratory and others' have linked HIV PIs with the activation of endoplasmic reticulum (**ER**) stress and oxidative stress, as well as an increase in inflammatory cytokine production from several cell types including macrophages, hepatocytes, intestinal epithelial cells and adipocytes. However, the underlying cellular and molecular mechanisms remain to be fully identified and therapeutic strategies are currently unavailable. Understanding the root cause of these chronic side effects and implications for HIV-infected patients will be critical to the design of effective interventions to combat the metabolic and cardiovascular diseases in a population chronically exposed to HAART.

B. HIV PI-Induced Dyslipidemia

Alterations in serum lipids of the HIV infected population have been noted since the beginning of the 1990s. Before treatments began, patients often had a decrease in LDL and HDL plasma concentrations. NRTI treatment alone seemed to increase LDL to presumable baseline levels, without any effect on HDL, yet multi-drug treatments tended to increase serum triglycerides. In the late 1990s, effort was put forth to tease apart the effect of infection versus therapies on this phenomenon.

Two hypotheses began these studies. First, the initial rise in serum lipid levels of HIV patients observed by clinicians at the start of treatment could have been partly due to immune reconstitution phenomena (*26*). This is a robust inflammatory response when HIV viral load decreases a few months to a year after initiation of treatment. At the same time, there has been an increase in average serum lipid levels in the general population due to poor diet and increasing age, and the HIV-HAART cohort is no different.

Despite these facts, it has been found in numerous long- and short-term studies, as well as in healthy versus HIV-infected persons, that HAART, specifically PIs, induces dyslipidemia (*20, 22, 27-32*). Often, clinicians combat this phenomenon with lipid-lowering drugs. At the same time, research has been attempting to determine which anti-HIV drugs induce the most change in lipid composition, and the mechanism underlying these changes.

Lipid homeostasis is centrally controlled by the liver. When fats are consumed in the diet, lipids are packaged into chylomicrons in the intestines whose final fate is the liver through an apoE endocytosis pathway. In order to effectively transport these to peripheral tissues, the liver packages triglycerides (**TG**) and cholesterol into very low density lipoproteins (VLDL). VLDLs circulate and the TGs inside are taken up by muscle and adipose tissue after hydrolysis by lipase. The remnants are called intermediate density lipoproteins (IDL) which can be endocytosed by cells or further converted to low density lipoproteins (LDL) by lipases on the surface of cells. LDLs are cholesterol rich particles endocytosed through apoB-100, mostly in the liver or adipose tissue, and pathologically by macrophages. Another type of lipoprotein is high density (HDL), which is a way peripheral tissues 'send back' lipids, cholesterols, and proteins to the liver in an attempt not to be overloaded with these potentially toxic substances, as well as signal to the liver to stop synthesizing VLDLs.

HAART appears to affect many aspects of this pathway. Some studies have found that NNRTIs may even be able to increase HDL (*33*), a clinical advantage for dyslipidemic patients leading some to want to alter regimens to decrease PIs and increase NNRTIs (*34, 35*). In fact, there were successful studies in switching from PI-based treatments to NNRTI or NRTI-only regimes with success in attenuating dyslipidemia (*35-37*). However, the effectiveness of PIs against HIV cannot be disputed. When PIs were added to the regimen in the mid-90s, there was a drastic decrease in patients who succumbed to opportunistic infections. The benefits of PIs far outweigh the side effects, but determining the mechanism behind these side effects may lead to alternative therapies in conjunction with PI use, or better-designed PIs.

IV. Endoplasmic Reticulum Stress

A. HIV PI-induced Metabolic Diseases and NAFLD Connection

In HIV PI-induced metabolic dysfunctions, many features are similar to those observed in nonalcoholic fatty liver disease (**NAFLD**). NAFLD is a clinical term to describe a phenomenon in which patients have a fatty liver similar in all aspects to an equivalent alcoholic subject. Induction of NAFLD has been described in a range of conditions, such as obesity and diabetes, as well as induction by a variety of drugs. Donnelly and colleagues were able to demonstrate that the majority of hepatic lipids in patients with NAFLD come from peripheral non-esterified fatty acids (NEFA) (predominately from adipose tissue) and *de novo* lipogenesis (DNL) in the liver, not the diet (*38*).

Patients receiving HIV PIs acquire metabolic complications that are too similar to NAFLD patients to ignore a connection. Indeed, HIV PIs have been clearly shown to alter lipid and carbohydrate metabolism pathways, the underlying mechanism of NAFLD (*39*). Although

HIV PI-induced NAFLD is not an entity of its own, many patients taking HIV PIs may have NAFLD with absolutely no symptoms, as does the majority of the overweight population. However, other patients progress to nonalcoholic steatohepatitis (NASH), which occurs with excess inflammation and scarring, potentially causing severe damage to the liver. In fact, many studies have found NASH in greater than 50% of HAART-treated patients undergoing liver histopathological assessments (*40-42*). Above all, NAFLD/NASH is most likely part of HIV PI-induced metabolic diseases due to the strong correlations of hyperglycemia, insulin resistance, and dyslipidemia. Indeed, a connection is apparent between western diet-induced NAFLD and HIV PIs – the induction of endoplasmic reticulum (**ER**) stress.

ER stress activation has been linked to various human diseases such as diabetes, cardiovascular diseases, and NAFLD/NASH (*43-48*). Concurrently, recent studies have shown that HIV PIs induce ER stress in many cell types including hepatocytes, macrophages and intestinal epithelial cells (*49-56*). Our laboratory has also identified that HIV PI-induced ER stress is partially due to depletion of ER calcium stores (*51*), and is linked to upregulation of sterol regulatory element binding proteins (**SREBP**) and dysregulation of lipid metabolism in hepatocytes (*49, 57, 58*). The similarities of HIV PI-induced ER stress and underlying ER stress in NAFLD must be further probed in order to discover the mechanism underlying HIV PI side effects.

B. Endoplasmic Reticulum Stress and the Unfolded Protein Response

Numerous cellular pathways can be altered in times of stress, leading to cellular aberrations and dysfunction. In the realm of over-nutrition and its complications, ER stress is arguably the most common and important (*59-62*). ER stress is linked to multiple harmful pathways including the cellular inflammatory cascade and lipid metabolism dysregulation since

the ER is central for protein folding, secretions (e.g. cytokines), calcium homeostasis, and lipid synthesis.

Inducing ER stress is relatively effortless *via* depletion of ER calcium stores, changes in ER lipid membrane composition, reactive oxygen species (ROS), or accumulation of misfolded proteins. When triggered, the ER signals to the cell through the unfolded protein response (**UPR**) to aid in increased productions of proteins needed for protein folding, while decreasing transcription and increasing degradation of other non-essential proteins. If the UPR is unable to return the ER to homeostastic conditions, it will trigger apoptosis.

A central component of the UPR is an ER chaperone protein, BiP/GRP78. In homeostatic conditions, BiP/GRP78 is bound to three ER membrane resident proteins, but an insult that alters ATP in the lumen, decreases ER calcium stores, or increases a demand of protein folding causes GRP78 to unbind. The three proteins, ER transmembrane kinase/endoribonuclease (**IRE1**), doubled-stranded RNA-activated protein kinase-like ER kinase (**PERK**), and activating transcription factor 6 (**ATF-6**), triggers a cascade upon their release which ultimately leads to the activation of transcription factors that upregulate protein chaperones, proteasome components, and with continuous activation, turns on GADD-153/**CHOP** (C/EBP homologous protein) which can activate apoptosis (see Figure 4).

1. IRE1

Upon release from GRP78, IRE1 transautophosphorylates, activating its RNase activity. Its target is X-box-binding protein 1 (**XBP-1**) transcript, of which it removes an intron, and XBP-1 is re-ligated into XBP-1^{s}. There are multiple targets of XBP1^{s}, including ER protein chaperones and upregulation of itself (*63-65*). However, beyond the traditional genes it activates, XBP-1 action has now been shown to be more diverse.

In fact, XBP-1's ability to induce many ER proteins, and increase expansion of the rough ER (*66*) has demonstrated its necessity in ER biogenesis. Specific and elaborate knockout models have demonstrated this further when the ER was poorly developed and secretory cells subsequently failed to function (*67*, *68*). Sriburi *et. al* have found that overexpression of XBP-1^{s} in pre-adipocytes induces upregulation of the rate limiting enzyme in phosphatidylcholine synthesis (CTP:phosphocholine cytidylyltransferse or CTT) (*66*, *69*). As this is the major phospholipid found in the ER membrane, it follows that XBP-1 increases ER biogenesis by both stimulation of ER proteins and membrane components.

2. PERK

The PERK pathway is another UPR leg. When released, PERK transautophosphorylates, activating its kinase domain. The major result of this is phosphorylation of eukaryotic translation initiation factor 2α (eIF2α). In the phosphorylated state, this essential component of the translational machinery cannot recycle GTP, inhibiting general translation but at the same time increasing the translation of mRNAs which contain internal ribosome entry sites, such as activating transcription factor (**ATF**)**-4**, BiP/GRP78, and SREBP-1 (*70*-*72*).

ATF-4 is a well studied protein involved in the UPR [reviewed in (*73*)]. This transcription factor is heavily involved in increasing amino acid metabolism and protein transport [reviewed in (*74*) and (*75*)]. Importantly, ATF-4 also upregulates stress-related transcription factors ATF-3 and CHOP. CHOP is a central transcription factor involved in cellular perturbations, including inhibition of adipocyte differentiation (*76*-*78*), and ultimately inducing apoptosis. However, this is another example of the necessity of balance, as although high induction of ATF-4 will lead to CHOP activation, complete absence will affect adipose lipogenesis (*79*).

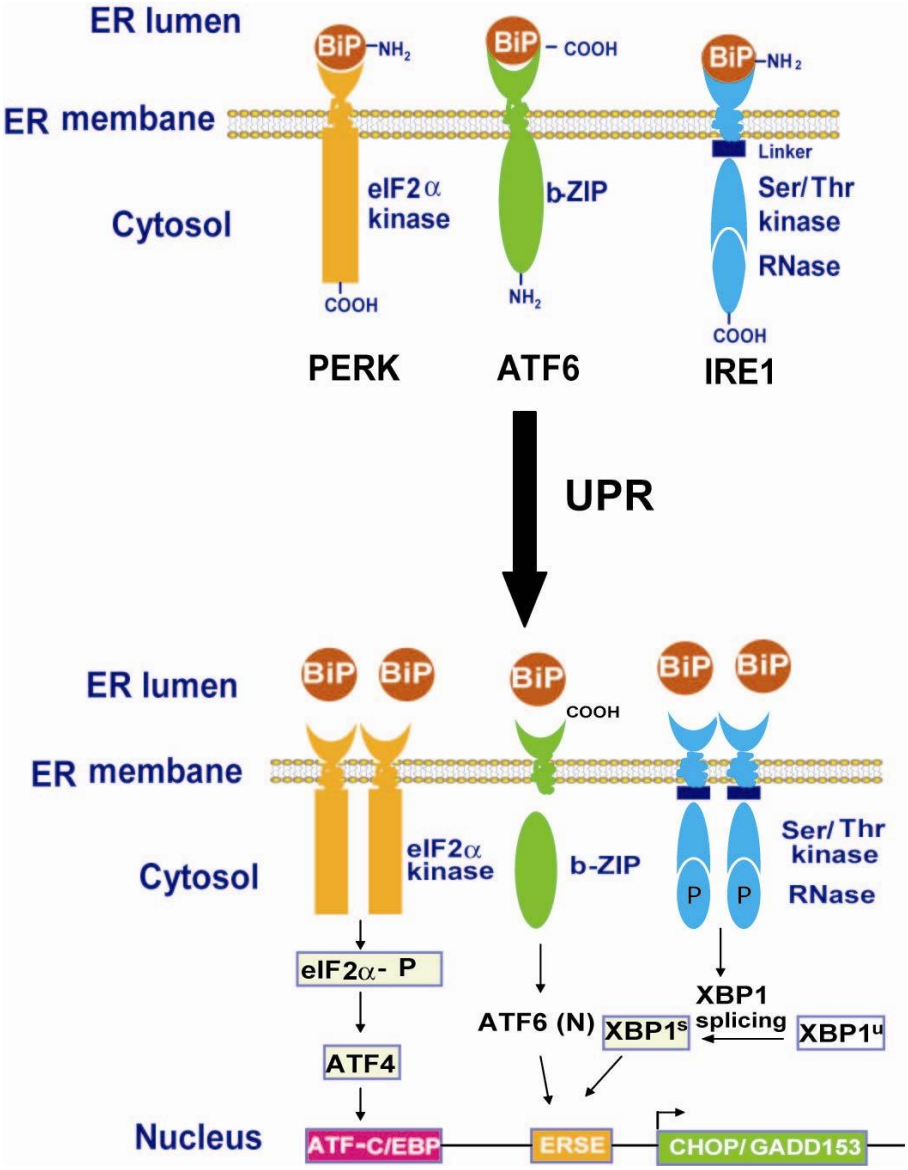

Figure 4. Depiction of the UPR. At times of ER stress, the UPR is activated to aid in return to homeostasis. Shown are the central proteins and downstream transcription factors involved in this pathway. BiP (GRP78) - ER protein chaperone; PERK, ATF-6, IRE-1 - ER transducer proteins; ATF-4, XBP-1^{S}, ATF-6 - downstream transcription factors.

SREBPs are additional transcription factors found in the ER membrane. There are three isoforms - SREBP-1a, -1c, and -2. SREBP-1c is involved in fatty acid synthesis and lipogenesis, -2 in cholesterol synthesis, and -1a in both pathways. The SREBPs are retained in the ER via insulin-induced gene (Insig) binding to SREBP cleavage activating protein (SCAP)-bound SREBP. At times of sensed decreases in cholesterol or fatty acids, SCAP-SREBP dissociates from Insig and relocates to the Golgi where SREBP is cleaved by two site proteases (S1P and S2P). The active form then translocates to the nucleus, activating genes for synthesis such as 3-hydroxy-3-methylgutaryl-CoA (HMG-CoA) synthase, HMG-CoA reductase, squalene synthase, acetyl-CoA carboxylase, and fatty acid synthase, as well as upregulation of themselves. Thus, ER stress induction not only alters protein production, but also cholesterol and fatty acid synthesis.

Normally, SREBPs are released when there is a sense of depletion of cholesterol or lipids in the ER membrane. However, SREBP1 processing is also regulated through PERK-eIF2α. In fact, knockout of PERK substantially decreases active SREBP1 in mammary glands (*80*). This is most likely a result from the recent finding that SREBP1 contains an internal ribosome entry site (*70*). Therefore, activation of ER stress will redundantly lead to active SREBP1 through both upregulation of translation and release protein from the membrane.

3. ATF-6

There are two genes encoding ATF-6, α and β. Both produce functional ATF-6 ER transmembrane proteins that can play redundant roles for one another. When either/both are released from GRP78, they translocate to the Golgi via a localization signal that was hidden when in the bound form. In the Golgi, ATF-6 is cleaved by the same proteases that process SREBPs, releasing the active cytoplasmic domain which is a transcription factor. ATF6α

heterodimerizes with XBP-1^{s} and upregulates genes with the ER stress-response element in their promoters, including GRP78 (*81*) and other ER chaperone proteins as well as XBP-1 and CHOP [reviewed in (*82*)].

C. ER Stress and Induction of Apoptosis

When activation of the UPR fails to bring a cell back to homeostasis, chronic ER stress can induce apoptosis. Activation of apoptosis occurs through a few routes, one of which is the transcription factor CHOP, and another is IRE1 activation (*83, 84*) (Figure 5). In addition, there exist multiple caspases resident in the ER (*85*), but it is still not elucidated how directly these caspases are involved in UPR-induced apoptosis, or if the mitochondrial apoptotic pathway is more essential. A major basis for confusion lies in the fact that calcium leaks from the ER at this late stage, triggering the mitochondrial stress pathway (*86, 87*).

Multiple investigators have noted the link of CHOP and apoptosis induction (*88, 89*). Indeed, overexpression of CHOP promotes cell death while overexpressing GRP78 can block CHOP-mediated cell cycle arrest and apoptosis (*90*). This role of CHOP may be directly attributed to CHOPs ability of transcriptionally repressing anti-apoptotic Bcl-2 (*91, 92*). CHOP also transcriptionally activates ER oxidase 1α (ERO1α), which oxidizes the ER, promoting disulfide bond formations. However, an accumulation of ERO1α may promote hyperoxidation in the lumen, inducing release of Ca^{2+} and downstream apoptotic inductions (*89, 93, 94*).

D. ER Stress and Activation of the Inflammatory Cascade

Many inflammatory pathways can be traced to the activation of mitogen-activated protein kinases (MAPKs). MAPKs are serine-threonine protein kinases expressed in most cell types. The

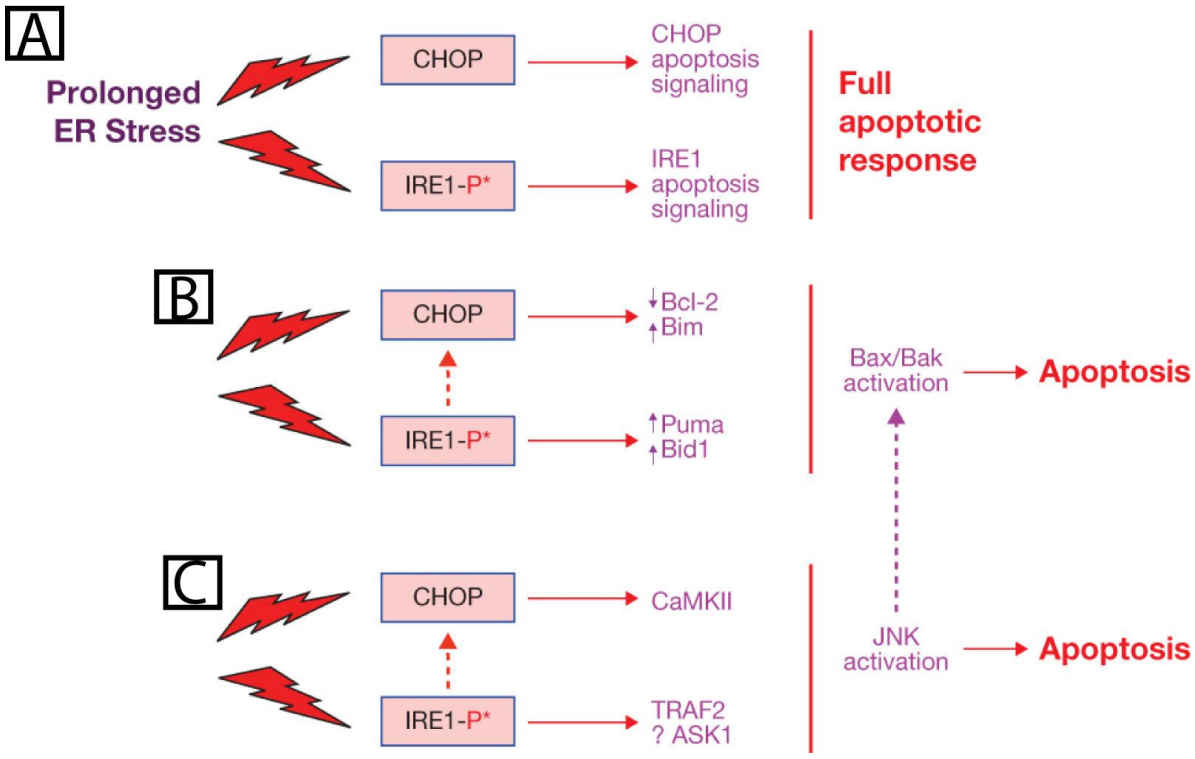

Figure 5. Potential pathways between ER stress activation and cellular apoptosis. After prolonged ER stress, cells may undergo apoptosis do to inability to return to homeostasis. As demonstrated in the current literature, after prolonged ER stress, apoptosis can be induced through CHOP upregulation (**A**). In addition, activated IRE1 can lead to upregulation of CHOP, activating apoptosis downstream (**B, C**). Reprinted by permission from Macmillan Publishers Ltd: [Nature Publishing Group] (*87*), 2004.

three ‘most important’ and well known MAPK pathways are Extracellular Signal-Regulated Kinases (ERK), c-Jun NH(2)-terminal protein Kinases (JNK), and p38 kinases. ERK 1 and 2 are involved in ‘pro-growth’ cascades, often being triggered by growth factors and cytokines. The p38 kinases are heavily involved in cytokine expression in immune cells, and as such, are targets of research in areas such as asthma and autoimmunity. The pathway of interest here, JNK, is activated upon stress responses that inhibit protein synthesis, such as ER stress (*95*). Activation of the JNK pathway is often investigated during drug research since it can be activated in numerous ways, induces inflammatory cytokine production, and is linked to cell death/apoptosis (*96*, *97*).

Although it was known that ER stress could activate JNK (*95*), it was Urano *et. al* who demonstrated it was through the IRE1 pathway (*83*). This direct connection has given a secure base of an ER stress activation and inflammatory disease link. HIV PI-induced risk factors of atherosclerosis, as well as atherosclerosis itself, have inflammatory components. Therefore, the issue of ER stress-induced inflammation will continue to be discussed in subsequent sections.

V. Autophagy

A. Autophagy Pathways

Autophagy was first defined in yeast, and has since been described in all eukaryotics. In yeast, autophagy serves to aid in times of starvation, while induction of the pathway in mammals is increasingly more diverse but is still essentially a self-protective cellular pathway. In mammals, autophagy can be activated by multiple stimuli including viral infection, perceived starvation, organelle dysfunction, and even ER stress. However, just as in the case of the UPR, autophagy has the ability to increase cellular damage or cell death when over-stimulated. This

has added autophagy as a third class of cell death (*98*), beyond the classical apoptotic and necrotic pathways.

There are three main subdivisions of autophagy - macroautophagy, microautophagy, and chaperone-mediated autophagy. These three pathways differ by how cytoplasmic components are delivered to the lysosome. Macroautophagy is the classical pathway first described in yeast, where cytoplasmic constituents are sequestered in autophagosomes, which later fuse with a lysosome to degrade the material for recycling or energy. In contrast, microautophagy occurs when a lysosome engulfs the material directly through invagination of its own membrane (*99, 100*). Chaperone-mediated utilizes a specific protein signal (KFERQ) that is recognized by HSC70 chaperone to traffic a protein directly to the lysosome [reviewed in (*101*)]. In addition, as the autophagic field expands, other pathways are continuing to be identified. However, it is not clear if these subsets are separate autophagic pathways or just alterations from the three pathways described above. For example, mitophagy, when mitochondria are selectively degraded, is most likely one selective form of microautophagy (*99, 102*).

Macroautophagy is the classical and well-understood pathway of autophagic research. It is non-specific in its uptake of material, and may be a major pathway by which lipid stores are regulated in cells (*103*). As it is the focus during our investigations, it will be the implied pathway when speaking of autophagy induction.

1. Formation of Autophagosomes

As stated above, cell death can occur through autophagy. Visualization of a cell in the midst of death can allow determination of which pathway is taken. In necrosis (accidental death), swelling of the cell and its organelles occurs due to loss of plasma membrane integrity and a consequent influx of ions and fluid. Apoptosis (self-destruction) is noted by shrinkage of the cell

and its organelles as the plasma membrane remains intact longer. In addition, apoptotic cells often have chromatin condensation, nuclear fragmentation, and blebs of membrane later in time. Autophagy is unique in that the cells appear under normal morphology at low magnification, yet upon close inspection, there is vacuolization in the cytoplasm and autophagosome formation.

At initiation of autophagy, autophagic-specific proteins begin to aggregate at a cistern-double membrane termed the pre-autophagosomal nucleation site (**PAS**) (*104*). This membrane than elongates and encloses around the cytosolic component(s), and is termed the autophagosome (*105*). Via vesicle-mediated transport, the autophagosome starts to accumulate lysosomal membrane proteins and pumps (*106*), and later fuses with a lysosome at the outer membrane, leaving the inner membrane to contain the cytoplasmic content within the lysosome (*107*). The final step is degradation of the inner membrane and components by hydrolases, and transport of products into the cytoplasm for metabolic purposes.

Each vesicle in this pathway can easily be defined by its properties. The initial autophagic vacuole (**AVi**), or autophagosome, is at physiologic pH without any lysosomal proteins. In the degradative autophagic vacuole (**AVd**) or late autophagosome, the vesicle is acidic and contains lysosomal proteins. Another distinguishing factor of these two vesicles from other organelles is their smoothness of membranes compared to the lysosome and ER, and their half-lives are actually only 8 minutes (*108*). After outermembrane fusion of the autophagosome with a lysosome, the vesicle is determined an autophagolysosome (*109*).

2. Few Key Proteins

There are currently at least 31 proteins identified to be specifically involved in autophagy (*110*) (see Figure 6 for a simplification of their involvement). Most of these proteins were first identified in the yeast model, and are named autophagy-related genes (**Atg**). Many of these have

analogues in mammalian cells, and have been named differently when found in these models, confusing the nomenclature of present day investigations. Both names will be given here to clarify the discussion below.

In addition to Atgs, other proteins involved in autophagy induction but not specific to autophagy also exist. For macroautophagy, the most classically understood activation is that of nutrient deprivation. In a nutrient-rich environment, growth factors stimulate the eukaryotic cell, and activate P13K Class I proteins. These proteins activate AKT, which results in activation of serine/threonine protein kinase target of rapamycin complex 1 (TORC1), an indirect inhibitor of Atg1 and direct inhibitor of Atg13. Hence, lack of nutrients leads to Atg1 activation.

Active Atg1/ULK1 and Atg13 associate with each other and translocate to the PAS. Inhibition by TORC1 can occur at this point via phosphorylating Atg13, destabilizing this complex. Nevertheless, after Atg13-Atg1/ULK1 is associated with the membrane, Atg17/FIP200 is localized to the complex, which leads to the recruitment of the transmembrane protein Atg9. Atg9 is particularly important as it membrane sequesters, allowing elongation of the PAS (*111*).

In addition to Atg9, the Atg13-Atg1 complex also activates Atg6/Beclin1, allowing the interaction with P13K class III proteins. The Atg6-PI3K complex recruits Atg14, and together activates the next complex that includes Atg12. Atg12 is conjugated to Atg5 via the catalysis of Atg7 (an ubiquitin E1-like enzyme) and Atg10 (E2-like). Atg12-Atg5 interacts with Atg16L, oligomerizes, and is involved in the recruitment of Atg8/LC3.

3. LC3 and Importance in Autophagy Detection

LC3 was first identified as microtubule associated protein light chain 3 (MAP-LC3). It is a constitutive cytosolic protein, activated when cleaved by a cysteine-protease (Atg4). Once cleaved, Atg7 (E1 like) and Atg3 (E2-like) catalyze the conjugation of exposed C-terminal

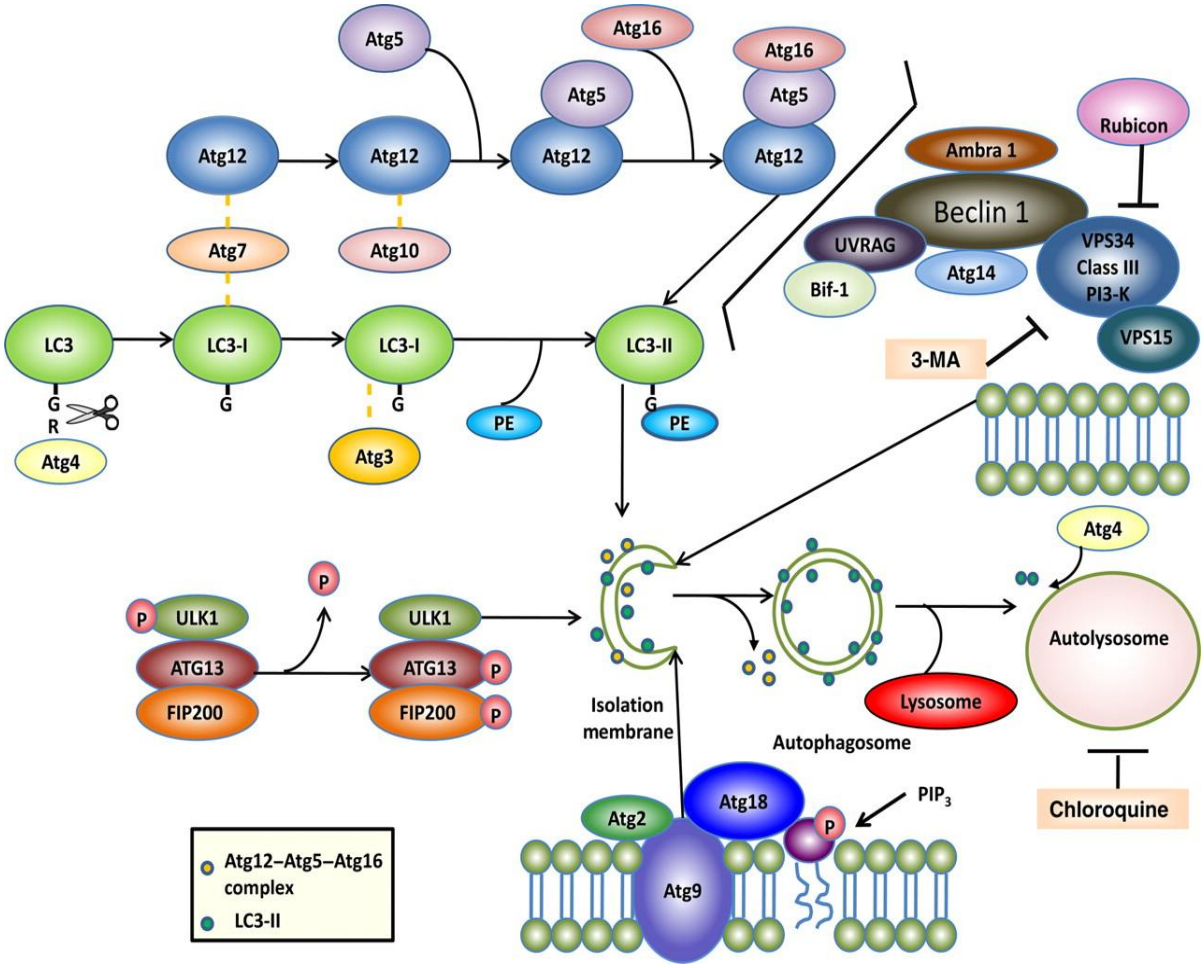

Figure 6. Schematic diagram depicting the molecular aspects of autophagosome formation. Shown is a simplified depiction of autophagy induction to autophagosome formation. As eluted to in the text, the complexity of autophagy, and numerous proteins involved, complicates the ability to draw the pathway as known today. Modifed by permission from Experimental Biology and Medicine(*112*), 2011.

glycine to phosphatidylethanolamine (PE) (*112, 113*). In this conformation, LC3 can associate to both the inner and outer limiting membranes of the phagosome. It is important to note that activation of LC3 is necessary, but not sufficient, as many other proteins and processes contribute to vacuole formation (*113*).

LC3 has been used extensively in autophagy research. During Western blot, one can analyze activation of LC3 as the free cytosolic form (I) migrates a Bis-tris gel slower than the lipidated form (II). During autophagy, the II:I ratio increases as more LC3 is activated (*114*). Another common method utilizes a plasmid expressing GFP-tagged LC3. After stably transfecting a cell line, autophagy increase can be followed by fluorescent-punctate formations in the cytoplasm as the expressed GFP-LC3 relocates to autophagosomes (*115*).

B. Autophagy and ER Stress

Autophagy and ER stress pathways are not disconnected from one another as previously assumed. In contrast, activation of both can aid in cell survival at times of stress. Autophagy offers an alternative pathway for degradation of proteins when ER-activated proteasomes can no longer handle the load (*116-121*). In addition, activation of cell death of each pathway may be interlinked. Classic knowledge is based on ER stress activating apoptosis through CHOP upregulation [reviewed in (*89*)] and autophagy-mediated cell death via a completely separate process. However, recent findings demonstrate that these two cell death pathways are interlinked [partially reviewed in (*122*)].

Prolonged UPR activation has been shown to lead to autophagy-induced cell death (*117*), and inhibition of autophagy increases cell viability with prolonged ER stress (*123-125*). The exact mechanism of how ER stress induces autophagy is still being investigated. Recently, it was found that ER stress activation can inhibit Akt phosphorylation, the upstream inducer of

autophagy at times of perceived starvation (*126*). However, the responsible protein(s) are still not known, and may even be cell-type specific [reviewed in (*127*)].

Another link is hypothesized to occur through the PERK pathway of the UPR (*128, 129*). Some studies have shown that PERK phosphorylation of eIF2α leads to an upregulation of LC3 (*120*). Yet, it has not been elucidated if this is directly due to eIF2α phosphorylation inducing LC3 translation, or through ATF-4 activation increasing *Atg12* transcription (*130, 131*).

Even more, one study has seen a strong link between activation of ER stress, increased autophagy induction, and increased SREBP activity leading to lipid overload in hepatocytes (*57*), although a mechanism was not proposed. Another group has demonstrated the capability of SREBP-2 to directly upregulate the expression of autophagy essential proteins (*132*), giving significance to a previous finding that cholesterol depletion leads to autophagy induction in multiple cell lines (*133*). Although SREBPs are not a current forefront of proposed activators of autophagy, it is probable that at times of cellular stress SREBPs are involved in processing lipid droplets through the autophagic pathway for ATP production.

VI. Adipocytes

A. Cellular Properties

1. Physiology

In the last two decades, the complexity of adipose tissue has become apparent. Investigations surrounding the biological impact of obesity, insulin resistance, and the Metabolic Syndrome have surged, resulting in a more intricate understanding of 'fat.' Now we know that adipose tissue (**AT**) is not only highly specialized to store energy for long term, but also is a central endocrine organ. Therefore, AT is inherently involved in the interplay of inflammatory

cascades and energy metabolism, which are important players in metabolic disorders. Even more, sick fat, or adiposopathy, has been coined an independent endocrine disease (*134*).

AT is an assortment of adipocytes, macrophages, and endothelial cells. In addition, these different cell-types are connected to one another through a complex mixture of proteins and proteoglycans in the extracellular matrix. Nevertheless, there is no rejecting the centrality of adipocytes in this tissue.

To understand the adipocyte, it is important to grasp the path it takes to become a mature cell. Adipocytes begin first as mesenchymal stem cells (MSCs) (although this has recently been debated as touched upon later). MSCs are multipotent stem cells, and as such, can follow multiple pathways to terminate as an osteoblast, chorocyte, or adipocyte (*135, 136*). Determination of lineage is dependent on small molecule signals and the extracellular environment (*137*), though complete understanding of this process is still lacking (*136*). Within adipogenesis, the normal pathway begins with MSCs proliferating and then differentiating into adipose-derived stem cells (ASCs) (*138*), most likely through activation via bone morphogenic protein 4 (BMP) (*139*). ASCs continue with proliferation and differentiation into fibroblast-like pre-adipocytes which are particular cells that can migrate, proliferate, and further differentiate into round adipocytes (*140*).

Pre-adipocytes are fibroblastic in both morphology and gene characteristics. In fact, a common cell line used in the study of adipocyte metabolism and differentiation is 3T3-L1, which is also commonly utilized in fibroblast studies. Induction of differentiation from the pre-adipocyte to mature adipocyte is rather simple, and can translate between cell cultures of differing species with slight modifications. The mechanism of a differentiation adipocyte is nonetheless a bit complex.

2. Differentiation

Understanding of adipogenesis began with cellular models, though more is now known through tissue modeling and *in vivo* studies. *In vitro*, the initiation of differentiation occurs at growth arrest via cell-cell contact. In tissue, this occurs through a combination of cell contact with other pre-adipocytes, as well as signals from neighboring adipocytes and stromal cells. After induction, the profile of genetic expression changes through adipogenic transcription factors, including peroxisome proliferator activated receptor γ (**PPARγ**), retinoid X receptor (**RXR**), and CCAAT enhancer binding proteins (**C/EBP**)α and β.

a. C/EBPs

The C/EBP family is named after their ability to interact with a cytidine-cytidine-adenosine-adenosine-thymidine (CCAAT) box motif on DNA, present in many promoters. There are six members in the family, of which α, β, δ, and ζ are involved in adipocyte differentiation. C/EBPβ and δ are involved early in the differentiation process – their maximal protein levels in 3T3-L1 culture is within four hours of induction, and only lasts two days (*141, 142*). C/EBPβ is transcriptionally activated by cAMP response element binding protein (CREBP) (*143*), and transcriptionally activates C/EBPα and PPARγ for the next steps of differentiation. C/EBPβ and δ may have a redundancy in action, as knockout of either one alone results in normal adipose physiology in mice, but a double knockout have markedly reduced AT mass (*144*). After activation, both C/EBPα and PPARγ autoinduce, and coinduce, to keep levels high throughout differentiation (*145-147*).

b. PPARγ

PPARγ is arguably the most important of these factors. For one, overexpression of PPARγ in fibroblasts induces adipogenesis without any other stimulation, while a dominant

negative mutant of the protein results in inhibition of full differentiation (*148*). Knockout of PPARγ in mice results in embryonically lethal day 10 due to malformation of the placenta. The heterozygote mouse model gives us more information as these mice develop very minimal AT (*149*).

PPARγ is a member of the PPAR family, which also includes α and β/δ nuclear receptor members. Upon activation with ligands, these PPARs dimerize with RXR, and act as transcription factors to control lipid metabolism and fuel dispersion. In AT, PPARγ increases insulin sensitivity as well as regulates TG storage, besides its role in adipogenesis (*150*). As such, a dominant-negative form of PPARγ in adipose tissue leads to insulin insensitivity, decreased glucose metabolism, and increased release of FAs – which can also be an issue clinically (*151*).

There are two isoforms of PPARγ, of which the second is dominant in adipocytes (PPARγ2), and most important in adipogenesis (*152*). There are five domains of the protein: *A/B* at the N-terminus, *C* which is the DNA-binding domain (DBD), flexible hinge region (*D*), ligand binding domain (*E*) and F at the C-terminus. The DBD binds to peroxisome proliferator hormone response elements (PPREs) on the genomic DNA (sequences of which are AGGTCAXAGGTCA).

PPARγ has a distinct and broad range of ligands including prostaglandin, polyunsaturated fatty acids (FA), non-steroidal anti-inflammatories, and the glitazone class of diabetic medications. Once activated, PPARγ goes on to transcriptionally activate a large number of adipose genes including adipocyte fatty acid-binding protein aP2 (*153*), lipoprotein lipase (*154*), lipid droplet-associated protein cidec (*155*), lipase ATGL (*156*), and perilipin (*157*). The trend of these genes revolves around lipid metabolism and lipid droplet formations.

c. Other Important TFs

Another protein that has been marked for involvement in adipogenesis is ADD1 (adipocyte determination and differentiation-dependent factor)/SREBP1. ADD1 and SREBP-1a/1c are all encoded in the same gene via alternative promoters, thus giving the protein involved here a double label (*158*). As discussed above, SREBPs are heavily involved in cholesterol and lipid synthesis, and ADD1/SREBP-1c does much the same within the first day of adipogenesis (*159*).

3. Lipid Droplet

The complexity of lipid droplet (LD) formation has been increasingly realized in the past decade. LD is now considered a dynamic intracellular organelle by many experts (*160*). In adipocytes, the LD is large (most other cells it is only $1/50^{th}$ of that found in adipocytes). At its core, the droplet is composed of TGs and cholesterol esters, surrounded by a phospholipid monolayer. In addition, there is a coat of proteins with unique functions to help package the TGs, as well as protect the droplet.

a. LD Proteins

The knowledge of LD protein functions are in the beginning stages, while control of their expression and the targeting to the LD are unknown. The most studied protein is perilipin, which is so similar to adipose differentiation-related protein (ADRP, also called adipophilin) and tail-interactin protein (TIP47) in sequence that these three proteins are placed into one protein family (PAT for Perilipin/ADRP/TIP47). In addition, two more proteins have been added to this family, S3-12 and OXPAT, which also share the N-terminal motif of the PAT domain.

Perilipin is a regulator of lipolysis. The half life of perilipin associated to a LD is about 40 hours, while free perilipin is quickly degraded (*161*). At this position, perilipin is also

associated with Comparative Gene Identificant-58 (CGI-58) (*162*), which together inhibit hormone sensitive lipase (HSL) and adipose triglyceride lipase (ATGL) from gaining access to the inner TGs.

In unstimulated conditions, perilipin remains associated with CGI-58 on the LD droplet, and HSL is sequesterd in the cytosol. With cellular stimulations that increase cAMP levels (ex. catecholamines and glucocoricoids), protein kinase A (PKA) is activated and multi-phosphorylates perilipin (*163*), as well as HSL. These phosphorylations result in activation of lipolysis two fold. First, phosphorylated perilipin no longer associates with CGI-58. Released CGI-58 then activates ATGL, allowing its interaction with LD. ATGL cleaves TG and releases one FA and diacylglycerol (*163*). At the same time, phosphorylated HSL colocalizes with phosphorylated perilipin (*164*), where it cleaves the diacylglycerol to release another FA and monoacylglycerol. The last is cleaved by monoacylglycerol lipase to release the last FA and a glycerol (*165*).

In addition to perilipin and CGI-58, other LD proteins include TIP47, a ubiquitously expressed protein. TIP47 coats early forming LDs (*166, 167*), and has also been shown to compensate for loss of ADRP (below) (*168*). Hickenbottom *et. al* were able to obtain the crystal structure of TIP47 in 2004, and found that there are many parallels of TIP47 and apoliproteins A and E structures, as well as a high structural match with N-terminal apoliprotein E (*164*). This finding is functionally important, demonstrating structural similarities of cellular LDs and serum lipid droplets that may be exploited in the future.

ADRP is another ubiquitously expressed protein (*169*), constitutively bound to the LD. Functionally, ADRP replaces TIP47 on the small LDs. During the progression of differentiation, ADRP RNA and protein levels decrease while perilipin proteins increase and coat larger LDs of

late adipogenesis (*166, 167, 170*). However, in other cell types that store lipids, such as hepatocytes, ADRP and perilipin both equally coat the LD. As such, ADRP can compensate for a loss of perilipin at least to an extent (*170-172*).

b. LDs and the ER

Formation of LDs is at this time only hypothesized and not concretely described. One highly supported model portrays the LD to bud off the ER membrane at points of neutral lipid accumulations. Others hypothesize the LD and ER remain attached, allowing the accumulation and recycling of proteins (*173*).

In an elegant study done by Robenek *et. al*, freeze-fracture replica immunolabeling (FRIL) was used to identify where LD proteins were located (*174*). In their images, the ER appears to be holding the LD 'like an egg-cup,' with the ER adjacent to, and not interconnected with, the LD membrane. ADRP and perilipin were found to be located in the limiting membrane, at the interface of the core lipid and cytoplasm, and ADRP was found in the ER membrane in concentrated areas that were the closest distance to LDs.

Despite the controversy of the origin of the LD, the importance of the ER in LD biogenesis and maintenance remains. Of particular interest in this arena is CTP:phosphocholinecytidylyltransferase (CCT), the rate limiting enzyme for phosphatidylcholine (PtdCho) synthesis (a major lipid in LD, the other being phosphatidylethanolamine). This enzyme, as well as others involved in this pathway, is enriched at the RER, however, it is unclear what signal occurs to stimulate/inhibit CCT. What is known is that lack of CCT can result in fusion of LDs (*175*).

B. Adipose Tissue

The majority of the population despises AT due to its depleasing asthetic nature.

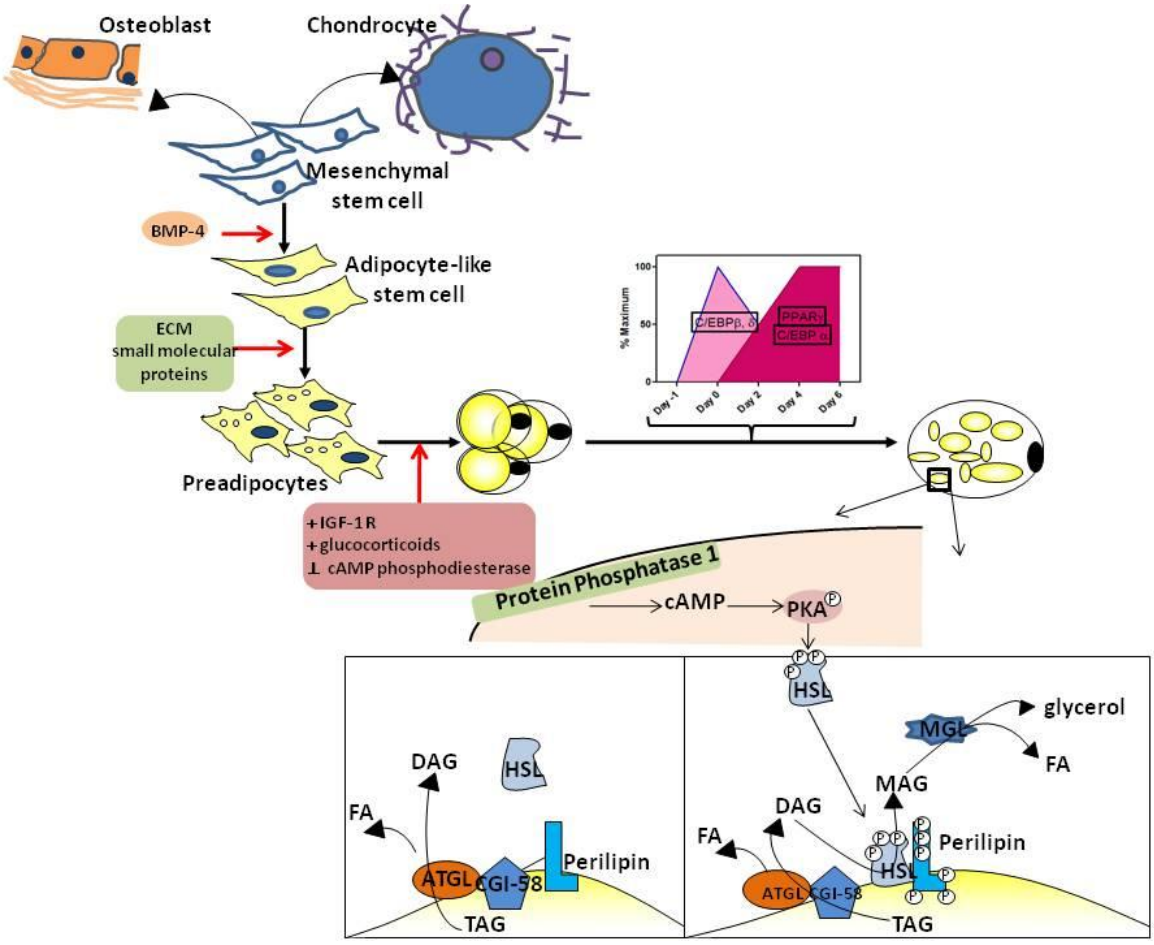

Figure 7. Depiction of the lineage and maturation of adipocytes. The start of adipogenesis can be traced to the mesenchymal stem cell (MSC) differentiating to an adipose-derived stem cell (ASC). Pre-adipocytes are then induced by small molecules such as insulin growth factor (IGF)-1 receptor activation, as well as cell-cell contact. Transcription factor C/EBPβ is subsequently induced, leading to the activation of PPARγ and C/EBPα transcription factors. At this point, upregulation of proteins necessary in lipid droplet formation occur. The last stage depicted here is activation of hydrolysis at the lipid droplet by cellular cAMP increases (see Section VIA. 3a.).

However, AT is a complex organ responsible for organ insulation, excess energy storage, and is heavily involved in the endocrine system (*176*, *177*). The condition of AT can determine lipidemia and insulin sensitivity, as well as the inflammatory state of the body.

There are slight differences between AT depots, and this may stem from embryogenesis. AT is often suspected to arise from the mesoderm (*178*), but some fat pads may actually be generated from the neural crest (*179*). The differences between depots are seen both chemically and physiologically. It was found in the late 1990s that preadipocytes isolated from different depots have different adipogenic induction responses (*180*) and gene expressions (*181*), but these differences are still not well understood.

Physiologically, it has been long understood that those with increased visceral adipose mass have a higher risk of cardiovascular disease, although those with the same BMI but more subcutaneous mass do not have the same risk. However, the differences that lead to detrimental risks are still not understood. Basic researchers have probed the physiology of visceral versus subcutaneous depots for a decade now with no concrete results. In HIV treatment, different drugs have differential effects on fat tissue - the RTIs seem to decrease subcutaneous depots while the HIV PIs increase visceral adipose mass (*182*) (termed HAART-induced lipodystrophy). The result is a substantial increased risk of cardiovascular disease in HAART-treated patients, and this can be attributed directly to PIs (*22*).

C. ER Stress in the Adipocyte

1. Basal Involvement of the UPR in Adipogenesis

As previously discussed, ER stress does not have a clear-cut product. Although the UPR is understood to aid a cell in returning to homeostasis, it can lead to detrimental cellular effects when overstimulated, and even when understimulated. One such example of this is XBP-1^{s}. In

the adipocytes, the close interplay of ER biogenesis and LD formation relies on tight control of XBP-1^s. As previously discussed, overexpression of XBP-1^s can lead to upregulation of CTT (*66, 69*), and knockout inhibits pre-adipocyte differentiation with only XBP-1^s (not unspliced) able to rescue this phenotype (*183*).

In vivo, XBP-1 knockout mice die *in utero* (*67*). Therefore, to study the importance of XBP-1 in AT, we must turn to a model that expresses XBP-1 only in the liver. These mice also prematurely die. In fact, death occurs during the neonatal starvation period, partially due to negligible white adipose mass (*69*).

In addition to the role XBP-1 may play in CCT and LD biogenesis, XBP-1^s has been shown by Sha *et. al* to upregulate C/EBPα (*183*). Conversely, C/EBPβ increases transcription of XBP-1. Therefore, XBP-1 is integral in the differentiation process, playing roles in both maturation of the cell and transcriptional activities.

Beyond the IRE1-XBP1 pathway, other components of the UPR may be involved in adipogenesis, although more investigations need to be completed to clarify these mechanisms. For the ATF6 pathway, knockout mice of either ATF6α or β do not show any striking physiological changes as there is redundancy between the two isoforms. However, it is proposed ATF6α is the more essential isoform for the ER stress pathway as ATF6α and not β induces genes with the ER stress-response element in their promoters (*184*). More important in this section, ATF6α can upregulate XBP-1. As ATF6α and XBP-1^s can heterodimerize, it should be determined if this formation is important in XBP-1 upregulation of C/EBPα or CCT.

SREBP-1c is another transcription factor heavily involved in adipogenesis. Although not deemed a UPR component, SREBPs can be activated during ER stress. SREBP-1c has a dual name of adipocyte determination and differentiation 1 (ADD1). Overexpression of

ADD1/SREBP1c leads to an increase of LD formation in pre-adipocytes (*185*), and this may be due to activation of a lipid activating PPARγ (*186*). However, conditional overexpression in mice inhibits normal white adipose tissue growth (*185*). *In vivo*, PPARγ levels were lowered compared to wild-type mice. The paradoxical differences of *in vivo* and *in vitro* models may be due to timing of knockdown of SREBP1c, but this needs to be further investigated, especially as SREBP1c has more recently been shown to directly activate C/EBPβ (*187*).

Lastly, the PERK pathway has also been found to be important during differentiation of adipocytes *in vitro*. PERK to ATF-4 activation has been shown to be important in activation of genes involved in lipogenesis (*80*). Knockdown of this pathway does not inhibit adipogenesis, but reduces the accumulation of lipids involved in this process. More significantly, ATF-4 activates CHOP, a known inhibitor of adipogenesis. CHOP can heterodimerize with C/EBP transcription factors (hence it's name). When in this conformation, the C/EBPs can not bind to their normal DNA targets, ultimately leading to inhibition of their actions, including activation of adipogenesis (*76, 78*).

2. UPR Activation in AT and Disease

Activation of the UPR has the potential of inducing deleterious cellular effects. In AT, the majority of this is manifested as inhibition of pre-adipocyte differentiation and induction of the inflammatory cascade, of which both are induced by HIV PIs.

The description of the intrinsic involvement of the UPR in adipogenesis above demonstrates how alteration of the UPR can influence differentiation. Direct examples of this have been shown in previous studies. For example, Basseri *et. al* treated murine 3T3-L1 cells with the chemical chaperone 4-phenylbutyrate, a repressor of the UPR, which attenuated

differentiation in this cellular model (*188*). At the same time, Shimada *et. al* demonstrated that the compound K-7174 could inhibit differentiation through overactivation of ER stress (*189*).

HIV PIs have been shown to differentially affect adipogenesis (28-36). However, results in the literature are contradictory and lack mechanistic explanations. For example, a few results state RITV does not inhibit differentiation of adipogenesis, and others state it significantly inhibits this pathway. Reasons for such contradiction derive from differences in differentiation techniques and subjectivity of certain assays. In addition, most studies focused on the possibility of inhibition of differentiation, and not the mechanism of this phenomenon. From the above information give, it could follow the mechanism underlying HIV PI-induced alteration in adipogenesis is induction of ER stress.

Many metabolic diseases have been shown to have underlying pathology in AT. In addition to altering capacity of lipid storage, these diseases also have underlying inflammation. As previously noted, there is now known to be a direct link between the UPR and inflammation. One of the first cell-types demonstrated to have this link was macrophages. Here, it has been repeatedly demonstrated that lipid-laden macrophages (the core of an atherosclerotic plaque) secrete multiple pro-inflammatory cytokines such as TNF-α and IL-6. In addition, HIV PIs can induce this pro-inflammatory state directly in this cell type through the activation of the UPR and upregulation of the mRNA binding protein HuR (*51, 52, 190, 191*).

Investigations into mechanisms underlying obesity and diabetes has demonstrated how inflammation in AT can detrimentally alter human physiology. With increasing overload, adipocytes begin to hypertrophy, becoming stressed and signaling this with a release of proinflammatory cytokines. These cytokines cause an infiltration of circulating macrophages, which engulf over-stressed or dying cells, forming characteristic crown-like structures.

Interestingly, HIV patients on HAART therapy appear to be in the same state as an obese individual in terms of inflammation and dysfunction in AT. Patients often have a decrease in insulin sensitivity, as well as having dyslipidemia and liver disease as previously discussed.

The inflammatory cascade has been shown to be induced by HIV PIs in adipocytes (*192-194*). In addition, this activation may be an underlying factor of inhibition of differentiation. In fact, exposure of pre-adipocytes to TNF-α alone is enough to inhibit induction of PPARγ and C/EBPα (*195*). However, the mechanistic induction of the inflammatory cascade in adipocytes is the key to determine how HIV PIs have these detrimental affects.

Even beyond the potential of inhibiting differentiation, induction of inflammation can lead to insulin resistance in AT (*196, 197*). This connection is already widely known, and will not be discussed in further detail here. For an in-depth discussion of the connection between inflammation and insulin resistance, please see reviews [(*198, 199*)]. Instead, our focus now turns to ER stress link with insulin resistance.

A key study in this field was done by Djedaini and colleagues. When a human adipocyte cell line was treated with LOPV, there was an increase of ER stress activation as well as a decrease of IRS1 phosphorylation (*54*). What linked these two phenomena was eIF2-α phosphorylation. When cells were treated with salubrinal, a small molecule that specifically inhibits eIF2-α phosphorylation, there was a slight decrease in IRS1 phosphorylation. However, when they added minimal concentrations of LOPV with salubrinal, there was a significant decrease of IRS1 phosphorylation, suggesting a synergistic effect of the two drugs and the role eIF2α plays in LOPV-induced adipocyte insulin resistance.

Activation of the UPR leading to a decrease in insulin signaling may only be part of the story. Others have shown that HIV PIs can actually directly inhibit the glucose transporter (*200*).

It has been proposed that this inhibition induces a starvation-like state in the cell with the decrease of intracellular glucose, causing activation of ER stress. This would lead to a decrease in insulin signaling, propagating insulin resistance further. At this point, adipocytes would rely heavily on lipids, hydrolyzing triglyceride stores and thus increasing NEFA release, causing lipotoxicity and insulin resistance at the physiological level. More research is clearly needed to determine which pathway or proteins HIV PIs induce/inhibit when they first come into contact with an adipocyte. Only then can we be certain of the consequences of a given structure on the drugs currently on the market.

D. Autophagy and Lipid Metabolism in the Adipocyte

In adipocytes, the importance of autophagy and cellular lipid metabolism goes beyond what was previously discussed. Of one particular note is that components of the autophagosome may be necessary for lipid droplet formations (*201*). Shibata *et. al* have demonstrated that LC3-II does not only colocalize to autophagasomes, but also LDs in hepatocytes and cardiac myocytes, suggesting a flux of lipid metabolism in the cell dependent on this pathway (*201*). These findings were followed with an investigation in murine adipocytes, demonstrating that LC3 colocalizes to LDs in differentiating cells (*202*). In addition, siRNA of LC3 drastically decreased the ability of adipogenesis (*202*).

Beyond Shibata *et. al*'s study, knockout models have demonstrated how essential autophagy is in adipogenesis. Baerga *et. al* were able to establish this by first showing the significant increase of autophagosome formations during induction of adipogenesis, followed by the inhibition of differentiation in a knockout *atg5* mouse model (*203*). Using this model, Baerga *et. al* saw both *in vitro* and *in vivo* that inhibition of autophagy restrained maturation of pre-adipocytes, resulting in a marked reduction of WAT in neonatal mice. Interestingly, when

knockout murine embryonic fibroblasts were induced to differentiate, cells that began to mature died through apoptosis, while those in the same culture that did not begin to differentiate remained alive. This study was followed by another with an adipose-specific deletion of *atg7* (*204*), a gene encoding an essential protein upstream of Atg5. Interestingly, WAT tissue of this knockout model was more characteristic of BAT in both morphology (smaller cells and LDs) and enzyme levels. The importance of Atg7 in adipogenesis was confirmed by Sing *et. al* who knockdown the same gene but used slightly different cell lines and mouse model (*205*). However, both groups came upon the same finding that the autophagic pathway is essential in adipogenesis.

The trigger of autophagy activation during adipogenesis is not currently known. PPARγ may be involved. In one cancer cell line, it was found that PPARγ targets can then activate the autophagy pathway (*206*). However, there is another study that contradicts these findings (*207*), and such investigations have not yet been repeated in an adipocyte model. Nonetheless, the summation of above experiments does demonstrate that autophagy is essential in adipogenesis and LD formation. Differing, a decrease of autophagy in the liver leads to lipid overload in hepatocytes. Intuitively, the difference lies in the biology of the two cell types, where adipocytes are normally storing lipids and hepatocytes are not. In metabolic disease states, it is easy to conceive how dysregulation of autophagy could ultimately lead to fatty liver with increased TG storage in the liver and decreased storage in AT.

In addition to its role in adipogenesis, autophagy may help control the inflammatory cascade in adipocytes. Adiponectin, the adipocyte-specific anti-inflammatory cytokine, is negatively correlated with diseases such as atherosclerosis and insulin resistance. In

overexpanded or stressed tissue, there is a decrease of adiponectin secretion (*208*), and an increase of macrophage-inducing TNF-α, IL-6, and MCP-1 as discussed previously.

HIV PIs have been repeatedly reported to decrease adiponectin, from the RNA level to secretion. Interestingly, adiponectin can alleviate ER stress (*209*). Zhou and colleagues have shown that ER stress initiation is sufficient to decrease adiponectin release. In animal models, they reported stabilization of adiponectin decreased obesity-induced ER stress in AT. Moreover, induction of autophagy could alleviate ER stress responses in the cell, stabilizing adiponectin secretions. More investigations are neded to determine if upregulation of autophagy could ultimately lead to therapeutic options for metabolic diseases.

However, the understanding of HIV PI-induced metabolic disease does not just center at AT lipid metabolism and inflammation, but also other key organ systems including the liver. Interplay between the liver and AT is central in lipidemia, serum glucose levels, and potential of fatty deposits in the liver. Therefore, the next section will focus on how HIV PIs disrupt normal liver metabolism.

VII. Liver

The liver is centrally involved in many metabolic diseases due to its role in lipid homeostasis, bile acid synthesis, and gluconeogenesis. In HIV PI-induced metabolic alterations, the liver plays a substantial role since it is the first organ to come in contact with this drug class, and responsible for their metabolism. Therefore, a majority of investigations focusing on HIV PI side effects have focused at the liver and hepatocytes for underlying mechanisms to explain disease.

Interestingly, some of this work has found that HIV PIs have a similar affect in the liver as a Western diet, inducing components of NASH. As discussed in Section IV A, a central factor

of NASH is accumulation of hepatic lipids from NEFA and DNL, not the diet as intuitively thought. In HIV PI treatment, alteration of AT lipid metabolism can lead to an overload of lipid dumping at the liver, which may be the mechanism underlying HIV PI-induced NASH.

In addition, insulin resistance is another central manifestation of NASH. In respect to HIV PI-induced NASH, it has been hypothesized that although HIV PIs can induce insulin resistance in both adipocytes and hepatocytes, HIV PIs first target a decrease in peripheral glucose uptake, and chronic treatment alters hepatic glucose production (*210, 211*). In fact, chronic inflammation may be the underlying instigator of insulin insensitivity, especially at induction of macrophage infiltration in AT (*212*). The resulting alterations of lipid metabolism in AT, with continuous pathophysiology in the liver, ultimately leads to insulin resistance and liver steatosis.

While pathology is occurring in AT as discussed previously, HIV PIs also induce insulin insensitivity in hepatocytes. Interestingly, the ability of HIV PIs to induce the UPR may be the mechanism underlying the hepatic insulin insensitivity (*44*). In NASH mouse models, as well as human liver biopsies of NAFLD patients, a link between increased IRE1α and JNK has been found (*213, 214*). It is hypothesized that the instigator of ER stress (whether it be increased need of protein folding or TG synthesis, or drugs such as HIV PIs) increases IRE1α. IRE1α then activates JNK, inducing the inflammatory cascade. In addition, JNK inhibits insulin receptor action by phosphorylating insulin receptor substrate (IRS)-1.

Insulin also inhibits VLDL secretion through suppression of ApoB100 packaging of TGs (*215-217*). Loss of insulin sensitivity would potentially lead to increased VLDL secretion. However, during HIV PI pathology, this may not simply be the case. Instead, activation of ER stress itself can lead to degradation of ApoB100 (*218*), which may occur through the autophagy

pathway (*219*). In addition, HIV PIs stimulate active SREBP-1 (*49, 220, 221*), the transcription factor important in *de novo* lipogenesis. Therefore, increased stimulation to release VLDLs due to loss of insulin sensitivity may not be able to compensate for the increased buildup of TGs in hepatocytes.

Many investigators in this field have proposed that much of HIV PI-induced hepatocyte pathology is through ER stress and the UPR (*49, 222-224*). However, autophagy may also be an important player as it now understood to be centrally involved in lipid metabolism. When autophagy is directly inhibited in hepatocytes, lipids accumulate in droplets (*205*), and this is not due to increased triglyceride synthesis nor decreased VLDL secretions (*225*). Mice lacking autophagy in the liver have enlarged lipid laden livers with increased triglyceride and cholesterol levels (*205*).

At this time, the connection of UPR, autophagy, and hepatic lipid metabolism is not well elucidated. Rather, only speculative links of the three have been made. What is clear by the information reviewed here is that both the UPR and autophagy are central in cellular homeostasis and lipid regulation. Therefore, disruption of one, or both, can have detrimental effects in both the AT and liver.

CHAPTER II: Materials and Methods

Materials

Antibodies: Antibodies against C/EBP homologous protein (CHOP), activating transcription factor-4 (ATF-4), X-box-binding protein-1 (XBP-1), Lamin B, phosphorylated and total AKT, HuR, CUGBP-1, and horseradish peroxidase (HRP)-conjugated donkey anti-goat IgG were bought from Santa Cruz Biotechnology (Santa Cruz, CA). LC3B antibody was obtained from Cell Signaling (Danvers, MA). p62, as well as HRP-conjugate goat anti-rabbit and anti-mouse IgG, were purchased from Bio-Rad (Hercules, CA).

Protein Assay and Western Blot Analysis*:* Bio-Rad protein assay reagent, Criterion XT Precast Gel, and Precision Plus Protein Kaleidoscope Standards were obtained from Bio-Rad (Hercules, CA). Chemiluminescence Reagent was purchased from PerkinElmer Life Sciences. For ELISA, all antibodies and avidin-HRP were purchased through eBioscience (San Diego, CA), while the standard recombinant mouse TNF-α and IL-6 were obtained from BioLegend (San Diego, CA).

RNA Analysis*:* RNeasy MinElute Cleanup Kit was purchased from Qiagen. High-Capacity cDNA Reverse Transcription Kit came from Applied Biosytems.

Chemicals and Drugs*:* Ritonavir, lopinavir, and darunavir were obtained from the National Institutes of Health (NIH). MK-0518 (Raltegravir) was obtained from Merck. Thapsigargin (TG), Dimethyl Sulfoxide molecular biology grade (DMSO), 3-Isobutyl-1-methylxanthine (IBMX), rosiglatizone, phosphatase inhibitor mix, dexamethasone, and hydrocortisone were obtained from Sigma Aldrich (St. Louis, MO).

Stains: Oil Red O and Nile Red powder were obtained from Sigma Aldrich.

Cell Culture Techniques

Maintenance and Products: All cell lines and primary cells were maintained in 5% CO_2 at 37ºC. Dulbecco's Modified Eagle Medium (DMEM) and tryspin with 0.25% EDTA was purchased from Gibco (Invitrogen). Newborn Calf and Fetal Bovine Serum were from Atlanta Biologicals (Lawrenceville, GA). Penicillin-Streptomycin was bought through CellGro (Manassas, VA).

Murine NIH 3T3-L1: Cells were obtained from ATCC (Manassas, VA), and maintained in DMEM containing 10% Newborn Calf Serum (NCS) and 1% Penicillin-Streptomycin (P-S). When cells reached 80% confluency, they were subcultured by removing media, washed with Phosphate Buffer Saline (PBS), and trypsinized with 0.25% Trypsin-EDTA. To induce differentiation, cells were grown to confluency, at which time media was changed to DMEM containing 10% Fetal Calf Serum (FCS), 1% P-S, plus 0.5 µM IBMX, 0.8 µM insulin, and 1 µM dexamethasone. Cells were cultured for three days and media then changed to DMEM with 10% FCS/1% P-S, and 0.8 µM Insulin. After two days, media was subsequently changed to DMEM with 10% FCS/1% P-S and cultured until 80% of cells visually appeared differentiated (at least 8 total days) (*226*).

Human Simpson-Golbai-Behmel Syndrome (SGBS) pre-adipocytes were a kind gift from Dr. Martin Wabitsch, University of Ulm, Germany (*227*). SGBS cells were maintained in DMEM/F12 with 10% FCS/1% P-S, Biotin, and Pentothenate. Cells were induced to differentiate at confluency in serum free DMEM/F12 with 0.01 mg/mL Transferrin, $2x10^{-8}$ M insulin, $1x10^{-7}$ M cortisol, and 0.2 nM T3. For the first 3 days, this media was also supplemented with 25 nM dexamethasone, 500 µM IBMX, and 2 µM rosiglitazone, then these three

components were not used for the rest of differentiation. Cells were used in experiments after 80% of cells visually appeared differentiated (average 2 weeks).

Adipocyte stem cells (ASC) were a kind gift from Dr. Shawn E. Holt, Virginia Commonwealth University. ASC cells were maintained and induced to differentiate in the same manner as 3T3 cells, except the DMEM used was low glucose instead of normal high glucose.

293-FT cells were obtained from ATCC (Manassas, VA). Cells were maintained in DMEM containing 10% FCS, 1% P-S, and 1% Non-Essential Amino Acids (NEAA), and kept under selection with G418 Neomycin.

Human HepG2 cells were obtained from ATCC (Manassas, VA). Cells were maintained in 10% FBS/1% P-S with 1% NEAA. Cells were subcultured at 90% confluency using 0.25% trypsin-EDTA. Cells were treated at 70% density.

Isolation of Primary Adipocytes: After mice were euthanized, the gonadal fat pad was excised from mice and placed in 37°C KRH buffer (1 mM $CaCl_2$, 1.2 mM $MgS0_4$, 1.2 mM KH_2PO_4, 1.4 mM KCl, 2 mM Pyruvic Acid, 10 mM HEPES with 4 mM $NaHCO_3$, 130 mM NaCl and 0.8333% BSA in water) (*228*). Tissue was minced until all fragments were no bigger than 1 mm and placed in 1 mg/mL Type 1 collagenase (Worthington Biochemical) in KRH, and digested for 30 min in a rotating water incubator at 37°C. Suspension was filtered through a 20 µM flat filter, washed two times in fresh KRH to remove bound collagenase, and full adipocytes removed from the top layer with a Pasteur pipette. The remaining solution was centrifuged at 300 g for 5 min, supernatant removed, and pellet resuspended in Primary Medium (DMEM containing 10% FBS, 1% P-S, 3 µM Biotin, 100 µM ascorbic acid, 4 nM insulin and 8.3 mM L-glutamine). Full adipocytes were also plated in Primary Medium, as well.

After confluency of pre-adipocytes, cells were induced to differentiate by adding 1 µg/mL insulin, 1 µM dexamethasone, 0.5 mM IBMX, and 1 µM rosiglitazone to Primary Media for 3 days, then media was supplemented with insulin and rosiglitazone for 3 days. Cells were thereafter cultured with Primary Media for 6 more days for full differentiation to occur.

Isolation of Primary Hepatocytes: Primary hepatocytes were isolated from male Sprague-Dawley rats (250-300 g), as well as C57BL/6 WT and CHOP-/- mice using the collagenase-perfusion technique of Bissell and Guzelian (*229*). Trypan blue exclusion was used to determine cell viability (>90%) before plating monolayers on collagen-coated plates (60-mm or 6-wells). Cells were cultured in serum-free Williams' E medium containing dexamethasone (0.1 µM), penicillin (100 units/mL), and thyroxine (1 µM). Media was changed and cells treated 6 hours (for rat) and 4 hours (for mouse) after plating.

In Vitro Studies

Nuclear Protein Extraction: For UPR activation analysis in adipocytes, nuclear extract was isolated from cells (*230*). Cells were rinsed with PBS and scraped with 1mL cold PBS, pelleted at 100 g x 10 min, and resuspended in Buffer A (10 mM HEPES, 1 mM EDTA), 0.5 mM DTT, 0.25 mM PMSF, 50 mM NaF, 2 mM NA metavanadate, and 5 mg/mL leupeptin and pepstatin). Suspension was homogenized through a needle/syringe then centrifuged at 1000 g for 10 min and supernatant placed in a separate tube with 0.5 M NaCl and left on ice for 1 h before flash frozen. Pellet was washed in 250 mL Buffer A with 250 mM sucrose and pelleted at 1000g for 10 min, resuspended in 100 mL Buffer A with 0.5 M NaCl, and 10 µL of 10% NP-40, left on ice for 1 h and centrifuged at 5000 g for 5 min. The nuclear extract was flash frozen. Proteins were later resolved on a 10% Bis-Tris gel at 100 V, and transferred at 360 mA.

Western Blot Analysis - Autophagy: For LC3 and p62 analysis, total cell extract was obtained by washing cells with cold PBS followed by scraping with RIPA buffer (1% NP-40, 0.5% sodium deoxycholate, 0.1% SDS, 0.25 mM PMSF, 5 mg/mL Aprotinin, and 1 mM sodium orthovanadate). Cells were lysed using an automatic homogenizer at 4ºC for 1 min, and samples were left at 4°C for 30 min before spun at 8,000 g for 8 min. Supernatants were stored at -80°C. Proteins were later resolved on a 12-15% Bis-Tris gel at 100 V and transferred at 90 mA overnight at 4ºC.

For both ER stress and autophagy analysis, immunoblots were blocked for one hour at room temperature with 5% nonfat milk in Tris-buffered saline (TBS). Membranes were incubated with primary antibodies in 2.5% milk-TBS, (5% BSA-TBS with 0.5% Tween-20 for LC3B). Secondary antibodies were incubated in 2.5% milk-TBST. Immunoreactive bands were detected using horseradish peroxidase-conjugated secondary antibody and chemiluminescence. The density of immunoblot was analyzed using Image J or Quantity One (Biorad) computer software.

RNA Isolation and Real-Time Quantitative RT-PCR: Total cellular RNA was isolated from adipocytes after treatment using Qiagen RNeasy MinElute Kit, or hepatocytes using Promega RNA Elute Kit. Total RNA (2 μg) was used for first-strand cDNA synthesis using High-Capacity cDNA Reverse Transcription Kit. The primers for mRNA levels analyzed are shown in Tables 1 and 2. iQ SYBER Green Supermix (Bio-Rad) was used as a fluorescent dye to detect the presence of double-stranded DNA. The mRNA values for each gene were normalized to internal control β-actin mRNA. The ratio of normalized mean value for each treatment group to vehicle control group was calculated.

Target mRNA	Forward Primer	Reverse Primer
Actin	ACCACACCTTCTACAATCAG	ACGACCAGAGGCATACAG
Adiponectin	GATGCAGGTCTTCTTGGTC	CCCACACTGAACGCTGAG
ATF-4	CCTAGGTCTCTTAGATGACTATCTGGAGG	CCAGGTCATCCATTCGAAACAGAGCATCG
ATG12	AAGATGTCGGAAGATTCAGAG	TCCTACAGCCTTCAGCAG
BECN1	TCTAAGGAGTTGCCGTTATAC	CCAGTGTCTTCAATCTTGCC
C/EBPα	GACAAGAACAGCAACGAG	GTCAACTCCAGCACCTTC
C/EBPβ	CGACGAGTACAAGATGCG	CTGCTCCACCTTCTTCTG
CHOP	GTCCCTGCCTTTCACCTTGG	GGTTTTTGATTCTTCCTCTTCG
CUGBP1	CCTGGCTGGTCTGAACAC	CCCTGCTGAACTGGTGAG
CYP27A1	GACACTGCCGCCTTCATC	GCCATTCAGGTATCGCTTCC
CYP7A1	CAGAAGCATAGACCCAAGTG	GTAGCAGAAGGCATACATCC
FXRα	GGACGGGATGAGTGTGAAG	ATCTGTGGCTGAACTTGAGG
HMGCOAR	GCCGTCATTCCAGCCAAG	CGTTGTAGCCGCCTATGC
HuR	ACACTGAACGGCTTGAGAC	ACCCTGGAGTTGATGATTCG
IL-6	GAGGATACCACTCCCAACAGACC	AAGTGCATCATCGTTGTTCATACA
LPL	GTCTAACTGCCACTTCAACC	CACCCAACTCTCATACATTCC
LXRα	GCTCTGCTCATTGCCATCAG	TGTTGCAGCCTCTCTACTTGGA
Perilipin	ACGAGGAGGAGGAAGAAGAG	AGGTCACTGCGGAGATGG
PPARα	ATGGAGACCTTGTGTATGGC	GGCAGCAGTGGAAGAATCG
PPARγ	ACTCGCATTCCTTTGACATC	TCGCACTTTGGTATTCTTGG
SREBP-1c	CCACTAGAGGTCGGCATGGT	TCCCTTGAGGACCTTTGTCATT
TNF-α	GCCTCCCTCTCATCAGTTC	ACTTGGTGGTTTGCTACG
VSP34	CTCTCCTCTCATTACACCAACC	CATCAGCAAATCCTCATCATCG
ULK2	GAGCAGCAGCAGAGCAAG	GCCAGCATAACACCACAGG
XBP-1sp	TGAGTCCGCAGCAGGTG	GACAGGGTCCAACTTGT
XBP-1usp	CGCAGCACTCAGACTATG	TTCCTCCAGACTAGCAGAC

Table 1. Real-time RT-PCR primers specific for mouse mRNA. Real-time RT-PCR primer sequences used for mouse-specific mRNA analysis in this dissertation. Sequences are written 5' to 3'.

RAT

Target mRNA	Forward Primer	Reverse Primer
Actin	TATCGGCAATGAGCGGTTCC	AGCACTGTGTTGGCATAGAGG
ATF-4	GGTTCTCCAGCGACAAGG	GGTTTCCAGGTCATCCATTC
ATG12	CCCAGAAACAGCCATCCC	GTCTCCTACAGCCTTCAGC
BECN1	ACGCTGTTTGGAGATGTTG	TTCTGCCACCACCTTTCG
CHOP	GGAGCAGGAGAATGAGAG	GACAGACAGGAGGTGATG
CYP27A1	TGGAGCAAGTGATGAGAC	CAAACTATGACGCAGATGG
CYP7A1	GACACAGAAGCATTGACC	GTAACAGAAGGCATACATCC
HMGCOAR	GGACCAACCTTCTACCTCAG	ACAACTCACCAGCCATCAC
SREBP-1	CATCAACAACCAAGACAGTG	GAAGCAGGAGAAGAGAAGC
ULK1	CCAGCAACATCCGAGTCAAG	ACATAGGAGAGCCACAGAGC
VPS34	AACAAGCAGCACACTCTCAG	CCAACCAATCCACCTTCACC

HUMAN

Target mRNA	Forward Primer	Reverse Primer
Actin	GCGTGACATTAAGGAGAAG	GAAGGAAGGCTGGAAGAG
ATF-4	CAACAACAGCAAGGAGGATG	AATTGGGTTCACCGTCTGG
CHOP	CTGAATCTGCACCAAGCATGA	AAGGTGGGTAGTGTGGCCC
SREBP-1	GGTCGTAGATGCGGAGAAG	TGATGGAGGAGCGGTAGC
XBP-1sp	GCTGAAGAGGAGGCGGAAG	GAAAGGGAGGCTGGTAAGG
XBP-1usp	TCCGCAGCACTCAGACTAC	TCCAAGTTGTCCAGAATGCC

Table 2. Real-time PCR primers specific to Rat and Human mRNA, respectively. Real-time RT-PCR primer sequences used for rat and human-specific mRNA analysis in this dissertation. Sequences are written 5' to 3'.

Enzyme-Linked Immunosorbent Assay (ELISA): For analysis of cytokine secretions, ELISA method was utilized. Cells were treated with HIV PIs for the noted times, and culture media collected. Cells were lysed with total lysis buffer and total protein concentrations of viable cells determined using Bio-Rad Protein Assay. 96-well plates were coated with antibody against IL-6 or TNF-α for 2-3 h at 37ºC, and then blocked overnight. 100 µL of diluted samples were added the next day, followed by addition of Biotin-conjugated anti-antibody. After washing, Avidin-HRP was added prior to the substrate. Plates were read at 450 nM after termination of enzyme reaction by adding 100 µL 2 N H_2SO_4. Total amounts of cytokine were normalized to total protein of cells and expressed as ng/mg proteins.

Analysis of Apoptosis by Annexin V and Propidium Iodine Staining: 3T3-L1s were treated with HIV PIs for 24 h, and culture media and trypsinized cells were collected and spun at 2,000 rpm for 5 min. Cells were stained with Annexin V-FITC and propidium iodine using BD ApoAlert Annexin V kit, according to the protocol recommended by the manufacturer. Stained cells were analyzed by two-color flow cytometry. Annexin V-FITC and propidium iodide emissions were detected in the FL1 and FL3 channels respectively of a Cytomics FC 500 flow cytometer (Beckman Coulter, Fullerton, CA). Analysis was stopped at a 20,000 cell count.

SGBS cells were plated in 6-well dishes, and treated with HIV PIs for 24 h. Cells were stained with Annexin V-FITC and propidium iodine using the same kit and protocol as above. Images were immediately acquired using a FITC filter, followed by a TRITC filter on fluorescent miscroscope (Olympus, Center Valley, PA) using a 40 × objective lens.

Assay of Endoplasmic Reticulum Calcium Pools: Non-differentiated 3T3-L1 cells were grown on 22 x 40-mm coverslips and treated for 24 h. Cells were loaded with 4 µM Fura-2 AM and ER calcium stores were analyzed by stimulation with 1 µM thapsigargin (TG). Fluorescent

images (510-nm emission after alternate 340- and 380-nm excitation) before and after addition of TG were collected at 15-ms intervals through a cooled CCD camera. The 340:380 ratios of 20 individual cells in these images were analyzed using TILLvisION v3.1 imaging software. The standard curve generated using a Fura-2 calcium imaging calibration kit to convert Fura-2 fluorescence measurements into estimates of free Ca^{2+} concentration (*51*).

Nile Red staining: Cells were plated on 60-mm glass coverslips in 6-well dishes, and at confluency, were treated with relevant HIV PIs while concurrently being induced to differentiate. After the noted times, cells were fixed in 3.7% paraformaldehyde-PBS for thirty min, rinsed with PBS, and stained with working solution of Nile Red (100 ng/mL) for 10 min. Samples were washed three times with PBS, 15 min each, and coverslips mounted. Images were obtained with a 40× objective using a FITC filter on a fluorescent microscope (Olympus, Center Valley, PA).

Oil Red O staining (ORO): Cells were plated on 60-mm glass coverslips in 6-well dishes, and at confluency, were treated with relevant HIV PIs while concurrently being induced to differentiate. After the noted times, cells were fixed in 3.7% paraformaldehyde-PBS for 30 min, rinsed with PBS, and stained with working solution of Oil Red O (5 mM) for 2 h followed by three washes of PBS 15 min each. Coverslips were mounted and images obtained using a 40 × lens objective of a light microscope (Motic BA200).

MATLAB Assessment of lipid droplet: 3T3-L1 cells were plated on 60-mm glass coverslips in 6-well dishes, and at confluency, were treated with HIV PIs while concurrently being induced to differentiate. After 14 days, cells were fixed in 3.7% paraformaldehyde-PBS for 30 min, and rinsed in PBS. Cells were mounted and images obtained using a 40 × objective of an upright light microscope (Motic BA200). Images were processed using a previously published

custom-made MATLAB (MathWorks) code (*231*), and the lipid droplet number, areas, and %-area occupied were then determined.

PPARγ Promoter Activity: A PPARγ luciferase reporter and firefly luciferase assay system (Promega) were used in this experiment. 293 cells were transfected with either pGL3-Luc control vector or pGL3 containing a PPARγ responsive element (PPRE) tagged to *luciferase* using Fugene transfection reagent (Roche). Luciferase catalyzes coelenterazine to coelenteramide, releasing light, immediately after transcription. Therefore, after treatment with HIV PIs for 24 h, cells were lysed in luciferase lysis buffer (containing DTT) obtained from the manufacturer. 40 µg of protein was used to measure with 80 µL luciferase assay by a luminometer. The GFP fluorescence was detected first, followed by injection of substrate to detect luciferase activity. Activity was normalized to GFP from viable cells.

mRNA Stability: 3T3-L1 cells were treated with vehicle control (DMSO) or HIV PIs for 2 h before the addition of actinomycin D (5.0 or 10.0 µg/mL) (time 0). Total cellular RNA was extracted at 0.25, 0.5, 1, 2, 4, and 6 h after actinomycin D addition. PPARγ mRNA levels were determined by real-time RT-PCR as previously described. Results are expressed as the percentage of the mRNA at time 0.

In Vitro Pulldown: Biotinylated mRNA construction: Primers for both the PPARγ 3'UTR (1564-1769, 205 bp) and CDS (46-1563, 1517 bp) were designed to include a T7 promoter sequence as well as restriction enzyme sites. For 3'UTR, forward primer: 5'CCAAGCTTCTAATACGACTCACTATAGGGCTGGATGGAGGAAAGTCCCACC3' and reverse primer: 5'AATGTGGTAATTTTTAATATTA3'. CDS forward primer: 5'CCAAGCTTCTAATACGACTCACTATAGGGCTGGATGGGTGAAAACTCTGGG3' and reverse primer: 5'AATACAAGTCCTTGTAGATC3'. 1 µg template was then added to a PCR

mixture containing T7 RNA polymerase and biotin-cytidine 5'-triphophate (CTP). This product was purified with DNase, a G-50 column, and RNA precipitation.

Analysis of RNA binding proteins bound to biotinylated RNA were done as previously described (*232*). Briefly, 120 µg of total cell lysate protein from 3T3-L1 cells treated for 24 h with HIV PIs was added to paramagnetic streptavidin-conjugated Dynabeads M-280 (Dynal, Oslo, Norway). 0.6 µg biotinylated PPARγ 3'UTR or CDS were incubated for 30 min at RT, after which beads were washed to remove non-specific binding. The mixture was subsequently boiled and protein separated on a 10-12% Tris-HCl SDS PAGE gel. The membranes were blotted with antibodies against HuR, CUGBP-1 and Actin for loading control.

RNA Immunoprecipitation: To assess the association of endogenous HuR and CUGBP1 with endogenous PPARγ mRNA, immunopreicipitation (IP) of RNA binding protein complexes was performed. 3T3-L1 cells were treated with HIV PIs or DMSO control for 24 h, and then harvested in PBS with rubber policemen. Cells were pelleted, and resuspended in approximately two cell pellet volumes of polysome lysis buffer (PLB: 100 mM KCl, 5 mM $MgCl_2$, 10 mM HEPES, 0.5% Nondiet P-40 with 1 mM DTT, 100 U/ml RNaseOUT, 0.2% vanadylribonucleoside complex, 0.2 M PMSF, 1g/ml pepstatin A, 5 g/mL bestatin, and 20 g/mL leupeptin). Protein G-Sepharose beads were swollen 1:1 (v/v) in NT2 buffer (see above) supplemented with 5% BSA. 5 mg cellular 3T3-L1 proteins were added to 100 µL aliquot of preswollen protein A bead slurry and incubated for 4 h at RT in the presence of excess (30 µg) antibody (IgG1, anti-HuR, or anti-CUGBP-1). Proteins were digested via Proteinase K (0.5 mg/mL) at 55ºC for 20 min, and bead-free supernatants were extracted with phenol:chloroform:isoamylalcohol. RNA was precipitated with $1/10^{th}$ volume 3 M NaAc (pH 5.2), 150 µg/mL glycogen, and 2.5 volumes of 100% ethanol. The precipitates were dissolved in

15 µL nuclease-free water. RNA in IP materials was reverse transcribed and used to detect presence of PPARγ mRNA by real-time RT PCR.

Effect of CUGBP1 and HuR overexpression on 3'UTR PPARγ: The 3'UTR of PPARγ was cloned into pEGFP-C3 expression vector. 293 cells were stably transfected with pEGFP-C3-mPPARγ-3'UTR. CUGBP1 was cloned into pcDNA3.1 vector and HuR into pcDNA3-TAP. 293 stable cells of GFP-PPARγ-3'UTR were transfected with either pcDNA3-CUGBP1 or pcDNA3-HuR-TAP using FuGENE HD (Roche) for 48 h according to the manufacture's protocol. GFP protein expression was than determined by Western blot analysis.

Monodansylcadaverine (MDC) Stain: Cells were plated in 6-well dishes with coverslips, and treated with HIV PIs or vehicle control for 24 or 48 h. Cells were then stained with 25 µM MDC (Sigma) in PBS for 10 min at 37°C, followed by fixation in 3.7% paraformaldehyde-PBS for 15 min. Cells were washed and mounted in the dark with antifade mounting media. Images were obtained with both 40 and 60 × objective lenses with a DAPI filter on a fluorescent microscope (Olympus, Center Valley, PA).

Transmission Electron Microscopy (TEM): 3T3-L1, HepG2, and RPH cells were plated on Permanox Quantity dishes (Nalgene Nunc International, Rochester NY), and treated with HIV PIs for 24 or 48 h. Cells were rinsed with PBS and fixed with 2% glutaraldehyde for 1 h, rinsed in 0.1 M cacodylate buffer, and fixed for another hour with 1% osmium tetroxide in 0.1M cacodylate buffer. Samples were further washed, dehydrated with gradient ethanol and infiltrated with a 50/50 mixture of 100% ethanol/PolyBed 812 resin for overnight, and further infiltrated with pure PolyBed. Samples were embedded using fresh PolyBed 812 and polymerized in a 60ºC oven for 2 days. Samples were sectioned with a Leica EM UC6i Ultramicrotome (Leica Microsystems) and stained with 5% uranyl acetate and Reynold's Lead Citrate, followed by

scoping using a JEOL JEM-1230 TEM (JEOL USA) with a Gatan Ultrascan 4000 digital camera (Gatan Inc, Pleasanton CA).

Construction of GFP-tagged LC3B Stable Cell Line: A pEGFP-C3 vector containing LC3B was a kind gift from Dr. Sarah Spiegel (Virginia Commonwealth University). 2 x 10^6 Cells were transfected with 2 µg of plasmid with 5 µL FuGENE HD for 24 h according to the manufacture's protocol. Stable clones were selected with 60 µg of G418.

Retroviral – GFP-LC3: GFP-LC3BI under SV promoter in the retroviral vector pBABE was purchased from AddGene. Plasmid was replicated in E. coli α-competent cells and purified with a ZR plasmid mini prep (Zymo research), and DNA eluted with 0.1 TE (pH 8.0). Retroviral particles were constructed in 293-FT cells by cotransfection with 1 µg pBab3-puro-GFP-LC3BI (or control vector), 0.1 µg pCMV-VSV-G, and 0.9 µg pMDLg/pREE using $CaCl_2$ and HEPES mixture. Infectious particles were harvested from culture supernatants 72 h after transfection and media was passaged through a 0.45 µM filter. Particles were purified by adding PEG 6000 (8.5%) with 0.4 M NaCl O/N at 4ºC, rotating. Samples were centrifuged at 4800 rpm for 30 min, and viral particles resuspended in sterile PBS at 1:100 of original volume of media.

3T3-L1 cells were infected with GFP-LC3 retrovirus at a 1:50 PFU in the presence of 8 µg/µL of polybrene for 48 h. Stably infected cells were selected with puromycin (5 ng/mL).

Lentiviral - ATF-4 shRNA: Small hairpin RNA (shRNA) specifically targeting mouse ATF-4 in a lentiviral vector, TRC1-pLKO.1-puro vector, was purchased from Sigma. Sequence of ATF-4 shRNA used was target to the coding region: 5'CGGACAAAGATACCTTCGAGTCT3'. Plasmid was replicated in E. coli α-competent cells and purified with a large-scale purification of DNA by cesium chloride gradient. Briefly, 1 liter of transformed bacterial cells were pelleted and resuspended inTris-EDTA with 25% (w/v)

sucrose. Cells were lysed in the presence of lysozyme, EDTA, and RNase, followed by Triton-X. Supernatant was collected after spinning at 25,000 rpm for 2 h, and cesium chloride added. After addition of ethidium bromide, samples were spun at 4,000 rpm for 15 min to remove protein, and then spun for 18-20 h at 45,000 rpm. The lowest band identified as DNA was collected, and ethidium bromide removed with water saturated butanol. Sample was dialysized O/N in deionized water containing 0.01 M Tris-HCl, 0.001 M EDTA, and 0.03 M NaAc. Plasmid was purified with phenol/chloroform extraction followed by ethanol precipitation. Plasmid was resuspended in Tris-Hcl/EDTA (TE pH 8.0).

Lentiviral particles were constructed in 293-FT cells. Cells were transfected with 3 µg pCMV-VSV-G, 2 µg pCMV-RSV-Rev, 5 µg pMDLg/pREE, and 10 µg pLKO1-ATF4shRNA or plasmid or control scramble using $CaCl_2$ and HEPES mixture. Infectious lentivirus was harvested from culture supernatants 24, 48, and 72 h after transfection. Particles were purified as described above. 3T3-L1 cells were infected with lentivirus in the presence of 8 µg/µL of polybrene at a 1:50 PFU for 48 h. Successfully infected cells were selected with puromycin (5 ng/mL). Silencing was confirmed by Western blot analysis and real-time RT-PCR.

Lentiviral - CHOP shRNA: CHOP small hairpin (sh)RNA was designed through siRNA Target Finder (Ambion). The sequences of 3 CHOP shRNAs were as follows: shRNA1 is 5'-CTGGAAGCCTGGTATGAGGA-3', shRNA2 is 5'-GGAAACGGAAACAGAGTGGTC-3', and shRNA3 is 5'-GCAGGAAATCGAGCGCCTGAC-3', with shRNA1 used in the majority of experiments shown here and elsewhere (*53*). shRNA was placed in pLentiLox, and plasmids purified the same as above. The recombinant lentiviral particles were produced following the same protocol as above for ATF-4 shRNA. 3T3-L1 cells were infected in the presence of 8 µg/µL of polybrene lentivirus at a 1:50 PFU for 48 h. Successfully infected cells were selected

with neomycin (30 µg/mL). Silencing was confirmed by Western blot analysis and real-time RT-PCR.

Lentiviral - CHOP overexpression: For overexpression of CHOP, the mouse cDNA of CHOP was subcloned into pLVX-AcGFP-N1 (Clonetech) from BamHI and EcoRI sites and N-terminus of CHOP was fused with GFP. Lentiviral particles were packaged and tittered as previously described (*232*). 3T3-L1 cells were incubated with lentivirus at a multiplicity of infection of 50 for 48 hours in the presence of polybrene (8 µg/mL). Cells were selected with puromycin (5 ng/mL). Efficiency was confirmed by real-time RT-PCR and Western blot analysis.

In Vivo Studies

Mouse Care and Treatments: C57BL/6 male mice were purchased from Jackson Laboratories. CHOP knockout mice, with a C57BL/6 background were previously acquired by our laboratory. All mice were housed under identical conditions and given free access to water and food. The VCU Animal Care Facility complies with all Federal and State laws regarding the use and care of experimental animals, and with Public Health Service Policy on Humane Care and Use of Laboratory Animals (NIH Guide for Grants and Contracts, Vol. 14, No. 8, June 255, 1985). The American Association currently accredits the facilities and care program for Accreditation of Laboratory Animal Care (AAALAC - #00036). It is also USDA inspected (#52-R-0007) and Animal Welfare Assurance #A3281-001.

Animals were kept under full-time veterinary supervision. Mice were weaned at 4 weeks of age and fed *ad libitum* a standard mouse chow diet. At 8 weeks of age, mice were divided into control and HIV PI treated groups, and gavaged for 8 weeks. All mice were fed on a high fat diet (HFD) during treatments to both mimic a typical patient on HIV PI treatment, and obtain more

adipose at time of sacrifice. Mice were observed daily for signs of distress, injury, and illness, and if had such signs, were immediately euthanized. At the end of the time point, mice were euthanized by anesthesia before harvesting any tissue, which is consistent with the recommendations by the Panel on Euthanasia of the American Veterinary Medical Association.

Western Blot Analysis: For analysis of protein expression, adipose or liver tissue was lysed (100 mg) in total lysis buffer (TLB; 1 mL) (20 mM Tris-HCl, 1% NondietP-40, 150 mM NaCl, 2 mM EDTA, 0.10% SDS, 20 mM NaF, 1 mM $NaVO_4$, and 2x protease and phosphatase inhibitor (Sigma)) via homogenization immediately after obtaining from -80ºC storage. Samples were centrifuged at 6,000 rpm for 6 min and the lipid layer removed. Cells were spun again, and supernatants aliquoted in 100 µL in -80ºC. For protein concentration measurement, samples were diluted 1:10 in TLB and measured using BioRad Protein Assay. 100 µg of protein was boiled and separated on 10% SDS-PAGE gel for UPR activation analysis, or 12% SDS-PAGE gel for autophagy activation analysis. Immunoblots were treated the same as for *in vitro* analysis.

RNA Isolation and Real-Time Quantitative PCR: For analysis of mRNA levels, adipose or liver tissue was lysed (100 mg) in Qiazol Tryzol Reagent (1 mL) (Qiagen) via homogenization immediately after obtaining from -80ºC storage. 200 µL of chloroform was added to each sample, vigorously shaken, and centrifuged 15 min at 12,000 rpm. Supernatant was placed in new tubes, and 2.5x 100% ethanol, 0.3 M NaAc, and 150 µg/mL glycogen added. Samples were placed O/N at -20ºC. The next day, samples were spun for 15 min at 12,000 rpm and pellets washed with 70% ethanol. Pellets were dried and resuspended in 15 µL nuclease-free water. Samples were reverse transcribed and analyzed by real-time RT-PCR (as in *in vitro*).

Immunohistochemistry of Adipose Tissue: Adipose tissue was fixed in 10% neutral buffered formalin immediately after isolation from animals. Samples were washed in PBS and

transferred to 70% ethanol. Formalin-fixed tissues were then embedded in paraffin, and sectioned at 5 µM. Paraffin on slides was heated in an oven at 45ºC for one h, and deparaffinized by running a xylene-drenched q-tip over slices. Slides were immersed in 0.3% v/v H_2O_2/methanol for 10 min and washed in deionized water. Samples were blocked by first washing in 50 mM PBS-0.02% Tween 20 and processed with a Vectastain Elite ABC Kit (Vector Laboratories). Briefly, tissue was covered in blocking solution (10% serum) for 20 min, blotted, and incubated for 1 h with primary antibody (anti Mac-2, Cederlane Laboratories). Samples were washed, and then incubated for 30 min with diluted biotinylated secondary antibody (anti-Rat). After washing, samples were incubated for 30 min with ABC reagent, washed for 5 min, and DAB (3, 3'-diaminobenzidine) substrate added for 2 min. Samples were counterstained in hematoxylin for 20 s, dehydrated through increasing concentrations of ethanol to xylene and coversliped with Permount. Images were obtained using a Motic BA200 microscope (Motic Instruments, Inc, Baltimore, MD).

Statistical analysis

Student's *t* test was employed to analyze the differences between sets of data. Statistics were performed using Prism 5 (GraphPad, San Diego, CA). All numerical results are represented as mean ± standard error (SE) from at least three separate experimental data sets.

CHAPTER III: HIV Protease Inhibitors Dysregulate Adipogenesis through Endoplasmic Reticulum Stress Activation and Alteration of PPARγ mRNA Stability

STUDY RATIONALE

Our laboratory has a long standing interest in the metabolic side effects of HIV protease inhibitors (PIs). Although the inclusion of HIV PIs in patient treatment has had a profund impact in the clinical history of HIV, PIs are linked to deleterious effects including early induction of insulin resistance, dysregulation of lipid metabolism, and inflammation, all of which are cornerstones of cardiovascular disease (*15, 22, 31*).

During the last decade, an extensive effort has been put forth to study the mechanism underlying HIV PI-induced side effects. Both *in vitro* and *in vivo* animal studies from our laboratory and others have linked HIV PIs with the activation of endoplasmic reticulum (ER) stress, oxidative stress, induction of apoptosis, and inflammatory cytokine production in several metabolically important cell types (*51-53, 233-235*). One tissue of particular interest is adipose tissue (AT) as pathology in AT can be central in the inflammatory state, insulin resistance, dyslipidemia and altered body morphology (*134, 236-238*). However, HIV PI-induced pathology in AT is not well understood. Investigators have focused on the ability of HIV PIs to differentially alter adipocyte maturation, but results have been contradictory, confusing, and lack elucidation of underlying mechanisms (*21, 192, 193, 239-245*).

Activation of ER stress induces the unfolded protein response (UPR), extensively shown to alter cellular lipid metabolism when upregulated (*58, 80, 246-248*). ER stress can also lead to the cellular inflammatory response (*83, 95*) and even apoptosis (*88, 89*). Therefore, strong activation of this pathway can result in multiple cellular aberrations, leading to detrimental effects in metabolically active tissue such as AT.

In this study, we attempt to elucidate the underlying mechanism of HIV PI-induced lipid metabolism dysregulation in adipocytes. Here, we demonstrate multiple deleterious effects of HIV PIs in adipocytes such as alteration of differentiation, induction of inflammation, and cell death, all of which may be linked to HIV PI-induced ER stress. We also show how HIV PIs alter gene regulation during adipogenesis, further explaining the phenomenon of HIV PI-induced adipocyte lipid metabolism dysfunction.

RESULTS

HIV PIs activate the UPR in murine and human adipocytes, in a time and dose-dependent manner

HIV PIs ritonavir (RITV) and lopinavir (LOPV) have been reported in separate studies to induce ER stress and to disrupt lipogenesis in adipocytes (*54, 241*). Our previous studies have shown that activation of ER stress plays a critical role in HIV PI-induced dysregulation of lipid metabolism in macrophages and hepatocytes (*49, 51*). In order to determine whether HIV PIs have similar effects on the UPR activation in adipocytes as they do in other cell types, mouse 3T3-L1 pre- and mature adipocytes were treated with seven available HIV PIs for various time periods (1-24 h) and the protein levels of the UPR-specific genes, CHOP, ATF-4, and XBP-1, were detected by Western blot analysis. We found only some HIV PIs induced UPR activation in mature adipocytes, and had less effect on pre-adipocytes. LOPV, RITV, saquinavir (SQV), and indinavir (IDV) induced significant activation of the UPR, while amprenavir (AMPV), darunavir (DRV) and tipranavir (TPV) only had modest or no activation. We therefore split these HIV PIs into two groups: ER stress inducers and non-inducers. Interestingly, those in the non-inducer group have much lower incidences of inducing dyslipidemia in patients compared to those in the inducer group (*249, 250*).

Based on the most updated January 2011 guidelines of US Department of Health and Human Services for Use of Antiretrovial Agents in HIV-1-infected Adults and Adolescents, HIV PIs are still listed as key components of preferred HAART regimens and will continue to be important drugs for the foreseeable future. With the ability to maintain viral load suppression superior to some other HIV PIs, LOPV coformulated with RITV (4/1) has remained a frequently used treatment in the clinic. As LOPV/RITV is also in the ER stress inducer group and is known

to induce metabolic side effects in the clinic, we focused on this combination during the subsequent studies.

Shown in Figure 8, we found UPR activation by these HIV PIs peak between 4 and 7 h. To determine if this activation was specific (i.e. dose-dependent), we treated 3T3-L1s with increasing doses of HIV PIs at 6 h, and found LOPV and LOPV/RITV dose-dependently increased CHOP and ATF-4 expression in differentiated adipocytes (Figure 10A,B), but had no significant effect on XBP-1 protein expression (data not shown). In human SGBS adipocytes, both RITV and LOPV increased CHOP and ATF-4 expression in a similar manner (Figure 10C). 3T3-L1 pre-adipocytes had comparatively less activation of the UPR than mature adipocytes (Figure 9). In addition, RITV was the more significant activator of the UPR in pre-adipocytes, compared to LOPV's higher activity in mature adipocytes. These differences may be attributable to the variation of cell type physiology.

To ascertain if HIV PI-induced increase of UPR transcriptional factors also occurs at the transcriptional level, we treated both pre- and differentiated 3T3-L1s 1-24 h and obtained total RNA. mRNA levels of UPR essential genes were determined by real-time RT-PCR. We found a peak increase of mRNA levels at 4 h. As shown in Figure 11, 3T3-L1 and SGBS cells treated with HIV PIs for 4 h demonstrated a dose-dependent increase of CHOP and ATF-4. Interestingly, LOPV tended to be a more significant activator of the UPR in this assay as well.

To determine if this phenomenon was specific to cell culture, we treated C57BL/6 4 week-old male mice fed a high fat diet with LOPV/RITV 4:1 (38mg/kg) or control solution for 2 months. Mice were sacrificed, and the gonadal fat pad analyzed for UPR protein and mRNA levels. In Figure 12, we demonstrate HIV PI LOPV/RITV increased both protein and mRNA levels of UPR ATF-4, CHOP, and spliced XBP-1 *in vivo*.

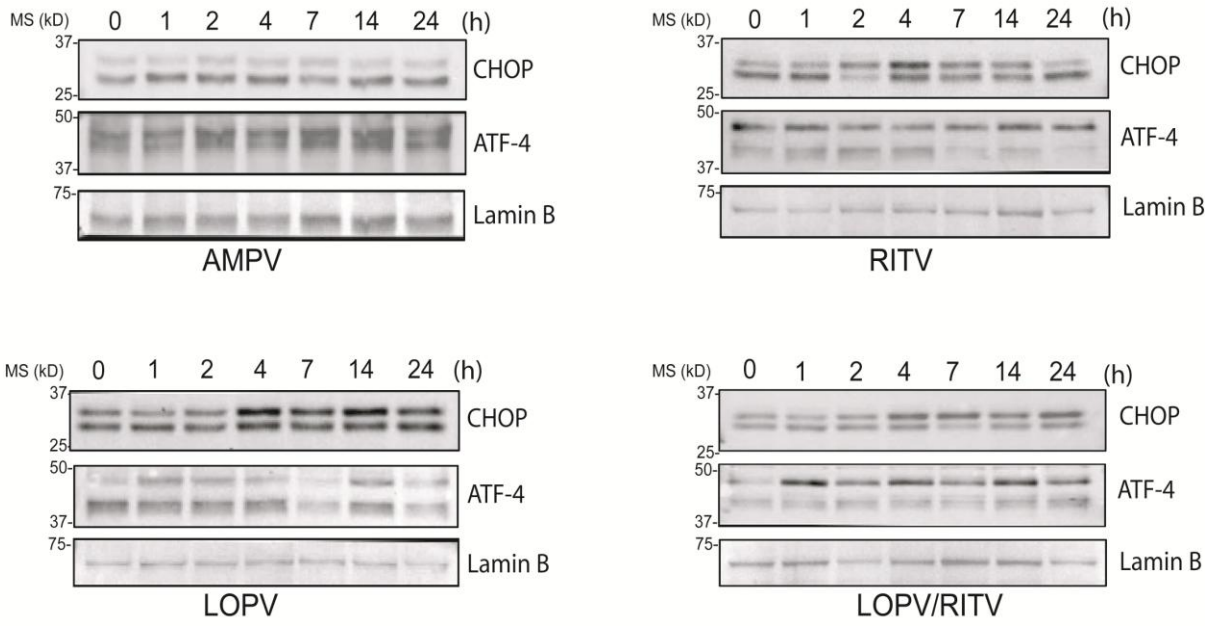

Figure 8. HIV PIs time-dependently activate the UPR in differentiated 3T3-L1s. Differentiated 3T3-L1s were treated with AMPV, RITV, LOPV, or LOPV/RITV (12.5 μM) for 1-24 h. Representative immunoblots from four separate experiments against CHOP, ATF-4, and Lamin B of nuclear extracts.

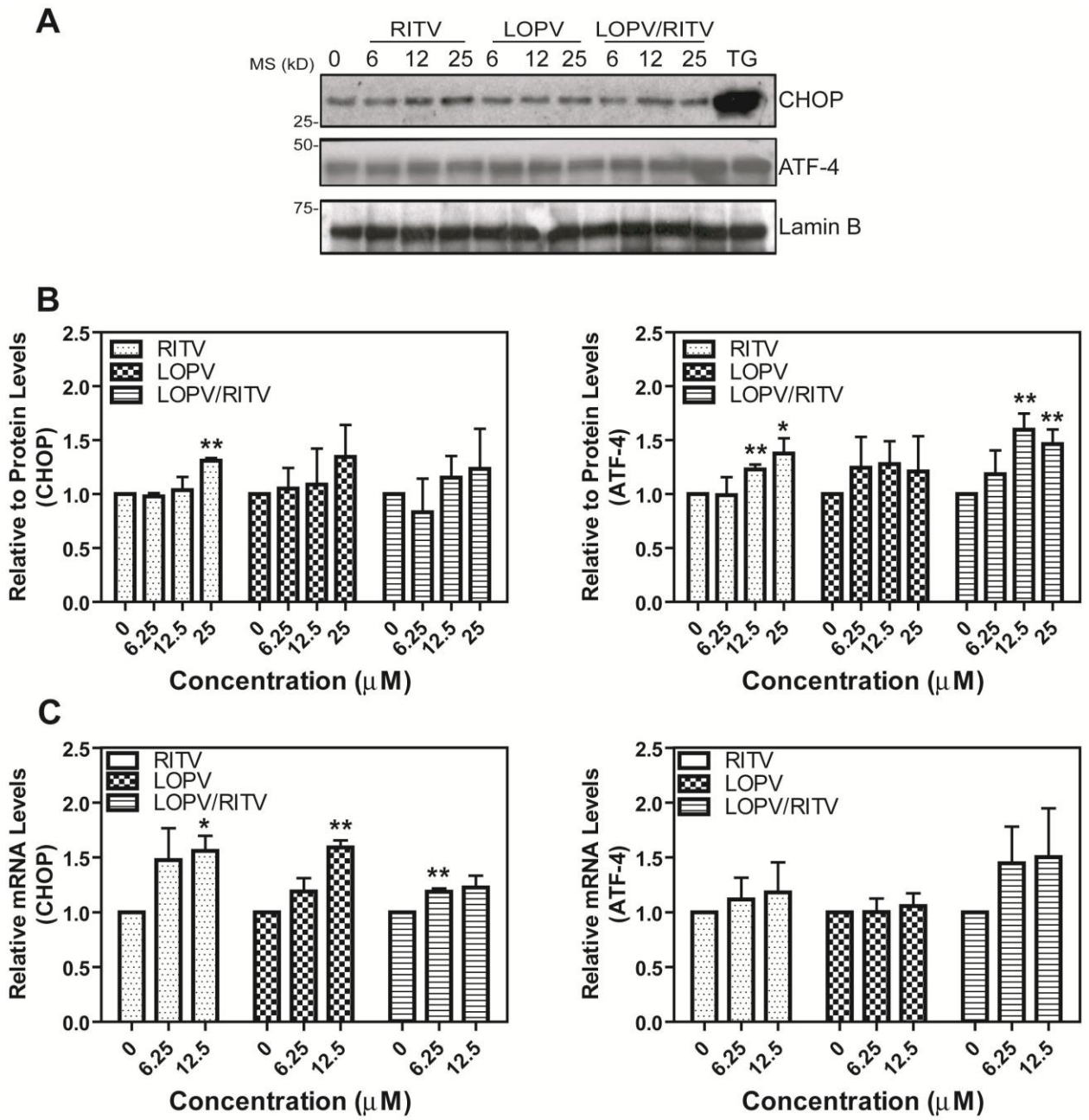

Figure 9. HIV PIs dose-dependently activate the UPR in non-differentiated 3T3-L1s. Non-differentiated 3T3-L1s were treated with increasing concentrations of RITV, LOPV, or LOPV/RITV. **A)** Representative immunoblots against CHOP, ATF-4, and Lamin B from nuclear extracts of cells treated 6 h. **B)** Density of immunoblots were determined by Image J. Relative protein levels were normalized using Lamin B as loading control. **C)** Relative mRNA levels of CHOP and ATF-4 of cells treated for 4 h and analyzed by real-time RT-PCR. β-Actin was used as an internal control. **B,C)** Values are means ± SE of four independent experiments. *$p<0.05$, **$p<0.005$

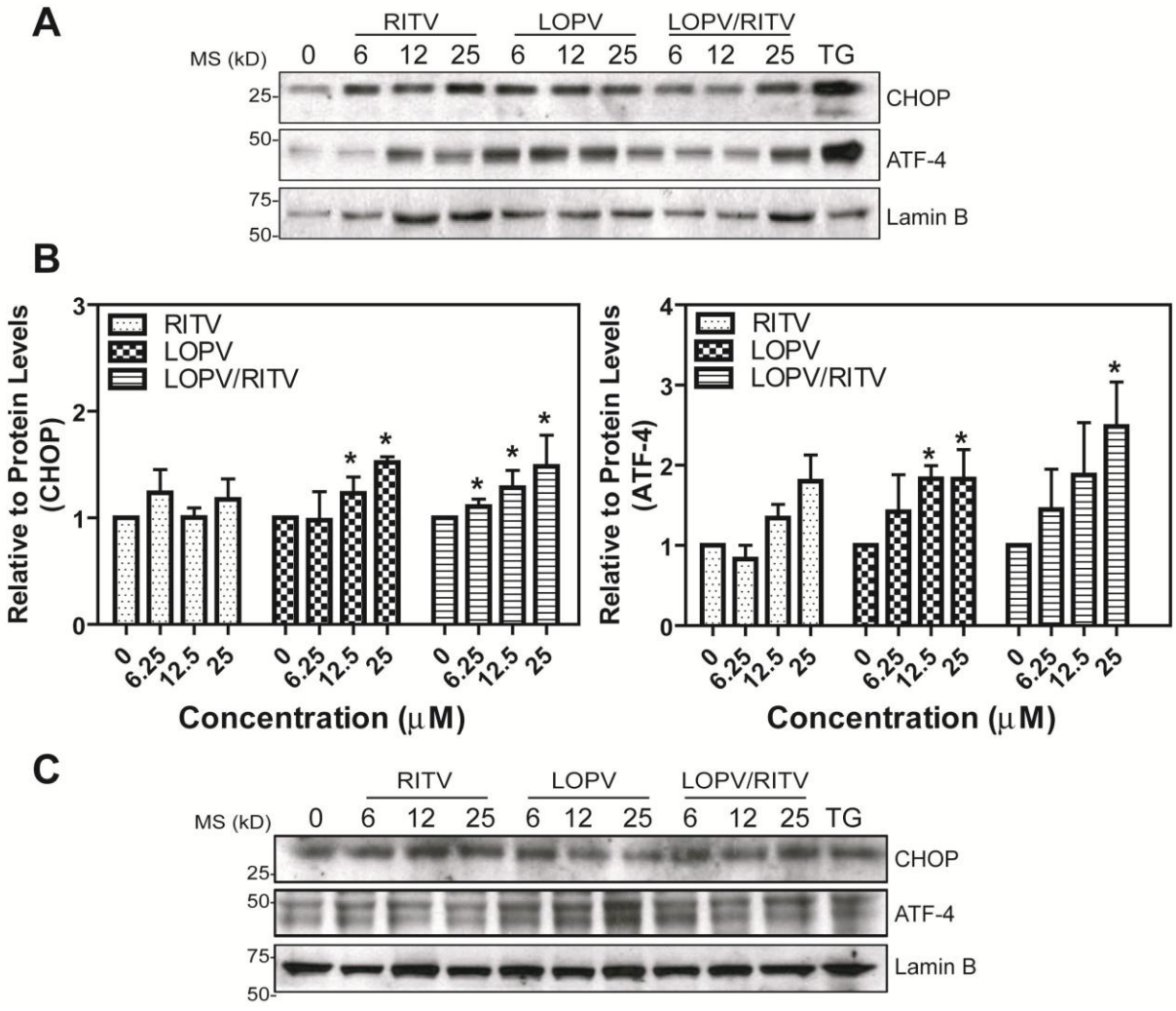

Figure 10. HIV PIs activate the UPR in differentiated murine and human adipocytes. Differentiated 3T3-L1s **(A, B)** and SGBS **(C)** were treated for 6 h with increasing concentrations of RITV, LOPV, and LOPV/RITV. Representative immunoblots against CHOP, ATF-4, and Lamin B from nuclear extracts are shown. **B)** Density of immunoreactive bands were determined by Image J with Lamin B as loading control. Values are mean ± SE of three independent experiments; *p<0.05.

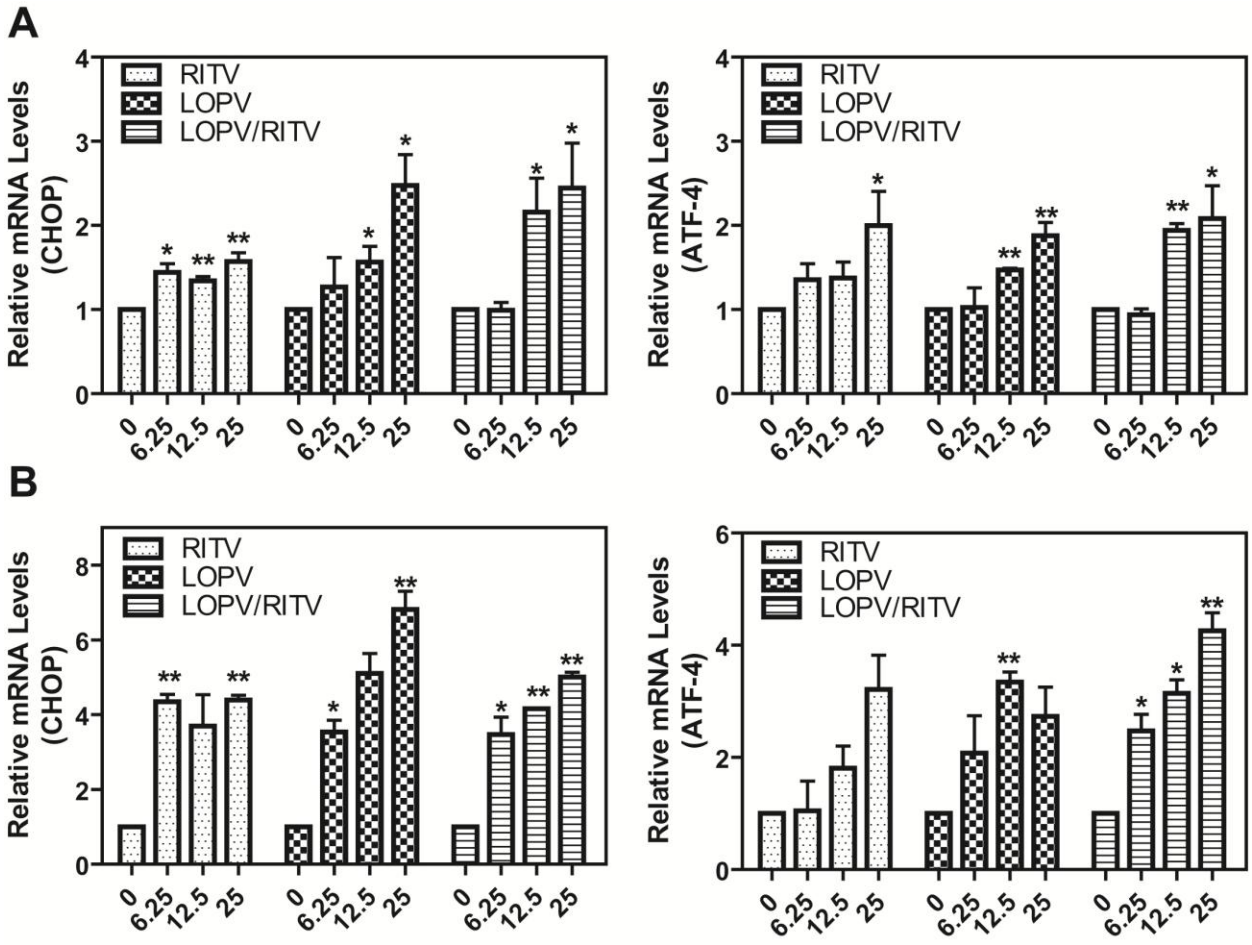

Figure 11. HIV PIs induce transcriptional increase of UPR genes in adipocytes. transcriptional level of UPR genes in adipocytes. Differentiated 3T3-L1s **(A)** and SGBS **(B)** were treated with increasing doses of RITV, LOPV, or LOPV/RITV for 4 h. mRNA levels were analyzed by real-time RT-PCR with β-Actin internal control. Values are mean ± SE of three independent experiments; *p<0.05, **p<0.005.

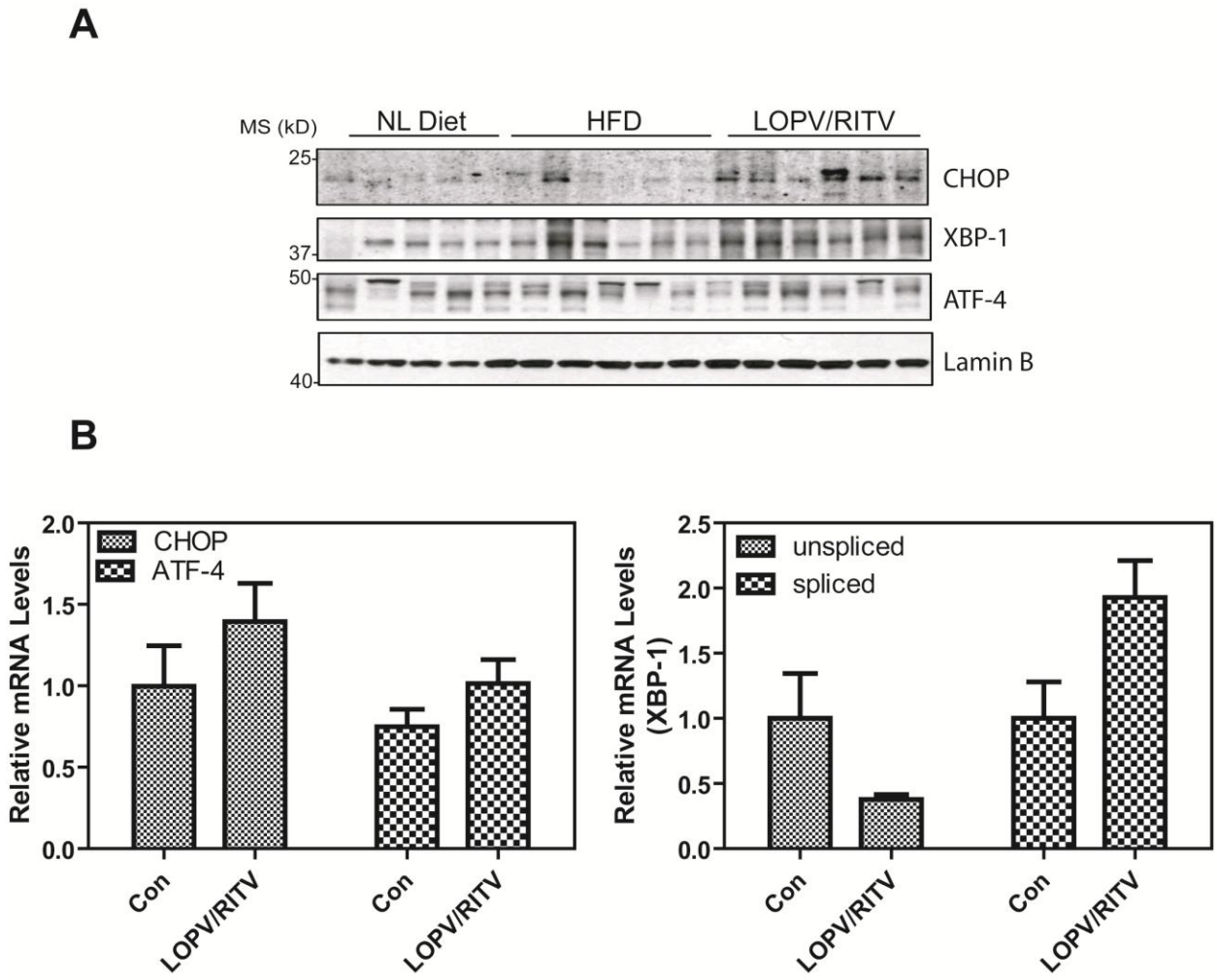

Figure 12. LOPV/RITV induces ER stress *in vivo*. C57BL/6 male mice were gavaged with 4:1 LOPV/RITV or control solution for eight weeks. At time of sacrifice, gonadal fat pads were obtained and analyzed for protein **(A)** and mRNA levels **(B)**. Values are mean ± SE from two independent experiments; n=5 normal chow (NL Diet), n=6 high fat diet (HFD) and LOPV/RITV.

Effect of HIV PIs on ER calcium stores in adipocytes

ER stress can be activated by a number of insults, one of which is depletion of ER calcium stores leading to altered cellular calcium homeostasis. Thapsigargin (TG), a sarcoplasmic/ER calcium ATPase inhibitor, depletes the ER calcium stores and activates the UPR in many different cells (*251, 252*). We have previously shown RITV depletes ER calcium in macrophages leading to UPR activation (*51*). We further examined the effect of LOPV and RITV (12.5 μM) on ER calcium stores in adipocytes by treating 3T3-L1s for 24 h. The ER calcium content was determined using the fluorescent calcium indicator fura-2/AM as described previously (*51*). As shown in Figure 13, both RITV- and LOPV-treated cells markedly reduced the response to TG compared to DMSO control, indicating that ER calcium stores were depleted.

HIV PIs induce cell death in adipocytes

We have previously shown that HIV PI-induced ER stress is correlated to the induction of cell apoptosis in both macrophages and hepatocytes at clinically relevant concentrations (*49, 52*). We further examined whether HIV PIs would have a similar affect in adipocytes, which could potentially account for dysregulation of lipid metabolism in patients. Non-differentiated and differentiated 3T3-L1s were treated with different concentrations of HIV PIs, vehicle control DMSO, or positive control thapsigargin (TG) for 24 h. Cells were collected, stained with annexin V-FITC and propidium iodide, and analyzed by flow cytometry. As shown in Figure 14, both LOPV and RITV increased cell death dose-dependently in differentiated 3T3-L1s. As similar to our other assays, non-differentiated 3T3-L1s did not have as significant an increase of HIV PI-induced cell death, but the trend remained the same (data not shown). In addition, differentiated SGBS cells demonstrated a much similar phenomenon as murine adipocytes (Figure 15).

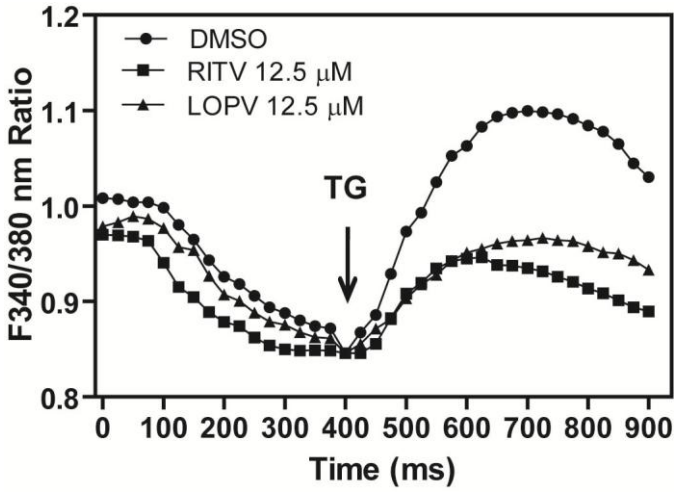

Figure 13. HIV PIs deplete ER calcium stores in 3T3-L1s. Non-differentiated 3T3-L1s were treated with RITV or LOPV (12.5 μM) or DMSO control for 24 h. ER calcium stores were assessed by Fura-2 AM fluorescence ratio of 340:380 nm in individual cells before and after addition of thapsigargin 100 nM. Representative tracing for a summation of at least 15 cells is shown, out of two independent experiments.

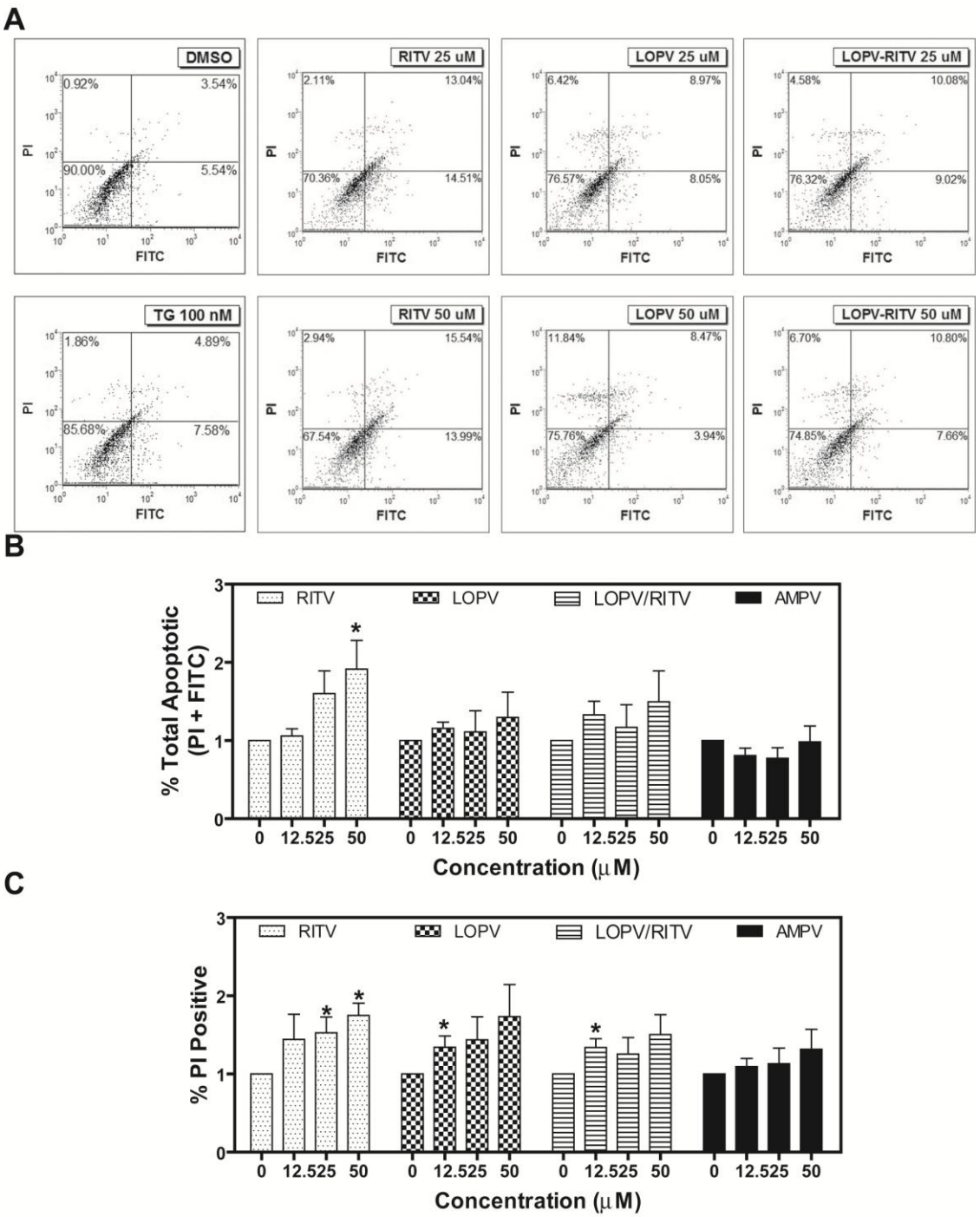

Figure 14. HIV PIs induce cell death in differentiated 3T3-L1s. Differentiated 3T3-L1s were treated with increasing concentration of HIV PIs, vehicle control (DMSO) for 24 h, then stained with Annexin V-FITC and propidium iodide. The percentages of apoptotic and necrotic cells were analyzed by flow cytometry. **A)** Represenative plots. **B, C)** Relative amount of apoptotic and necrotic cells. Values are mean ± SE for four independent experiments. Statistical signficiance relative to vehicle control (0): *p<0.05.

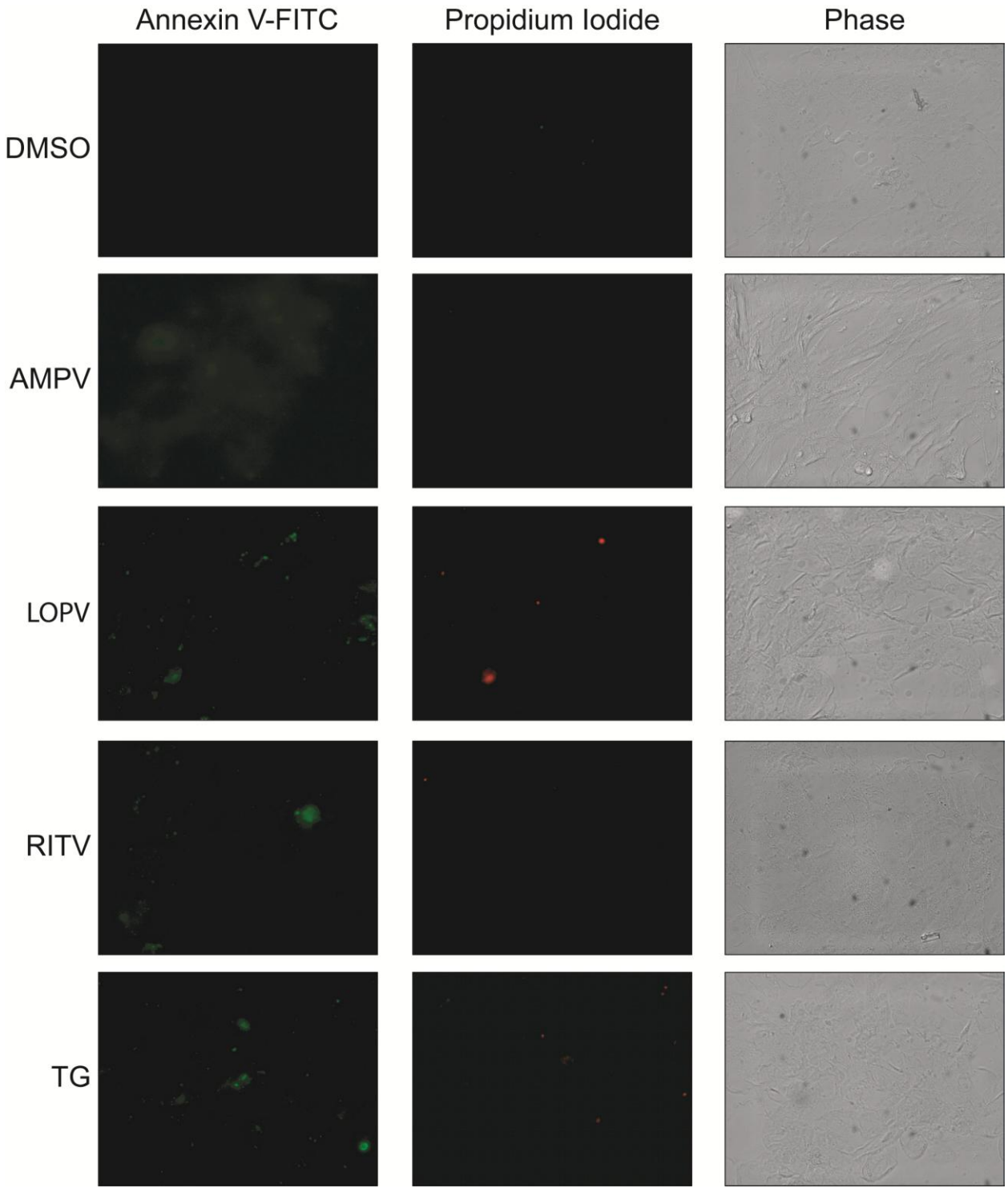

Figure 15. HIV PIs induce cell death in SGBS cells. Non-differentiated SGBS cells were treated with 25 µM HIV PIs, DMSO control, or positive control thapsigargin (TG) for 24 h. Cells were stained with Annexin V-FITC and propidium idodide, and images obtained using a fluorescent microscope with a 40 × objective.

HIV PIs activate the inflammatory cascade in adipocytes

Inflammation is a major cornerstone of metabolic diseases, as well as atherosclerosis. It is well demonstrated that inflammation in AT is an underlying issue in diabetes mellitus (*196, 199*). We have previously demonstrated that HIV PIs activate the inflammatory cascade, as well as stabilize mRNA transcripts of IL-6 and TNF-α in macrophages (*232*). To determine if this was also true in adipocytes, we treated murine 3T3-L1s with HIV PIs for 12, 24, and 48 h, and analyzed culture media by ELISA. At 48 h, there was an increase of IL-6 secretion from these cells. This was found to be a dose-dependent occurrence in mature adipocytes, while pre-adipocytes did not demonstrate this phenomenon (Figure 16).

In addition to pro-inflammatory cytokine secretion, crown structure formation is another hallmark of inflamed AT. Resident macrophages are activated by over expanded and stressed adipocytes (*253-255*), and call in circulating macrophages. Activated macrophages than attempt to engulf dying or stressed cells, and can be visualized in tissue stained with anti-macrophage antibodies. We wanted to determine if HIV PIs can induce this inflammatory response in our animal model. Therefore, gonadal AT of C57BL/6 mice treated with LOPV/RITV for 8 weeks was fixed, dehydrated and placed in paraffin. 0.5 μM slices were stained for presence of macrophages, and counterstained for nuclei visualization. As seen in Figure 17, there was only a slight difference found between control and mice treated with HIV PIs. This is most likely due to the already stressed tissue from mice being fed a high fat diet for a long period, as this diet has already been shown to induce crown structure in AT (*256*). However, it was promising to find the slight increase of crown-like structures in LOPV/RITV treated mice, supporting the hypothesis that HIV PIs increase AT inflammation.

A

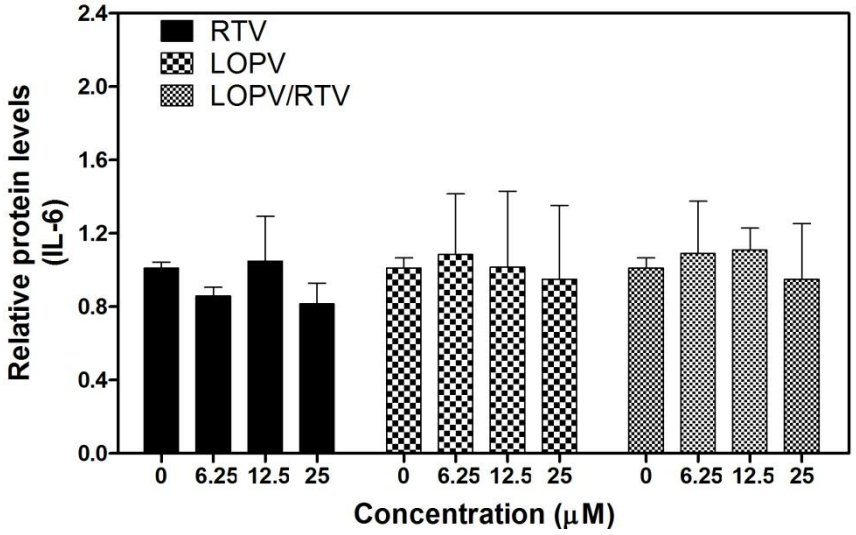

B

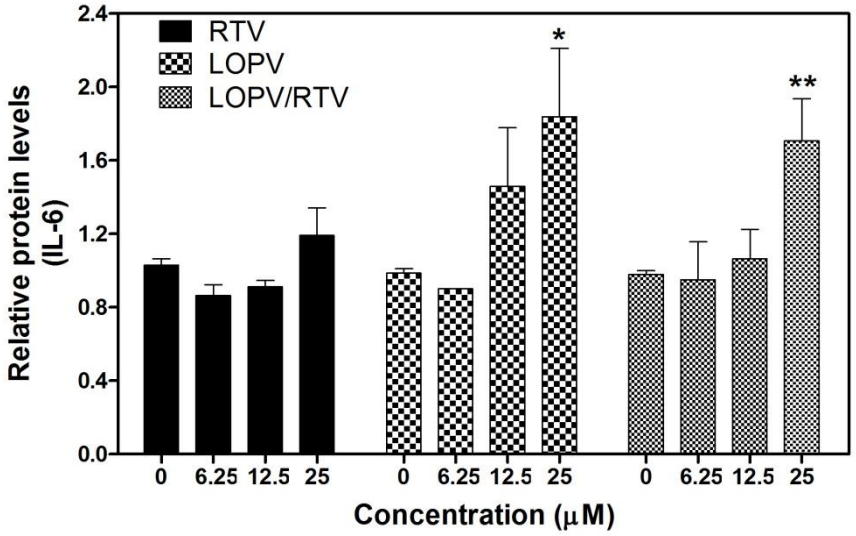

Figure 16. HIV PIs increase inflammatory cytokines in differentiated 3T3-L1s. A) Non-differentiated and **B)** differentiated 3T3-L1s were treated with increasing concentrations of RITV, LOPV, or LOPV/RITV for 48 h. Culture media analyzed by ELISA. Relative IL-6 levels were determined with total cellular protein as control. Values are mean ± SE from three independent experiments. Statistical significance relative to DMSO control (0); *$p<0.05$, **$p<0.005$.

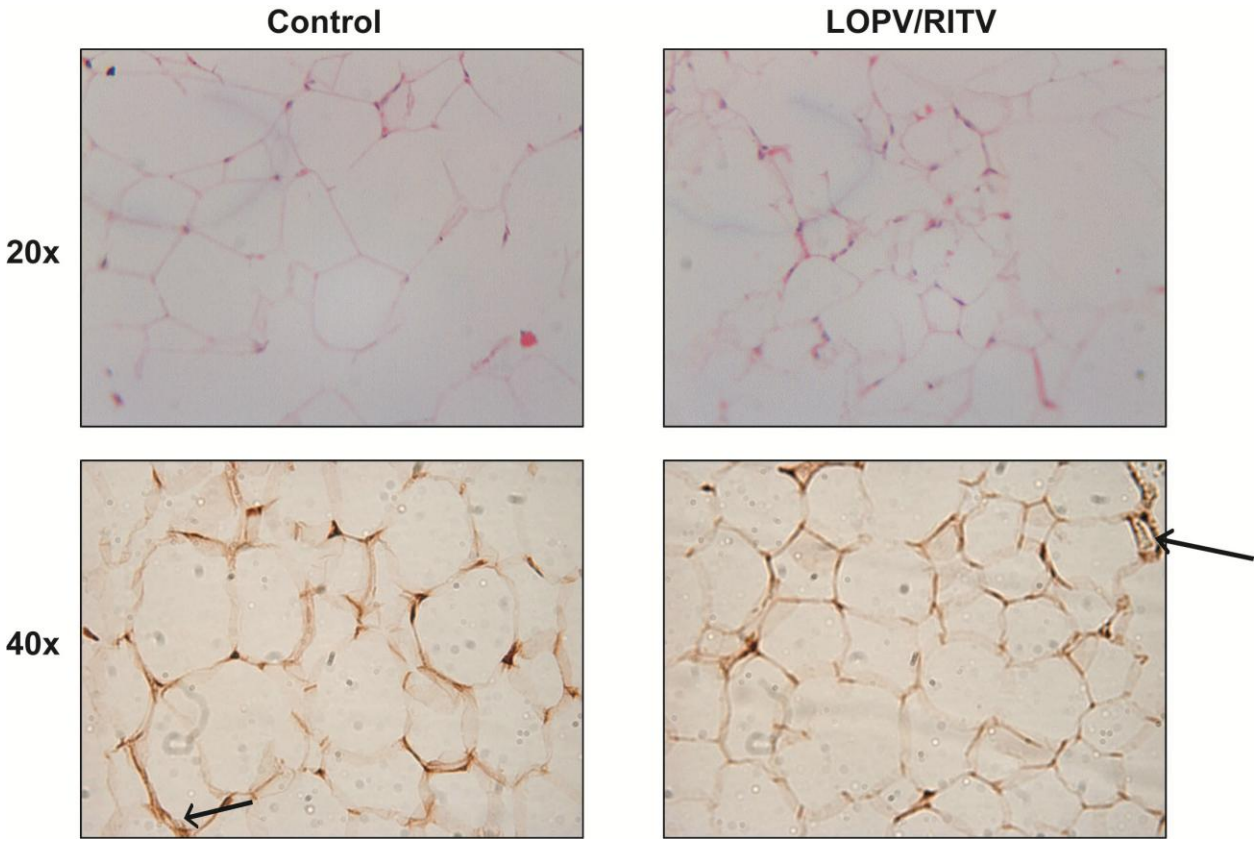

Figure 17. LOPV/RITV slightly increases inflammation *in vivo*. C57BL/6 male mice were fed a high fat diet and gavaged with 4:1 LOPV/RITV or control solution for 8 weeks. Gonadal fat pads were fixed, stained with anti-Mac2, and counterstained for nuclei. Images were acquired using a light microscope with 20 × and 40 × objective lenses.

Effects of HIV PIs on intracellular lipid accumulation in adipocytes

Previous studies have shown that HIV PIs can affect adipocyte differentiation, but with contradictory results (*242, 257, 258*). To specifically determine the effect of individual HIV PIs on adipocytes differentiation, we first monitored the effect of HIV PIs on intracellular lipid droplet formation using Nile Red, a fluorescent dye that specifically stains lipid droplets (*259*). As shown in Figure 18A, when murine pre-adipocytes were induced to differentiate while concurrently treated, HIV PIs differentially affected intracellular lipid accumulation. Specifically, RITV increased lipid accumulation compared to control, while LOPV and LOPV/RITV inhibited lipid accumulation. We further verified our observations using another common neutral lipid stain, Oil Red O in 3T3-L1 cells (Figure 18B). Similar results were obtained with human SGBS cells stained with Oil Red O (Figure 18C). To increase accuracy and avoid subjectivity, we also quantitated both the number and size of lipid droplets that accumulated in 3T3-L1 cells when induced to differentiate in presence of HIV PIs using a MATLAB program previously written and published (*231*) (Figure 19). These combined findings enabled us to more definitively ascertain the effect of HIV PIs on adipocyte differentiation compared to what was previously published in the literature, as well as determine the extent of effect at the LD level.

HIV PIs alter PPARγ at the transcriptional and posttranscriptional levels

To ascertain the mechanism underlying LOPV-inhibition of differentiation and RITV-induction of differentiation, we first analyzed the activity of the PPARγ promoter in the presence of HIV PI treatment. As discussed previously, PPARγ is an essential transcription factor involved in adipogenesis. Although we expected LOPV to inhibit PPARγ, and RITV to either

have no affect or induce the promoter leading to more lipid accumulation, we found all HIV PIs to significantly inhibit promoter activity (Figure 20). We further analyzed PPARγ mRNA levels. In non-differentiated cells, mRNA levels could not be accurately assessed as PPARγ is not yet upregulated at this stage. In differentiated 3T3-L1s, we found significant decreases of PPARγ mRNA at 4 h, with complete rebound by 6 h of treatment (Figure 21A). However, RITV induced an increase of mRNA stability compared to DMSO control (Figure 21B).

In attempt to elucidate how RITV inhibits PPARγ promoter activity but increases mRNA stability, we investigated the role of RNA binding proteins in 3T3-L1s treated with LOPV and RITV. We have previously shown that HIV PIs can increase the stabilizing mRNA binding protein HuR in macrophages, leading to increased translation of IL-6 (*191, 232*), and hypothesized that LOPV/RITV may have a similar role in PPARγ stabilization.

We therefore completed a pulldown assay in which 3T3-L1s were treated for 24 h with either RITV or LOPV (12.5 μM) or DMSO control. 5 mg of total cell lysate was incubated with biotinylated beads previously incubated with anti-HuR or anti-CUGBP1 antibody. Protein was digested and RNA precipitated. Bound mRNA was analyzed by real-time RT-PCR, using IgG1-incubated bead samples as a control. As shown in Figure 22, RITV and not LOPV significantly increased mRNA binding proteins to associate with PPARγ. In order to clarify this was a specific binding, we completed an *in vitro* binding assay. Supportive of the putative binding sites found in mRNA PPARγ sequence (Figure 23A), we found significant HuR and minimal CUGBP-1 to bind to the 3'UTR, and only HuR binding minimally to the CDS (Figure 24B).

In addition, when 293 cells were transfected with plasmid containing the 3'UTR of PPARγ in a GFP-expression vector, overexpression of either HuR or CUGBP-1 increased GFP

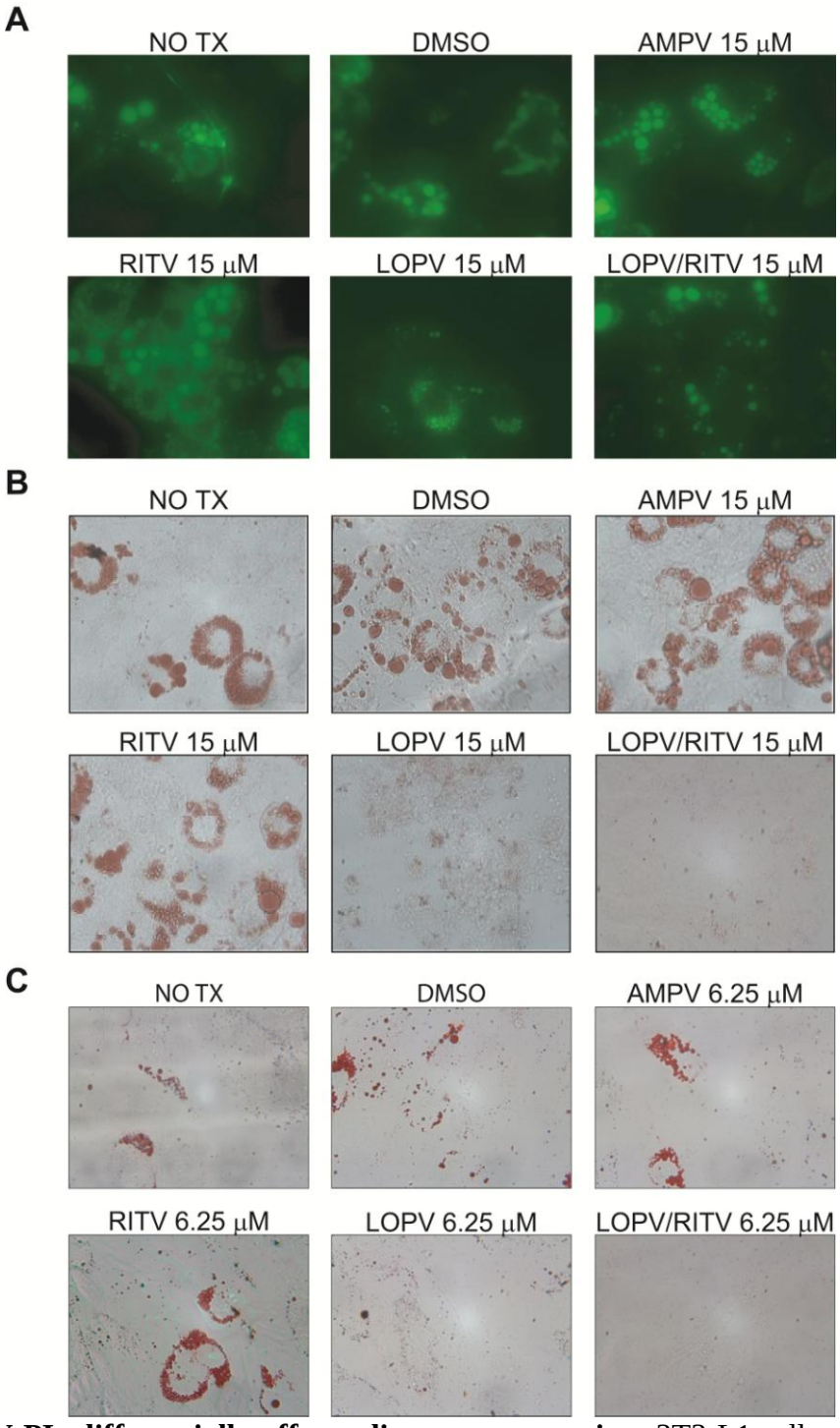

Figure 18. HIV PIs differentially affect adipocyte maturation. 3T3-L1 cells were induced to differentiate while concurrently treated with HIV PI. Cells were fixed after 8 days and stained with **A)** Nile Red and images acquired on a fluorescent microscope or **B)** Oil Red O (40 ×). **C)** SGBS cells were treated in the same manner as 3T3-L1s and stained with Oil Red O after 10 days (40 ×). Images are representative of three individual experiments.

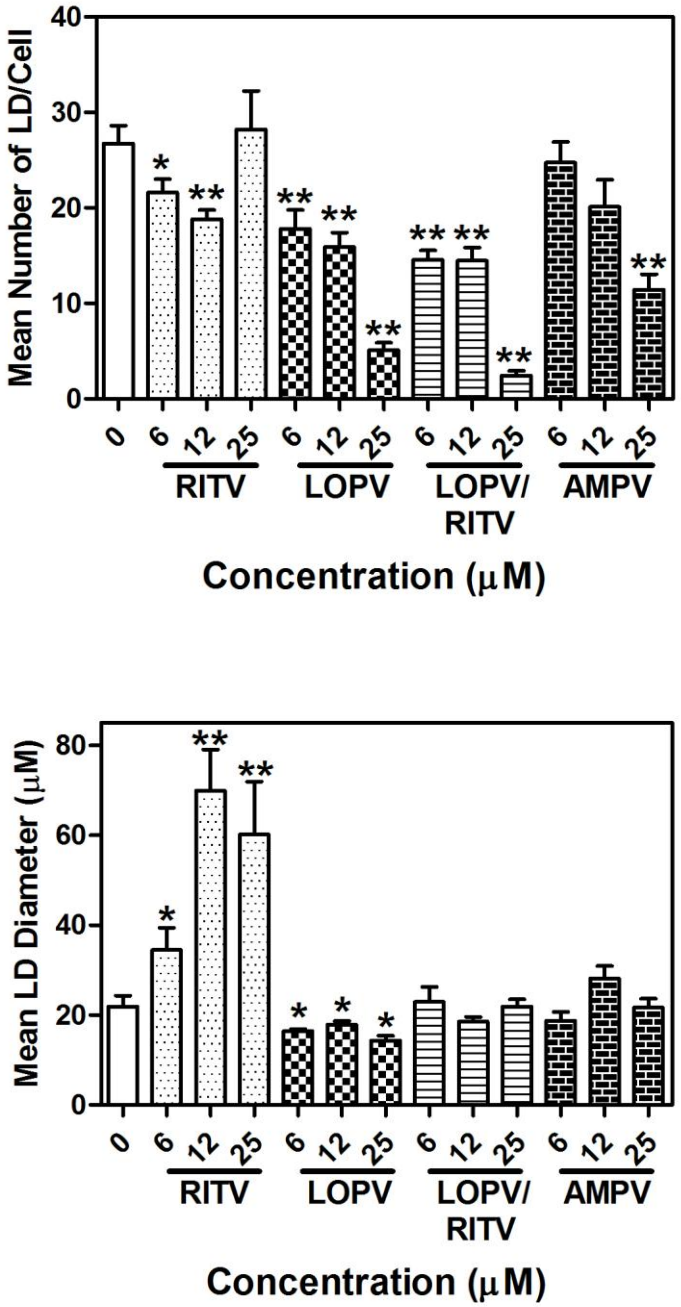

Figure 19. HIV PIs differentially affect LD number and size in differentiating 3T3-L1s. 3T3-L1s were induced to differentiate in the presence of increasing concentrations of HIV PIs. After 2 weeks, cells were fixed and imaged using a 40 × objective on a light microscope. Images were analyzed via MATLAB for both lipid droplet (LD) number and diameter. Values are mean ± SE of three independent experiments; *p<0.05, **p<0.005.

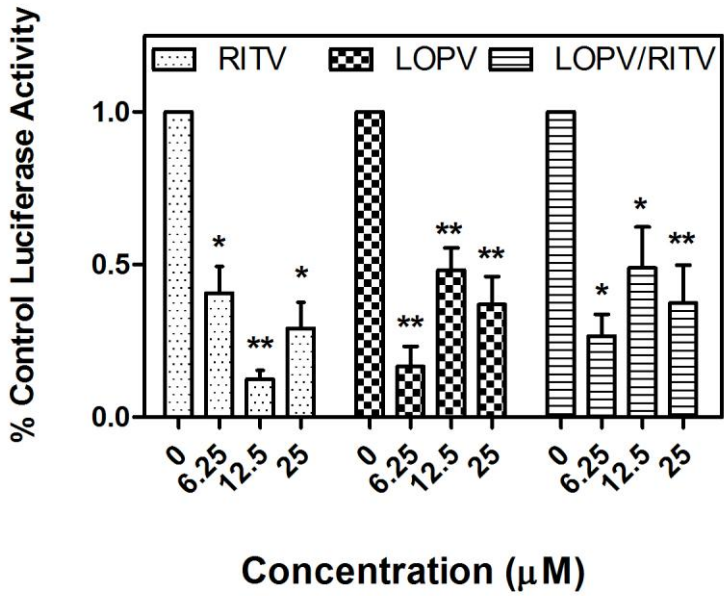

Figure 20. HIV PIs inhibit activity of the PPARγ promoter. 293 cells were transfected with a plasmid with the PPARγ promoter controlling luciferase expression for 48 h. Cells were subsequently treated with increasing concentrations of HIV PIs or control DMSO for 6 h. Relative luciferase activity was analyzed with total protein levels as control. Values were subtracted from treated 293 cells transfected with empty plasmid. Values are mean ± SE of ten independent experiments. *p<0.05, **p<0.001 compared to DMSO (0).

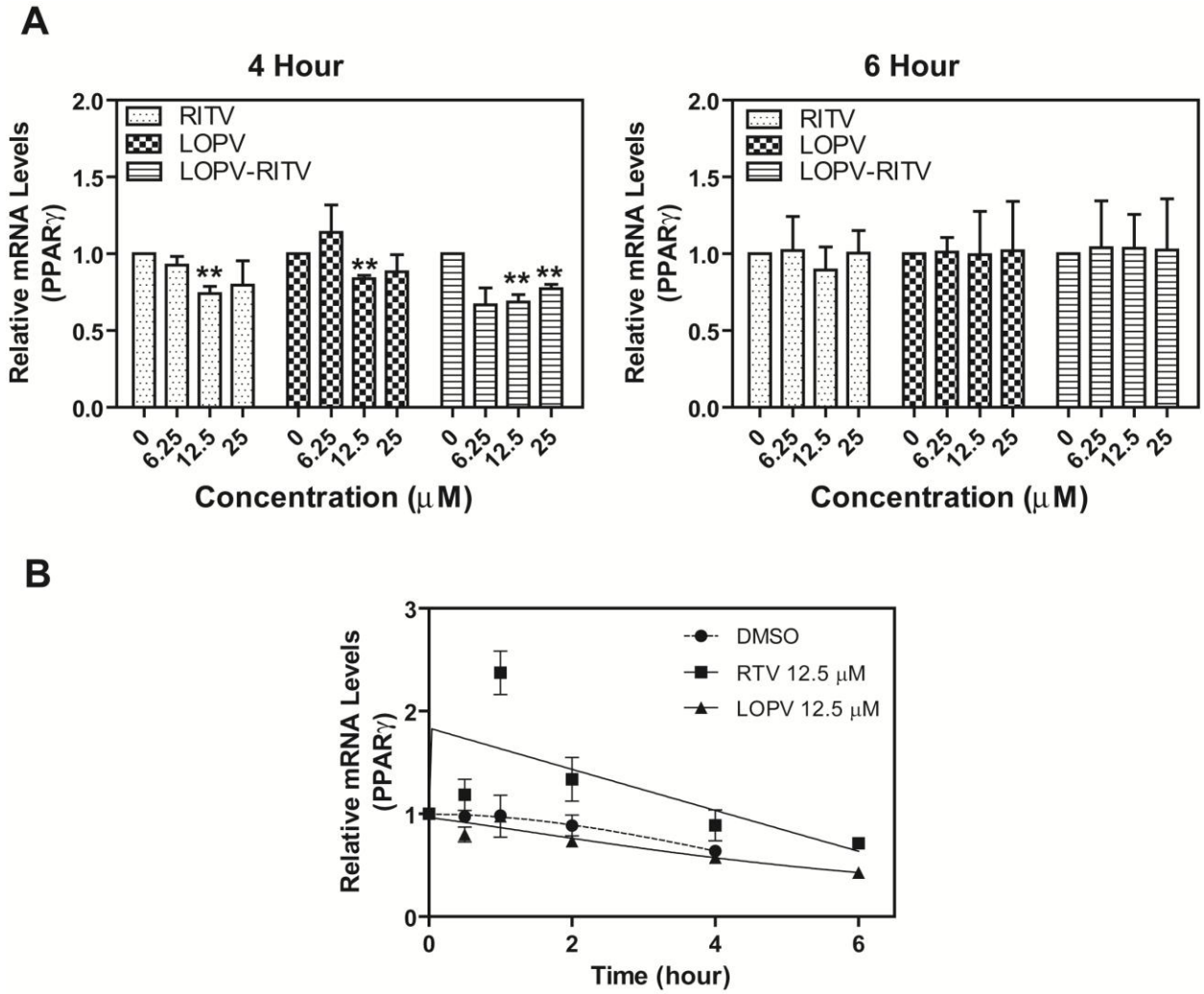

Figure 21. HIV PIs differentially alter PPARγ mRNA levels. A) Differentiated 3T3-L1s were treated with increasing concentrations of HIV PIs for 4 or 6 h. Relative mRNA levels were determined by real-time RT-PCR with β-Actin as internal control. Values are mean ± SE from four independent experiments: **p<0.005 compared to DMSO (0) control. **B)** 3T3-L1s were treated with 12.5 μM RITV or LOPV for 2 h, followed by the addition of ActinomycinD (10 μg) (time 0). Total RNA was isolated from cells at 0.5, 1, 2, 4, and 6 h, and PPARγ mRNA levels analyzed as above. Results are expressed as the percentage of the mRNA at time 0 using a two phase exponential decay analysis of n =2.

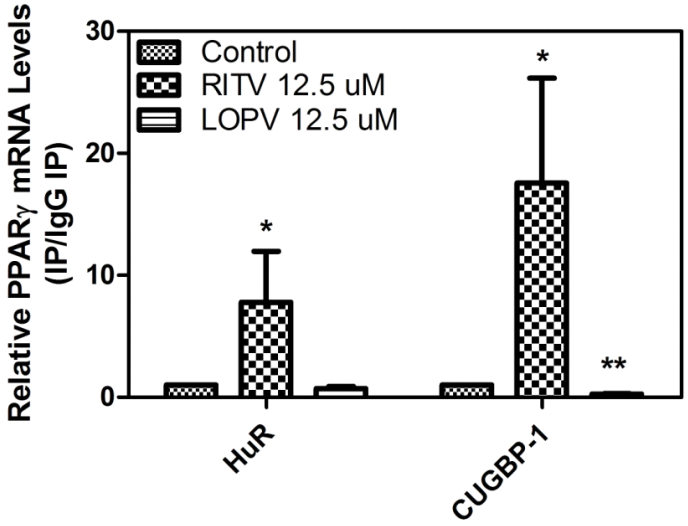

Figure 22. *In vivo* pulldown of PPARγ mRNA after treatment with HIV PIs in 3T3-L1 cells. 3T3-L1 cells were treated with RITV 12.5 µM, LOPV 12.5 µM, or DMSO control for 24 h. 3 mg protein equivalent was added to preswollen and antibody labeled Sepharose beads, and rotated at RT for 4 h. RNA in IP materials was reverse transcribed to detect the presence of PPARγ mRNA. Values are mean ± SE from four independent experiments: *$p<0.05$, **$p<0.001$.

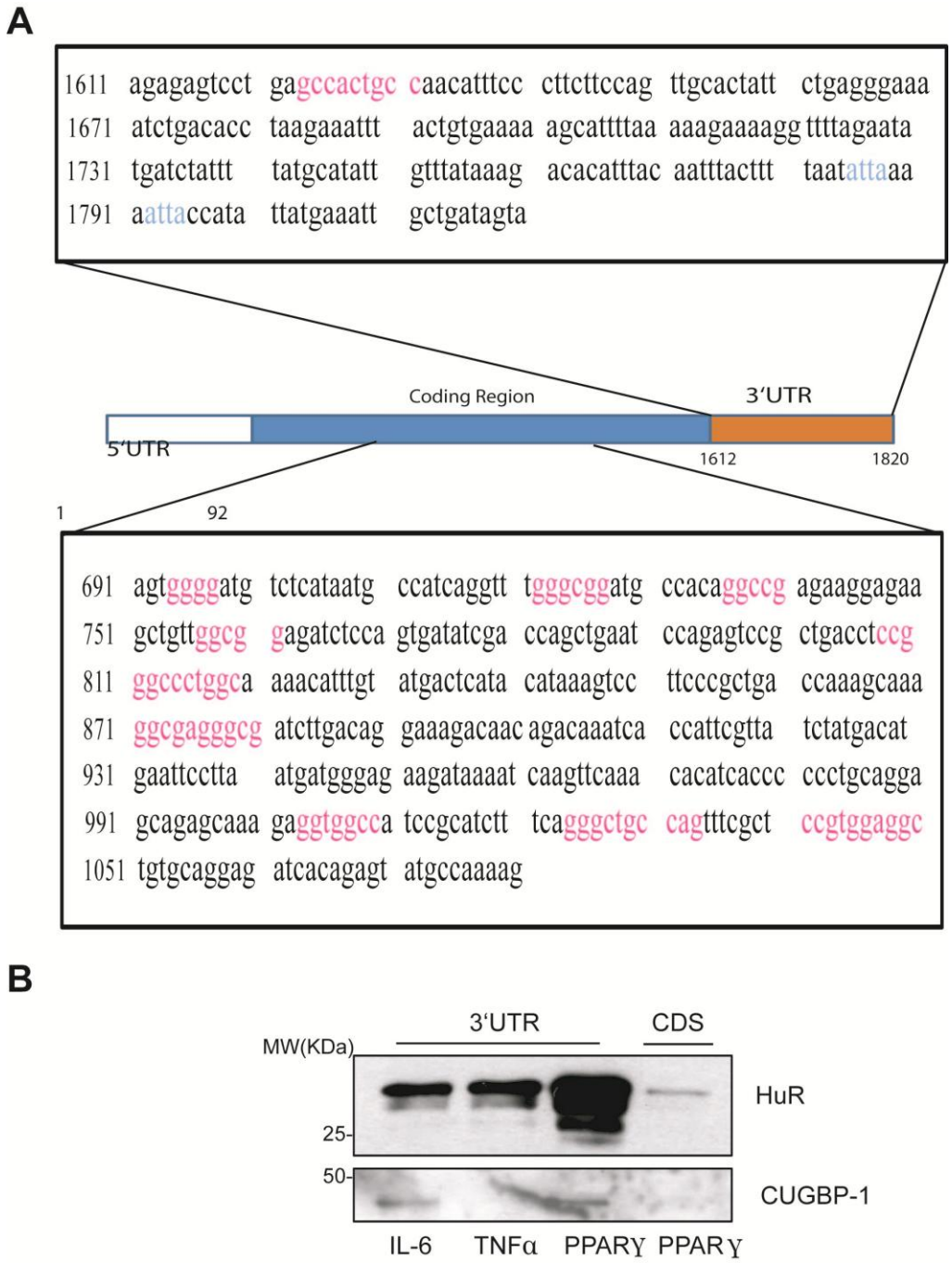

Figure 23. HuR and CUGBP-1 bind to PPARγ. A) Putative binding cites of HuR (Blue) and CUGBP1 (Pink) in the mRNA sequence of PPARγ. **B)** Biotinylated mRNA of the 3'UTR and CDS of PPARγ were incubated with total 3T3-L1 protein lysates. mRNA-protein complex was pulled down with Streptavidin Dynabeads. Shown are representative immunoblots of four independent experiments against HuR and CUGBP-1 of IP material. The 3'UTR of IL-6 and TNF-α are shown as positive control (results previously published (*191*, *232*)).

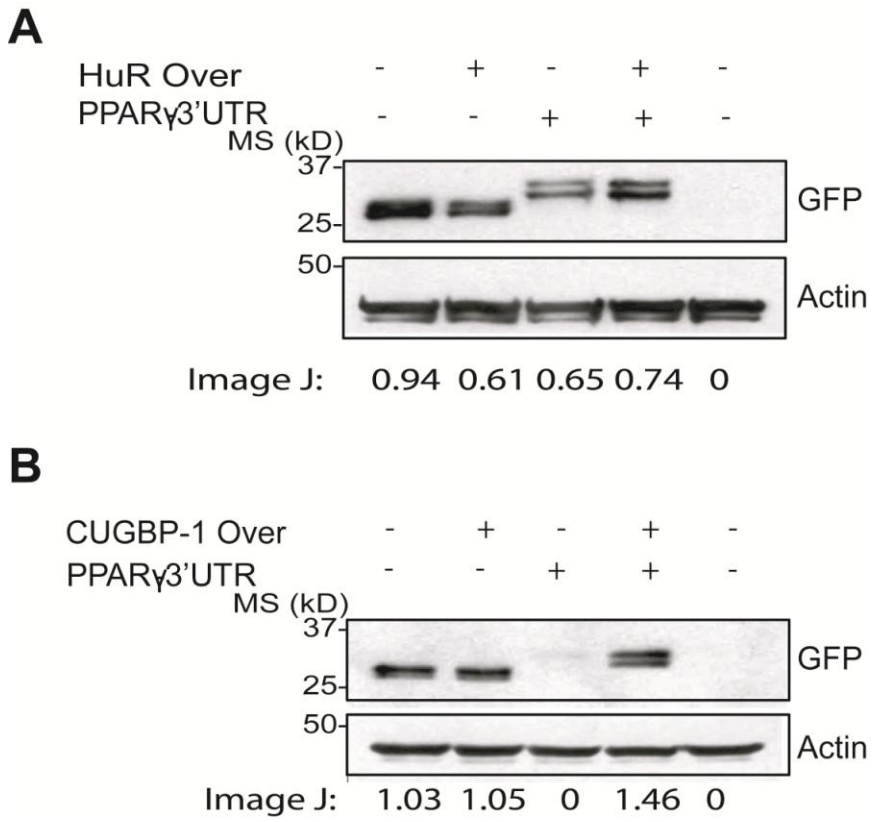

Figure 24. 3'UTR PPARγ activity is increased with HuR and CUGBP-1 overexpression. 293 cells were co-transfected with the 3'UTR region of PPARγ inserted in a GFP-expressing vector with either **(A)** HuR or **(B)** CUGBP-1 under constitutive CMV control. Vectors with no insert were used as control. After 48 h, activity of 3'UTR was determined with total cell lysates. Shown are representative immunoblots against GFP and Actin from three independent experiments. Last lane is no transfection control.

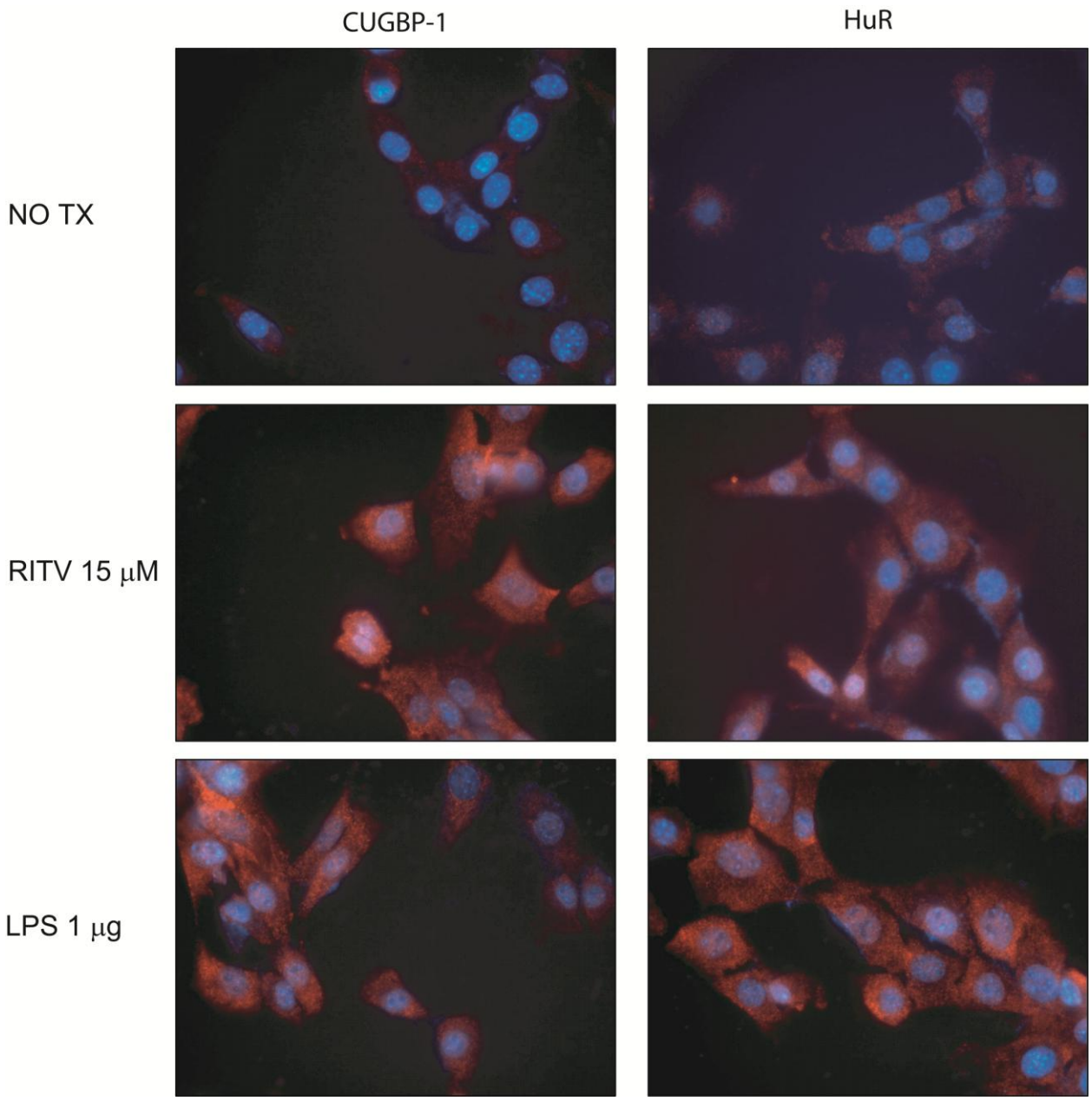

Figure 25. RITV increases HuR and CUGBP-1 translocation in 3T3-L1s. 3T3-L1 cells were treated with RITV (15 μM) or purified lipopolysaccharide (LPS – total 1 μg) for 24 h. Cells were fixed and stained with anti-HuR or -CUGBP-1, and images acquired using a confocal microscope with a 60 × oil immersion lens. Shown are representative images from two independent experiments.

expression compared to empty GFP plasmid (Figure 24). We also have preliminary data that RITV treatment of 3T3-L1s increases translocation of HuR and CUGBP-1, indicating activation of protein (Figure 25). Taken together, these results indicate RITV increases HuR and CUGBP-1 activation and binding to PPARγ mRNA, which has the ability to then increase stability. This can ultimately lead to an increased in LD formations during adipogenesis.

Effect of CHOP on HIV PI-induced alterations of intracellular lipid accumulation in adipocytes

The differential affects of RITV and LOPV on PPARγ mRNA stability needs to be further investigated. However, we still hypothesize that this, and other alterations, may be at least partially explained by HIV PI-induced UPR. Therefore, to identify this potential link, we isolated primary adipocytes from C57BL/6 wild-type and $CHOP^{-/-}$ mice with a C57BL/6 background. Isolated primary adipocytes were induced to differentiate while concurrently treated with HIV PIs for 10-days. Intracellular lipid droplets were stained with Oil Red O. As shown in Figure 26, similar to the findings in cultured murine and human adipocytes, LOPV and LOPV/RITV significantly inhibited intracellular lipid accumulation in wild-type mouse adipocytes. However, in the absence of CHOP, LOPV and LOPV/RITV had less effect on intracellular lipid accumulation. Also of note, AMPV (a non-inducer of ER stress) did induce lipid accumulation and its effect also was abrogated in absence of CHOP.

In addition, total RNA was analyzed from the gonadal fat pads of mice gavaged for eight weeks with LOPV/RITV and control solution. Preliminary data suggests a slight abrogration of HIV PI-induced lipid dysregulation and inflammation in AT with absence of CHOP (Figure 27). However, as $CHOP^{-/-}$ does not result in a significant decrease of these pathologies, another pathway may also be involved in HIV PI-induced lipid dysregulation in adipocytes.

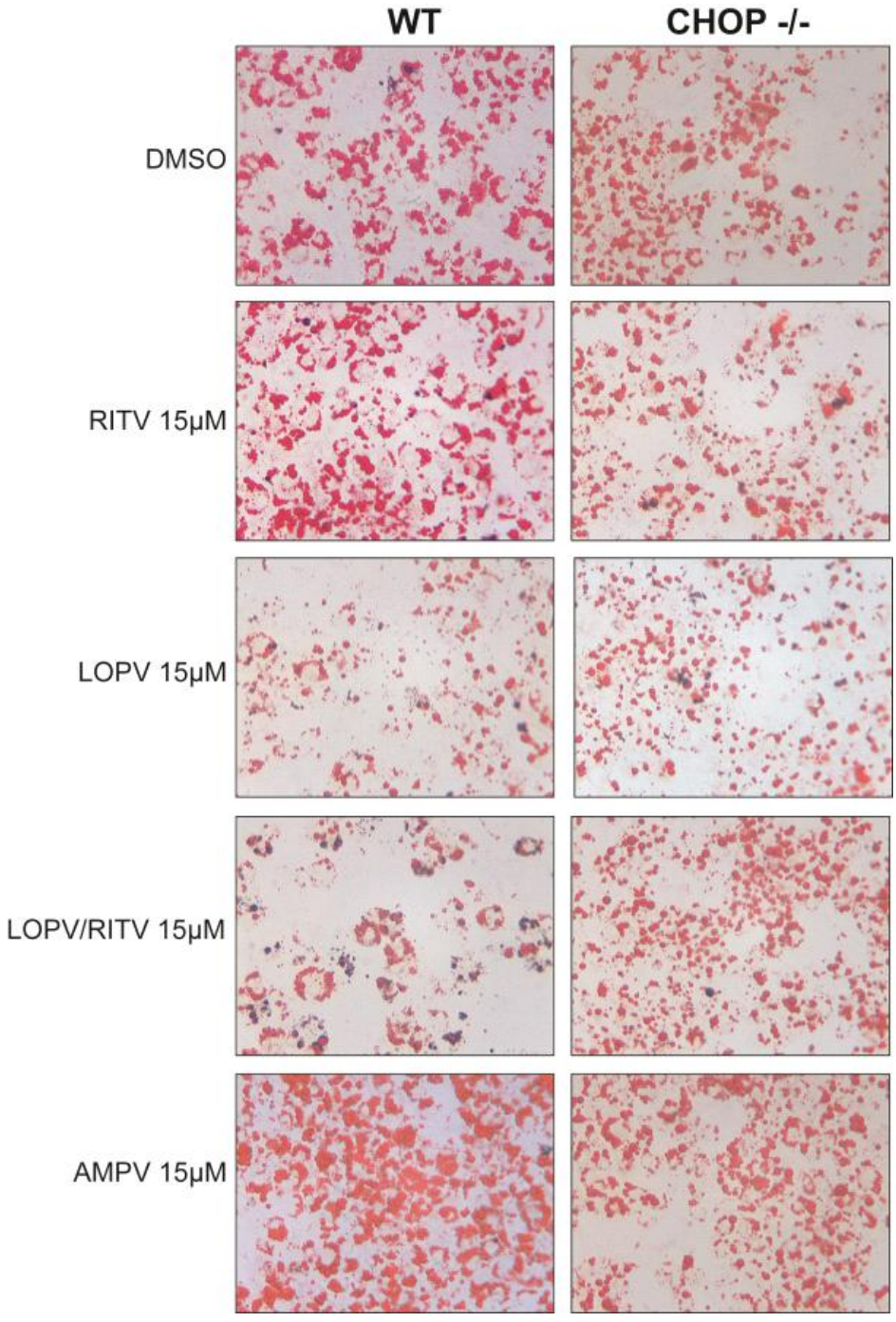

Figure 26. HIV PI-induced alteration of adipogenesis is abrogated in absence of CHOP. Primary murine pre-adipocytes were isolated from CHOP$^{-/-}$ and wild type (WT) mice. Cells were induced to differentiate while concurrently treated with HIV PIs, and stained with Oil Red O after 10 days. Images were acquired with a 40 × objective lens. Representative images of two independent experiments are shown.

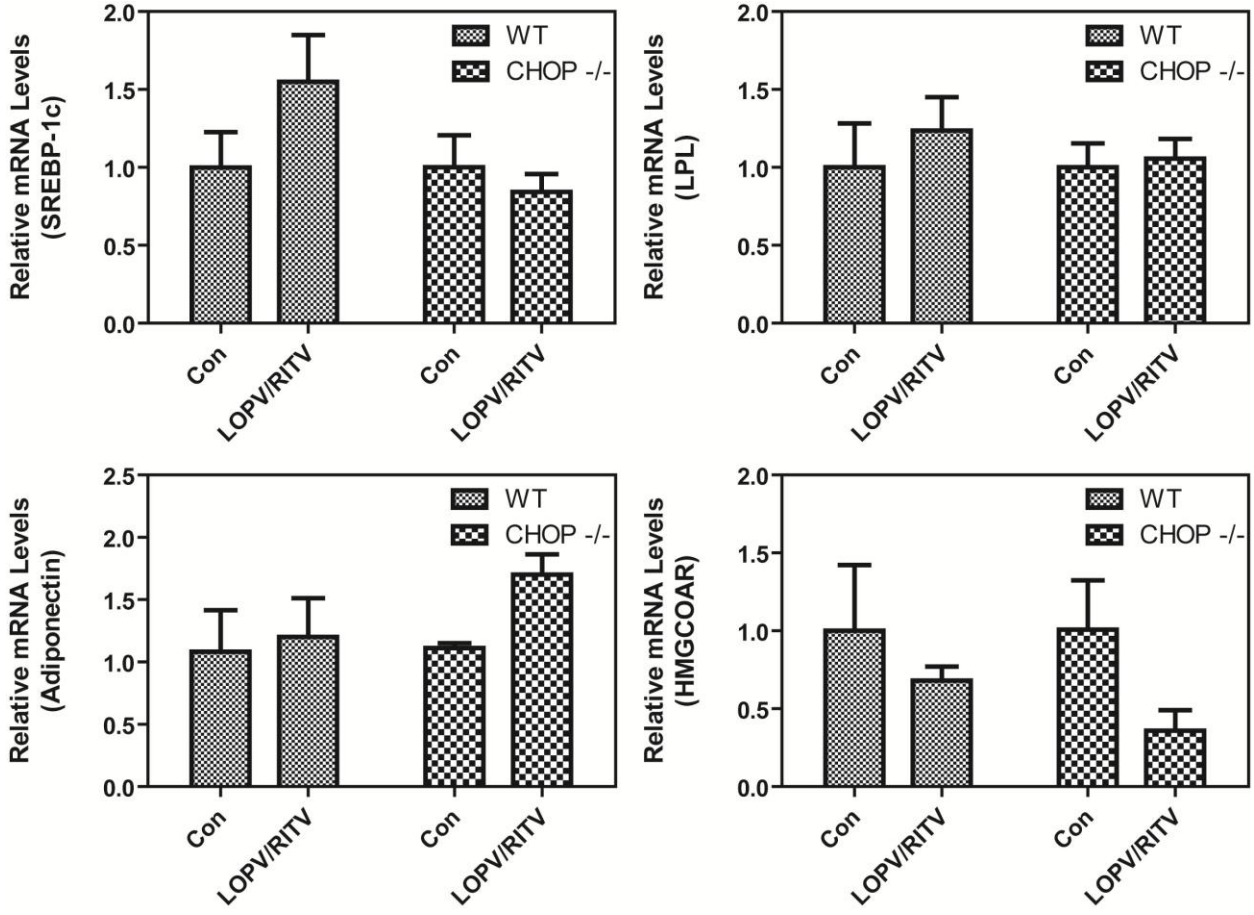

Figure 27. CHOP knockout may abrograte HIV PI-induced lipid metabolism dysregulation and inflammation in AT. Male and female C57BL/6 WT and CHOP$^{-/-}$ mice were fed a high fat diet and gavaged with either 4:1 LOPV/RITV or control solution for 8 weeks. mRNA from gonadal fat pads were analyzed by real-time RT-PCR with β-Actin as internal control. Value means ± SE are shown; n=6.

SIGNIFICANCE

Although HIV PIs are extremely effective in decreasing viral load, HIV patients are at increased risk of developing metabolic syndrome and cardiovascular diseases on this regimen (*9, 22*). Understanding the cellular mechanism underlying these complications is essential in development of alternative and improved therapies for chronically infected patients.

The field of ER stress and the UPR has gained great attention during the last decade. The UPR signaling pathway plays an important role in regulating normal functions of various cells including hepatocytes, β-cells, and macrophages. Consequently, dysregulation of the UPR signaling pathway has been implicated in various human diseases such as diabetes, fatty liver, and cardiovascular diseases (*45-47*). Previous studies from our laboratory suggest that activation of ER stress represents an important cellular mechanism underlying HIV PI-induced inflammation and dyslipidemia (*49-53, 190, 232*). In addition, Djedaini *et. al* have recently shown a correlation of HIV PI-induced insulin resistance and the ER stress in adipocytes (*54*). However, little is currently understood of the mechanism underlying HIV PI-induced lipid metabolism dysregulation.

Here, we have shown that HIV PIs induce ER stress in a time and dose-dependent manner, similar to macrophages and hepatocytes (Figures 8-11). There was, however, a differential effect in differentiated versus non-differentiated adipocytes, likely owing to the fibroblastic-like physiology of preadipocytes. There has not yet been a study defining HIV PI-induced alterations in fibroblasts, illuminating the nonsignificant induction of cell death and inflammatory response we found in 3T3-L1 preadipocytes. Nonetheless, we found slight increases in UPR protein and mRNA levels in our preadipocyte cell lines. We hypothesize this is do to our particular cell culture methods which commit the cell line to the adipocyte lineage.

In addition, not all HIV PIs activated the UPR to the same level, which may be explained by pharmacokinetic differences within this drug class. HIV PIs differ in molecular weight, ionization, and lipophilicity, all of which determine rate of transport through cellular membranes. While molecular weight and ionization for HIV PIs are similar and associated with passive diffusion, the lipophilicity (oil-water partition coefficient, or logP) differs. A strong correlation has been reported between log P and the intracellular accumulation of HIV PIs (*260*). The log P of AMPV and DRV are in the poor range of permeability while that of LOPV, RITV, ATZ, IDV, SQV, and NEFV are very permeable. These differences correlate strongly with our categorization of ER stress inducer and non-inducers. While pharmacokinetic studies have not been completed to determine the significance of these log P differences, the connection is notable and may be one molecular contribution to differences in dyslipidemia induction in the clinic.

We have found that HIV PIs which induce high levels of the UPR also alter adipogenesis and lipid metabolism. Specifically, RITV and LOPV differentially affect both LD number and size (Figure 19). However, while RITV significantly decreased LD number, it also increased LD diameter. This data suggests LD fusion, as could occur at times of ER stress with alteration of CTT function (*175*). In addition, while higher concentrations of RITV increased lipid droplet formations, the physiological concentration in the clinical LOPV/RITV formulation inhibited lipid accumulation (6.25 µM). At the same time, LOPV dose-dependently inhibited differentiation. Taken together, there was a synergistic inhibition of LOPV-RITV in the clinically relevant 4:1 formulation at physiological concentration (12.5 µM).

We hypothesized the induction of ER stress may be the cause of these alterations, as the ER and LD organelles are so closely intertwined (*66, 69, 173, 174*). Indeed, knockout of CHOP,

a downstream UPR transcription factor, abrogated HIV PI-induced adipogenesis dysregulation (Figure 26). In addition, we show preliminary data that this difference occurs *in vivo*. When CHOP$^{-/-}$ mice are fed LOPV/RITV (4:1) for 8 weeks, the lipogenesis transcription factor SREBP-1c, as well as lipid protein lipase (LPL) is not upregulated in AT of CHOP$^{-/-}$ as it is in wild-type mice.

Some of the alterations in differentiation by HIV PIs can also be explained by affects on PPARγ. Particularly, we have found an increased binding of mRNA binding proteins HuR and CUGBP1 to PPARγ mRNA when 3T3-L1s were treated with RITV, but not LOPV (Figure 22). We have previously shown HIV PIs can increase HuR translocation from the nucleus to cytoplasm, indicating activation (*232*), and have seen similar occurrences in 3T3-L1s (Figure 25). However, we have not yet determined a direct mechanism by which RITV results in activation of HuR and CUGBP1, although we hypothesize it is connected with our UPR activation findings.

Some of our other findings also brought more questions. One example is from our AMPV treatments. AMPV is an ER stress non-inducer and shown in the clinic to have minimal lipid profile alterations. However, in cells treated with physiological concentrations (12.5 μM), we saw an increased lipid accumulation during adipogenesis which was abrogated with loss of CHOP. In addition, knockout of CHOP did not completely abrogate LOPV and RITV lipid metabolism alterations *in vitro* or *in vivo*, suggesting other pathways may be involved.

It has recently been shown that autophagy is upregulated in visceral and not subcutaneous fat pads (*261*), a similar distribution of which HIV PIs also affect fat depots in patients. This pathway has also been shown to be involved in cellular lipid recycling and metabolism (*205*). We therefore began to investigate if HIV PI-induced dysregulation of adipocyte lipid metabolism

could be explained through this pathway. Our findings on this matter are intriguing, and can be found in the next chapter of this dissertation.

CHAPTER IV: HIV Protease Inhibitors LOPV and RITV Induce Autophagosome Accumulations in Adipocytes

STUDY RATIONALE

Autophagy is a catabolic pathway in which intracellular components are degraded for energy production. Recently, autophagy has been shown to be strongly involved in lipid metabolism. Within adipocytes, autophagy aids in lipid store turnover and adipogenesis (*262-264*). Loss of the autophagic pathway results in inhibition of differentiation *in vitro* and decreased white adipose tissue size and distribution *in vivo*.

Recent investigations have shown HIV PIs nelfinavir (NFV) and saquinavir (SQV) to induce autophagy in cancer cells (*233, 234, 265*). However, little is known whether HIV PIs can induce autophagy in adipocytes, and if this is involved in dysregulation of lipid metabolism.

There is growing evidence that ER stress can activate autophagy (*119, 120, 125, 209*). While this is hypothesized to occur for nascent protein degradation, other mechanistic inductions are ill-defined. We have previously demonstrated that HIV PIs significantly activate the UPR in adipocytes. Yet, not all HIV PI perturbations could be thoroughly explained by this pathway. We therefore began to investigate if autophagy induction is also involved in HIV PI-induced dysregulation of adipocyte lipid metabolism. After finding that autophagy is induced by these drugs, we further pursued how HIV PI-induced ER stress and autophagy are connected.

RESULTS

Effect of HIV PIs on autophagy activation in adipocytes

LC3B western blot analysis is a common method in determining activation of autophagy (*266*). At autophagic induction, cytosolic LC3B-I is cleaved and lipidated to form membrane-associated LC3B-II. To determine if HIV PIs increase the ratio of LC3BII:I, non-differentiated and differentiated 3T3-L1 cells were treated with HIV PIs (12.5 μM) for various time points (12, 24, and 48 h), and total cell lysates separated on a 12% SDS-PAGE gel. Peak conversion was found to occur at 48 h, and cells were treated dose-dependently at this time point. Greater activation of LC3B was found in differentiated 3T3-L1s than non-differentiated (Figure 28), but both were significant. Similar results were seen in a human adipocyte cell line (ASC) (Figure 29).

HIV PIs increase autophagosomes in 3T3-L1s

Although immunoblotting LC3B is a frequent method used in autophagy detection, there remain many pitfalls in this assay that cannot be simply addressed in one experiment (*12*, *13*). Therefore, we further confirmed the effect of HIV PIs on autophagosome accumulation using electron microscopy, the current gold standard of autophagy induction. As shown in Figure 30, there was a significant increase of autophagosome density with LOPV, LOPV/RITV, and RITV treatments in 3T3-L1 cells.

Second Generation HIV PI Darunavir does not activate autophagy

Darunavir (DRV), with RITV boost, now surpasses LOPV/RITV prescription numbers in the clinic. In fact, the newest HIV treatment guidelines recommend treatment-naïve patients beginning HAART regimens containing HIV PIs to be treated with DRV/RITV (4:1). As there is

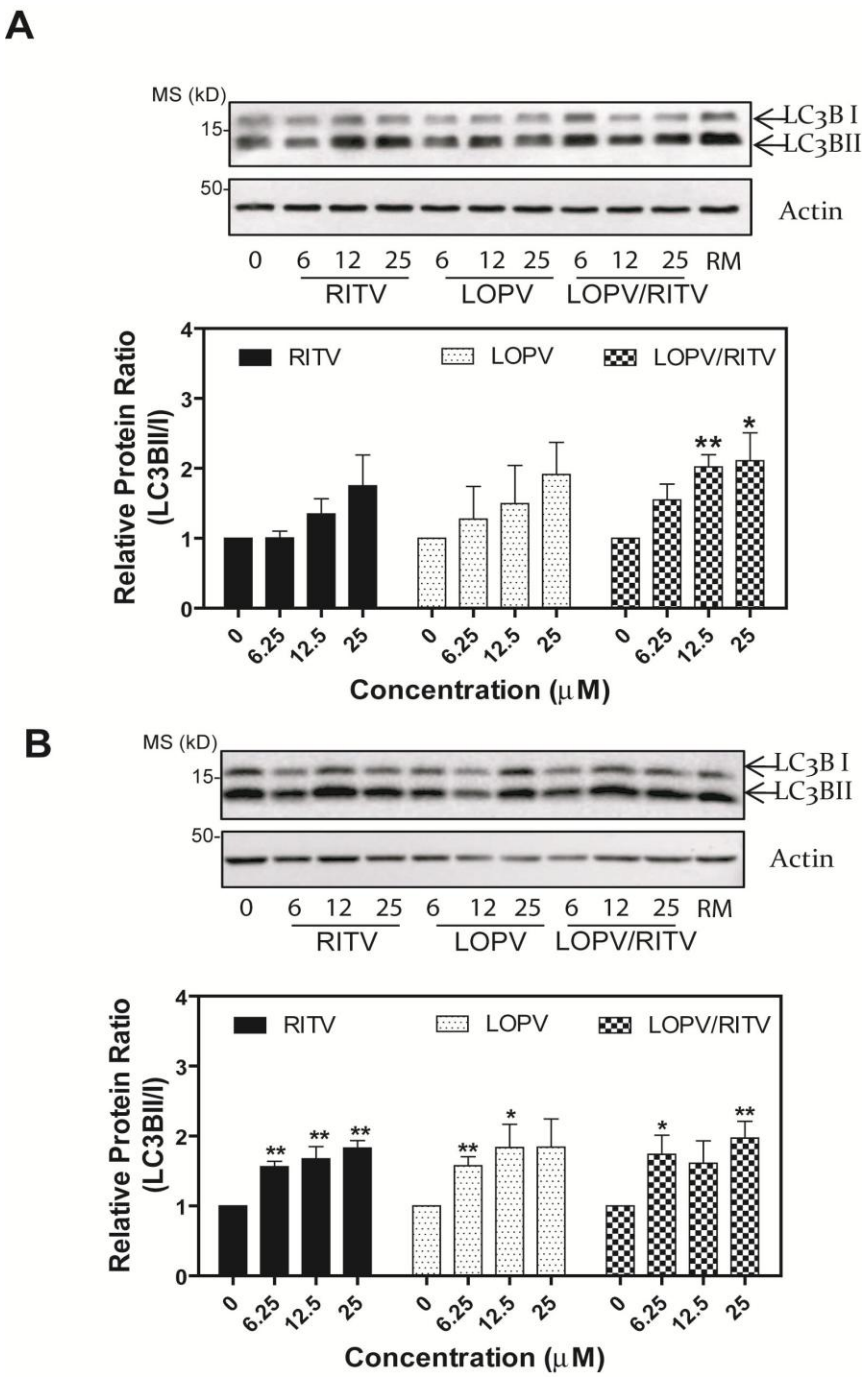

Figure 28. HIV PIs increase LC3B II:I ratio. A) Non-differentiated and **B)** differentiated 3T3-L1s were treated with increasing concentrations of HIV PIs for 48 h. Representative immunoblots against LC3B and Actin are shown. Densitometry was determined using Quantity One. Values are means ± SE from four independent experiments; * $p<0.05$, ** $p<0.005$

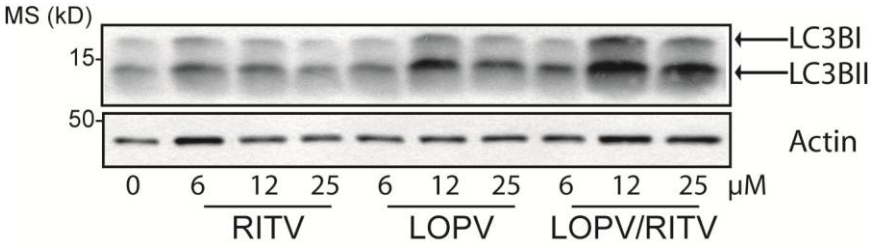

Figure 29. HIV PIs increase LC3B II:I ratio in human ASCs. Human adipose stem cells were induced to differentiate and then treated with increasing concentrations of HIV PIs for 48 h. Representative immunoblots of LC3B and Actin from two separate experiments are shown.

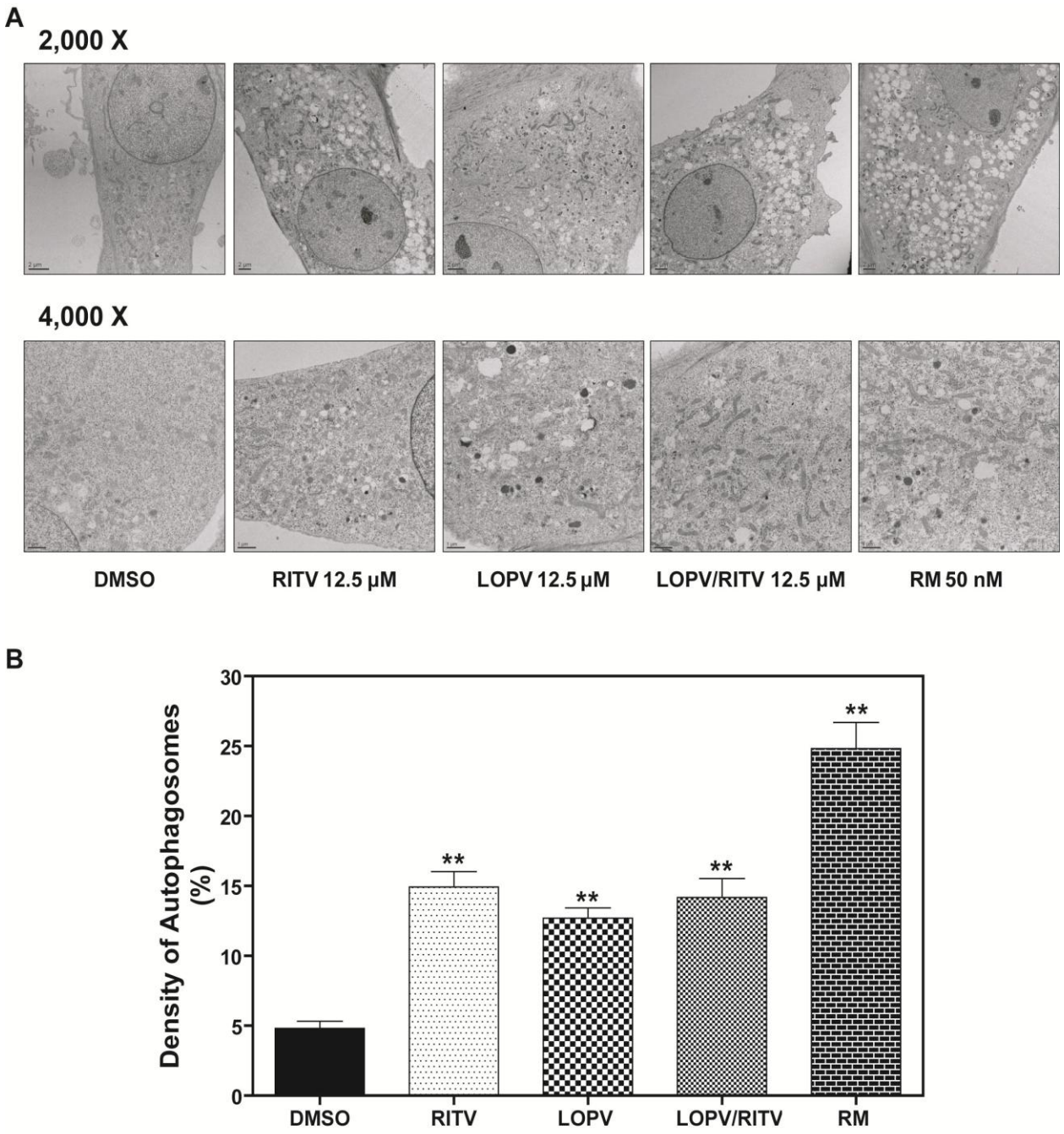

Figure 30. HIV PIs quantifiably increase autophagosomes in 3T3-L1 cells. Non-differentiated 3T3-L1s were treated with 12.5 µM HIV PIs, 50 nM Rapamycin (RM), or DMSO control for 48 h. Cells were processed for transmission electron microscopy as described in "Methods." **A)** Representative images for each treatment at 2,000 × and 4,000 ×. **B)** The density of autophagosomes were determined by point counting at 4,000 ×. Statistical significance relative to vehicle control: **p<0.05x10^5.

currently no clinical evidence suggesting DRV has metabolic side effects, and we previously found little activation of the UPR by DRV, we tested whether DRV induces autophagy similarly as LOPV/RITV. As shown in Figure 31, DRV did not significantly increase LC3B conversion or autophagosome formation compared to control.

Effect of HIV PIs on autophagic flux

The increase of autophagosome number does not always indicate increase of autophagic activity. Accumulation of autophagosomes can be caused by an increase in the induction of autophagy and/or an impairment of autophagolysosomal maturation. We therefore examined the effect of HIV PIs on autophagic flux.

Monodansylcadaverine (MDC) is an autofluorescent drug that naturally accumulates in lower pH vesicle membranes, which is characteristic of late autophagosomes (*115*). When non-differentiated 3T3-L1 cells were treated with HIV PIs and subsequently stained with MDC, HIV PI treatment did increase punctate staining, but did not appear to be dose-dependent (Figure 32). In addition, results did not appear to quantitatively define HIV PI-induced autophagosome induction as our previous assays. As MDC staining is already cited to not be the most reliable assay due to high dependence on intracellular pH, vacuole pH, and therefore differences in cellular environment, we continued our investigations to a p62 analysis.

p62 is nuclear membrane protein found to have an LC3-interacting region (LIR) by which it binds to specific residues of LC3. p62 can serve as a link between LC3B and ubiquitinated substrates, and has been proposed to be specifically degraded through the autophagic pathway (*267, 268*). Therefore, the activity of autophagy should inversely correlate with p62 protein levels. As seen in Figure 33, when differentiated 3T3-L1 adipocytes were treated with HIV PIs, there is an accumulation of p62 at higher (25 μM) concentrations.

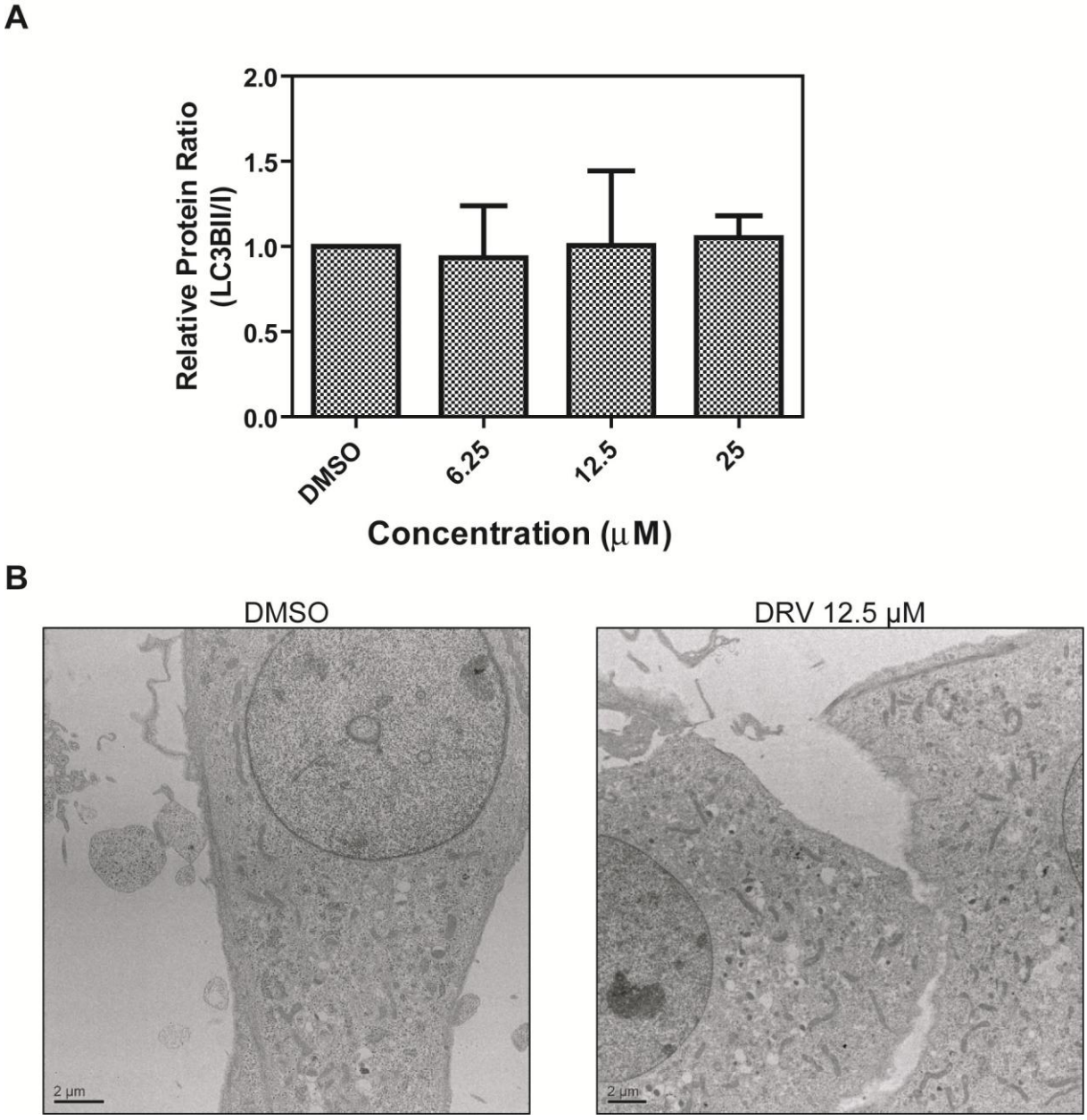

Figure 31. Darunavir does not significantly activate autophagy in 3T3-L1s. A) Differentiated 3T3-L1s were treated with increasing concentrations of darunavir (DRV) or DMSO control for 48 h. Density of immunoreactive bands against LC3B and Actin was determined by Quantity One. Value means ± SE are shown. **B)** Non-differentiated 3T3-L1s were treated with 12.5 μM of DRV for 48 h, and cells analyzed by electron microscopy. Representative images at 2,000 × are shown.

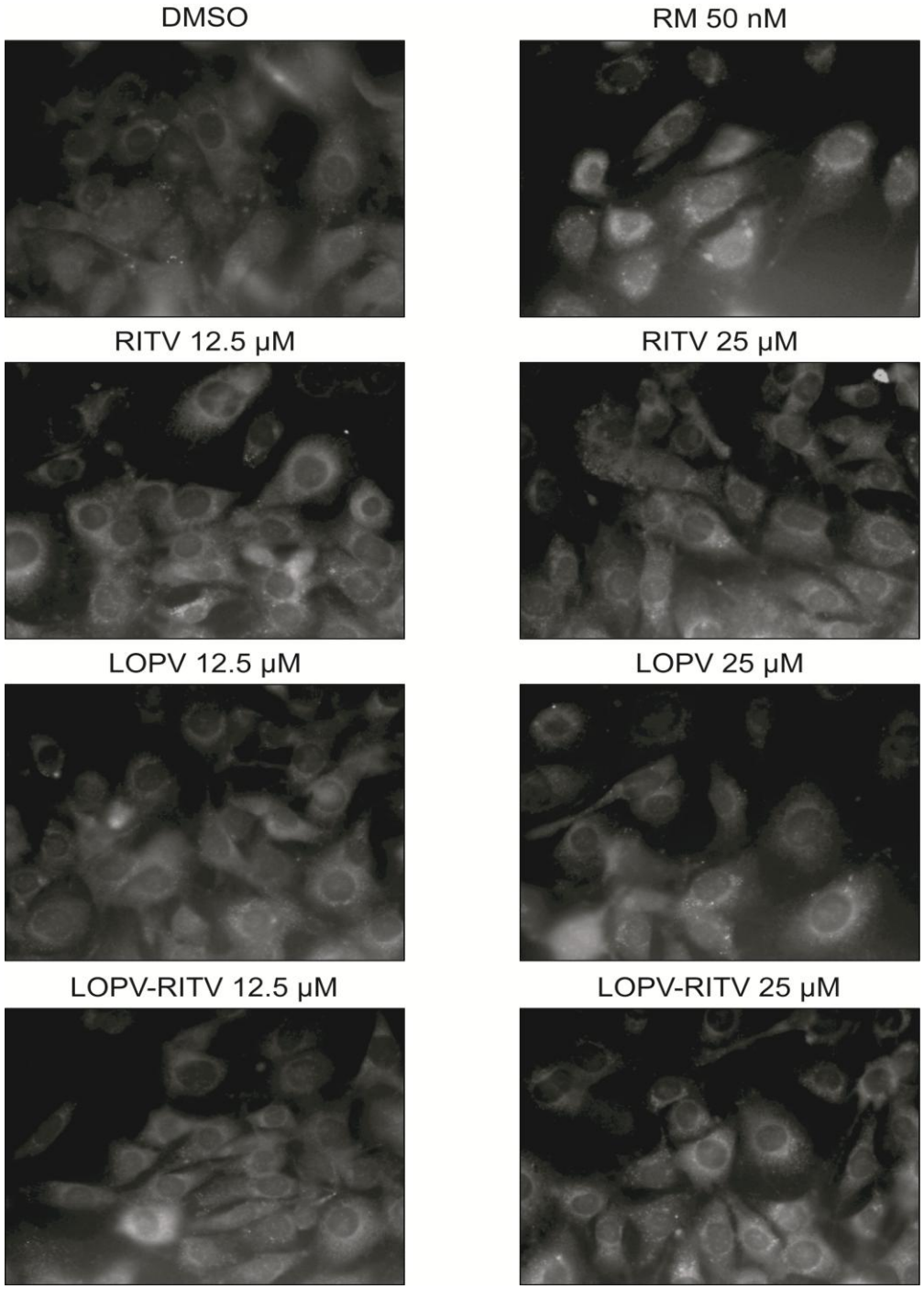

Figure 32. HIV PIs increase late autophagosome accumulation without dose-dependence. Non-differentiated 3T3-L1 cells were treated with HIV PIs (12.5 or 25 µM), rapamycin (RM) 50 nM, or DMSO control for 24 h. Cells were stained with 25 µM MDC for 5 min at 37ºC. Images were acquired on a fluorescent microscope with a 60 × objective. Micrographs were desaturated for easier visualization of punctuate. Images are representative of four separate experiments.

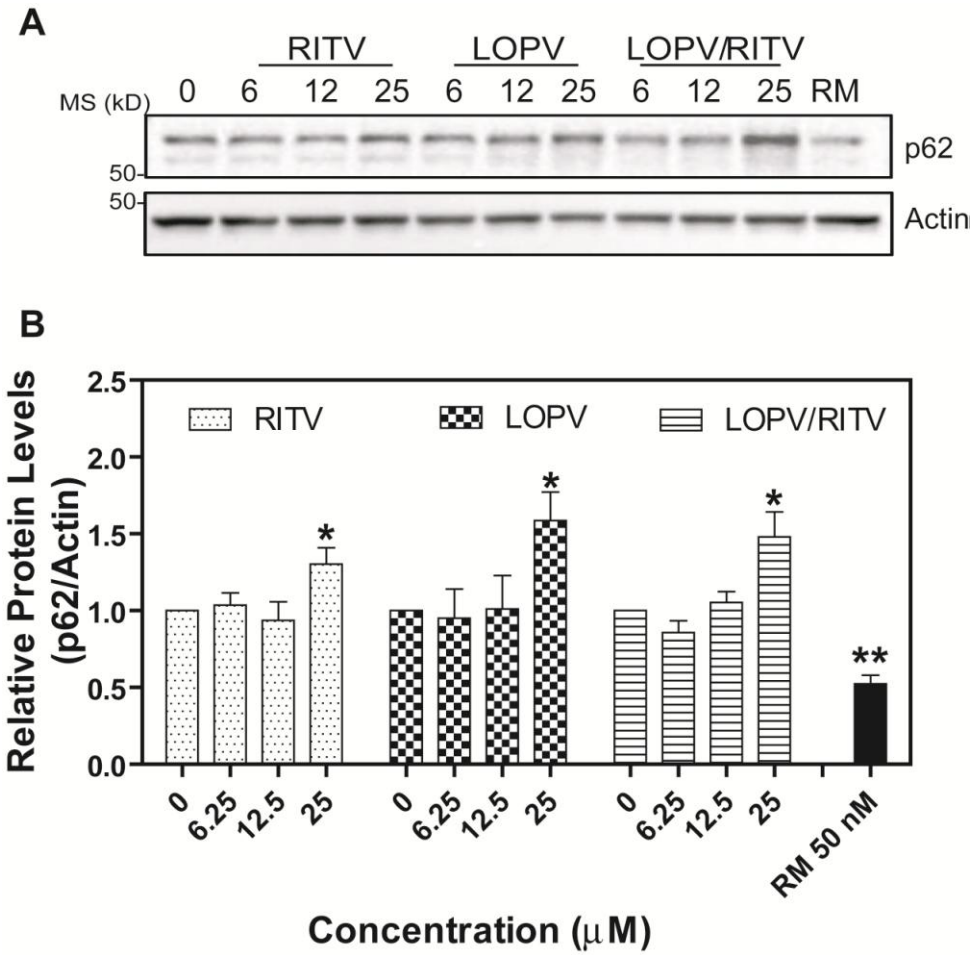

Figure 33. Effect of HIV PIs on p62 degradation. Differentiated 3T3-L1s were treated with increasing concentrations of HIV PIs for 48 h, and total cell lysates analyzed. **A)** Representative immunoblots of p62 and Actin. **B)** Relative protein level of p62 was determined by Quantity One using Actin as loading control. Values are mean ± SE of three independent experiments. Statistical significance relative to DMSO contol (0); *p<0.05, **p<0.005.

However, this may be attributable to inhibition of the proteasome (see Discussion).

To further follow this observation, we examined the effect of HIV PIs on degradation of GFP-tagged LC3B. When cells are transfected with a plasmid containing this construct, green punctuate are formed at the induction of autophagy as GFP-LC3BII accumulates at autophagosomes, versus a homogenous cytoplasmic green from GFP-LC3BI (Figure 34A). However, as these autophagosomes mature into autolysosomes, the LC3B on the internal membrane is degraded while GFP is released into the cytosol. This can be tracked by Western blot analysis. We found an accumulation of GFP when 3T3-L1 cells infected with a retrovirus containing this construct were treated with HIV PIs, with more accumulation at 48 than 24 h (Figure 34 B,C). This suggests that the fusion of autophagosomes with lysosomes is being completed in the presence of HIV PIs.

Effect of CHOP and ATF-4 on HIV PI-Induced Autophagy

In order to identify the potential link between HIV PI-induced ER stress and subsequent autophagy induction, we first examined the effect of CHOP on HIV PI-induced autophagy stress by overexpressing and knocking down CHOP with constructed lentiviral vectors (see Methods). With knockdown of CHOP, we saw a decrease of total LC3B protein levels, while overexpression had little affect (Figure 35A). In addition, there was a slight decrease of total LC3B, and insignificant alterations of LC3BII:I when 3T3-L1s overexpressing CHOP were treated with HIV PIs (Figure 35B).

There is current growing evidence of a PERK-autophagy link (*120, 130, 269*). As ATF-4 is upstream of CHOP, and HIV PIs significantly increased ATF-4 in our model, we next

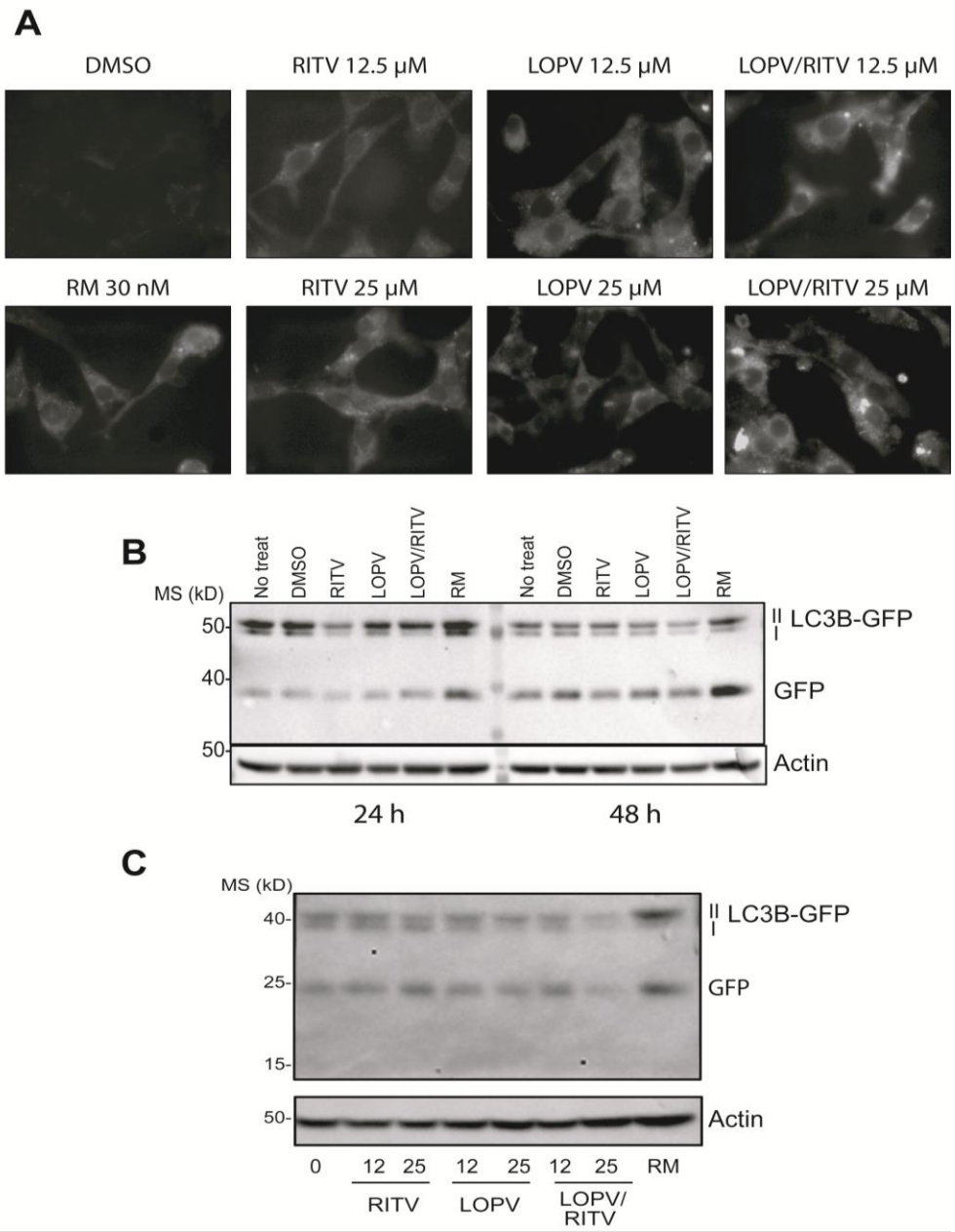

Figure 34. Effect of HIV PIs on GFP-LC3B cleavage. A) 3T3-L1 cells were stably transfected with a plasmid containing GFP-tagged LC3B, and treated with HIV PIs, rapamycin (RM), or vehicle control (DMSO) for 48 h. The fluorescence images were recorded using a 60 × oil lens with FITC filter. Micrographs are desaturated for easier visualization. **B)** 3T3-L1 cells were infected with a retrovirus containing GFP-LC3B and treated with individual HIV PIs (12.5 μM) for 24 or 48 h. Shown are representative immunoblots against GFP and Actin. **C)** 3T3-L1 cells infected with retroviral GFP-LC3B were treated with HIV PIs (12.5 or 25 μM) for 48 h. Representative images of GFP-LC3 and free GFP are shown.

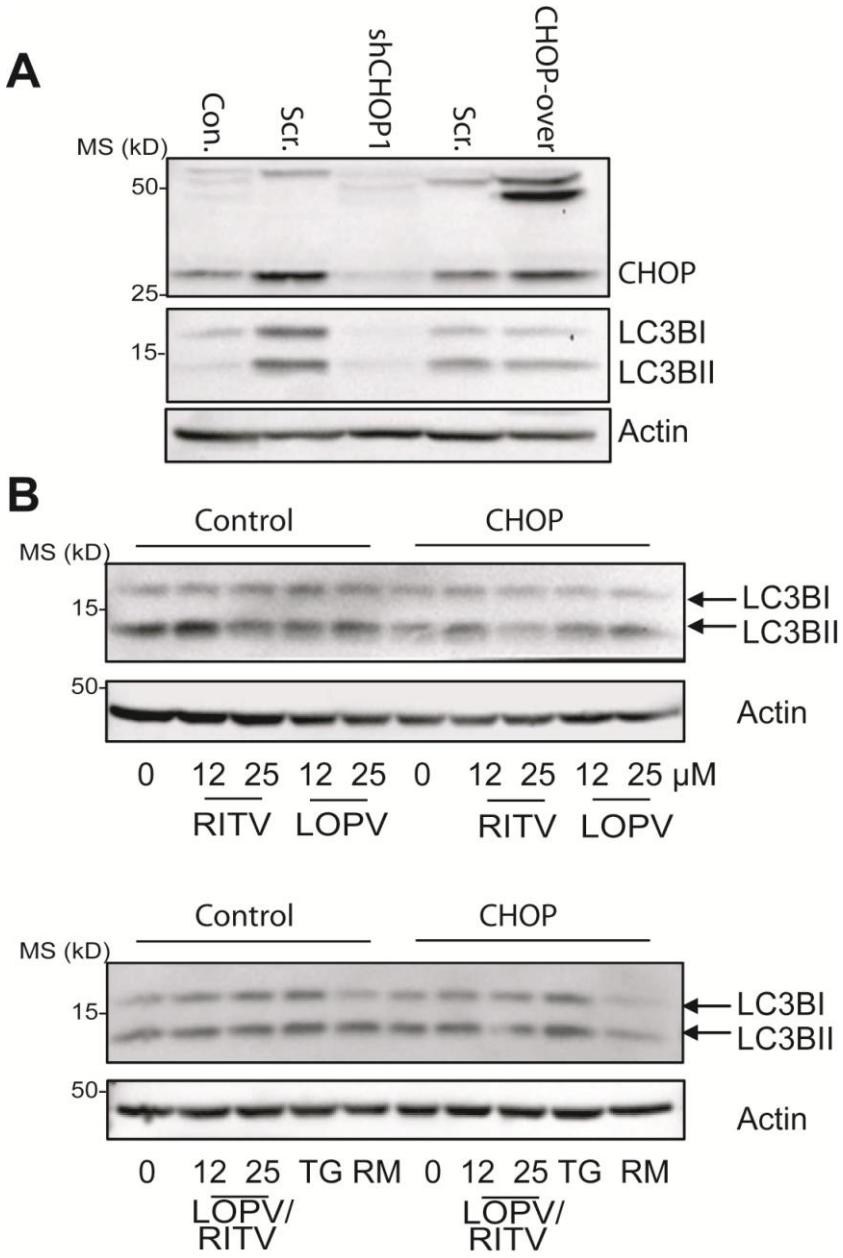

Figure 35. CHOP and HIV PI-induced LC3B. A) 3T3-L1s were infected with lentivirus containing either shRNA against CHOP (shCHOP1), recombinant GFP-CHOP (CHOP-over), or control virus for 48 h. Total cell lysates were used for Western blot analysis. Shown are representative immunoblots against CHOP, LC3B, and Actin as loading control. **B)** 3T3-L1 cells were infected with recombinant constitutively active CHOP or control virus. Stable colonies were treated with HIV PIs (12 or 25 µM), DMSO control (0), or positive controls (TG and RM 50 nM) for 24 h. Shown are representative immunoblots against LC3B and Actin from two separate experiments.

examined whether ATF-4 is the connecting link of HIV PI-induced UPR and autophagy. Using a lentiviral shRNA specifically targeting mouse ATF-4, mRNA ATF-4 level was successfully down-regulated by more than a 50% in 3T3 cells (Figure 36A). The downregulation of ATF-4 in 3T3-L1s inhibited both LOPV- and LOPV/RITV-induced increases of total LC3B protein, but had no effect on RITV-induced increase of LC3B. In addition, conversion of LC3BII:I was not significantly altered in this model. However, the results demonstrate that HIV PI-induced UPR may lead to an increased ability of autophagosome formation with increased substrate LC3B.

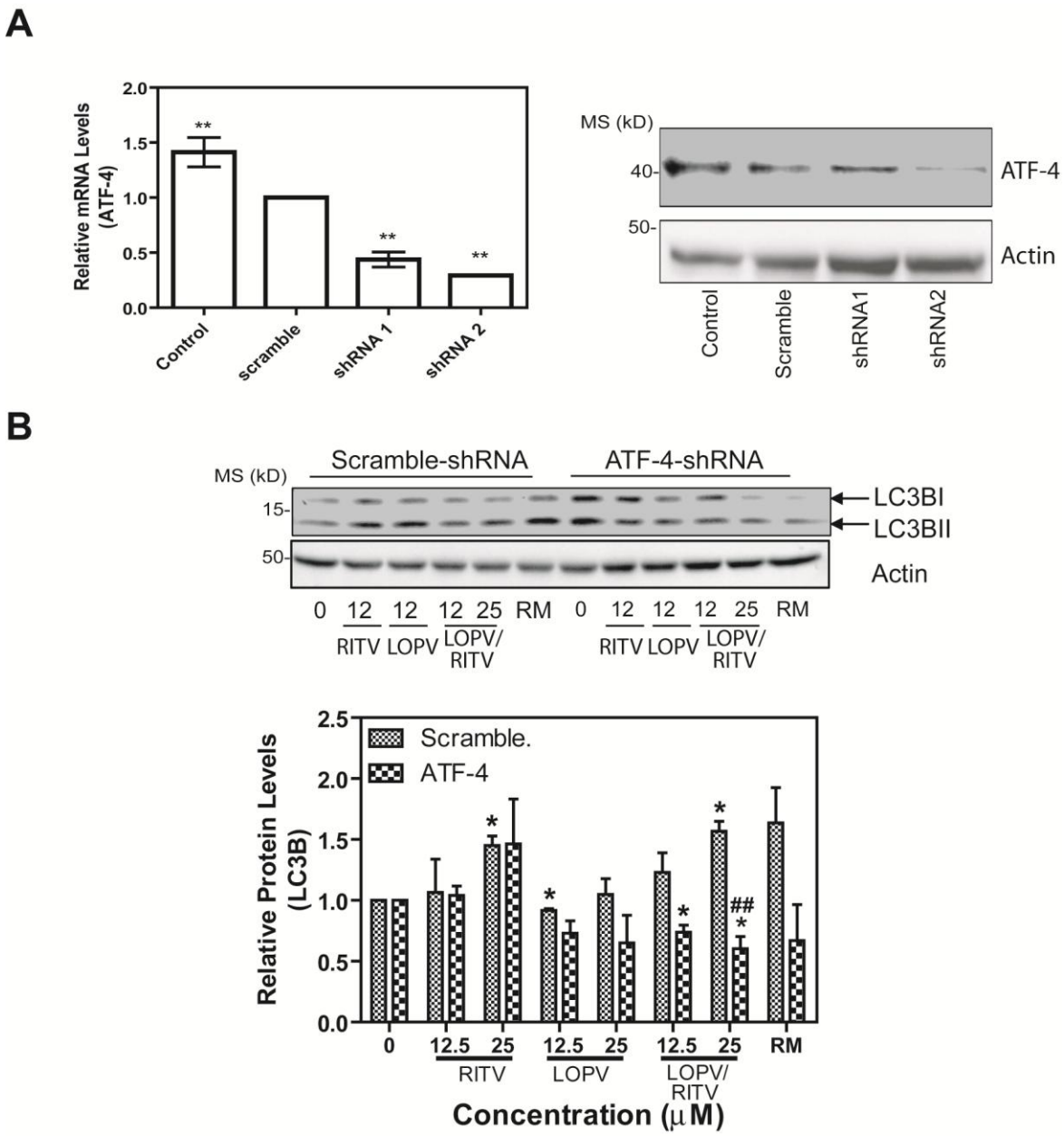

Figure 36. ATF-4 and HIV PI-induced LC3B. 3T3-L1s were infected with lentiviral shRNA specific to ATF-4, or scramble control. Stable colonies were selected using puromycin. **A)** The knockdown efficiency of shRNA was determined by real-time RT-PCR and Western blot analysis. **B)** Stable colonies of 3T3-L1 cells infected with control or shRNA lentivirus were treated with HIV PIs (12 and 25 μM), DMSO (0), or rapamycin (RM) 50 nM for 24 h. Representative immunoblots are shown. Relative protein levels of LC3B using Actin as loading control were determined with Quantity One. Values are mean ± SE of three independent experiments; *p<0.05 compared to vehicle control; ##p<0.005 compared to control shRNA.

SIGNIFICANCE

HIV PI therapy will not, and should not, be discontinued in the near future due to their high effectiveness in controlling viral load in patients. Instead, investigators now need to focus on inhibiting HIV PI-induced risks of metabolic syndrome and cardiovascular disease (*22, 31, 236*). Elucidating the effects of this drug class can have on the metabolically important adipose tissue, and central adipocytes, is essential in development of improved therapies.

In order to fully understand HIV PI-induced lipid metabolism dysregulation in adipocytes, we turned to the autophagic pathway. Autophagy has been recently identified as a new cellular target for dysregulation of lipid metabolism and accumulation (*262*). In addition, autophagy is also shown to be involved in body lipid profile and pathologically in metabolic diseases such as obesity (*261, 270*).

We have shown that some HIV PIs induce autophagy dose-dependently in mouse and human adipocytes (Figures 28, 29). In fact, the HIV PIs we have found that do not induce autophagy fall under the 'UPR non-inducer' subclass (i.e. DRV - Figure 31). In addition, autophagy activation did not occur to the same extent in non-differentiated as differentiated adipocytes, similar to our HIV PI-induced UPR results.

By using TEM, we have further supporting evidence that HIV PIs LOPV and RITV siginificantly upregulate autophagosome production (Figure 30). This upregulation does not seem to be through inhibition of autophagsome-lysosome fusion (Figures 33, 34). In this regard, we would like to address the accumulation of p62 with higher concentrations of HIV PI treatments. The nuclear membrane protein p62 has been proposed to be degraded specifically through autophagy. Therefore, the activity of autophagy should inversely correlate with p62 protein levels (*267, 271, 272*). However, we disagree with the specificity of this assay as other

sub-populations of p62 may also exist (*273*). Particularly, one recent publication has demonstrated that p62 associates with the 26S proteasome, and inhibition of proteasome activity leads to p62 accumulation (*274*). HIV PIs have already been shown to inhibit the activity of the 26S proteasome dose dependently, with LOPV and RITV inhibiting chymotryptic activity 50-60% at 25 µM (*223*). In our findings, p62 did not accumulate until this concentration. In addition, HIV PIs did not inhibit autolysosome cleavage of the GFP-LC3 construct. Taken together, we do not believe HIV PIs are inhibiting autophagic flux, although further assays are needed to definitively ascertain this observation.

We have demonstrated that HIV PIs activate the UPR at an earlier time point than autophagy, and many similarities of activation occur for both pathways. Therefore, we next aimed to determine a link between HIV PI-induced UPR and autophagy. We began this investigation with CHOP, as we had seen abrogation of HIV PI-induced adipocyte lipid metabolism dysregulation with absence of CHOP. Indeed, CHOP knockout decreased total LC3B, but CHOP overexpression had only a slight effect on HIV PI-induced LC3B protein. However, this could be accounted for an already saturated system, and further incricate studies need to be completed to fully elucidate this result.

We next went upstream to ATF-4, as others have already shown a PERK-pathway connection with autophagy induction (*120, 130, 269*). We show ATF-4 knockout abrogates LOPV and LOPV/RITV upregulation of LC3B protein. As written in the final discussion, Rzymski *et. al* have recently shown ATF-4 to bind to the 5'UTR of the LC3B promoter at times of hypoxia-induced ER stress (*130*). As with our studies, when ATF-4 was knockdown with siRNA there was a decrease in total LC3B protein levels. However, our results also suggest CHOP plays a major role in ER stressed-induced autophagy. While CHOP is downstream of

ATF-4, if the findings of Rzymski *et. al* hold true, knockdown of CHOP should have little to no affect on LC3B levels. We did not find this to be the case, and have additional data that suggests CHOP plays a major role in ER-stress induced autophagy in hepatocytes (Chapter 5). Therefore, CHOP may act separately independently of ATF-4 in activating autophagy, as has been suggested by others (*275*).

HIV PI cellular alterations are indeed complex, but our studies are beginning to piece together how HIV PIs induced lipid metabolism dysregulation. We have already shown HIV PIs to differentially activate ER stress and autophagy in adipocytes. We hypothesize inhibition of HIV PI-induced ER stress will relieve downstream activation of autophagy and lipid metabolism dysregulation. Such a hypothesis has translated well to another central cell type in lipid metabolism regulation, hepatocytes, as shown in the next chapter.

CHAPTER V: Raltegravir Inhibits LOPV/RITV-Induced Autophagosome Accumulation in Hepatocytes

STUDY RATIONALE

Although HAART has drastically decreased the mortality of those living with HIV, it has also been linked to cardiovascular complications, with recent demonstrations that the PI component is much to blame (*21-23, 276*). In addition, many of these patients also have non-alcoholic fatty liver disease (NAFLD), or even nonalcoholic steatohepatitis (NASH) (*40, 41*), which is correlated with HIV PI-induced insulin resistance and visceral fat hypertrophy.

Endoplasmic reticulum (ER) stress may be a central pathway involved in HIV PI-induced NAFLD. In nutrient-induced NAFLD, saturated fatty acids induce ER stress, activating deleterious pathways that lead to increased inflammation and insulin resistance (*58, 246, 277, 278*). We have previously shown that HIV PIs induce ER stress and its signaling pathway, the unfolded protein response (UPR), leading to lipid metabolism dysregulation in hepatocytes (*49, 50, 222*). Some HIV PI-induced lipid accumulation in hepatocytes is also directly attributed to an increased activation of sterol regulatory element binding protein (SREBP)-1, a lipogenic transcription factor activated at times of ER stress (*70, 279*).

Autophagy is another cellular pathway now known to be involved in hepatocyte lipid metabolism regulation. Although autophagy was first defined as a degradative pathway to remove accumulated proteins, infectious particles, or supply the cell with ATP, it is now known that this pathway is also involved in lipolyis and LD turnover (*205, 280*). When autophagy is inhibited in hepatocytes, LDs increase (*205*) not due to increased triglyceride synthesis nor decreased VLDL secretions (*225*). In addition, mice lacking autophagy have enlarged lipid laden

livers with increased triglyceride and cholesterol levels (*205*). Therefore, we hypothesize that alterations in autophagy could be another underlying mechanism in HIV PI-associated NAFLD.

Recently, we have demonstrated that the integrase inhibitor raltegravir (MK-0518) can inhibit HIV PI-induced lipid metabolism dysregulation in hepatocytes (*222*). In addition, we have shown HIV PIs to significantly induce autophagy in adipocytes. Using hepatic cell lines and primary cells, we aimed to determine if raltegraivir inhibits LOPV/RITV-induced lipid accumulation through autophagy. In addition, we further elucidated a link between HIV PI-induced ER stress and autophagy.

RESULTS

Raltegravir inhibits HIV PI-induced lipid accumulation in hepatocytes

We have previously shown that HIV PIs with metabolic side effects in the clinic increase fatty liver *in vivo*, and alter lipid metabolism in hepatocytes *in vitro* (*49, 222*). In addition, we now have evidence that raltegravir can inhibit LOPV/RITV hepatocyte lipid accumulation as shown in both Figure 37 and (*222*). However, the mechanism behind this inhibition is not fully elucidated, only partially explained by an abrogation of UPR activation (*222*).

HIV PI combination LOPV/RITV 4:1 induces autophagy in hepatocytes

As autophagy is now known to be a major pathway involved in lipid metabolism (*205, 225*), we next tested if LOPV/RITV alteration of lipid metabolism in hepatocytes could also be explained by an alteration of autophagy. As previously mentioned, activation of LC3B from cytosolic (I) to cleaved and lipidated form (II) is frequently analyzed by Western blot to determine if autophagosome numbers are increasing (*266*). We found that in a both time and dose-dependent manner, LOPV/RITV did increase LC3BII:I ratio in rat and mouse primary hepatocytes (Figure 38), as well as a human hepatocyte cell line (HepG2 - data not shown). As 24 h was the peak activation, we used this time point for subsequent experiments.

Raltegravir inhibits LOPV/RITV induction of autophagy

We next wanted to elucidate if raltegravir, an anti-retroviral with little known clinical lipid side effects, activated autophagy similarly as LOPV/RITV which has a high clinical lipid side effect profile. Rat primary hepatocytes (RPH) were treated with increasing concentrations of raltegravir at 24 h. As seen in Figure 39A, there was actually a trend of decreasing LC3BII:I

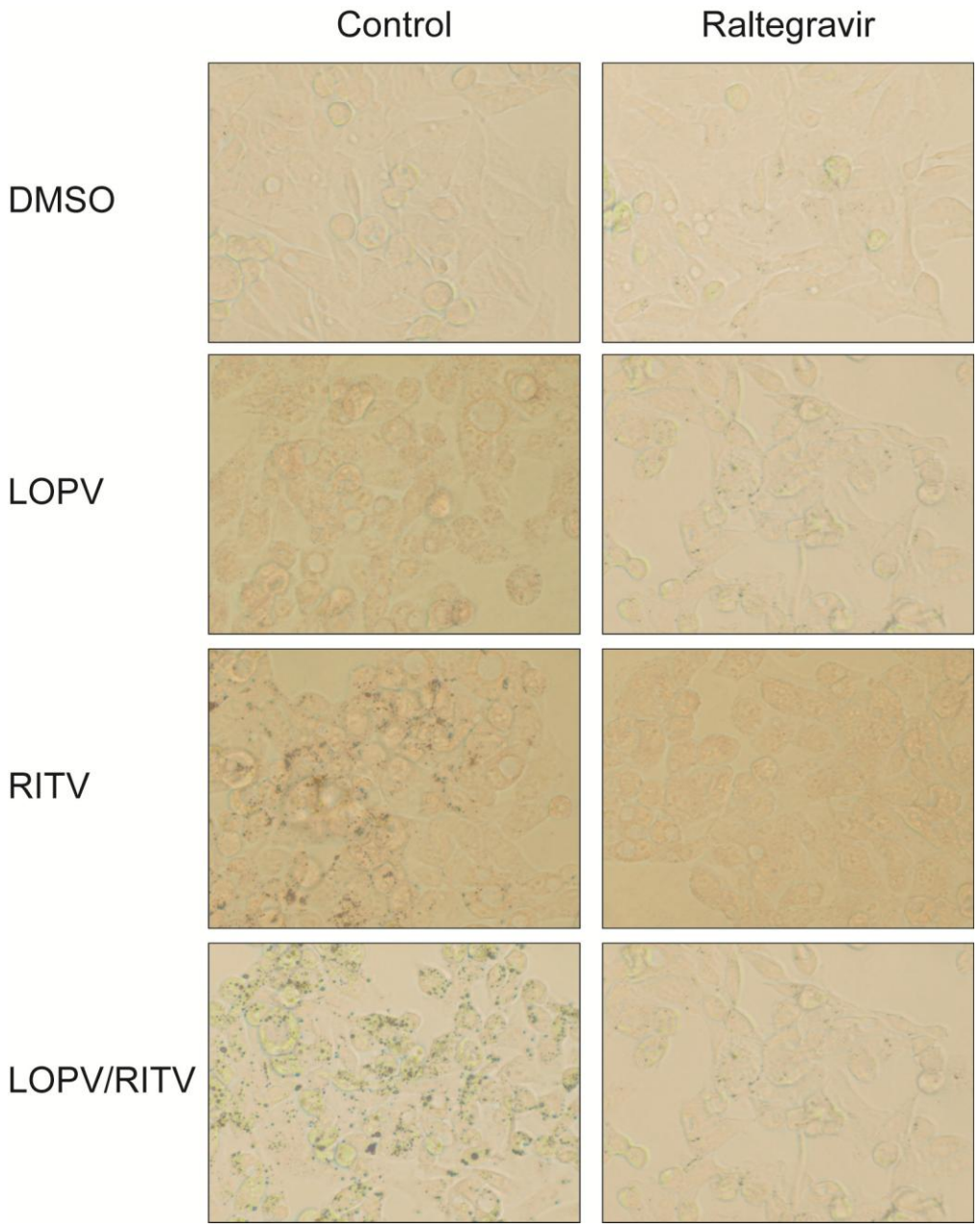

Figure 37. Raltegravir abrogates LOPV/RITV-induced lipid accumulation in rat primary hepatocytes. RPH were treated with raltegravir (25 µM) and LOPV/RITV (25 µM) together or alone for 48 h. Cells were fixed and stained with Oil Red O and analyzed using a light microscope at with a 40 × objective lens. Shown are representative images from three independent experiments.

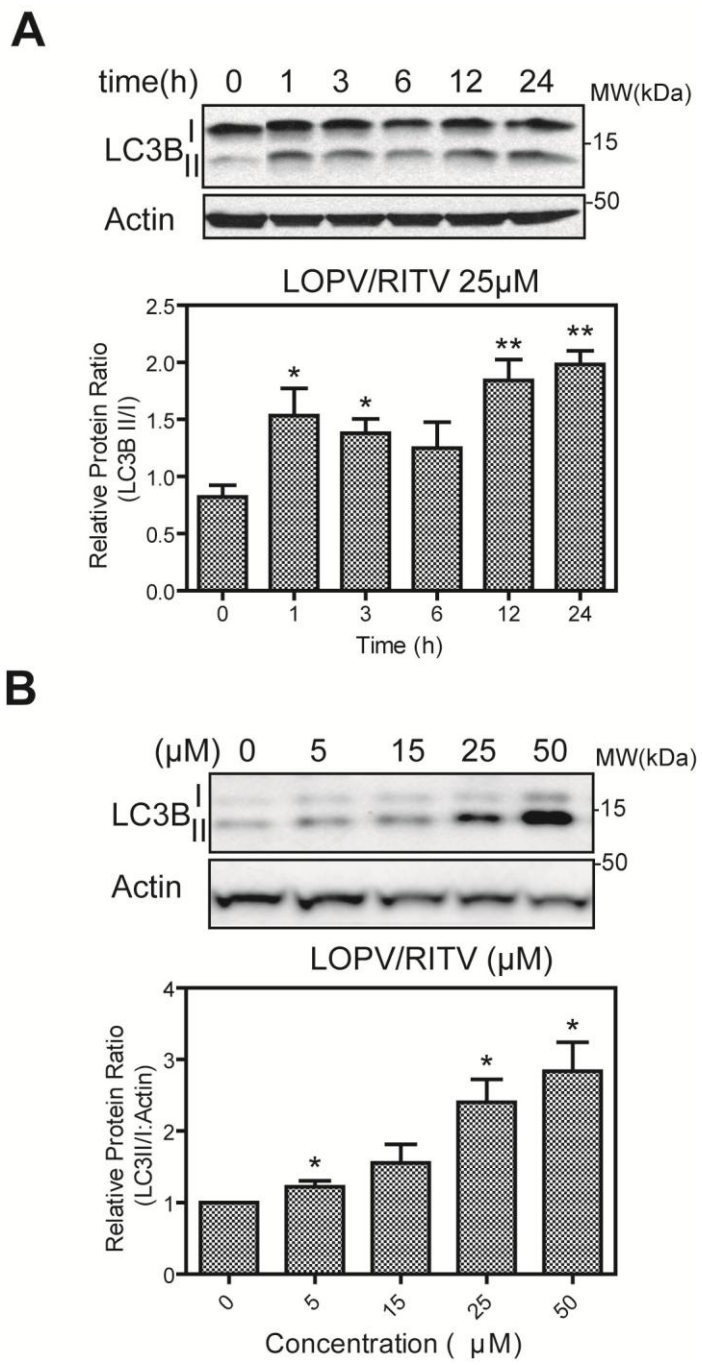

Figure 38. LOPV/RITV 4:1 increases LC3BII:I in rat and mouse primary hepatocytes. A) RPH were treated with 25 μM LOPV/RITV for 0, 1, 3, 6, 12, or 24 h and **B)** MPH were treated with increasing concentrations of LOPV/RITV at 24 h. Representative immunoblots of LC3B and Actin are shown. Densitometry was determined using Image J with Actin as loading control. Values are mean ± SE of three independent experiments; *$p<0.05$ and **$p<0.005$ compared to vehicle control (0).

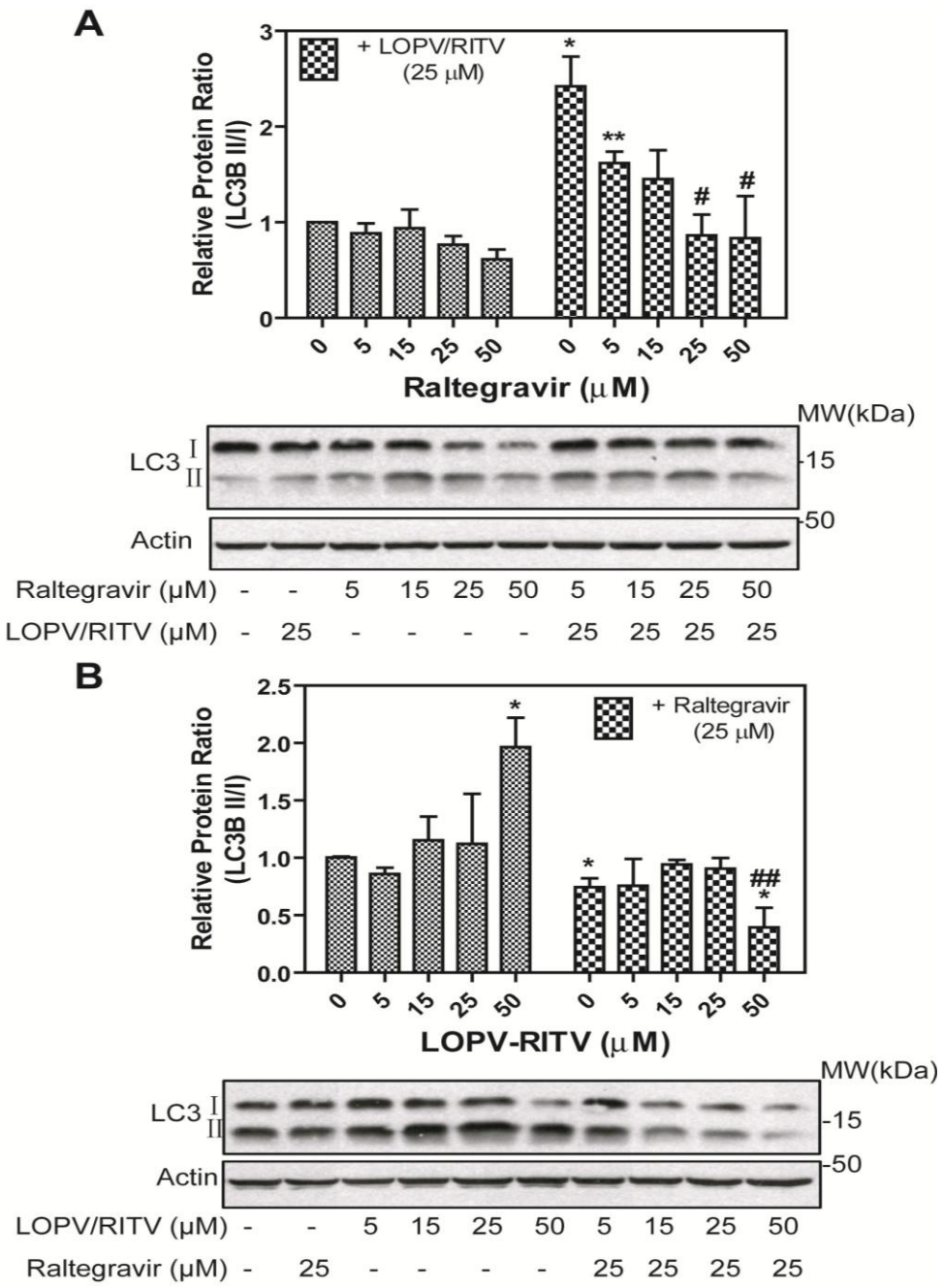

Figure 39. Raltegravir abrogrates LOPV/RITV-induced LC3BII:I in hepatocytes. RPH were treated with increasing concentrations of raltegravir with or without LOPV/RITV 25 μM **(A)** or increasing concentrations of LOPV/RITV with or without raltegravir 25 μM **(B)** for 24 h. Representative immunoblots against LC3B and Actin are shown. Densitometry was determined with Image J. Values are mean ± SE of three independent experiments; *p<0.05 compared to vehicle control; #p<0.05 and ##p<0.005 compared to same dose of single treatment.

ratio with raltegravir treatment. In addition, when added to increasing concentrations of LOPV/RITV treatments, raltegravir significantly inhibited LOPV/RITV dose-dependent increase of LC3BII:I. Increasing concentrations of raltegravir given with 25 μM of LOPV/RITV showed a dose-dependent decrease in LC3BII:I ratio (Figure 39A,B).

HepG2 cells were treated with 25 μM raltegravir and/or LOPV/RITV for 24 hours, and mRNA analyzed by real-time RT-PCR. As shown in Figure 40, LOPV/RITV significantly increased the transcripts of proteins important in macroautophagy induction (Atg12 and Beclin1 (BECN1)), while raltegravir abrogated this. ULK1 and VPS34, also essential proteins for macroautophagy, followed the same trend although increases in mRNA levels by LOPV/RITV were not statistically significant compared to control.

To ascertain if autophagosomes were indeed increased by LOPV/RITV, and if that increase was abrograted by raltegravir, we assessed treated RPH with both monodansylcadaverine (MDC) stain and transmission electron microscopy (TEM). MDC is a fluorescent dye that normally accumulates in high pH vacuoles, such as late autophagosomes. We found that indeed LOPV/RITV treatment increased MDC accumulations, and raltegravir significantly inhibited this (Figure 41). This held true for the gold standard of autophagy induction, TEM (Figure 42).

Inhibition of autophagy induction by raltegravir is CHOP-Dependent

There is growing evidence of a UPR and autophagy link (*129, 130*). From previously acquired datat, we hypothesized raltegravir inhibition of LOPV/RITV-induced autophagy could occur via inhibition of UPR induction. We have previously shown HIV PIs induce CHOP at both

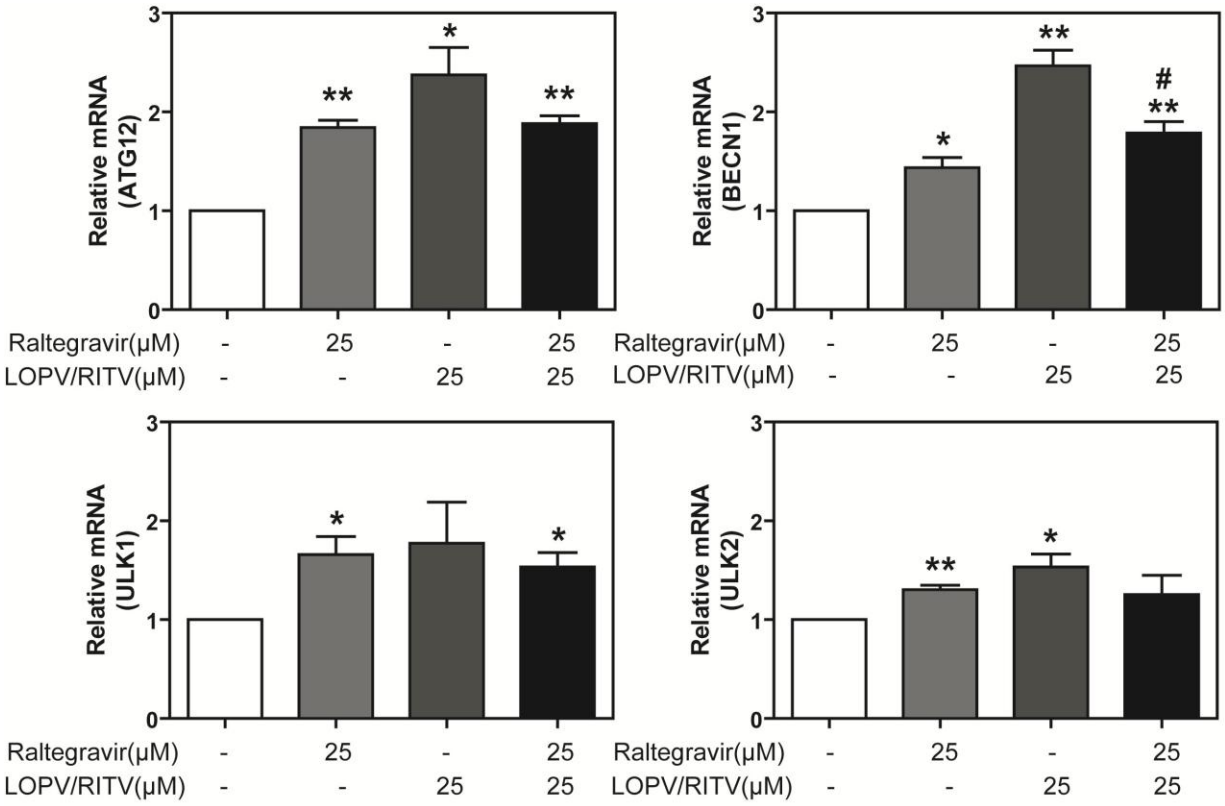

Figure 40. Raltegravir abrogrates HIV PI-induced autophagy at the mRNA level. RPH were treated with raltegravir (25 μM) and LOPV/RITV (25 μM) separately or in combination for 24 hours. Relative mRNA levels of Atg12, Beclin 1(BECN1), ULK1 and 2 were determined by real-time RT-PCR with β-Actin as internal control. Values are mean ± SE from three independent experiments. Statistical significance *p<0.05, **p<0.005 compared to vehicle control (-/-) and #p<0.05 compared to LOPV/RITV alone.

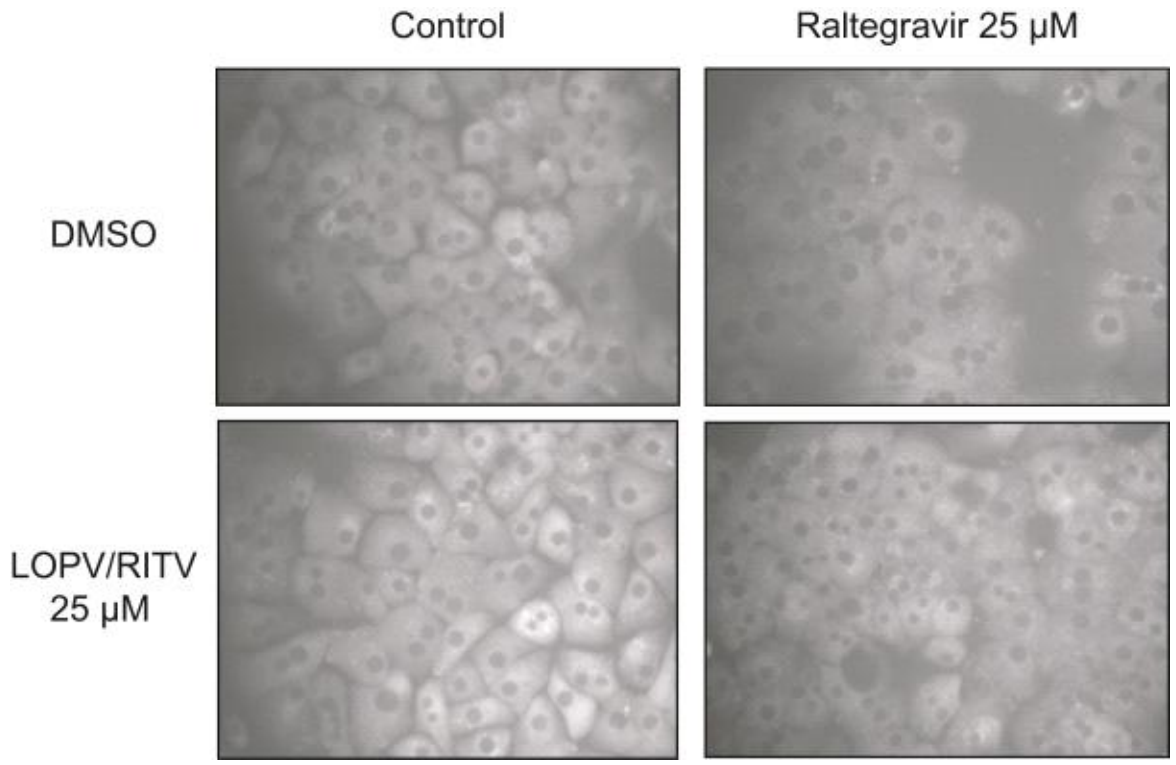

Figure 41. Raltegravir abrogrates LOPV/RITV-induced late autophagosome accumalation in rat primary hepatocytes. RPH were treated with raltegravir (25 µM) and LOPV/RITV (25 µM) separately or combined for 24 h. Cells were stained with MDC, and fluorescence images immediately acquired using a 60 × oil lens with a DAPI filter. Micrographs were desaturated for easier visualization of punctuates. Images representative of three independent experiments.

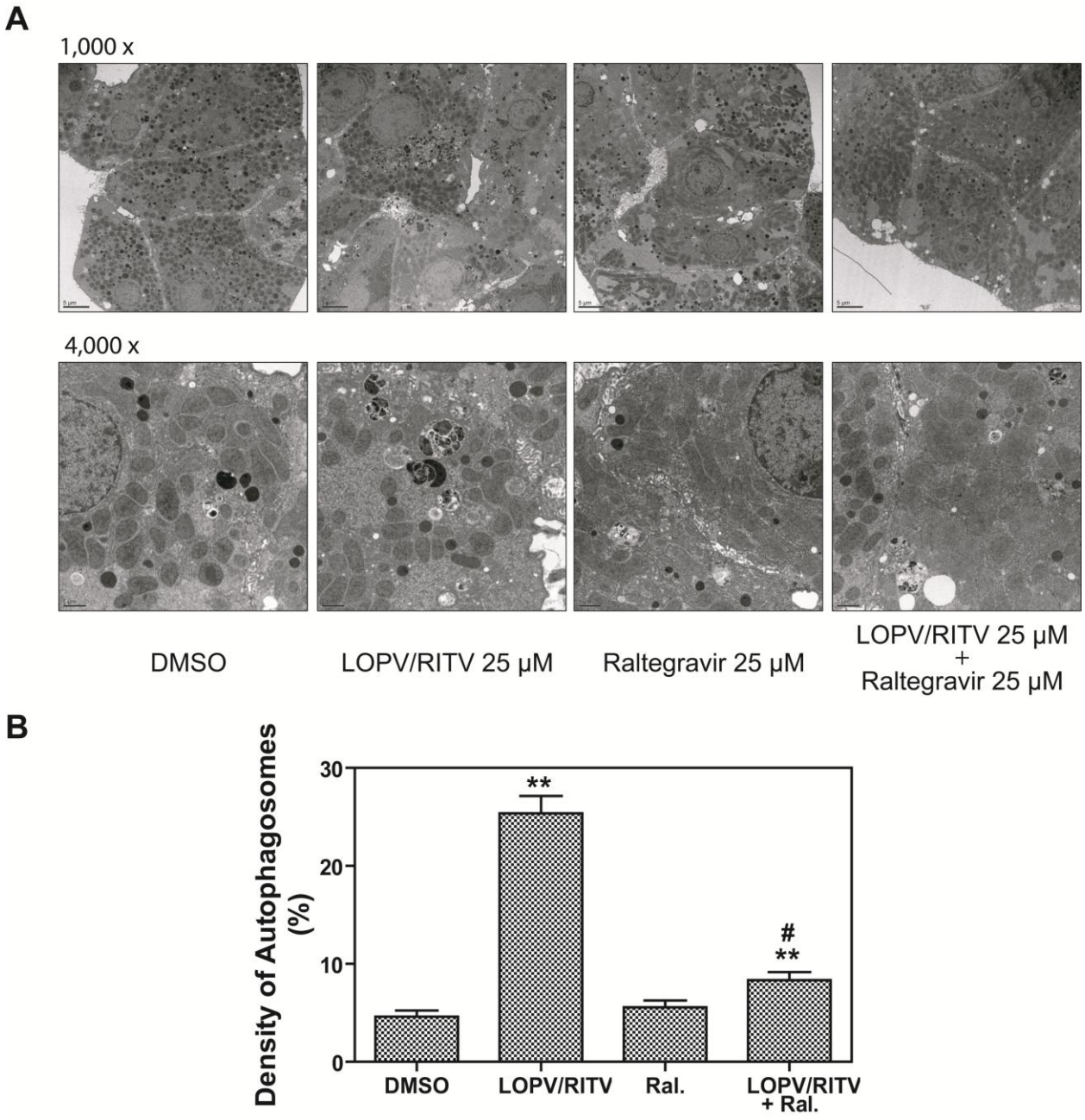

Figure 42. Raltegravir abrogates HIV PI-induced autophagy induction in hepatocytes. RPH were treated with raltegravir (25 µM) and LOPV/RITV (25 µM) separately or combined for 24 h, and cells processed for transmission electron microscopy as described in "Methods." **A)** Representative images at 4,000 ×. **B)** Density of autophagosomes were determined by point counting at 4,000 × using a 1.5 cm lattice. Point counts were completed in at least 15 cells per treatment, 4 images per cell.

time and dose-dependent manners in numerous cell types (*49*, *51*, *53*). In addition, we have shown that HIV PI-induced liver fat accumulation is altered in CHOP$^{-/-}$ mice relative to their wild type counterpart. Raltegravir inhibited LOPV/RITV lipid accumulations in murine livers *(222)*, and we had preliminary evidence this was altered with loss of CHOP.

Therefore, we turned to our CHOP$^{-/-}$ model to determine if raltegravir abrogation of LOPV/RITV-induced autophagy was through the CHOP pathway. As seen in Figure 43, raltegravir failed to inhibit LOPV/RITV-induced LC3B conversion with the absence of CHOP. This demonstrates a vital role of the CHOP pathway in the mechanism underlying raltegravir inhibition of LOPV/RITV-induced autophagy.

We repeated this investigation *in vivo*. As shown in Figure 44, preliminary data suggested raltegravir did inhibit LOPV/RITV-induced LC3B protein in C57BL/6 fed a normal diet. This was followed by a larger experiment in which C57BL/6 wild-type and CHOP$^{-/-}$ male mice were treated with control solution, LOPV/RITV, raltegravir, or both (50mg/kg) for 4 weeks. Livers were isolated for protein analysis by Western blot. As seen in Figure 45, we saw a significant decrease of LOPV/RITV-increased total LC3B with raltegravir treatment, with was abrogated with loss of CHOP.

LOPV/RITV and Raltegravir Effects on Autophagic Flux

In our animal experiments, alteration of LC3BII:I was not as significant as total LC3B changes. While lack of raltegravir conversion was abrogated with loss of CHOP, all other treatments were not significant in both experiments (Figures 44, 45). Some of our hypotheses to explain these results include a low ‘n’ for treatment groups, degradation of small-short lived proteins in our lysates, and/or an alteration of autophagy flux. We therefore further investigated

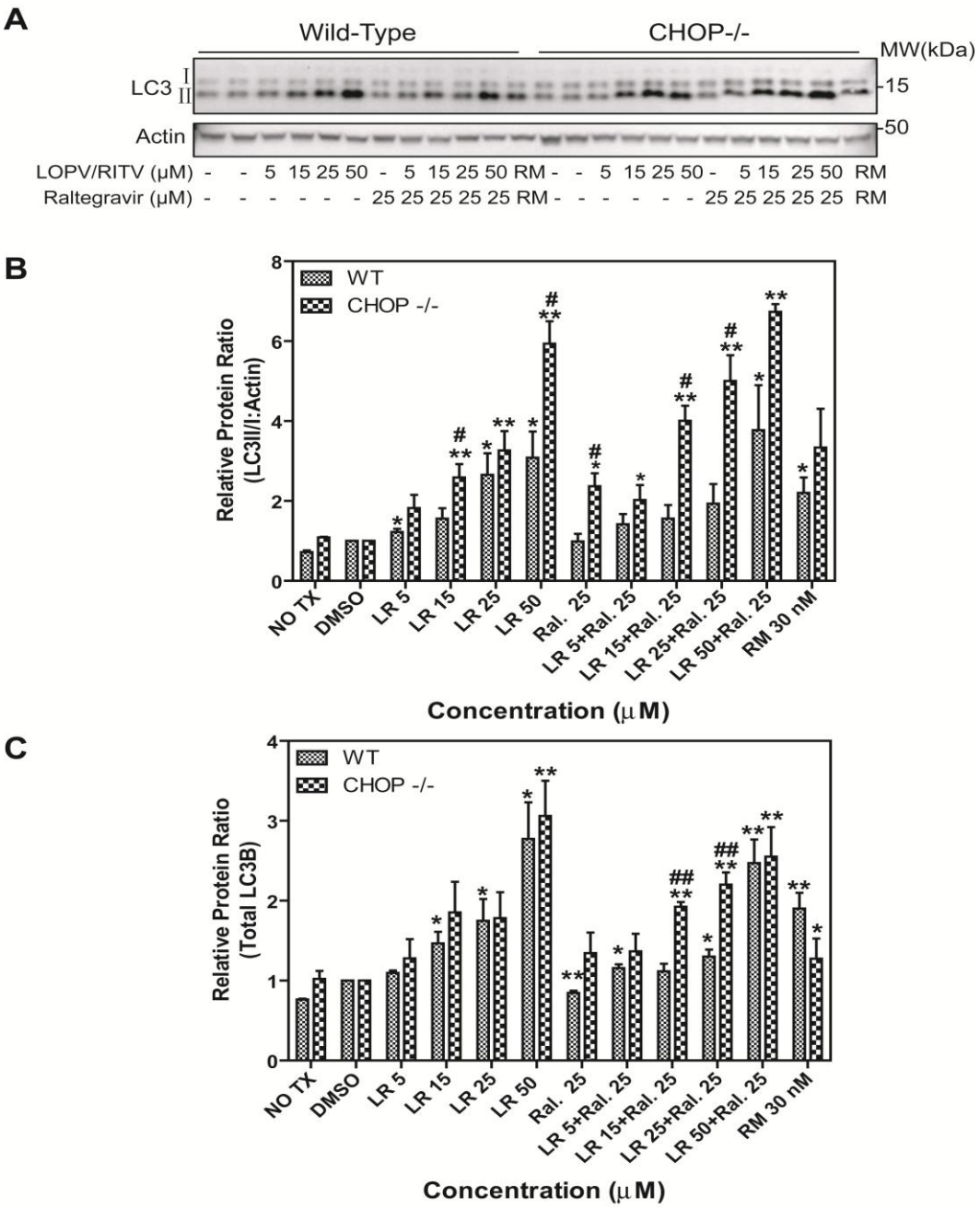

Figure 43. CHOP plays a central role in raltegravir inhibition of LOPV/RITV-induced LC3BII:I. MPH from wild-type and CHOP$^{-/-}$ C57BL/6 male mice were isolated and treated as shown for 24 h. **A)** Representative immunoblots against LC3B and Actin. Denisty of immunoreactive bands was analyzed by Quantity One and relative protein levels determined with Actin as loading control. **B)** Ratio of LC3BII/I and **C)** total LC3B protein. Values are mean ± SE of three independent experiments. Statistical significance *p<0.05, **p<0.005 compared to vehicle control and #p<0.05, ##p<0.005 compared to equivalent treatment of wild-type cells.

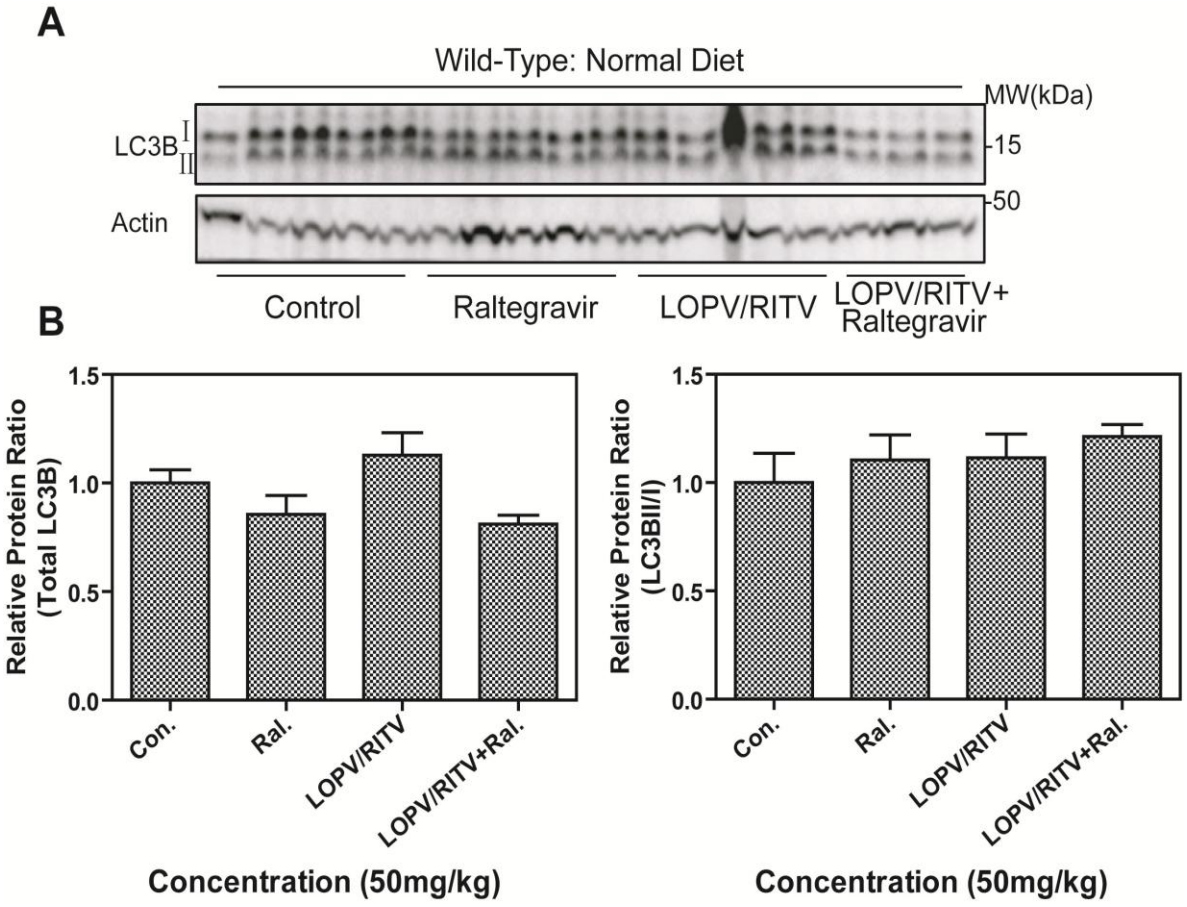

Figure 44. Raltegravir inhibits LOPV/RITV-induced LC3B. C57BL/6 wild-type male mice were fed a normal chow diet and treated with LOPV/RITV (50mg/kg) and raltegravir (50mg/kg), separately or in combination for 4 weeks. Protein from liver samples was analyzed by Western blot. **A)** Immunoblots against LC3B and Actin. **B)** Relative protein ratios using Actin as loading control of total LC3B and LC3BII:I. Values are mean ± SE. n=5 for control (Con.), Raltegravir (Ral.), and LOPV/RITV, while n=3 for LOPV/RITV+Raltegravir.

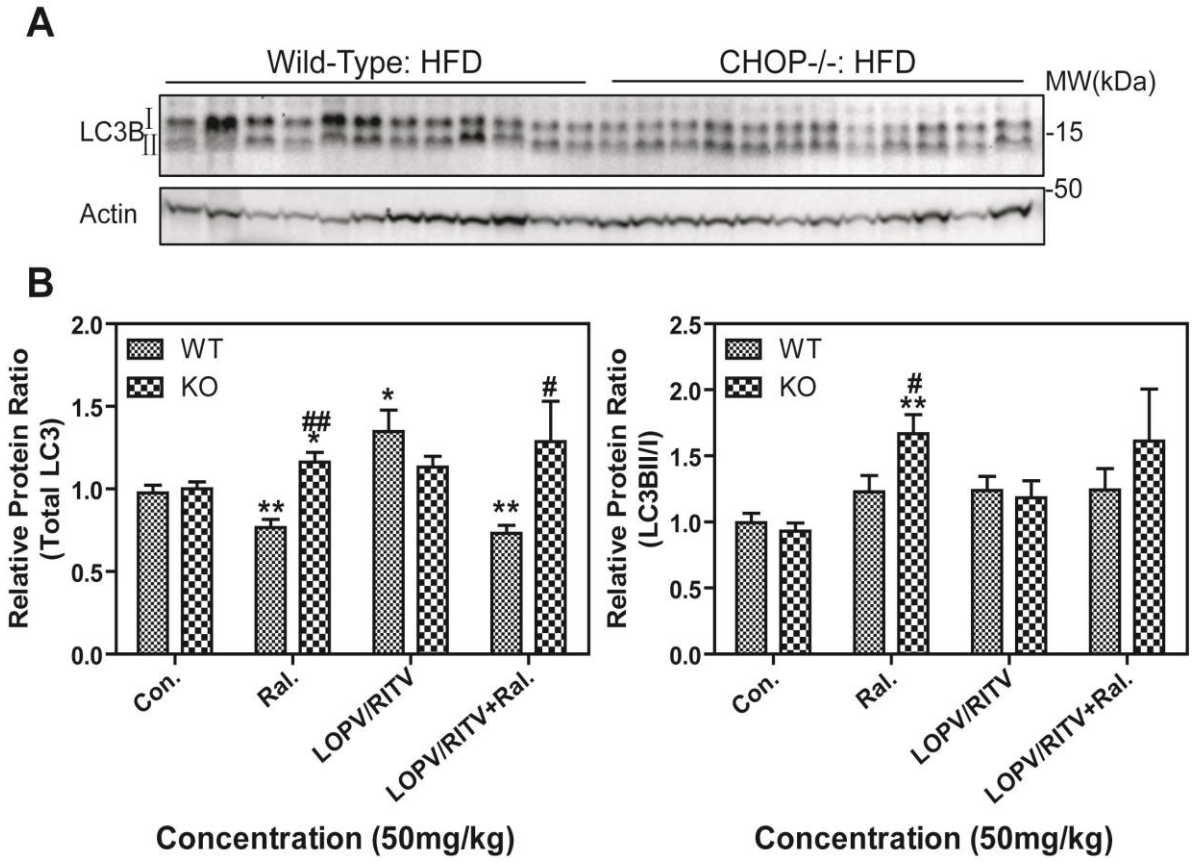

Figure 45. Raltegravir lack of autophagy induction relies on CHOP. C57BL/6 wild-type and CHOP$^{-/-}$ male mice were fed a high fat diet and treated with LOPV/RITV (50mg/kg) or raltegravir (50mg/kg) in combination or separately for 4 weeks. Protein from liver samples was analyzed by Western blot. **A)** Representative immunoblots against LC3B and Actin. **B)** Relative protein levels with Actin as loading control of total LC3B and LC3BII:I. Values are mean ± SE. n=5; *p<0.05, **p<0.005 compared to control; #p<0.05 and ##p<0.005 compared to wild-type.

how autophagy flux is altered in our models.

As explained in Chapter 4, p62 is a nuclear membrane protein proposed to be specifically degraded through autophagy (*267*). We analyzed p62 levels of WT and CHOP$^{-/-}$ MPH treated with increasing concentrations of LOPV/RITV with or without 25 μM raltegravir. As shown in Figure 46, p62 accumulated at higher concentrations of LOPV/RITV, even in the presence of raltegravir (which did not induce accumulation alone). Loss of CHOP abrogated this accumulation. While p62 accumulation may be partially explained by inhibition of proteasome by LOPV/RITV (Chapter 4), the CHOP pathway is shown here to also be involved in this accumulation. We therefore continue our studies to determine if LOPV/RITV did indeed inhibit autophagolysosome action.

HepG2 cells were stably transfected with a plasmid containing GFP-tagged LC3B. As shown in Figure 47A, raltegravir successfully inhibited LOPV/RITV-induced GFP-punctate, supporting our previous results. When autophagosomes fuse with lysosomes, LC3BII is degraded, while the GFP is released to the cytoplasm as it is resistant to these proteases (*281*, *282*). When lysosomal activity is inhibited by pH neutralization (i.e. NH_4Cl) or protease inhibitors (i.e. Leupeptin), GFP-LC3BII cleavage will not occur, and GFP will not accumulate in the cytoplasm. As shown in Figure 47B, addition of lysosomal inhibitors did decrease GFP accumulation compared to control. However, LOPV/RITV treatment slightly increased GFP accumulation.

We further analyzed autophagy flux by inhibiting lysosomal action in RPH treated with LOPV/RITV and raltegravir. As shown in Figure 48, we have preliminary data suggesting both LOPV/RITV and raltegravir do not induce LC3B conversion. Rather, LOPV/RITV treated in the presence of lysosomal inhibitors did not induce LC3BII accumulation any more than lysosomal

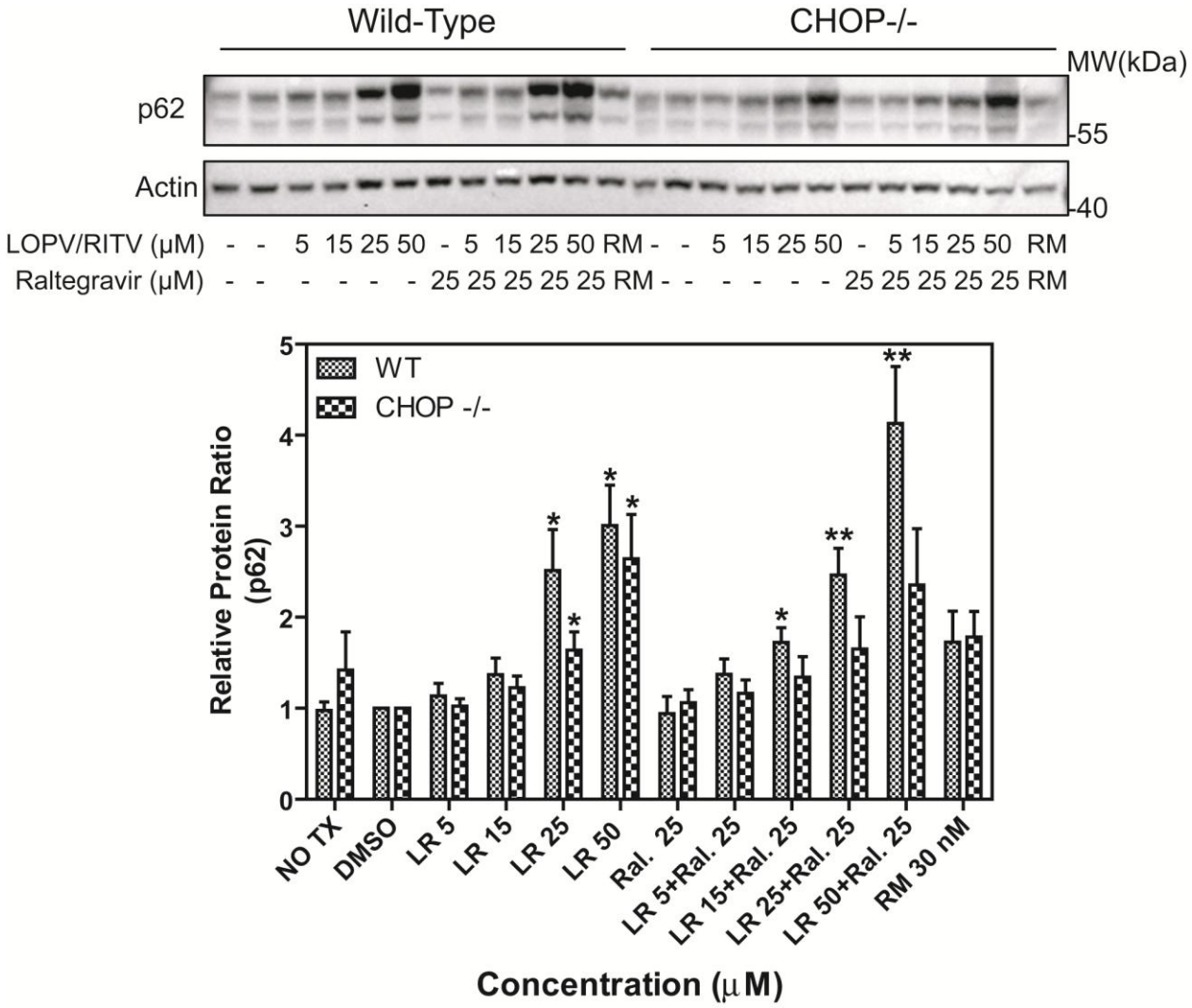

Figure 46. p62 accumulates with high concentrations of LOPV/RITV treatment. MPH from wild-type and CHOP$^{-/-}$ C57BL/6 male mice were isolated and treated as shown for 24 h. Shown are relative immunoblots against p62 and Actin. Relative protein levels of p62 were determined by Quantity One with Actin as loading control. Values are mean ± SE of three independent experiments. *p<0.05 **p<0.05 compared to DMSO control.

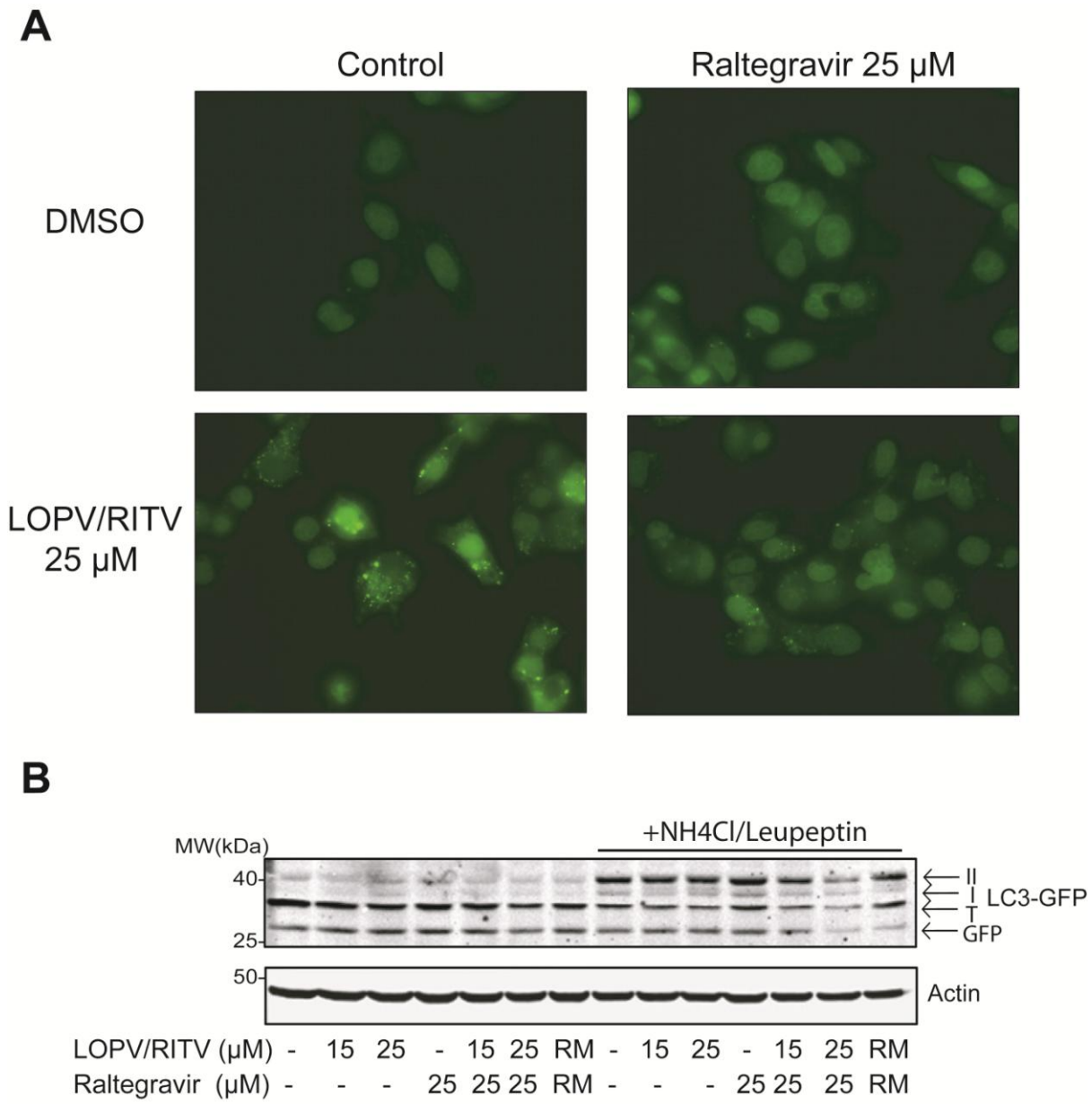

Figure 47. Affect of HIV PIs and raltegravir on GFP-LC3 cleavage in HepG2 cells. HepG2 cells were stably transfected with a plasmid containing GFP-tagged LC3B. **A)** Cells were treated with 25 µM LOPV/RITV and 25 µM raltegravir (separately or in combination) for 24 h. Fluorescent images were acquired using a 60 × oil lens and a FITC filter. **B)** Cells were treated with 15 or 25 µM LOPV/RITV with or without 25 µM raltegravir for 24 h, in the presence or absence of lysosomal inhibitors (100 µM leupeptin/25 mM NH_4Cl). LC3B-GFP and free GFP levels were determined by Western blot analysis using GFP antibody and Actin as loading control. Shown are representative images from at least three independent experiments.

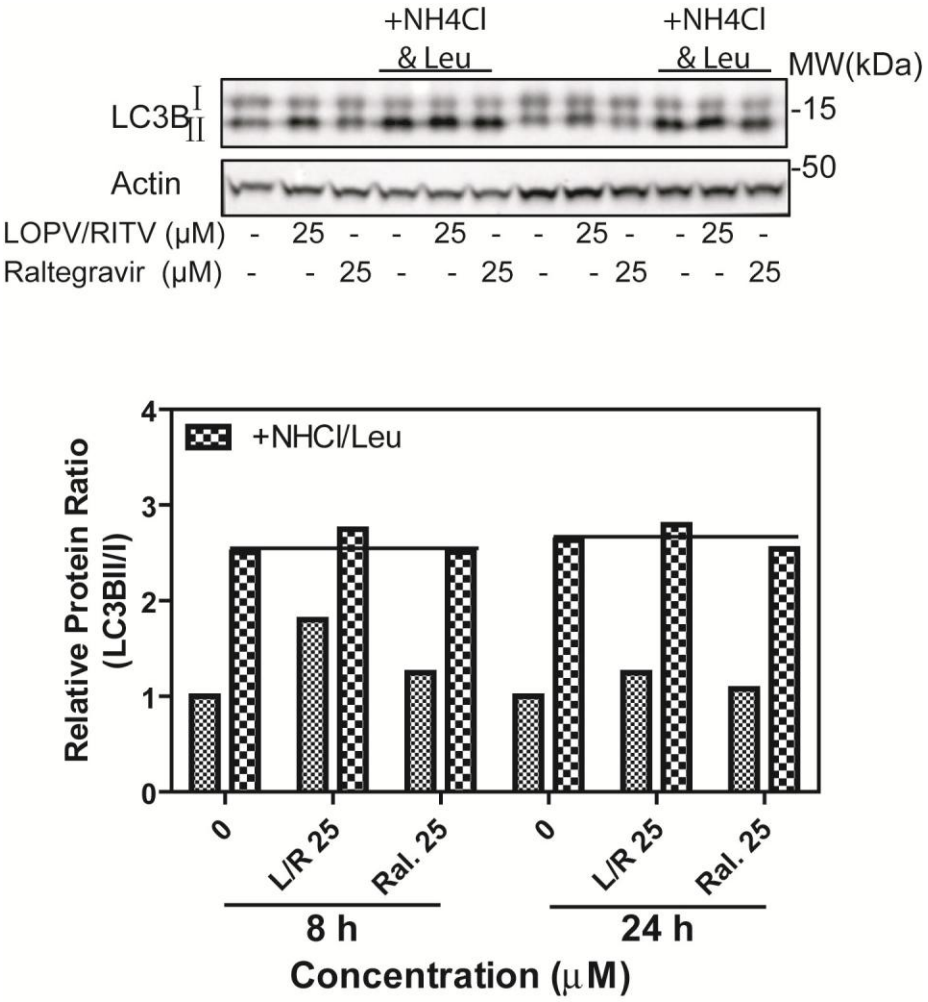

Figure 48. LOPV/RITV and raltegravir may not increase LC3BI activation. RPH hepatocytes with pretreated with 25 mM NH_4Cl/100 μM Leupeptin for 2 hours, followed by 25 μM LOPV/RITV (L/R) or raltegravir (Ral.) for 24 h. Shown are representative immunoblots against LC3B and Actin. Densitometry was determined by Quantity One with Actin as loading control.

inhibitor alone. Rather, accumulation of LC3BII:I in previous Western blots may be due to an inhibition of LC3BII degradation instead of increased LC3BI activation. This inhibition may then be relieved with raltegravir.

SIGNFICANCE

Debatably one of the most severe side effects of HIV PIs is the induction of NAFLD (*42, 283*). Fatty liver can result in insulin resistance and dyslipidemia, contributing to the atherosclerotic risk in this patient population. Therefore, understanding the mechanism underlying HIV PI-induced fatty liver will aid in future alternative therapies.

Autophagy is now understood to be central in cellular lipid metabolism. In addition, autophagy has been recently shown to play key roles in metabolic diseases such as obesity and NAFLD (*99, 103, 284*). In the liver, basal autophagy is important in degradation of misfolded proteins and nonfuctional organelles, but alterations in the pathway can lead to induction of inflammation, cell death (*285*), and lipid overload (*205*). These are in fact the same pathologies noted with HIV PIs (*49, 191, 232*). Therefore, we completed this study to investigate if HIV PI hepatic alterations could be due to alterations in autophagy.

We show LOPV/RITV to time and dose-dependently increase autophagy. At this time, we cannot definitvely state whether the increase of LC3BII and late autophagosome accumulations are directly through induction of the pathway or inhibition of autophagolysosome action. Although p62 did dose-dependently accumulate in MPH with LOPV/RITV treatment, we believe this is in fact is due to HIV PI inhibition of proteasome activity (please see Chapter 4 and final Discussion). However, preliminary evidence with the use of lysosomal inhibitors demonstrates LOPV/RITV can not induce an increase of LC3B accumulation farther than lysosomal inhibition alone. Further studies using lysosomal inhibitors need to be completed to

fully elucidate if LOPV/RITV inhibits autophagolysosome action beyond its ability to inhibit proteasome action.

What we found most intriguing was the integrase inhibitor raltegravir was able to abrogate LOPV/RITV-induced autophagy (Figures 39-42). We have previously shown raltegravir to inhibit LOPV/RITV lipid accumulations in hepatocytes (*222*), and this finding implied a novel mechanism underlying this phenomenon.

HIV PIs significantly activate CHOP in multiple cell types including hepatocytes, as well as *in vivo* mouse models (*49, 51, 53*). Autophagy is now known to be induced through the UPR (*116, 117, 128*). We therefore investigated if raltegravir's ability to inhibit LOPV/RITV-induced autophagy was through the CHOP pathway. Indeed, the loss of CHOP abrogated this phenomenon (Figures 43-45), and this occurred for both total LC3B protein and LC3BII:I ratio increases. However, knockout of CHOP resulted in an increase of LOPV/RITV-induced LC3BII:I, with no alteration at the total LC3B level (Figure 43). This contradiction may be due to autophagolysosome inhibition, and we are currently investigating if this is the case.

In short summary, addition of raltegravir suppresses LOPV/RITV-induced lipid accumulation through alterations of the autophagy pathway. This phenomenon is shown here to be through the UPR-CHOP pathway. Therefore, we hypothesize that inhibition of HIV PI-induced ER stress by alternative therapies will significantly aid in reducing HIV PI-induced dysregulation of lipid metabolism that leads to clinical metabolic diseases.

CHAPTER VI: Final Discussion

Successful therapy for HIV-infected patients has increased greatly in the past decade. HAART no longer just includes inhibiting viral reverse transcription and protease, but also inhibition of viral fusion and integration. The success of the HIV PI class in suppressing patient viral load is undeniable, especially in treatment-experienced patients (*286, 287*). Although the benefit of HIV PIs is greater than the risk, large side effects still remain. Unfortunately, these include long-term metabolic complications including dyslipidemia, insulin resistance, and lipodystrophy, all of which are high risk factors for atherosclerosis and heart disease (*19, 21, 22, 276*). In order to decrease the risk to benefit ratio, the mechanism underlying HIV PI-induced metabolic side effects needs to be addressed and resolved through alteration of HIV PI structures or inclusion of alternative therapies in the regimen.

Abnormalities seen in the clinic begin at the cell. Therefore, to understand how HIV PIs induce dyslipidemia and lipodystrophy, the mechanism by which HIV PIs modify cellular lipid metabolism needs to be elucidated. While it is often difficult to determine which cellular pathways are implicated in drug-induced pathologies, ER stress and autophagy are already shown to be directly involved in cellular lipid metabolism.

We hypothesize HIV PIs dysregulate lipid metabolism in adipocytes by activating ER stress and autophagy. In addition, while we have previously shown HIV PIs to dysregulate lipid metabolism in hepatocytes through ER stress, autophagy dysregulation may also play a role. Finally, we surmise inhibiting HIV PI-induced ER stress will abrogate lipid metabolism dysregulation in these metabolically important cell types.

HIV PIs in Adipocytes

When it comes to investigating cellular mechanisms underlying HIV PI side effects, surprisingly little work has been accomplished in adipocytes. Until the last decade, the complexity of adipocytes and adipose tissue had hindered in depth studies in this field as well as metabolic disease research. In the 2000s, HIV PI affects in adipocytes focused on inhibition of differentation. As a result of these investigations, there was much contradiction as well as little insight into mechanistic explanations.

Contradictions began in 1998 with the first two major studies in this realm. Here, HIV PI alterations of adipogenesis showed opposite results with IDV and RITV. While using the same cell lines, very similar culture conditions, and Oil Red O staining, Gagnon *et. al* found IDV and RITV to potentiate differentiation (*288*), while Zhang *et. al* found inhibition (*245*). In addition, Zhang *et. al* also found AMPV, a drug with little metabolic side effects, to also inhibit differentiation.

More results followed suit, and included almost all HIV PIs (*156, 192, 193, 239-244, 289, 290*). Due to these inconsistencies, our studies began with preliminary results already published. We began simply by optimizing differentiation protocols for our cellular models to ensure downstream assays were finding conclusions in differentiated, and not partially differentiated, adipocytes. As pre-adipocytes are fibroblastic in nature, we felt a mixed cellular population would distort the results.

Once our methods were confirmed, we did one large experiment to determine HIV PI affects on 3T3-L1 differentiation by treating cells while concurrently inducing adipogenesis. We found this assay to be extremely concentration-dependent, with some HIV PIs (IDV, SQV, NFV) inducing complete cell death at reported patient serum concentrations. This may explain

contradictions in the literature as such a large range of concentrations were used between investigators.

It is important to note at this point the concentrations chosen in our studies. While plasma concentrations can vary greatly in patients due to a variety of factors such as health, individuality, and drug regimens, mean plasma concentrations are given in a number of clinical investigations. Of particular importance is what is deemed effective plasma concentrations of each HIV PI, as often the plasma concentration is 10 times higher than the mononuclear intracellular concentrations (*291*). For LOPV/RITV, the current published data states an average mean concentration of 6 µg/mL, and for LOPV a peak concentration at about 12.5 µg/mL, for those on LOPV:RITV 800/100 mg once a day or 400/100 two dimes a day (*292, 293*). Given the molecular weight, this translates to around 10 µM for RITV and 25 µM for LOPV. Other HIV PIs also do not differ much in clinical plasma concentrations compared to those treatments we show here as physiological (ex. IDV is 15 µg/mL which is almost 25 µM (*294*)).

For our studies, another important factor to consider is the actual accumulation of HIV PIs in non-target cells (i.e. hepatocytes and adipocytes). For Chapter 5, we are confident of the concentrations used as HIV PIs are susceptible to first-pass metabolism, and therefore concentrations experienced by hepatocytes is as high, if not higher, than that measured in patient serum. In addition, we have already shown HIV PIs to accumulate intracellularly in hepatocytes (*49*).

In terms of adipose tissue, it is key to realize that HIV PIs are highly lipophilic, and can accumulate in AT by passive diffusion and physical dissolution in the neutral fats (*295*). However, limited quantitative studies have confirmed the actual concentration of PIs in AT versus serum levels in patients. Others have shown HIV PIs to accumulate intracellularly in

cultered mouse and human adipocytes (*244*, *290*, *296*), and we have preliminary data suggesting the same in our cellular model. Although numerical concentration of HIV PIs in AT is not well published, we believe plasma concentration is highly representative given the above data, the accumulation by diffusion, and knowledge that AT is a well vascularized organ.

Therefore, when analyzing results from our investigations, and those in the literature, the clinically relevant concentrations must be considered. We are now confident of the results shown in Chapter 3 due to these above careful considerations, numerous repeats, and different assays used to analyze HIV PI-alteration of adipogenesis. Of particular significance is the clarification we found of RITV's effects on adipogenesis. We have found with Oil Red O staining, as well as analysis of LD size and numbers by MATLAB, that there is no increase of lipid accumulations compared to control at physiological concentrations of RITV (6.25 µM), while accumulations occur at higher concentrations. This may help explain both the contradictions in the literature, as well as the reason LOPV plus RITV combinations inhibit differentiation by 12.5-25 µM.

At the same time of these clarifications, we began investigating one cellular pathway involved in lipid metabolism, ER stress. In adipocytes, ER homeostasis is essential in LD droplet formations and lipolysis (see Chapter I VI A 3b). We therefore hypothesized that HIV PIs induce ER stress upstream of adipogenesis alterations in adipocytes.

The unfolded protein response (UPR) is the signaling pathway induced at times of ER stress activation. In the beginning figures of Chapter 3, we show LOPV and RITV, as well as the clinically relevant combination LOPV/RITV (4/1), time and dose-dependently increased the UPR transcription factors ATF-4 and CHOP. We have also found that HIV PIs which do not induce the UPR (AMPV and DRV) have minimal metabolic side effects in the clinical. This

correlation encouraged the remainder of our studies as the UPR may be a potential therapeutic target.

During this time, another group also found LOPV to induce ER stress in a human adipocyte cell line (SGBS) (*54*). Their investigations were able to correlate LOPV-induced ER stress and insulin signaling, but were unable to find a direct connection. While their results were only correlative and not involved in lipid metabolism, their findings are supportive of our studies. In addition, others have found the ability of ER stress activation to lead to inhibition of adipogenesis (*189*). This has been proposed to occur through CHOP.

CHOP is a C/EBP-homologous protein (hence its name) and can therefore dimerize with C/EBPs. C/EBPβ is essential in the induction of adipogenesis, while C/EBPα is involved in maintenance of differentiation (Background VI A 2a). When CHOP dimerizes with the C/EBPs, it inhibits their homodimerization necessary for binding to target promoters (*297, 298*). This ultimately leads to inhibition of differentiation (*76*).

We found that lack of CHOP abrogates HIV PI-induced alterations in adipogenesis. While in the literature many have published the ability of HIV PIs to alter adipogenesis (although with contradictions therein), we are the first to propose a substantial mechanism by which this may occur. We propose that an increase of ER stress can lead to upregulation of CHOP through transcription factor ATF-4, resulting in inhibition of differentiation by LOPV and LOPV/RITV.

However, the ability of RITV to induce lipid accumulations at higher concentrations grabbed our curiosity. RITV at 6.25 μM did increase CHOP mRNA and protein levels in differentiated adipocytes (Figures 10, 11). However, by 12.5 μM, this increase was not as great as that induced by LOPV, especially at the protein level. We hypothesize that although these

differences are slight, they may be enough to cause differential results in adipogenesis progression. This would especially be the case if CHOP is competitively binding to C/EBPs during differentiation. Given that CHOP$^{-/-}$ also abrogated RITV accumulations supports that both LOPV and RITV alterations in adipogenesis occur through the CHOP pathway.

We also serendipitously came upon another potential mechanism to explain the differential affects of LOPV and RITV. This occurred when we were testing whether HIV PIs could increase IL-6 mRNA stability through HuR binding in adipocytes as they do in macrophages (*232*). While our results were non-conclusive in this regard, we surprisingly found that HuR and CUGBP-1 (CUG_n triplet repeat RNA-binding protein) bound to PPARγ mRNA, and this was significantly increased with RITV, but not LOPV, treatment.

AU-rich elements (AREs) in the 3' untranslated region (3'UTR) allow for rapid decay of short-lived mRNAs. RNA binding proteins such as HuR increase mRNA stability via binding to these regions (*299, 300*). CUGBP-1 binds to CUG oligonucleotides, leading to alternative splicing and alteration in translation (*301, 302*).

Both HuR and CUGBP-1 have previously been reported to play a role in adipogenesis through postranscriptional regulation of C/EBPβ. CUGBP-1 was the first shown to bind to C/EBPβ (*301*). This binding resulted in differential translation of the C/EBPβ transcript, leading to production of short dominant-negative isoforms which bind and inhibit action of full C/EBPβ proteins. In adipocytes, this leads to inhibition of differentiation (*303*). More recently, HuR has also been demonstrated to complex with C/EBPβ. Rather than increasing C/EBPβ mRNA stability, HuR binding slowed translocation to the cytosol, also contributing to a delay in differentiation (*304, 305*). Therefore, both of these mRNA proteins may negatively regulate adipogenesis.

While this work is intriguing, we are the first to demonstrate a potential role of these binding proteins on PPARγ postranscriptional regulation. We have identified putative binding sites for both proteins, and demonstrated binding through an *in vitro* pulldown. Importantly, RITV treatment in 3T3-L1s increased both HuR and CUGBP-1 binding, with more significant binding found at the 3'UTR.

It remains to be asked why so many who study this essential transcription factor failed to note such a regulatory mechanism of its action. In fact, we believe the substantial induction of binding with RITV treatment allowed us to come upon this finding. In addition, another inquiry remains as to why both proteins bind to the 3'UTR. Intuitively, this result seems contradictory as HuR is thought to stabilize mRNA transcripts while CUGBP-1 destabilizes. In reality, these distinct classifications may not hold, as we have discussed above HuR binding actually slows C/EBPβ shuttling. In addition, CUGBP-1 may increase translation of some transcripts (*306*). Therefore, there is potential that these proteins are not having opposite effects when binding to PPARγ.

To boot, others in our laboratory have noticed competitive binding of HuR and CUGBP-1 on IL-6 mRNA in macrophages (*in progress*). Therefore, there is the possibility that this competition is also occurring in our model. The regulation of mRNA binding proteins and their subsequent actions is currently not well defined, and continuously investigated due to potential roles they play in many cellular pathways and correlated diseases. While this field is growing, we hope to gain a greater prospective of how, and why, HuR and CUGBP-1 bind to PPARγ mRNA.

Although one HIV PI induced binding significantly and the other did not, both LOPV and RITV significantly inhibited PPARγ promoter activity in our assay. This result is supportive of

current literature (*243, 258, 307, 308*). In addition, our findings were not dose dependent, which is supportive of other results that HIV PIs do not directly bind to the PPARγ promoter (*245*). While it is clear HIV PIs inhibit PPARγ promoter activity, some have reported no change in mRNA or protein levels of PPARγ with RITV treatments (*193, 241*), perhaps explained by postranscriptional modifications.

There are multiple lines of evidence that ER stress can lead to a decrease in PPARγ (*309-312*). What is not known is which component of the UPR is leading to this inhibition, or if another factor is contributing to the phenomenon. SREBP-1c is a lipogenic transcription factor located in the inactive form at the ER membrane, and can be released at times of ER stress (Background IV B2). Others have shown that HIV PIs alter the nuclear lamin A/C maturation (*239, 313, 314*), essential for normal nuclear penetration of SREBP-1 (*315, 316*). We have previously shown SREBPs to be upregulated at times of HIV PI-induced ER stress (*49*), and believe the same occurs in AT (Figure 27). However, in adipocytes SREBP-1c may not be adequately translocated into the nucleus at times of HIV PI treatments, failing to stimulate PPARγ. At the same time, HIV PIs may be increasing the mRNA stability of what transcript is produced, allowing for a quick rebound of levels. Future studies need to be completed to analyze the timing of all these alterations, as well as the extent PPARγ protein levels are changed in the cytosol and nucleus of cells treated with HIV PIs.

The centrality of ER stress induction and HIV PI alterations in adipogenesis is apparent in our work. We also consider our MATLAB data directly correlated to ER stress induction. CTP:phosphocholinecytidylyltransferase (CCT), the rate limiting enzyme for phosphatidylcholine (PtdCho) synthesis, is enriched in the rough ER (Background VI 3 b). Lipid droplet (LD) fusion can occur at times of ER stress when there is a decrease of CCT (*175*). In

Figure 19, RITV significantly decreased LD number while increasing LD diameter. This data suggests LD fusion. We hypothesize the induction of ER stress is the cause of this specific phenomenon, as the ER and LD organelles are so closely intertwined (*66, 69, 173, 174*). However, more intricate studies are needed to elucidate this phenomenon. These investigations will not only aid in understanding how HIV PIs act in adipocytes, but also allow deeper clarification of LD physiology.

HIV PIs in Adipocytes - Autophagy Induction

In order to further investigate HIV PI-induced lipid metabolism dysregulation in adipocytes, we turned to autophagy. We first began these studies when all the pathologies induced by HIV PIs could not be thoroughly explained through UPR induction. For instance, although we can visualize cell death in adipocytes chronically treated with HIV PIs, our apoptosis analysis was not as significant as expected (Figure 14). In addition, knockout of CHOP did not result in complete inhibition of LOPV and RITV alterations (Figures 26, 27).

At the same time of our ER stress studies, the role of autophagy in lipid metabolism was emerging in the literature. Autophagy has previously been shown to induce cell death and alter lipid metabolism (Background V A and VI D). In adipocytes, the significance of autophagy in physiology and pathology seems to be complex and only beginning to be understood. Recent work has demonstrated that knockdown of this pathway leads to inhibition of differentiation *in vitro*, and lack of white adipose tissue growth *in vivo* (*203, 263*). However, the control and intricacies of autophagy in fully differentiated adipocytes is not very well known. This is partially attributable to the essentiality of autophagy in differentiation, and therefore difficulty in knocking-down this pathway in mature cells and tissues through gene manipulation.

A few investigators have recently shown HIV PIs SQV, NFV, and an IDV analog induce autophagy in cancer cells (*233, 234, 265*). As seen in Chapter 4, we were able to demonstrate that HIV PIs ccan induce autophagy in metabolically important cells. Using multiple methods, we show that both RITV and LOPV induce autophagosome accumulations in both non-differentiated and differentiated adipocytes. In contrast, DRV, a second generation HIV PI which is not known to induce lipid metabolism alterations in the clinic, did not significantly increase either the UPR or autophagy (Figure 31).

Autophagic flux is just as important as autophagosome formation. If autophagosomes fail to fuse with, or be processed in, lysosomes, an accumulation of autophagosomes will occur and present as an induction of autophagy. There is often criticism when investigators fail to probe for alterations in autophagic flux, especially in the emerging field studying autophagy in adipogenesis (*280*). LC3B has been demonstrated to localize at LDs (*201, 317*). Therefore, autophagosomes may not only be engulfing LDs when recycling lipids, but LDs may also fuse directly to these vesicles. If flux is inhibited, there would be a lack of full lipid recycling. This would obviously lead to pathology on its own.

We found no evidence of inhibition of autophagosome maturation in our model. When analyzing our EM images, we visualized both early and late autophagosomes, as well as apparent autolysosomes (single membraned with highly degraded substances). We also examined for successful cleavage of GFP-LC3B. LC3B-II is already extensively shown to be localized to both the inner and outer membranes of autophagosomes (*318, 319*). Upon autophagosome-lysosome fusion, inner membrane LC3B is degraded with the cytosolic components while the outer membrane LC3B is removed by Atg4 through delipidation to be recycled (*320*). This same process will occur with the GFP-LC3B construct, but as GFP is much more resistant to

proteases, it is released into the cytosol at LC3B cleavage (*281, 282, 321*). Impediment of GFP cytosolic accumulation would suggest inhibition of autophagolysosome maturation, which does not occur in our assay (Figure 34).

Another flux assay we used was p62 degradation. The nuclear membrane protein p62 is used extensively in autophagy assays. p62 was found to have a LIR, and can serve as a linking protein between LC3B and ubiquitinated substrates (*267, 268, 322*). It has been proposed to be specifically degraded through autophagy, and therefore p62 protein levels should inversely correlate with autophagic flux (*267, 271, 272*). However, recent research has shown that there exist other sub-populations of p62 beyond those associated with autophagosomes (*273*). In addition, a recent publication has demonstrated that p62 associates with the 26S proteasome, and inhibition of proteasome activity leads to p62 accumulation (*274*).

HIV PIs have already extensively been shown to inhibit proteasome activity (*223, 323-325*). In addition, this inhibition is dose-dependent, with HIV PIs having moderate activity when compared to other pharmacological agents. HIV PI proteasome inhibition has been proposed to be the inducer of ER stress, as it will cause an inhibition of nascent protein degradation (*223*). In this particular study cited, while ER stress activation and proteasome inhibition occurred in HepG2 and 3T3-L1 cells with HIV PI treatments, it was not elucidated which activity occurred first. As we have not conducted sufficient studies to determine if direct inhibition of proteasome activity is the result of UPR activation, and the downstream affects shown, we cannot refute this as being a possible underlying mechanism. However, our previous data suggests that in fact accumulation of cholesterol in the ER membrane is the underlying issue, which would lead to inhibition of the Ca^{2+} ATP-pump, and result in depletion of ER Ca^{2+} stores (Figure 13 and (*51*)).

We hypothesize that the accumulation of p62 protein seen with the higher concentrations of HIV PIs in our assays is due to inhibition of proteasome activity, not inhibition of autophagolysosome activity (Figures 33, 47). While we are currently confident of our results demonstrating HIV PIs are inducing autophagy with no affect on flux, further experiments will be conducted in support of our work. One such study, of which we show in Chapter 5, is the use of lysosomal inhibitors to demonstrate accumulation of LC3BII is due to activation of autophagy and not inhibition of LC3BII degradation in the autophagolysosome (*281*).

An even better determinant is degradation of long-lived proteins. This classical method utilizes isotope-labeling of long-lived proteins. The output result may be the most precise measurement of autophagolysosome activity (*326, 327*). However, degradation of many long-lived proteins occurs through the proteasome. Therefore, to clarify the degradation pathway, inclusion of autophagy inhibitors (such as 3-methyladenine) is necessary. This leads to two pitfalls in the study. One, some inhibitors such as 3-methyladenine must be used at very high concentrations to fully inhibit autophagy. Another, HIV PI-inhibition of proteasomes may also affect the output of this assay. As such, positive and negative controls are even more essential in our particular investigations and will be considered in future experiments.

While flux is not apparently altered, LC3B protein increase may not be attributable only to increased autophagy. In contrast, we believe some of this protein is also aiding in LD fusions. LC3B has been demonstrated to localize at LDs (*201, 317*), and also be involved in lipososomal fusion in drosophili (*328*). In a recent study of hepatic stellate cells, it was shown that platelet-derived growth factor increased LC3B accumulation to LDs (*317*). While we are investigating different cell types with different drug treatments, this result demonstrates the capacity of an extracellular substance inducing differential localization of LC3B.

With the above studies, it can be hypothesized that HIV PIs induce an increase of LC3B protein levels, some of which will accumulate at adipocyte LDs (in a non-elucidated manner). With LC3B now shown to have tethering capacity, this protein may aid in the fusion of LDs, as well as direct fusion to autophagosomes. In addition, this increase of LC3B will allow more substrate for autophagosome production, a basis for the significant results shown in Chapter 4. Indeed, we have shown how HIV PIs can increase LC3B protein through the activation of ER stress.

We first investigated an HIV PI-induced UPR and autophagy link with the transcription factor CHOP, as we had seen $CHOP^{-/-}$ to abrogate HIV PI alterations in adipogenesis (Chapter 3). While knockdown of CHOP resulted in a decrease of LC3B protein levels in 3T3-L1s, CHOP overexpression did not affect LC3B in either non-treated or HIV PI treated 3T3-L1s (Figure 35). This could be due to the methods we used (GFP-tagged CHOP may impede action of CHOP) and/or an already saturated system. The next step will be to reintroduce CHOP into a $CHOP^{-/-}$ adipocyte and test LC3B response. In addition, we are continuing our experiments focused on HIV PI treated CHOP knockdown 3T3-L1s. Our initial results are very similar to our inhibition of adipogenesis assay, demonstrating the central role CHOP plays in HIV PI-induced dysregulation of lipid metabolism.

Nonetheless, we also wanted to determine if this connection also occurred upstream of CHOP. As previously mentioned, others have demonstrated a UPR-PERK-autophagy connection (*120, 130, 269*). ATF-4, the transcription factor activated through this pathway, is a direct activator of CHOP (*329, 330*). In addition, RITV, a dose-dependent activator of autophagy (shown by EM to even be a more significant than LOPV) activated ATF-4 more so than CHOP in our models. As shown, ATF-4 knockout abrogates LOPV and LOPV/RITV upregulation of

LC3B protein (Figure 36). These findings are most intriguing and well connected to above discussions. Please see HIV PI-Induced UPR and Induction of Autophagy below for a further discussion of this matter.

HIV PIs in Hepatocytes

In contrast to adipocytes, extensive work on HIV PI-induced metabolic side effects has focused in the liver and hepatocytes. The reasons are simple - the liver is central in many metabolic diseases, is one of the first organs HIV PIs come into contact, and is the major organ responsible for HIV PI metabolism. Nonetheless, it was not until most recent years that specific mechanisms underlying HIV PI-induced side effects in this organ were proposed.

Of most interest that formulated was the induction of ER stress. This mechanism seemed lucrative as it could so easily explain how one drug had so many deleterious cellular affects such as the inflammatory cascade, insulin resistance, and lipid metabolism dysregulation. In addition, more recent clinical findings demonstrate that many patients on HIV PIs have NAFLD, which ER stress has also been proposed to underlie (*213, 214*). Our laboratory has already extensively demonstrated that HIV PIs lead to the activation of the UPR in hepatocytes, and subsequent dysregulation of lipid metabolic-essential transcription factors (*49, 50, 222*).

More recently, autophagy is now understood to be a major player in lipid metabolism in hepatocytes, and may also underlie NAFLD/NASH (*205, 225, 284*). As we had investigated, and found, HIV PIs to induce autophagy in adipocytes, we were also interested if autophagy dysregulation was occurring in hepatocytes. And as shown in Chapter 5, this is indeed the case with LOPV/RITV 4:1.

We also took these findings a step further. Raltegravir, an integrase inhibitor, was found by our laboratory to not induce the UPR or lipid accumulations in hepatocytes as do HIV PIs.

Importantly, addition of raltegravir with LOPV/RITV treatment actually inhibited their induction of lipid accumulations (*222*). We hypothesized that this phenomenon could be explained through raltegravir-inhibition of LOPV/RITV-induced autophagy.

Indeed, as shown in Figures 39-42, raltegravir inhibits LOPV/RITV activation of autophagy. Excited by these findings, we moved forward to elucidate the mechanism. Significant evidence came by utilization of our previously acquired $CHOP^{-/-}$ model. Here, we found significant abrogation of raltegravir-inhibition of LOPV/RITV-induced LC3B conversion (Figure 43). However, *in vivo* raltegravir did not alter LOPV/RITV increased LC3BII:I, but only inhibited the total LC3B protein increase (Figures 44, 45).

We do not believe this result is a lack of correlation between our *in vitro* and *in vivo* assays. Isolation and separation of protein is in fact a crude method of analyzing *in vivo* processes, especially in tissue with high proteolytic enzymes such as the liver. Although all experiments were handled with as much care as possible, we cannot disprove that some of these small proteins were not degraded before analysis. In addition, the liver is composed of more than just hepatocytes, but also macrophages and endothelial cells. We have not analyzed if HIV PIs induce autophagy in either of these other cell types, and therefore cannot exclude that their alterations are not also affecting our Western results.

Upon further investigation of this data, we believe our *in vitro* results are translatable. In the wild type mice fed a normal diet, the 'n' may not be large enough. Additionally, in the high fat diet experiment, lack of raltegravir activation of LC3B is significantly abrogated with loss of CHOP. And although not significant with this 'n,' there is a trend loss in raltegravir inhibition of LOPV/RITV-induced LC3B activation. Nonetheless, more extensive investigations should be undertaken to definitively ascertain the *in vivo* ability of raltegravir inhibition in LOPV/RITV-

induced autophagy. One example would be the use of GFP-LC3B transgenic mice (*281*). This model allows direct monitoring of autophagosome formations by sectioning tissue and analyzing with fluorescent microscopy, and may aid greatly in our investigations.

Nevertheless, our *in vivo* results highly correlate to our results from Chapter 4. In fact, when CHOP is downregulated in 3T3-L1s, there was a total decrease of LC3B protein, not a decrease of LC3BII:I. Going farther upstream lead to this same finding. In fact, it has been proposed the PERK pathway connects ER stress to autophagy through ATF-4 transcriptional regulation of *LC3B*.

HIV PI-Induced UPR and Induction of Autophagy

Hypoxia is one known inducer of ER stress as protein folding is oxygen dependent (*331*). Autophagy induction has been shown to occur at times of oxygen depletion (*332, 333*), with a direct connection to ER stress proposed by Rzymski *et. al* in 2010 (*130*). In hypoxic conditions, this group found an upregulation of ATF-4 lead to a subsequent increase in LC3B protein. By using a siRNA targeted to ATF-4, they saw a decrease in total LC3B protein levels, as we have also shown in our model. Even more, they were able to define an ATF-4 binding site in the 5'UTR of the *LC3B* promoter, and demonstrated strong and specific binding at times of hypoxia.

ER stress can be induced by multiple mechanisms. Other investigators have proposed UPR-autophagy links during such differential alterations such as inhibition of nascent protein degradation (*131*), oxidative stress (*334*), and radiation (*129*). Our studies investigate only one mechanism of ER stress activation, but have many similarities to others who show a PERK-autophagy link. Particularly, HIV PIs significantly upregulate both ATF-4 and CHOP in all cell models we study, and knockdown of ATF-4 leads to a decrease in total LC3B protein levels.

Many investigators are under the impression that conversion of LC3B is the key necessary for increased autophagosome formation. While we do not refute the necessity of this, it should also follow that an upregulation of *LC3B* will ultimately lead to more of the substrate essential in autophagosome formation. In fact, our findings are highly supported by Rzymski's results that ATF-4 may be able to directly upregulate LC3B protein leading to autophagosome increase (*131, 335*).

Our results demonstrate that CHOP also plays a major role in HIV PI-induced ER stress and autophagy induction. Knockdown of CHOP caused a significant decrease in LC3B within adipocytes, and raltegravir inhibition of LOPV/RITV LC3B induction was dependent on CHOP in hepatocytes. These results are novel, and demonstrate an exclusive relationship downstream CHOP has on LC3B regulation.

We have not yet defined the mechanism underlying CHOP's ability to alter LC3B protein levels. Rouschoup *et. al* have recently shown CHOP to bind to the *Atg5* promoter (*275*). Atg5 is an E3-like ligase essential in LC3B lipidation, and therefore directly controls LC3BII:I levels. However, we have no current evidence this is occurring, and some of our results refute this hypothesis. Indeed, $CHOP^{-/-}$ primary hepatocytes resulted in increased LOPV/RITV-induced LC3B conversion relative to wild type control (Figure 43). More intricate assays are thus needed to determine if CHOP does indeed play a transcriptional role in autophagy regulation. This may be via Atg5, or one of the other 30+ proteins involved in autophagy.

Targeting HIV PI-Induced Metabolic Side Effects

While all our findings above are intriguing and give insight into a multitude of cellular pathways and regulations, the ultimate goal is unearthing a potential target to inhibit HIV PI-

induced cellular lipid metabolism dysregulation. Unfortunately, current approaches in the clinic do not target the issue at hand, but rather treat the symptoms.

For instance, when a physician notes an alteration in lipidemia, the first conclusion is often a change of diet with a lipid lowering agent. This may not be enough to combat cellular alterations induced by a chronic drug therapy. In addition, switching to alternative HAART regimens may not be beneficial to the patient due to viral load and mutations, physical condition of the patient such as ability to clear drug, and other induced side effects. Therefore, an optimal approach would be inhibition of HIV PI cellular perturbations that lead to these chronic clinical effects.

Some have attempted addition of direct interventions during HIV PI treatment. One such example is addition of thiazolidinediones, direct stimulators of PPARγ. These drugs are often used in the treatment of insulin resistance, but have also been shown to have great potential in treatment of genetic lipodystrophies (*336, 337*). However, addition of rosiglitazone did not improve lipid profile in patients on HIV PI-therapy (*338-340*). Probing into the molecular effects of HIV PIs gives the reasons for such a failure – as shown in our studies.

Others have attempted to add homeopathic agents into the treatment and test if this could alleviate some HIV PI side effects. There has not been any success in this avenue, either. Importantly, clinical investigators must be cautious in such studies. Although many herbs have minimal side effects, they may disrupt the metabolism of drugs, affecting the concentration and action of essential therapies such as HIV PIs. One well known example is St. John's wort, which inhibits cytochrome P450 3A4, the same enzyme that metabolizes HIV PIs.

While our laboratory was initially investigating such alternative therapies, focusing on the Chinese herbal medicine Berberine (*191*), the results we show here may ultimately change

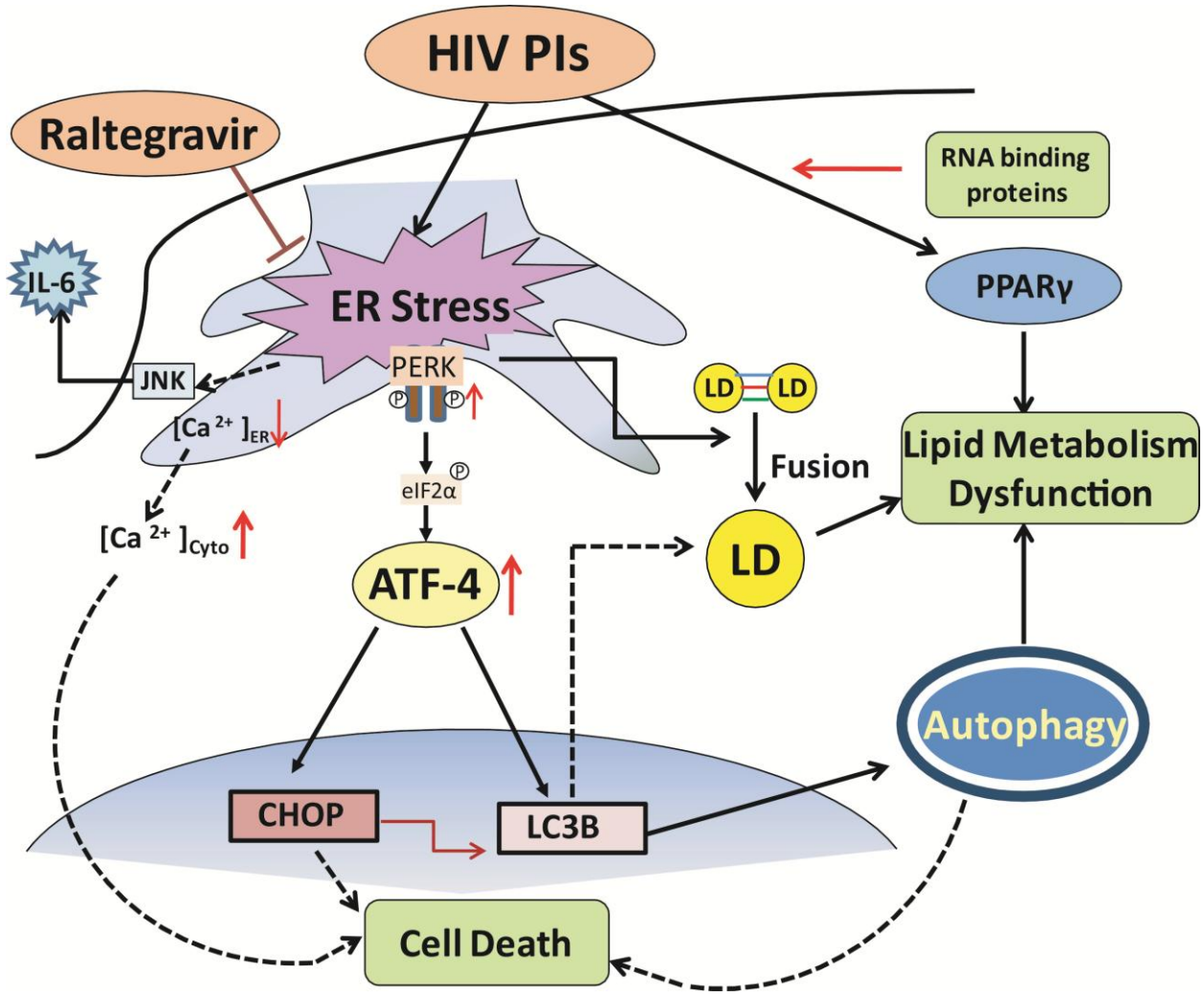

Figure 49: HIV PI-Induced ER stress activates autophagy and dysregulates cellular lipid metabolism. Our current model based on the findings presented in this dissertation.

focus to agents already within the HAART class. Specifically, we show raltegravir to inhibit LOPV/RITV-induced lipid accumulations in hepatocytes.

In the clinic, there is currently no data suggesting an unfavorable lipid profile in patients on raltegravir therapy (*341, 342*). In fact, some propose a switch from HIV PIs to raltegravir would be beneficial. A few clinical trials, such as the SWITCH study, have investigated this, but it is currently not recommended. While the results demonstrate an improvement of lipid profile, it is at the cost of worsening viral load (*343*), so much so that one study had to terminate early (*344*). It is apparent, however, that raltegravir can have a positive impact on HIV PI-induced lipidemia.

Our investigations demonstrate that raltegravir has a direct affect on these lipid metabolic alterations at the cellular level. However, our current studies with raltegravir are only completed in hepatocytes. While this is a key cell type involved in lipidemia, it must be determined if this phenomenon also occurs in adipocytes. One recent study has shown raltegravir to have no effects on adipogenesis of 3T3-L1s (*345*). This suggests to us that raltegravir may have similar beneficial results in adipocytes, and we will therefore continue our studies in this direction.

Conclusion

Chronic side effects induced by HIV PIs have placed a major pitfall on these otherwise beneficial agents. Elucidating HIV PI cellular metabolism alterations can lead to better therapies. We have shown that HIV PIs induce two major pathways involved in cellular lipid metabolism, ER stress and autophagy, which are not mutually exclusive. We propose raltegravir addition in HAART will relieve this activation, inhibiting HIV PI-induced lipid metabolism dysregulation. Future investigations should focus on the metabolic benefits of such a therapy.

References Cited

1. WHO, U. (2010) Global Summary of the AIDS Epidemic.
2. WHO, U. (2009) AIDS Epidemic Update.
3. Arien, K. K., Vanham, G., and Arts, E. J. (2007) Is HIV-1 evolving to a less virulent form in humans?, *Nat Rev Microbiol 5*, 141-151.
4. Fauci, A. S. (2003) HIV and AIDS: 20 years of science, *Nat Med 9*, 839-843.
5. Navia, M. A., Fitzgerald, P. M., McKeever, B. M., Leu, C. T., Heimbach, J. C., Herber, W. K., Sigal, I. S., Darke, P. L., and Springer, J. P. (1989) Three-dimensional structure of aspartyl protease from human immunodeficiency virus HIV-1, *Nature 337*, 615-620.
6. Kovalevsky, A. Y., Ghosh, A. K., and Weber, I. T. (2008) Solution kinetics measurements suggest HIV-1 protease has two binding sites for darunavir and amprenavir, *J Med Chem 51*, 6599-6603.
7. Mastrolorenzo, A., Rusconi, S., Scozzafava, A., Barbaro, G., and Supuran, C. T. (2007) Inhibitors of HIV-1 protease: current state of the art 10 years after their introduction. From antiretroviral drugs to antifungal, antibacterial and antitumor agents based on aspartic protease inhibitors, *Curr Med Chem 14*, 2734-2748.
8. Brik, A., and Wong, C. H. (2003) HIV-1 protease: mechanism and drug discovery, *Org Biomol Chem 1*, 5-14.
9. Flint, O. P., Noor, M. A., Hruz, P. W., Hylemon, P. B., Yarasheski, K., Kotler, D. P., Parker, R. A., and Bellamine, A. (2009) The role of protease inhibitors in the pathogenesis of HIV-associated lipodystrophy: cellular mechanisms and clinical implications, *Toxicol Pathol 37*, 65-77.

10. Paccou, J., Viget, N., Legrout-Gerot, I., Yazdanpanah, Y., and Cortet, B. (2009) Bone loss in patients with HIV infection, *Joint Bone Spine 76*, 637-641.

11. Ofotokun, I., and Weitzmann, M. N. (2010) HIV-1 infection and antiretroviral therapies: risk factors for osteoporosis and bone fracture, *Curr Opin Endocrinol Diabetes Obes 17*, 523-529.

12. Gibellini, D., De Crignis, E., Ponti, C., Borderi, M., Clo, A., Miserocchi, A., Viale, P., and Carla Re, M. (2010) HIV-1 Tat protein enhances RANKL/M-CSF-mediated osteoclast differentiation, *Biochem Biophys Res Commun 401*, 429-434.

13. Mallon, P. W., Miller, J., Cooper, D. A., and Carr, A. (2003) Prospective evaluation of the effects of antiretroviral therapy on body composition in HIV-1-infected men starting therapy, *AIDS (London, England) 17*, 971-979.

14. Martinez, E., Mocroft, A., Garcia-Viejo, M. A., Perez-Cuevas, J. B., Blanco, J. L., Mallolas, J., Bianchi, L., Conget, I., Blanch, J., Phillips, A., and Gatell, J. M. (2001) Risk of lipodystrophy in HIV-1-infected patients treated with protease inhibitors: a prospective cohort study, *Lancet 357*, 592-598.

15. Carr, A., Miller, J., Law, M., and Cooper, D. A. (2000) A syndrome of lipoatrophy, lactic acidaemia and liver dysfunction associated with HIV nucleoside analogue therapy: contribution to protease inhibitor-related lipodystrophy syndrome, *AIDS (London, England) 14*, F25-32.

16. Barbaro, G. (2007) Visceral fat as target of highly active antiretroviral therapy-associated metabolic syndrome, *Current pharmaceutical design 13*, 2208-2213.

17. Lee, H., Hanes, J., and Johnson, K. A. (2003) Toxicity of nucleoside analogues used to treat AIDS and the selectivity of the mitochondrial DNA polymerase, *Biochemistry 42*, 14711-14719.

18. Mallon, P. W. (2007) Pathogenesis of lipodystrophy and lipid abnormalities in patients taking antiretroviral therapy, *AIDS reviews 9*, 3-15.

19. Caron-Debarle, M., Boccara, F., Lagathu, C., Antoine, B., Cervera, P., Bastard, J. P., Vigouroux, C., and Capeau, J. (2010) Adipose Tissue as a Target of HIV-1 Antiretroviral Drugs. Potential Consequences on Metabolic Regulations, *Current pharmaceutical design*.

20. Friis-Moller, N., Weber, R., Reiss, P., Thiebaut, R., Kirk, O., d'Arminio Monforte, A., Pradier, C., Morfeldt, L., Mateu, S., Law, M., El-Sadr, W., De Wit, S., Sabin, C. A., Phillips, A. N., Lundgren, J. D., and group, D. A. D. s. (2003) Cardiovascular disease risk factors in HIV patients--association with antiretroviral therapy. Results from the DAD study, *AIDS (London, England) 17*, 1179-1193.

21. Calza, L., Manfredi, R., and Chiodo, F. (2004) Dyslipidaemia associated with antiretroviral therapy in HIV-infected patients, *The Journal of antimicrobial chemotherapy 53*, 10-14.

22. Group, D. A. D. S., Friis-Moller, N., Reiss, P., Sabin, C. A., Weber, R., Monforte, A., El-Sadr, W., Thiebaut, R., De Wit, S., Kirk, O., Fontas, E., Law, M. G., Phillips, A., and Lundgren, J. D. (2007) Class of antiretroviral drugs and the risk of myocardial infarction, *The New England journal of medicine 356*, 1723-1735.

23. Kaplan, R. C., Kingsley, L. A., Sharrett, A. R., Li, X., Lazar, J., Tien, P. C., Mack, W. J., Cohen, M. H., Jacobson, L., and Gange, S. J. (2007) Ten-year predicted coronary heart

disease risk in HIV-infected men and women, *Clinical infectious diseases : an official publication of the Infectious Diseases Society of America 45*, 1074-1081.

24. Grundy, S. M., Cleeman, J. I., Daniels, S. R., Donato, K. A., Eckel, R. H., Franklin, B. A., Gordon, D. J., Krauss, R. M., Savage, P. J., Smith, S. C., Jr., Spertus, J. A., and Costa, F. (2006) Diagnosis and management of the metabolic syndrome: an American Heart Association/National Heart, Lung, and Blood Institute scientific statement, *Current opinion in cardiology 21*, 1-6.

25. Martinez, E., Milinkovic, A., Buira, E., de Lazzari, E., Leon, A., Larrousse, M., Lonca, M., Laguno, M., Blanco, J. L., Mallolas, J., Garcia, F., Miro, J. M., and Gatell, J. M. (2007) Incidence and causes of death in HIV-infected persons receiving highly active antiretroviral therapy compared with estimates for the general population of similar age and from the same geographical area, *HIV Med 8*, 251-258.

26. Floris-Moore, M., Howard, A. A., Lo, Y., Arnsten, J. H., Santoro, N., and Schoenbaum, E. E. (2006) Increased serum lipids are associated with higher CD4 lymphocyte count in HIV-infected women, *HIV Med 7*, 421-430.

27. Pere, D., Ignacio, S. L., Ramon, T., Fernando, L., Alberto, T., Pompeyo, V., Juan, G., G, M. J., Paloma, G., Antonio, V., Jaime, C., Esteban, R., Bernardino, R., GA, M. L., Trinitario, S., Ferran, T., Juan Ramon, L., and Myriam, G. (2008) Dyslipidemia and cardiovascular disease risk factor management in HIV-1-infected subjects treated with HAART in the Spanish VACH cohort, *Open AIDS J 2*, 26-38.

28. Periard, D., Telenti, A., Sudre, P., Cheseaux, J. J., Halfon, P., Reymond, M. J., Marcovina, S. M., Glauser, M. P., Nicod, P., Darioli, R., and Mooser, V. (1999)

Atherogenic dyslipidemia in HIV-infected individuals treated with protease inhibitors. The Swiss HIV Cohort Study, *Circulation 100*, 700-705.

29. Tsiodras, S., Mantzoros, C., Hammer, S., and Samore, M. (2000) Effects of protease inhibitors on hyperglycemia, hyperlipidemia, and lipodystrophy: a 5-year cohort study, *Arch Intern Med 160*, 2050-2056.

30. Calza, L., Manfredi, R., Farneti, B., and Chiodo, F. (2003) Incidence of hyperlipidaemia in a cohort of 212 HIV-infected patients receiving a protease inhibitor-based antiretroviral therapy, *Int J Antimicrob Agents 22*, 54-59.

31. Carr, A., Samaras, K., Thorisdottir, A., Kaufmann, G. R., Chisholm, D. J., and Cooper, D. A. (1999) Diagnosis, prediction, and natural course of HIV-1 protease-inhibitor-associated lipodystrophy, hyperlipidaemia, and diabetes mellitus: a cohort study, *Lancet 353*, 2093-2099.

32. Purnell, J. Q., Zambon, A., Knopp, R. H., Pizzuti, D. J., Achari, R., Leonard, J. M., Locke, C., and Brunzell, J. D. (2000) Effect of ritonavir on lipids and post-heparin lipase activities in normal subjects, *Aids 14*, 51-57.

33. Garcia-Benayas, T., Blanco, F., de la Cruz, J. J., Senchordi, M. J., Gomez-Viera, J. M., Soriano, V., and Gonzalez-Lahoz, J. (2001) Role of nonnucleosides in the development of HAART-related lipid disturbances, *J Acquir Immune Defic Syndr 28*, 496-498.

34. Barragan, P., Fisac, C., and Podzamczer, D. (2006) Switching strategies to improve lipid profile and morphologic changes, *AIDS Rev 8*, 191-203.

35. Walli, R. K., Michl, G. M., Bogner, J. R., and Goebel, F. D. (2001) Improvement of HAART-associated insulin resistance and dyslipidemia after replacement of protease inhibitors with abacavir, *Eur J Med Res 6*, 413-421.

36. Ruiz, L., Negredo, E., Domingo, P., Paredes, R., Francia, E., Balague, M., Gel, S., Bonjoch, A., Fumaz, C. R., Johnston, S., Romeu, J., Lange, J., and Clotet, B. (2001) Antiretroviral treatment simplification with nevirapine in protease inhibitor-experienced patients with hiv-associated lipodystrophy: 1-year prospective follow-up of a multicenter, randomized, controlled study, *J Acquir Immune Defic Syndr 27*, 229-236.

37. Martinez, E., Arnaiz, J. A., Podzamczer, D., Dalmau, D., Ribera, E., Domingo, P., Knobel, H., Riera, M., Pedrol, E., Force, L., Llibre, J. M., Segura, F., Richart, C., Cortes, C., Javaloyas, M., Aranda, M., Cruceta, A., de Lazzari, E., and Gatell, J. M. (2003) Substitution of nevirapine, efavirenz, or abacavir for protease inhibitors in patients with human immunodeficiency virus infection, *N Engl J Med 349*, 1036-1046.

38. Donnelly, K. L., Smith, C. I., Schwarzenberg, S. J., Jessurun, J., Boldt, M. D., and Parks, E. J. (2005) Sources of fatty acids stored in liver and secreted via lipoproteins in patients with nonalcoholic fatty liver disease, *J Clin Invest 115*, 1343-1351.

39. Rector, R. S., Thyfault, J. P., Wei, Y., and Ibdah, J. A. (2008) Non-alcoholic fatty liver disease and the metabolic syndrome: an update, *World J Gastroenterol 14*, 185-192.

40. Ingiliz, P., Valantin, M. A., Duvivier, C., Medja, F., Dominguez, S., Charlotte, F., Tubiana, R., Poynard, T., Katlama, C., Lombes, A., and Benhamou, Y. (2009) Liver damage underlying unexplained transaminase elevation in human immunodeficiency virus-1 mono-infected patients on antiretroviral therapy, *Hepatology 49*, 436-442.

41. Lemoine, M., Barbu, V., Girard, P. M., Kim, M., Bastard, J. P., Wendum, D., Paye, F., Housset, C., Capeau, J., and Serfaty, L. (2006) Altered hepatic expression of SREBP-1 and PPARgamma is associated with liver injury in insulin-resistant lipodystrophic HIV-infected patients, *Aids 20*, 387-395.

42. Akhtar, M. A., Mathieson, K., Arey, B., Post, J., Prevette, R., Hillier, A., Patel, P., Ram, L. J., Van Thiel, D. H., and Nadir, A. (2008) Hepatic histopathology and clinical characteristics associated with antiretroviral therapy in HIV patients without viral hepatitis, *Eur J Gastroenterol Hepatol 20*, 1194-1204.

43. Gentile, C., Frye, M., and Pagliassotti, M. (2011) Endoplasmic reticulum stress and the unfolded protein response in nonalcoholic fatty liver disease, *Antioxid Redox Signal*.

44. Malhi, H., and Kaufman, R. J. (2011) Endoplasmic reticulum stress in liver disease, *J Hepatol 54*, 795-809.

45. Kaplowitz, N., Than, T. A., Shinohara, M., and Ji, C. (2007) Endoplasmic reticulum stress and liver injury, *Semin Liver Dis 27*, 367-377.

46. Toth, A., Nickson, P., Mandl, A., Bannister, M. L., Toth, K., and Erhardt, P. (2007) Endoplasmic reticulum stress as a novel therapeutic target in heart diseases, *Cardiovasc Hematol Disord Drug Targets 7*, 205-218.

47. Lin, J. H., Walter, P., and Yen, T. S. (2008) Endoplasmic reticulum stress in disease pathogenesis, *Annu Rev Pathol 3*, 399-425.

48. Yoshida, H. (2007) ER stress and diseases, *FEBS J 274*, 630-658.

49. Zhou, H., Gurley, E. C., Jarujaron, S., Ding, H., Fang, Y., Xu, Z., Pandak, W. M., Jr., and Hylemon, P. B. (2006) HIV protease inhibitors activate the unfolded protein response and disrupt lipid metabolism in primary hepatocytes, *American journal of physiology.Gastrointestinal and liver physiology 291*, G1071-1080.

50. Zhou, H., Pandak, W. M., Jr., and Hylemon, P. B. (2006) Cellular mechanisms of lipodystrophy induction by HIV protease inhibitors, *Future Lipidology 1*, 163.

51. Zhou, H., Pandak, W. M., Jr., Lyall, V., Natarajan, R., and Hylemon, P. B. (2005) HIV protease inhibitors activate the unfolded protein response in macrophages: implication for atherosclerosis and cardiovascular disease, *Molecular pharmacology 68*, 690-700.

52. Zhou, J., Lhotak, S., Hilditch, B. A., and Austin, R. C. (2005) Activation of the unfolded protein response occurs at all stages of atherosclerotic lesion development in apolipoprotein E-deficient mice, *Circulation 111*, 1814-1821.

53. Wu, X., Sun, L., Zha, W., Studer, E., Gurley, E., Chen, L., Wang, X., Hylemon, P. B., Pandak, W. M., Jr., Sanyal, A. J., Zhang, L., Wang, G., Chen, J., Wang, J. Y., and Zhou, H. (2010) HIV protease inhibitors induce endoplasmic reticulum stress and disrupt barrier integrity in intestinal epithelial cells, *Gastroenterology 138*, 197-209.

54. Djedaini, M., Peraldi, P., Drici, M. D., Darini, C., Saint-Marc, P., Dani, C., and Ladoux, A. (2009) Lopinavir co-induces insulin resistance and ER stress in human adipocytes, *Biochemical and biophysical research communications 386*, 96-100.

55. Cho, H. Y., Thomas, S., Golden, E. B., Gaffney, K. J., Hofman, F. M., Chen, T. C., Louie, S. G., Petasis, N. A., and Schonthal, A. H. (2009) Enhanced killing of chemo-resistant breast cancer cells via controlled aggravation of ER stress, *Cancer Lett 282*, 87-97.

56. Pyrko, P., Kardosh, A., Wang, W., Xiong, W., Schonthal, A. H., and Chen, T. C. (2007) HIV-1 protease inhibitors nelfinavir and atazanavir induce malignant glioma death by triggering endoplasmic reticulum stress, *Cancer Res 67*, 10920-10928.

57. Nishina, S., Korenaga, M., Hidaka, I., Shinozaki, A., Sakai, A., Gondo, T., Tabuchi, M., Kishi, F., and Hino, K. (2010) Hepatitis C virus protein and iron overload induce hepatic steatosis through the unfolded protein response in mice, *Liver Int 30*, 683-692.

58. Kammoun, H. L., Chabanon, H., Hainault, I., Luquet, S., Magnan, C., Koike, T., Ferre, P., and Foufelle, F. (2009) GRP78 expression inhibits insulin and ER stress-induced SREBP-1c activation and reduces hepatic steatosis in mice, *J Clin Invest 119*, 1201-1215.

59. Alhusaini, S., McGee, K., Schisano, B., Harte, A., McTernan, P., Kumar, S., and Tripathi, G. (2010) Lipopolysaccharide, high glucose and saturated fatty acids induce endoplasmic reticulum stress in cultured primary human adipocytes: Salicylate alleviates this stress, *Biochem Biophys Res Commun 397*, 472-478.

60. Boden, G., Duan, X., Homko, C., Molina, E. J., Song, W., Perez, O., Cheung, P., and Merali, S. (2008) Increase in endoplasmic reticulum stress-related proteins and genes in adipose tissue of obese, insulin-resistant individuals, *Diabetes 57*, 2438-2444.

61. Gregor, M. F., Yang, L., Fabbrini, E., Mohammed, B. S., Eagon, J. C., Hotamisligil, G. S., and Klein, S. (2009) Endoplasmic reticulum stress is reduced in tissues of obese subjects after weight loss, *Diabetes 58*, 693-700.

62. Sharma, N. K., Das, S. K., Mondal, A. K., Hackney, O. G., Chu, W. S., Kern, P. A., Rasouli, N., Spencer, H. J., Yao-Borengasser, A., and Elbein, S. C. (2008) Endoplasmic reticulum stress markers are associated with obesity in nondiabetic subjects, *J Clin Endocrinol Metab 93*, 4532-4541.

63. Yoshida, H., Matsui, T., Yamamoto, A., Okada, T., and Mori, K. (2001) XBP1 mRNA is induced by ATF6 and spliced by IRE1 in response to ER stress to produce a highly active transcription factor, *Cell 107*, 881-891.

64. Yoshida, H., Matsui, T., Hosokawa, N., Kaufman, R. J., Nagata, K., and Mori, K. (2003) A time-dependent phase shift in the mammalian unfolded protein response, *Dev Cell 4*, 265-271.

65. Lee, A. H., Iwakoshi, N. N., and Glimcher, L. H. (2003) XBP-1 regulates a subset of endoplasmic reticulum resident chaperone genes in the unfolded protein response, *Mol Cell Biol 23*, 7448-7459.

66. Sriburi, R., Jackowski, S., Mori, K., and Brewer, J. W. (2004) XBP1: a link between the unfolded protein response, lipid biosynthesis, and biogenesis of the endoplasmic reticulum, *J Cell Biol 167*, 35-41.

67. Reimold, A. M., Iwakoshi, N. N., Manis, J., Vallabhajosyula, P., Szomolanyi-Tsuda, E., Gravallese, E. M., Friend, D., Grusby, M. J., Alt, F., and Glimcher, L. H. (2001) Plasma cell differentiation requires the transcription factor XBP-1, *Nature 412*, 300-307.

68. Lee, A. H., Chu, G. C., Iwakoshi, N. N., and Glimcher, L. H. (2005) XBP-1 is required for biogenesis of cellular secretory machinery of exocrine glands, *Embo J 24*, 4368-4380.

69. Sriburi, R., Bommiasamy, H., Buldak, G. L., Robbins, G. R., Frank, M., Jackowski, S., and Brewer, J. W. (2007) Coordinate regulation of phospholipid biosynthesis and secretory pathway gene expression in XBP-1(S)-induced endoplasmic reticulum biogenesis, *J Biol Chem 282*, 7024-7034.

70. Damiano, F., Alemanno, S., Gnoni, G. V., and Siculella, L. (2010) Translational control of the sterol-regulatory transcription factor SREBP-1 mRNA in response to serum starvation or ER stress is mediated by an internal ribosome entry site, *Biochem J 429*, 603-612.

71. DeGracia, D. J., Kumar, R., Owen, C. R., Krause, G. S., and White, B. C. (2002) Molecular pathways of protein synthesis inhibition during brain reperfusion: implications for neuronal survival or death, *J Cereb Blood Flow Metab 22*, 127-141.

72. Yang, Q., and Sarnow, P. (1997) Location of the internal ribosome entry site in the 5' non-coding region of the immunoglobulin heavy-chain binding protein (BiP) mRNA: evidence for specific RNA-protein interactions, *Nucleic Acids Res 25*, 2800-2807.

73. Ameri, K., and Harris, A. L. (2008) Activating transcription factor 4, *Int J Biochem Cell Biol 40*, 14-21.

74. Rutkowski, D. T., and Kaufman, R. J. (2003) All roads lead to ATF4, *Dev Cell 4*, 442-444.

75. Wek, R. C., Jiang, H. Y., and Anthony, T. G. (2006) Coping with stress: eIF2 kinases and translational control, *Biochem Soc Trans 34*, 7-11.

76. Batchvarova, N., Wang, X. Z., and Ron, D. (1995) Inhibition of adipogenesis by the stress-induced protein CHOP (Gadd153), *EMBO J 14*, 4654-4661.

77. Clarke, S. L., Robinson, C. E., and Gimble, J. M. (1997) CAAT/enhancer binding proteins directly modulate transcription from the peroxisome proliferator-activated receptor gamma 2 promoter, *Biochem Biophys Res Commun 240*, 99-103.

78. Adelmant, G., Gilbert, J. D., and Freytag, S. O. (1998) Human translocation liposarcoma-CCAAT/enhancer binding protein (C/EBP) homologous protein (TLS-CHOP) oncoprotein prevents adipocyte differentiation by directly interfering with C/EBPbeta function, *J Biol Chem 273*, 15574-15581.

79. Wang, C., Huang, Z., Du, Y., Cheng, Y., Chen, S., and Guo, F. (2010) ATF4 regulates lipid metabolism and thermogenesis, *Cell Res 20*, 174-184.

80. Bobrovnikova-Marjon, E., Hatzivassiliou, G., Grigoriadou, C., Romero, M., Cavener, D. R., Thompson, C. B., and Diehl, J. A. (2008) PERK-dependent regulation of lipogenesis

during mouse mammary gland development and adipocyte differentiation, *Proc Natl Acad Sci U S A 105*, 16314-16319.

81. Haze, K., Yoshida, H., Yanagi, H., Yura, T., and Mori, K. (1999) Mammalian transcription factor ATF6 is synthesized as a transmembrane protein and activated by proteolysis in response to endoplasmic reticulum stress, *Mol Biol Cell 10*, 3787-3799.

82. Davenport, E. L., Morgan, G. J., and Davies, F. E. (2008) Untangling the unfolded protein response, *Cell Cycle 7*, 865-869.

83. Urano, F., Wang, X., Bertolotti, A., Zhang, Y., Chung, P., Harding, H. P., and Ron, D. (2000) Coupling of stress in the ER to activation of JNK protein kinases by transmembrane protein kinase IRE1, *Science 287*, 664-666.

84. Klee, M., Pallauf, K., Alcala, S., Fleischer, A., and Pimentel-Muinos, F. X. (2009) Mitochondrial apoptosis induced by BH3-only molecules in the exclusive presence of endoplasmic reticular Bak, *Embo J 28*, 1757-1768.

85. Breckenridge, D. G., Germain, M., Mathai, J. P., Nguyen, M., and Shore, G. C. (2003) Regulation of apoptosis by endoplasmic reticulum pathways, *Oncogene 22*, 8608-8618.

86. Rizzuto, R., and Pozzan, T. (2006) Microdomains of intracellular Ca2+: molecular determinants and functional consequences, *Physiol Rev 86*, 369-408.

87. Rao, R. V., Poksay, K. S., Castro-Obregon, S., Schilling, B., Row, R. H., del Rio, G., Gibson, B. W., Ellerby, H. M., and Bredesen, D. E. (2004) Molecular components of a cell death pathway activated by endoplasmic reticulum stress, *J Biol Chem 279*, 177-187.

88. Oyadomari, S., and Mori, M. (2004) Roles of CHOP/GADD153 in endoplasmic reticulum stress, *Cell Death Differ 11*, 381-389.

89. Tabas, I., and Ron, D. (2011) Integrating the mechanisms of apoptosis induced by endoplasmic reticulum stress, *Nat Cell Biol 13*, 184-190.

90. Rao, R. V., Peel, A., Logvinova, A., del Rio, G., Hermel, E., Yokota, T., Goldsmith, P. C., Ellerby, L. M., Ellerby, H. M., and Bredesen, D. E. (2002) Coupling endoplasmic reticulum stress to the cell death program: role of the ER chaperone GRP78, *FEBS Lett 514*, 122-128.

91. McCullough, K. D., Martindale, J. L., Klotz, L. O., Aw, T. Y., and Holbrook, N. J. (2001) Gadd153 sensitizes cells to endoplasmic reticulum stress by down-regulating Bcl2 and perturbing the cellular redox state, *Mol Cell Biol 21*, 1249-1259.

92. Chiribau, C. B., Gaccioli, F., Huang, C. C., Yuan, C. L., and Hatzoglou, M. (2010) Molecular symbiosis of CHOP and C/EBP beta isoform LIP contributes to endoplasmic reticulum stress-induced apoptosis, *Mol Cell Biol 30*, 3722-3731.

93. Marciniak, S. J., Yun, C. Y., Oyadomari, S., Novoa, I., Zhang, Y., Jungreis, R., Nagata, K., Harding, H. P., and Ron, D. (2004) CHOP induces death by promoting protein synthesis and oxidation in the stressed endoplasmic reticulum, *Genes Dev 18*, 3066-3077.

94. Li, G., Mongillo, M., Chin, K. T., Harding, H., Ron, D., Marks, A. R., and Tabas, I. (2009) Role of ERO1-alpha-mediated stimulation of inositol 1,4,5-triphosphate receptor activity in endoplasmic reticulum stress-induced apoptosis, *J Cell Biol 186*, 783-792.

95. Kyriakis, J. M., Banerjee, P., Nikolakaki, E., Dai, T., Rubie, E. A., Ahmad, M. F., Avruch, J., and Woodgett, J. R. (1994) The stress-activated protein kinase subfamily of c-Jun kinases, *Nature 369*, 156-160.

96. Xia, Z., Dickens, M., Raingeaud, J., Davis, R. J., and Greenberg, M. E. (1995) Opposing effects of ERK and JNK-p38 MAP kinases on apoptosis, *Science (New York, N.Y.) 270*, 1326-1331.

97. Tournier, C., Hess, P., Yang, D. D., Xu, J., Turner, T. K., Nimnual, A., Bar-Sagi, D., Jones, S. N., Flavell, R. A., and Davis, R. J. (2000) Requirement of JNK for stress-induced activation of the cytochrome c-mediated death pathway, *Science (New York, N.Y.) 288*, 870-874.

98. Hotchkiss, R. S., Strasser, A., McDunn, J. E., and Swanson, P. E. (2009) Cell death, *N Engl J Med 361*, 1570-1583.

99. Mijaljica, D., Prescott, M., and Devenish, R. J. (2010) Autophagy in disease, *Methods in molecular biology (Clifton, N.J.) 648*, 79-92.

100. Todde, V., Veenhuis, M., and van der Klei, I. J. (2009) Autophagy: principles and significance in health and disease, *Biochim Biophys Acta 1792*, 3-13.

101. Li, W., Yang, Q., and Mao, Z. (2011) Chaperone-mediated autophagy: machinery, regulation and biological consequences, *Cell Mol Life Sci 68*, 749-763.

102. Tolkovsky, A. M. (2009) Mitophagy, *Biochim Biophys Acta 1793*, 1508-1515.

103. Kovsan, J., Bashan, N., Greenberg, A. S., and Rudich, A. (2010) Potential role of autophagy in modulation of lipid metabolism, *Am J Physiol Endocrinol Metab 298*, E1-7.

104. Suzuki, K., Kirisako, T., Kamada, Y., Mizushima, N., Noda, T., and Ohsumi, Y. (2001) The pre-autophagosomal structure organized by concerted functions of APG genes is essential for autophagosome formation, *Embo J 20*, 5971-5981.

105. Juhasz, G., and Neufeld, T. P. (2006) Autophagy: a forty-year search for a missing membrane source, *PLoS Biol 4*, e36.

106. Dunn, W. A., Jr. (1990) Studies on the mechanisms of autophagy: maturation of the autophagic vacuole, *J Cell Biol 110*, 1935-1945.

107. Dunn, W. A., Jr. (1994) Autophagy and related mechanisms of lysosome-mediated protein degradation, *Trends Cell Biol 4*, 139-143.

108. Kawai, A., Uchiyama, H., Takano, S., Nakamura, N., and Ohkuma, S. (2007) Autophagosome-lysosome fusion depends on the pH in acidic compartments in CHO cells, *Autophagy 3*, 154-157.

109. Burman, C., and Ktistakis, N. T. (2010) Autophagosome formation in mammalian cells, *Semin Immunopathol 32*, 397-413.

110. Klionsky, D. J., Cregg, J. M., Dunn, W. A., Jr., Emr, S. D., Sakai, Y., Sandoval, I. V., Sibirny, A., Subramani, S., Thumm, M., Veenhuis, M., and Ohsumi, Y. (2003) A unified nomenclature for yeast autophagy-related genes, *Dev Cell 5*, 539-545.

111. Suzuki, K., and Ohsumi, Y. (2010) Current knowledge of the pre-autophagosomal structure (PAS), *FEBS Lett 584*, 1280-1286.

112. Ding, W. X., Manley, S., and Ni, H. M. (2011) The emerging role of autophagy in alcoholic liver disease, *Exp Biol Med (Maywood) 236*, 546-556.

113. Gimenez-Xavier, P., Francisco, R., Platini, F., Perez, R., and Ambrosio, S. (2008) LC3-I conversion to LC3-II does not necessarily result in complete autophagy, *International journal of molecular medicine 22*, 781-785.

114. Asanuma, K., Tanida, I., Shirato, I., Ueno, T., Takahara, H., Nishitani, T., Kominami, E., and Tomino, Y. (2003) MAP-LC3, a promising autophagosomal marker, is processed during the differentiation and recovery of podocytes from PAN nephrosis, *Faseb J 17*, 1165-1167.

115. Klionsky, D. J., Abeliovich, H., Agostinis, P., Agrawal, D. K., Aliev, G., Askew, D. S., Baba, M., Baehrecke, E. H., Bahr, B. A., Ballabio, A., Bamber, B. A., Bassham, D. C., Bergamini, E., Bi, X., Biard-Piechaczyk, M., Blum, J. S., Bredesen, D. E., Brodsky, J. L., Brumell, J. H., Brunk, U. T., Bursch, W., Camougrand, N., Cebollero, E., Cecconi, F., Chen, Y., Chin, L. S., Choi, A., Chu, C. T., Chung, J., Clarke, P. G., Clark, R. S., Clarke, S. G., Clave, C., Cleveland, J. L., Codogno, P., Colombo, M. I., Coto-Montes, A., Cregg, J. M., Cuervo, A. M., Debnath, J., Demarchi, F., Dennis, P. B., Dennis, P. A., Deretic, V., Devenish, R. J., Di Sano, F., Dice, J. F., Difiglia, M., Dinesh-Kumar, S., Distelhorst, C. W., Djavaheri-Mergny, M., Dorsey, F. C., Droge, W., Dron, M., Dunn, W. A., Jr., Duszenko, M., Eissa, N. T., Elazar, Z., Esclatine, A., Eskelinen, E. L., Fesus, L., Finley, K. D., Fuentes, J. M., Fueyo, J., Fujisaki, K., Galliot, B., Gao, F. B., Gewirtz, D. A., Gibson, S. B., Gohla, A., Goldberg, A. L., Gonzalez, R., Gonzalez-Estevez, C., Gorski, S., Gottlieb, R. A., Haussinger, D., He, Y. W., Heidenreich, K., Hill, J. A., Hoyer-Hansen, M., Hu, X., Huang, W. P., Iwasaki, A., Jaattela, M., Jackson, W. T., Jiang, X., Jin, S., Johansen, T., Jung, J. U., Kadowaki, M., Kang, C., Kelekar, A., Kessel, D. H., Kiel, J. A., Kim, H. P., Kimchi, A., Kinsella, T. J., Kiselyov, K., Kitamoto, K., Knecht, E., Komatsu, M., Kominami, E., Kondo, S., Kovacs, A. L., Kroemer, G., Kuan, C. Y., Kumar, R., Kundu, M., Landry, J., Laporte, M., Le, W., Lei, H. Y., Lenardo, M. J., Levine, B., Lieberman, A., Lim, K. L., Lin, F. C., Liou, W., Liu, L. F., Lopez-Berestein, G., Lopez-Otin, C., Lu, B., Macleod, K. F., Malorni, W., Martinet, W., Matsuoka, K., Mautner, J., Meijer, A. J., Melendez, A., Michels, P., Miotto, G., Mistiaen, W. P., Mizushima, N., Mograbi, B., Monastyrska, I., Moore, M. N., Moreira, P. I., Moriyasu, Y., Motyl, T., Munz, C., Murphy, L. O., Naqvi, N. I., Neufeld, T. P., Nishino, I., Nixon,

R. A., Noda, T., Nurnberg, B., Ogawa, M., Oleinick, N. L., Olsen, L. J., Ozpolat, B., Paglin, S., Palmer, G. E., Papassideri, I., Parkes, M., Perlmutter, D. H., Perry, G., Piacentini, M., Pinkas-Kramarski, R., Prescott, M., Proikas-Cezanne, T., Raben, N., Rami, A., Reggiori, F., Rohrer, B., Rubinsztein, D. C., Ryan, K. M., Sadoshima, J., Sakagami, H., Sakai, Y., Sandri, M., Sasakawa, C., Sass, M., Schneider, C., Seglen, P. O., Seleverstov, O., Settleman, J., Shacka, J. J., Shapiro, I. M., Sibirny, A., Silva-Zacarin, E. C., Simon, H. U., Simone, C., Simonsen, A., Smith, M. A., Spanel-Borowski, K., Srinivas, V., Steeves, M., Stenmark, H., Stromhaug, P. E., Subauste, C. S., Sugimoto, S., Sulzer, D., Suzuki, T., Swanson, M. S., Tabas, I., Takeshita, F., Talbot, N. J., Talloczy, Z., Tanaka, K., Tanaka, K., Tanida, I., Taylor, G. S., Taylor, J. P., Terman, A., Tettamanti, G., Thompson, C. B., Thumm, M., Tolkovsky, A. M., Tooze, S. A., Truant, R., Tumanovska, L. V., Uchiyama, Y., Ueno, T., Uzcategui, N. L., van der Klei, I., Vaquero, E. C., Vellai, T., Vogel, M. W., Wang, H. G., Webster, P., Wiley, J. W., Xi, Z., Xiao, G., Yahalom, J., Yang, J. M., Yap, G., Yin, X. M., Yoshimori, T., Yu, L., Yue, Z., Yuzaki, M., Zabirnyk, O., Zheng, X., Zhu, X., and Deter, R. L. (2008) Guidelines for the use and interpretation of assays for monitoring autophagy in higher eukaryotes, *Autophagy 4*, 151-175.

116. Kawakami, T., Inagi, R., Takano, H., Sato, S., Ingelfinger, J. R., Fujita, T., and Nangaku, M. (2009) Endoplasmic reticulum stress induces autophagy in renal proximal tubular cells, *Nephrology, dialysis, transplantation : official publication of the European Dialysis and Transplant Association - European Renal Association 24*, 2665-2672.

117. Yorimitsu, T., Nair, U., Yang, Z., and Klionsky, D. J. (2006) Endoplasmic reticulum stress triggers autophagy, *J Biol Chem 281*, 30299-30304.

118. Ding, W. X., and Yin, X. M. (2008) Sorting, recognition and activation of the misfolded protein degradation pathways through macroautophagy and the proteasome, *Autophagy 4*, 141-150.

119. Ding, W. X., Ni, H. M., Gao, W., Yoshimori, T., Stolz, D. B., Ron, D., and Yin, X. M. (2007) Linking of autophagy to ubiquitin-proteasome system is important for the regulation of endoplasmic reticulum stress and cell viability, *Am J Pathol 171*, 513-524.

120. Kouroku, Y., Fujita, E., Tanida, I., Ueno, T., Isoai, A., Kumagai, H., Ogawa, S., Kaufman, R. J., Kominami, E., and Momoi, T. (2007) ER stress (PERK/eIF2alpha phosphorylation) mediates the polyglutamine-induced LC3 conversion, an essential step for autophagy formation, *Cell Death Differ 14*, 230-239.

121. Yorimitsu, T., and Klionsky, D. J. (2007) Eating the endoplasmic reticulum: quality control by autophagy, *Trends in cell biology 17*, 279-285.

122. Thorburn, A. (2008) Apoptosis and autophagy: regulatory connections between two supposedly different processes, *Apoptosis 13*, 1-9.

123. Price, J., Zaidi, A. K., Bohensky, J., Srinivas, V., Shapiro, I. M., and Ali, H. (2010) Akt-1 mediates survival of chondrocytes from endoplasmic reticulum-induced stress, *Journal of cellular physiology 222*, 502-508.

124. Qin, L., Wang, Z., Tao, L., and Wang, Y. (2010) ER stress negatively regulates AKT/TSC/mTOR pathway to enhance autophagy, *Autophagy 6*, 239-247.

125. Ogata, M., Hino, S., Saito, A., Morikawa, K., Kondo, S., Kanemoto, S., Murakami, T., Taniguchi, M., Tanii, I., Yoshinaga, K., Shiosaka, S., Hammarback, J. A., Urano, F., and Imaizumi, K. (2006) Autophagy is activated for cell survival after endoplasmic reticulum stress, *Mol Cell Biol 26*, 9220-9231.

126. Gupta, A. K., Li, B., Cerniglia, G. J., Ahmed, M. S., Hahn, S. M., and Maity, A. (2007) The HIV protease inhibitor nelfinavir downregulates Akt phosphorylation by inhibiting proteasomal activity and inducing the unfolded protein response, *Neoplasia 9*, 271-278.

127. Schleicher, S. M., Moretti, L., Varki, V., and Lu, B. (2010) Progress in the unraveling of the endoplasmic reticulum stress/autophagy pathway and cancer: implications for future therapeutic approaches, *Drug Resist Updat 13*, 79-86.

128. Zhou, L., Zhang, J., Fang, Q., Liu, M., Liu, X., Jia, W., Dong, L. Q., and Liu, F. (2009) Autophagy-mediated insulin receptor down-regulation contributes to endoplasmic reticulum stress-induced insulin resistance, *Mol Pharmacol 76*, 596-603.

129. Kim, K. W., Moretti, L., Mitchell, L. R., Jung, D. K., and Lu, B. (2010) Endoplasmic reticulum stress mediates radiation-induced autophagy by perk-eIF2alpha in caspase-3/7-deficient cells, *Oncogene 29*, 3241-3251.

130. Rzymski, T., Milani, M., Pike, L., Buffa, F., Mellor, H. R., Winchester, L., Pires, I., Hammond, E., Ragoussis, I., and Harris, A. L. (2010) Regulation of autophagy by ATF4 in response to severe hypoxia, *Oncogene 29*, 4424-4435.

131. Milani, M., Rzymski, T., Mellor, H. R., Pike, L., Bottini, A., Generali, D., and Harris, A. L. (2009) The role of ATF4 stabilization and autophagy in resistance of breast cancer cells treated with Bortezomib, *Cancer Res 69*, 4415-4423.

132. Seo, Y. K., Jeon, T. I., Chong, H. K., Biesinger, J., Xie, X., and Osborne, T. F. (2011) Genome-wide Localization of SREBP-2 in Hepatic Chromatin Predicts a Role in Autophagy, *Cell Metab 13*, 367-375.

133. Cheng, J., Ohsaki, Y., Tauchi-Sato, K., Fujita, A., and Fujimoto, T. (2006) Cholesterol depletion induces autophagy, *Biochem Biophys Res Commun 351*, 246-252.

134. Bays, H. E., Gonzalez-Campoy, J. M., Henry, R. R., Bergman, D. A., Kitabchi, A. E., Schorr, A. B., and Rodbard, H. W. (2008) Is adiposopathy (sick fat) an endocrine disease?, *Int J Clin Pract 62*, 1474-1483.

135. Pittenger, M. F., Mackay, A. M., Beck, S. C., Jaiswal, R. K., Douglas, R., Mosca, J. D., Moorman, M. A., Simonetti, D. W., Craig, S., and Marshak, D. R. (1999) Multilineage potential of adult human mesenchymal stem cells, *Science 284*, 143-147.

136. Otto, T. C., and Lane, M. D. (2005) Adipose development: from stem cell to adipocyte, *Crit Rev Biochem Mol Biol 40*, 229-242.

137. Atmani, H., Chappard, D., and Basle, M. F. (2003) Proliferation and differentiation of osteoblasts and adipocytes in rat bone marrow stromal cell cultures: effects of dexamethasone and calcitriol, *J Cell Biochem 89*, 364-372.

138. Amos, P. J., Shang, H., Bailey, A. M., Taylor, A., Katz, A. J., and Peirce, S. M. (2008) IFATS collection: The role of human adipose-derived stromal cells in inflammatory microvascular remodeling and evidence of a perivascular phenotype, In *Stem cells*, pp 2682-2690.

139. Tang, Q. Q., Otto, T. C., and Lane, M. D. (2004) Commitment of C3H10T1/2 pluripotent stem cells to the adipocyte lineage, *Proc Natl Acad Sci U S A 101*, 9607-9611.

140. Liu, J., DeYoung, S. M., Zhang, M., Zhang, M., Cheng, A., and Saltiel, A. R. (2005) Changes in integrin expression during adipocyte differentiation, *Cell Metab 2*, 165-177.

141. Lane, M. D., Tang, Q. Q., and Jiang, M. S. (1999) Role of the CCAAT enhancer binding proteins (C/EBPs) in adipocyte differentiation, *Biochem Biophys Res Commun 266*, 677-683.

142. Darlington, G. J., Ross, S. E., and MacDougald, O. A. (1998) The role of C/EBP genes in adipocyte differentiation, *J Biol Chem 273*, 30057-30060.

143. Zhang, J. W., Klemm, D. J., Vinson, C., and Lane, M. D. (2004) Role of CREB in transcriptional regulation of CCAAT/enhancer-binding protein beta gene during adipogenesis, *J Biol Chem 279*, 4471-4478.

144. Tanaka, T., Yoshida, N., Kishimoto, T., and Akira, S. (1997) Defective adipocyte differentiation in mice lacking the C/EBPbeta and/or C/EBPdelta gene, *Embo J 16*, 7432-7443.

145. Christy, R. J., Kaestner, K. H., Geiman, D. E., and Lane, M. D. (1991) CCAAT/enhancer binding protein gene promoter: binding of nuclear factors during differentiation of 3T3-L1 preadipocytes, *Proc Natl Acad Sci U S A 88*, 2593-2597.

146. Schwarz, E. J., Reginato, M. J., Shao, D., Krakow, S. L., and Lazar, M. A. (1997) Retinoic acid blocks adipogenesis by inhibiting C/EBPbeta-mediated transcription, *Mol Cell Biol 17*, 1552-1561.

147. Shao, D., and Lazar, M. A. (1997) Peroxisome proliferator activated receptor gamma, CCAAT/enhancer-binding protein alpha, and cell cycle status regulate the commitment to adipocyte differentiation, *J Biol Chem 272*, 21473-21478.

148. Tamori, Y., Masugi, J., Nishino, N., and Kasuga, M. (2002) Role of peroxisome proliferator-activated receptor-gamma in maintenance of the characteristics of mature 3T3-L1 adipocytes, *Diabetes 51*, 2045-2055.

149. Barak, Y., Nelson, M. C., Ong, E. S., Jones, Y. Z., Ruiz-Lozano, P., Chien, K. R., Koder, A., and Evans, R. M. (1999) PPAR gamma is required for placental, cardiac, and adipose tissue development, *Molecular cell 4*, 585-595.

150. Lehrke, M., and Lazar, M. A. (2005) The many faces of PPARgamma, *Cell 123*, 993-999.

151. Savage, D. B., Tan, G. D., Acerini, C. L., Jebb, S. A., Agostini, M., Gurnell, M., Williams, R. L., Umpleby, A. M., Thomas, E. L., Bell, J. D., Dixon, A. K., Dunne, F., Boiani, R., Cinti, S., Vidal-Puig, A., Karpe, F., Chatterjee, V. K., and O'Rahilly, S. (2003) Human metabolic syndrome resulting from dominant-negative mutations in the nuclear receptor peroxisome proliferator-activated receptor-gamma, *Diabetes 52*, 910-917.

152. Camp, H. S., Ren, D., and Leff, T. (2002) Adipogenesis and fat-cell function in obesity and diabetes, *Trends Mol Med 8*, 442-447.

153. Tontonoz, P., Hu, E., and Spiegelman, B. M. (1994) Stimulation of adipogenesis in fibroblasts by PPAR gamma 2, a lipid-activated transcription factor, *Cell 79*, 1147-1156.

154. Schoonjans, K., Peinado-Onsurbe, J., Lefebvre, A. M., Heyman, R. A., Briggs, M., Deeb, S., Staels, B., and Auwerx, J. (1996) PPARalpha and PPARgamma activators direct a distinct tissue-specific transcriptional response via a PPRE in the lipoprotein lipase gene, *Embo J 15*, 5336-5348.

155. Kim, Y. J., Cho, S. Y., Yun, C. H., Moon, Y. S., Lee, T. R., and Kim, S. H. (2008) Transcriptional activation of Cidec by PPARgamma2 in adipocyte, *Biochem Biophys Res Commun 377*, 297-302.

156. Kim, J. Y., Tillison, K., Lee, J. H., Rearick, D. A., and Smas, C. M. (2006) The adipose tissue triglyceride lipase ATGL/PNPLA2 is downregulated by insulin and TNF-alpha in 3T3-L1 adipocytes and is a target for transactivation by PPARgamma, *Am J Physiol Endocrinol Metab 291*, E115-127.

157. Ohoka, N., Kato, S., Takahashi, Y., Hayashi, H., and Sato, R. (2009) The orphan nuclear receptor RORalpha restrains adipocyte differentiation through a reduction of C/EBPbeta activity and perilipin gene expression, *Mol Endocrinol 23*, 759-771.

158. Hua, X., Wu, J., Goldstein, J. L., Brown, M. S., and Hobbs, H. H. (1995) Structure of the human gene encoding sterol regulatory element binding protein-1 (SREBF1) and localization of SREBF1 and SREBF2 to chromosomes 17p11.2 and 22q13, *Genomics 25*, 667-673.

159. Kim, J. B., and Spiegelman, B. M. (1996) ADD1/SREBP1 promotes adipocyte differentiation and gene expression linked to fatty acid metabolism, *Genes Dev 10*, 1096-1107.

160. Farese, R. V., Jr., and Walther, T. C. (2009) Lipid droplets finally get a little R-E-S-P-E-C-T, *Cell 139*, 855-860.

161. Brasaemle, D. L., Barber, T., Kimmel, A. R., and Londos, C. (1997) Post-translational regulation of perilipin expression. Stabilization by stored intracellular neutral lipids, *J Biol Chem 272*, 9378-9387.

162. Yamaguchi, T., Omatsu, N., Morimoto, E., Nakashima, H., Ueno, K., Tanaka, T., Satouchi, K., Hirose, F., and Osumi, T. (2007) CGI-58 facilitates lipolysis on lipid droplets but is not involved in the vesiculation of lipid droplets caused by hormonal stimulation, *J Lipid Res 48*, 1078-1089.

163. Brasaemle, D. L., Subramanian, V., Garcia, A., Marcinkiewicz, A., and Rothenberg, A. (2009) Perilipin A and the control of triacylglycerol metabolism, *Mol Cell Biochem 326*, 15-21.

164. Hickenbottom, S. J., Kimmel, A. R., Londos, C., and Hurley, J. H. (2004) Structure of a lipid droplet protein; the PAT family member TIP47, *Structure 12*, 1199-1207.

165. Ahmadian, M., Wang, Y., and Sul, H. S. (2010) Lipolysis in adipocytes, *Int J Biochem Cell Biol 42*, 555-559.

166. Wolins, N. E., Skinner, J. R., Schoenfish, M. J., Tzekov, A., Bensch, K. G., and Bickel, P. E. (2003) Adipocyte protein S3-12 coats nascent lipid droplets, *J Biol Chem 278*, 37713-37721.

167. Wolins, N. E., Quaynor, B. K., Skinner, J. R., Schoenfish, M. J., Tzekov, A., and Bickel, P. E. (2005) S3-12, Adipophilin, and TIP47 package lipid in adipocytes, *J Biol Chem 280*, 19146-19155.

168. Sztalryd, C., Bell, M., Lu, X., Mertz, P., Hickenbottom, S., Chang, B. H., Chan, L., Kimmel, A. R., and Londos, C. (2006) Functional compensation for adipose differentiation-related protein (ADFP) by Tip47 in an ADFP null embryonic cell line, *J Biol Chem 281*, 34341-34348.

169. Brasaemle, D. L., Barber, T., Wolins, N. E., Serrero, G., Blanchette-Mackie, E. J., and Londos, C. (1997) Adipose differentiation-related protein is an ubiquitously expressed lipid storage droplet-associated protein, *J Lipid Res 38*, 2249-2263.

170. Bickel, P. E., Tansey, J. T., and Welte, M. A. (2009) PAT proteins, an ancient family of lipid droplet proteins that regulate cellular lipid stores, *Biochim Biophys Acta 1791*, 419-440.

171. Martinez-Botas, J., Anderson, J. B., Tessier, D., Lapillonne, A., Chang, B. H., Quast, M. J., Gorenstein, D., Chen, K. H., and Chan, L. (2000) Absence of perilipin results in leanness and reverses obesity in Lepr(db/db) mice, *Nat Genet 26*, 474-479.

172. Tansey, J. T., Sztalryd, C., Gruia-Gray, J., Roush, D. L., Zee, J. V., Gavrilova, O., Reitman, M. L., Deng, C. X., Li, C., Kimmel, A. R., and Londos, C. (2001) Perilipin ablation results in a lean mouse with aberrant adipocyte lipolysis, enhanced leptin production, and resistance to diet-induced obesity, *Proc Natl Acad Sci U S A 98*, 6494-6499.

173. Walther, T. C., and Farese, R. V., Jr. (2009) The life of lipid droplets, *Biochim Biophys Acta 1791*, 459-466.

174. Robenek H., B. I., Robenek M.J., Hofnagel O., Ruebel A., Troyer D., and Severs N.J. (2010) Topography of lipid droplet-associated proteins: insights from freeze-fracture replica immunogold labeling., *Journal of Lipids 2011*, 1-10.

175. Guo, Y., Walther, T. C., Rao, M., Stuurman, N., Goshima, G., Terayama, K., Wong, J. S., Vale, R. D., Walter, P., and Farese, R. V. (2008) Functional genomic screen reveals genes involved in lipid-droplet formation and utilization, *Nature 453*, 657-661.

176. Mohamed-Ali, V., Pinkney, J. H., and Coppack, S. W. (1998) Adipose tissue as an endocrine and paracrine organ, *International journal of obesity and related metabolic disorders : journal of the International Association for the Study of Obesity 22*, 1145-1158.

177. Ahima, R. S., and Flier, J. S. (2000) Adipose tissue as an endocrine organ, *Trends in endocrinology and metabolism: TEM 11*, 327-332.

178. Laharrague, P., and Casteilla, L. The emergence of adipocytes, *Endocr Dev 19*, 21-30.

179. Billon, N., Iannarelli, P., Monteiro, M. C., Glavieux-Pardanaud, C., Richardson, W. D., Kessaris, N., Dani, C., and Dupin, E. (2007) The generation of adipocytes by the neural crest, *Development 134*, 2283-2292.

180. Adams, M., Montague, C. T., Prins, J. B., Holder, J. C., Smith, S. A., Sanders, L., Digby, J. E., Sewter, C. P., Lazar, M. A., Chatterjee, V. K., and O'Rahilly, S. (1997) Activators of peroxisome proliferator-activated receptor gamma have depot-specific effects on human preadipocyte differentiation, *J Clin Invest 100*, 3149-3153.

181. Lefebvre, A. M., Laville, M., Vega, N., Riou, J. P., van Gaal, L., Auwerx, J., and Vidal, H. (1998) Depot-specific differences in adipose tissue gene expression in lean and obese subjects, *Diabetes 47*, 98-103.

182. Mallewa, J. E., Wilkins, E., Vilar, J., Mallewa, M., Doran, D., Back, D., and Pirmohamed, M. (2008) HIV-associated lipodystrophy: a review of underlying mechanisms and therapeutic options, *J Antimicrob Chemother 62*, 648-660.

183. Sha, H., He, Y., Chen, H., Wang, C., Zenno, A., Shi, H., Yang, X., Zhang, X., and Qi, L. (2009) The IRE1alpha-XBP1 pathway of the unfolded protein response is required for adipogenesis, *Cell Metab 9*, 556-564.

184. Adachi, Y., Yamamoto, K., Okada, T., Yoshida, H., Harada, A., and Mori, K. (2008) ATF6 is a transcription factor specializing in the regulation of quality control proteins in the endoplasmic reticulum, *Cell Struct Funct 33*, 75-89.

185. Shimomura, I., Hammer, R. E., Richardson, J. A., Ikemoto, S., Bashmakov, Y., Goldstein, J. L., and Brown, M. S. (1998) Insulin resistance and diabetes mellitus in transgenic mice expressing nuclear SREBP-1c in adipose tissue: model for congenital generalized lipodystrophy, *Genes Dev 12*, 3182-3194.

186. Kim, J. B., Wright, H. M., Wright, M., and Spiegelman, B. M. (1998) ADD1/SREBP1 activates PPARgamma through the production of endogenous ligand, *Proc Natl Acad Sci U S A 95*, 4333-4337.

187. Le Lay, S., Lefrere, I., Trautwein, C., Dugail, I., and Krief, S. (2002) Insulin and sterol-regulatory element-binding protein-1c (SREBP-1C) regulation of gene expression in 3T3-L1 adipocytes. Identification of CCAAT/enhancer-binding protein beta as an SREBP-1C target, *J Biol Chem 277*, 35625-35634.

188. Basseri, S., Lhotak, S., Sharma, A. M., and Austin, R. C. (2009) The chemical chaperone 4-phenylbutyrate inhibits adipogenesis by modulating the unfolded protein response, *J Lipid Res 50*, 2486-2501.

189. Shimada, T., Hiramatsu, N., Okamura, M., Hayakawa, K., Kasai, A., Yao, J., and Kitamura, M. (2007) Unexpected blockade of adipocyte differentiation by K-7174: implication for endoplasmic reticulum stress, *Biochem Biophys Res Commun 363*, 355-360.

190. Chen, L., Jarujaron, S., Wu, X., Sun, L., Zha, W., Liang, G., Wang, X., Gurley, E. C., Studer, E. J., Hylemon, P. B., Pandak, W. M., Jr., Zhang, L., Wang, G., Li, X., Dent, P., and Zhou, H. (2009) HIV protease inhibitor lopinavir-induced TNF-alpha and IL-6 expression is coupled to the unfolded protein response and ERK signaling pathways in macrophages, *Biochemical pharmacology 78*, 70-77.

191. Zha, W., Liang, G., Xiao, J., Studer, E. J., Hylemon, P. B., Pandak, W. M., Jr., Wang, G., Li, X., and Zhou, H. (2010) Berberine inhibits HIV protease inhibitor-induced inflammatory response by modulating ER stress signaling pathways in murine macrophages, *PLoS One 5*, e9069.

192. Jones, S. P., Janneh, O., Back, D. J., and Pirmohamed, M. (2005) Altered adipokine response in murine 3T3-F442A adipocytes treated with protease inhibitors and nucleoside reverse transcriptase inhibitors, *Antiviral Therapy 10*, 207-213.

193. Kim, R. J., Wilson, C. G., Wabitsch, M., Lazar, M. A., and Steppan, C. M. (2006) HIV protease inhibitor-specific alterations in human adipocyte differentiation and metabolism, *Obesity (Silver Spring, Md.) 14*, 994-1002.

194. Leroyer, S., Vatier, C., Kadiri, S., Quette, J., Chapron, C., Capeau, J., and Antoine, B. (2011) Glyceroneogenesis is inhibited through HIV protease inhibitor-induced inflammation in human subcutaneous but not visceral adipose tissue, *J Lipid Res 52*, 207-220.

195. Meng, L., Zhou, J., Sasano, H., Suzuki, T., Zeitoun, K. M., and Bulun, S. E. (2001) Tumor necrosis factor alpha and interleukin 11 secreted by malignant breast epithelial cells inhibit adipocyte differentiation by selectively down-regulating CCAAT/enhancer binding protein alpha and peroxisome proliferator-activated receptor gamma: mechanism of desmoplastic reaction, *Cancer Res 61*, 2250-2255.

196. Xu, H., Barnes, G. T., Yang, Q., Tan, G., Yang, D., Chou, C. J., Sole, J., Nichols, A., Ross, J. S., Tartaglia, L. A., and Chen, H. (2003) Chronic inflammation in fat plays a crucial role in the development of obesity-related insulin resistance, *J Clin Invest 112*, 1821-1830.

197. Bastard, J. P., Maachi, M., Lagathu, C., Kim, M. J., Caron, M., Vidal, H., Capeau, J., and Feve, B. (2006) Recent advances in the relationship between obesity, inflammation, and insulin resistance, *Eur Cytokine Netw 17*, 4-12.

198. Hotamisligil, G. S. (2006) Inflammation and metabolic disorders, *Nature 444*, 860-867.

199. Monteiro, R., and Azevedo, I. (2010) Chronic inflammation in obesity and the metabolic syndrome, *Mediators Inflamm 2010*.

200. Hertel, J., Struthers, H., Horj, C. B., and Hruz, P. W. (2004) A structural basis for the acute effects of HIV protease inhibitors on GLUT4 intrinsic activity, *J Biol Chem 279*, 55147-55152.

201. Shibata, M., Yoshimura, K., Furuya, N., Koike, M., Ueno, T., Komatsu, M., Arai, H., Tanaka, K., Kominami, E., and Uchiyama, Y. (2009) The MAP1-LC3 conjugation system is involved in lipid droplet formation, *Biochem Biophys Res Commun 382*, 419-423.

202. Shibata, M., Yoshimura, K., Tamura, H., Ueno, T., Nishimura, T., Inoue, T., Sasaki, M., Koike, M., Arai, H., Kominami, E., and Uchiyama, Y. (2010) LC3, a microtubule-associated protein1A/B light chain3, is involved in cytoplasmic lipid droplet formation, *Biochem Biophys Res Commun 393*, 274-279.

203. Baerga, R., Zhang, Y., Chen, P. H., Goldman, S., and Jin, S. (2009) Targeted deletion of autophagy-related 5 (atg5) impairs adipogenesis in a cellular model and in mice, *Autophagy 5*, 1118-1130.

204. Zhang, Y., Goldman, S., Baerga, R., Zhao, Y., Komatsu, M., and Jin, S. (2009) Adipose-specific deletion of autophagy-related gene 7 (atg7) in mice reveals a role in adipogenesis, *Proc Natl Acad Sci U S A 106*, 19860-19865.

205. Singh, R., Kaushik, S., Wang, Y., Xiang, Y., Novak, I., Komatsu, M., Tanaka, K., Cuervo, A. M., and Czaja, M. J. (2009) Autophagy regulates lipid metabolism, *Nature 458*, 1131-1135.

206. Zhou, J., Zhang, W., Liang, B., Casimiro, M. C., Whitaker-Menezes, D., Wang, M., Lisanti, M. P., Lanza-Jacoby, S., Pestell, R. G., and Wang, C. (2009) PPARgamma

activation induces autophagy in breast cancer cells, *Int J Biochem Cell Biol 41*, 2334-2342.

207. Yan, J., Yang, H., Wang, G., Sun, L., Zhou, Y., Guo, Y., Xi, Z., and Jiang, X. (2010) Autophagy augmented by troglitazone is independent of EGFR transactivation and correlated with AMP-activated protein kinase signaling, *Autophagy 6*, 67-73.

208. Kern, P. A., Di Gregorio, G. B., Lu, T., Rassouli, N., and Ranganathan, G. (2003) Adiponectin expression from human adipose tissue: relation to obesity, insulin resistance, and tumor necrosis factor-alpha expression, *Diabetes 52*, 1779-1785.

209. Zhou, L., Liu, M., Zhang, J., Chen, H., Dong, L. Q., and Liu, F. (2010) DsbA-L alleviates endoplasmic reticulum stress-induced adiponectin downregulation, *Diabetes 59*, 2809-2816.

210. Lee, G. A., Rao, M. N., and Grunfeld, C. (2005) The effects of HIV protease inhibitors on carbohydrate and lipid metabolism, *Curr HIV/AIDS Rep 2*, 39-50.

211. Woerle, H. J., Mariuz, P. R., Meyer, C., Reichman, R. C., Popa, E. M., Dostou, J. M., Welle, S. L., and Gerich, J. E. (2003) Mechanisms for the deterioration in glucose tolerance associated with HIV protease inhibitor regimens, *Diabetes 52*, 918-925.

212. Feldstein, A. E. (2010) Novel insights into the pathophysiology of nonalcoholic fatty liver disease, *Semin Liver Dis 30*, 391-401.

213. Hirosumi, J., Tuncman, G., Chang, L., Gorgun, C. Z., Uysal, K. T., Maeda, K., Karin, M., and Hotamisligil, G. S. (2002) A central role for JNK in obesity and insulin resistance, *Nature 420*, 333-336.

214. Ozcan, U., Cao, Q., Yilmaz, E., Lee, A. H., Iwakoshi, N. N., Ozdelen, E., Tuncman, G., Gorgun, C., Glimcher, L. H., and Hotamisligil, G. S. (2004) Endoplasmic reticulum stress links obesity, insulin action, and type 2 diabetes, *Science 306*, 457-461.

215. Borradaile, N. M., de Dreu, L. E., and Huff, M. W. (2003) Inhibition of net HepG2 cell apolipoprotein B secretion by the citrus flavonoid naringenin involves activation of phosphatidylinositol 3-kinase, independent of insulin receptor substrate-1 phosphorylation, *Diabetes 52*, 2554-2561.

216. Ota, T., Gayet, C., and Ginsberg, H. N. (2008) Inhibition of apolipoprotein B100 secretion by lipid-induced hepatic endoplasmic reticulum stress in rodents, *J Clin Invest 118*, 316-332.

217. Sidiropoulos, K. G., Meshkani, R., Avramoglu-Kohen, R., and Adeli, K. (2007) Insulin inhibition of apolipoprotein B mRNA translation is mediated via the PI-3 kinase/mTOR signaling cascade but does not involve internal ribosomal entry site (IRES) initiation, *Arch Biochem Biophys 465*, 380-388.

218. Qiu, W., Kohen-Avramoglu, R., Mhapsekar, S., Tsai, J., Austin, R. C., and Adeli, K. (2005) Glucosamine-induced endoplasmic reticulum stress promotes ApoB100 degradation: evidence for Grp78-mediated targeting to proteasomal degradation, *Arterioscler Thromb Vasc Biol 25*, 571-577.

219. Qiu, W., Zhang, J., Dekker, M. J., Wang, H., Huang, J., Brumell, J. H., and Adeli, K. (2011) Hepatic autophagy mediates endoplasmic reticulum stress-induced degradation of misfolded apolipoprotein B, *Hepatology 53*, 1515-1525.

220. Chow, W. A., Guo, S., and Valdes-Albini, F. (2006) Nelfinavir induces liposarcoma apoptosis and cell cycle arrest by upregulating sterol regulatory element binding protein-1, *Anticancer Drugs 17*, 891-903.

221. Nguyen, A. T., Gagnon, A., Angel, J. B., and Sorisky, A. (2000) Ritonavir increases the level of active ADD-1/SREBP-1 protein during adipogenesis, *Aids 14*, 2467-2473.

222. Cao, R., Hu, Y., Wang, Y., Gurley, E. C., Studer, E. J., Wang, X., Hylemon, P. B., Pandak, W. M., Sanyal, A. J., Zhang, L., and Zhou, H. (2010) Prevention of HIV protease inhibitor-induced dysregulation of hepatic lipid metabolism by raltegravir via endoplasmic reticulum stress signaling pathways, *The Journal of pharmacology and experimental therapeutics 334*, 530-539.

223. Parker, R. A., Flint, O. P., Mulvey, R., Elosua, C., Wang, F., Fenderson, W., Wang, S., Yang, W. P., and Noor, M. A. (2005) Endoplasmic reticulum stress links dyslipidemia to inhibition of proteasome activity and glucose transport by HIV protease inhibitors, *Mol Pharmacol 67*, 1909-1919.

224. Williams, K., Rao, Y. P., Natarajan, R., Pandak, W. M., and Hylemon, P. B. (2004) Indinavir alters sterol and fatty acid homeostatic mechanisms in primary rat hepatocytes by increasing levels of activated sterol regulatory element-binding proteins and decreasing cholesterol 7alpha-hydroxylase mRNA levels, *Biochemical pharmacology 67*, 255-267.

225. Singh, R. (2010) Autophagy and regulation of lipid metabolism, *Results and problems in cell differentiation 52*, 35-46.

226. Mottillo, E. P., Shen, X. J., and Granneman, J. G. (2007) Role of hormone-sensitive lipase in beta-adrenergic remodeling of white adipose tissue, *Am J Physiol Endocrinol Metab 293*, E1188-1197.

227. Wabitsch, M., Brenner, R. E., Melzner, I., Braun, M., Moller, P., Heinze, E., Debatin, K. M., and Hauner, H. (2001) Characterization of a human preadipocyte cell strain with high capacity for adipose differentiation, *Int J Obes Relat Metab Disord 25*, 8-15.

228. Kanda, H., Tamori, Y., Shinoda, H., Yoshikawa, M., Sakaue, M., Udagawa, J., Otani, H., Tashiro, F., Miyazaki, J., and Kasuga, M. (2005) Adipocytes from Munc18c-null mice show increased sensitivity to insulin-stimulated GLUT4 externalization, *J Clin Invest 115*, 291-301.

229. Bissell, D. M., and Guzelian, P. S. (1980) Degradation of endogenous hepatic heme by pathways not yielding carbon monoxide. Studies in normal rat liver and in primary hepatocyte culture, *J Clin Invest 65*, 1135-1140.

230. Thuillier, P., Baillie, R., Sha, X., and Clarke, S. D. (1998) Cytosolic and nuclear distribution of PPARgamma2 in differentiating 3T3-L1 preadipocytes, *J Lipid Res 39*, 2329-2338.

231. Or-Tzadikario, S., Sopher, R., and Gefen, A. (2010) Quantitative monitoring of lipid accumulation over time in cultured adipocytes as function of culture conditions: toward controlled adipose tissue engineering, *Tissue Eng Part C Methods 16*, 1167-1181.

232. Zhou, H., Jarujaron, S., Gurley, E. C., Chen, L., Ding, H., Studer, E., Pandak, W. M., Jr., Hu, W., Zou, T., Wang, J. Y., and Hylemon, P. B. (2007) HIV protease inhibitors increase TNF-alpha and IL-6 expression in macrophages: involvement of the RNA-binding protein HuR, *Atherosclerosis 195*, e134-143.

233. Gills, J. J., Lopiccolo, J., Tsurutani, J., Shoemaker, R. H., Best, C. J., Abu-Asab, M. S., Borojerdi, J., Warfel, N. A., Gardner, E. R., Danish, M., Hollander, M. C., Kawabata, S., Tsokos, M., Figg, W. D., Steeg, P. S., and Dennis, P. A. (2007) Nelfinavir, A lead HIV protease inhibitor, is a broad-spectrum, anticancer agent that induces endoplasmic reticulum stress, autophagy, and apoptosis in vitro and in vivo, *Clin Cancer Res 13*, 5183-5194.

234. McLean, K., VanDeVen, N. A., Sorenson, D. R., Daudi, S., and Liu, J. R. (2009) The HIV protease inhibitor saquinavir induces endoplasmic reticulum stress, autophagy, and apoptosis in ovarian cancer cells, *Gynecol Oncol 112*, 623-630.

235. Zhou, H., Pandak, W. M., Jr., and and Hylemon, P. B. (2006) Cellular mechanisms of lipodystrophy induction by HIV protease inhibitors, *Future Lipidology 1*, 163.

236. Fiorenza, C. G., Chou, S. H., and Mantzoros, C. S. (2011) Lipodystrophy: pathophysiology and advances in treatment, *Nat Rev Endocrinol 7*, 137-150.

237. Lionetti, L., Mollica, M. P., Lombardi, A., Cavaliere, G., Gifuni, G., and Barletta, A. (2009) From chronic overnutrition to insulin resistance: the role of fat-storing capacity and inflammation, *Nutrition, metabolism, and cardiovascular diseases : NMCD 19*, 146-152.

238. Virtue, S., and Vidal-Puig, A. (2010) Adipose tissue expandability, lipotoxicity and the Metabolic Syndrome--an allostatic perspective, *Biochim Biophys Acta 1801*, 338-349.

239. Caron, M., Auclair, M., Sterlingot, H., Kornprobst, M., and Capeau, J. (2003) Some HIV protease inhibitors alter lamin A/C maturation and stability, SREBP-1 nuclear localization and adipocyte differentiation, *AIDS (London, England) 17*, 2437-2444.

240. Cianflone, K., Zakarian, R., Stanculescu, C., and Germinario, R. (2006) Protease inhibitor effects on triglyceride synthesis and adipokine secretion in human omental and subcutaneous adipose tissue, *Antiviral Therapy 11*, 681-691.

241. Grigem, S., Fischer-Posovszky, P., Debatin, K. M., Loizon, E., Vidal, H., and Wabitsch, M. (2005) The effect of the HIV protease inhibitor ritonavir on proliferation, differentiation, lipogenesis, gene expression and apoptosis of human preadipocytes and adipocytes, *Hormone and metabolic research = Hormon- und Stoffwechselforschung = Hormones et metabolisme 37*, 602-609.

242. Jones, S. P., Waitt, C., Sutton, R., Back, D. J., and Pirmohamed, M. (2008) Effect of atazanavir and ritonavir on the differentiation and adipokine secretion of human subcutaneous and omental preadipocytes, *AIDS (London, England) 22*, 1293-1298.

243. Saillan-Barreau, C., Tabbakh, O., Chavoin, J. P., Casteilla, L., and Penicaud, L. (2008) Drug-specific effect of nelfinavir and stavudine on primary culture of human preadipocytes, *Journal of acquired immune deficiency syndromes (1999) 48*, 20-25.

244. Vernochet, C., Azoulay, S., Duval, D., Guedj, R., Cottrez, F., Vidal, H., Ailhaud, G., and Dani, C. (2005) Human immunodeficiency virus protease inhibitors accumulate into cultured human adipocytes and alter expression of adipocytokines, *The Journal of biological chemistry 280*, 2238-2243.

245. Zhang, B., MacNaul, K., Szalkowski, D., Li, Z., Berger, J., and Moller, D. E. (1999) Inhibition of adipocyte differentiation by HIV protease inhibitors, *The Journal of clinical endocrinology and metabolism 84*, 4274-4277.

246. Rutkowski, D. T., Wu, J., Back, S. H., Callaghan, M. U., Ferris, S. P., Iqbal, J., Clark, R., Miao, H., Hassler, J. R., Fornek, J., Katze, M. G., Hussain, M. M., Song, B., Swathirajan,

J., Wang, J., Yau, G. D., and Kaufman, R. J. (2008) UPR pathways combine to prevent hepatic steatosis caused by ER stress-mediated suppression of transcriptional master regulators, *Dev Cell 15*, 829-840.

247. Zheng, Z., Zhang, C., and Zhang, K. (2010) Role of unfolded protein response in lipogenesis, *World journal of hepatology 2*, 203-207.

248. Colgan, S. M., Tang, D., Werstuck, G. H., and Austin, R. C. (2007) Endoplasmic reticulum stress causes the activation of sterol regulatory element binding protein-2, *Int J Biochem Cell Biol 39*, 1843-1851.

249. Estrada, V., and Fuster, M. (2008) Darunavir in treatment-naive patients. The ARTEMIS study], *Enfermedades infecciosas y microbiologia clinica 26 Suppl 10*, 10-13.

250. Becker, S., and Thornton, L. (2004) Fosamprenavir: advancing HIV protease inhibitor treatment options, *Expert Opin Pharmacother 5*, 1995-2005.

251. Goudeau, H., and Goudeau, M. (1998) Depletion of intracellular Ca2+ stores, mediated by Mg2+-stimulated InsP3 liberation or thapsigargin, induces a capacitative Ca2+ influx in prawn oocytes, *Dev Biol 193*, 225-238.

252. Torres, M., Castillo, K., Armisen, R., Stutzin, A., Soto, C., and Hetz, C. (2010) Prion protein misfolding affects calcium homeostasis and sensitizes cells to endoplasmic reticulum stress, *PLoS One 5*, e15658.

253. Cinti, S., Mitchell, G., Barbatelli, G., Murano, I., Ceresi, E., Faloia, E., Wang, S., Fortier, M., Greenberg, A. S., and Obin, M. S. (2005) Adipocyte death defines macrophage localization and function in adipose tissue of obese mice and humans, *J Lipid Res 46*, 2347-2355.

254. Weisberg, S. P., McCann, D., Desai, M., Rosenbaum, M., Leibel, R. L., and Ferrante, A. W., Jr. (2003) Obesity is associated with macrophage accumulation in adipose tissue, *J Clin Invest 112*, 1796-1808.

255. Strissel, K. J., Stancheva, Z., Miyoshi, H., Perfield, J. W., 2nd, DeFuria, J., Jick, Z., Greenberg, A. S., and Obin, M. S. (2007) Adipocyte death, adipose tissue remodeling, and obesity complications, *Diabetes 56*, 2910-2918.

256. Murano, I., Barbatelli, G., Parisani, V., Latini, C., Muzzonigro, G., Castellucci, M., and Cinti, S. (2008) Dead adipocytes, detected as crown-like structures, are prevalent in visceral fat depots of genetically obese mice, *J Lipid Res 49*, 1562-1568.

257. Lenhard, J. M., Furfine, E. S., Jain, R. G., Ittoop, O., Orband-Miller, L. A., Blanchard, S. G., Paulik, M. A., and Weiel, J. E. (2000) HIV protease inhibitors block adipogenesis and increase lipolysis in vitro, *Antiviral Research 47*, 121-129.

258. Pacenti, M., Barzon, L., Favaretto, F., Fincati, K., Romano, S., Milan, G., Vettor, R., and Palu, G. (2006) Microarray analysis during adipogenesis identifies new genes altered by antiretroviral drugs, *AIDS (London, England) 20*, 1691-1705.

259. Greenspan, P., Mayer, E. P., and Fowler, S. D. (1985) Nile red: a selective fluorescent stain for intracellular lipid droplets, *J Cell Biol 100*, 965-973.

260. Ford, J., Khoo, S. H., and Back, D. J. (2004) The intracellular pharmacology of antiretroviral protease inhibitors, *J Antimicrob Chemother 54*, 982-990.

261. Kovsan, J., Bluher, M., Tarnovscki, T., Kloting, N., Kirshtein, B., Madar, L., Shai, I., Golan, R., Harman-Boehm, I., Schon, M. R., Greenberg, A. S., Elazar, Z., Bashan, N., and Rudich, A. (2011) Altered autophagy in human adipose tissues in obesity, *J Clin Endocrinol Metab 96*, E268-277.

262. Dong, H., and Czaja, M. J. (2011) Regulation of lipid droplets by autophagy, *Trends Endocrinol Metab 22*, 234-240.

263. Singh, R., Xiang, Y., Wang, Y., Baikati, K., Cuervo, A. M., Luu, Y. K., Tang, Y., Pessin, J. E., Schwartz, G. J., and Czaja, M. J. (2009) Autophagy regulates adipose mass and differentiation in mice, *The Journal of clinical investigation 119*, 3329-3339.

264. Zhang, Y., Goldman, S., Baerga, R., Zhao, Y., Komatsu, M., and Jin, S. (2009) Adipose-specific deletion of autophagy-related gene 7 (atg7) in mice reveals a role in adipogenesis, *Proceedings of the National Academy of Sciences of the United States of America 106*, 19860-19865.

265. You, J., He, Z., Chen, L., Deng, G., Liu, W., Qin, L., Qiu, F., and Chen, X. (2010) CH05-10, a novel indinavir analog, is a broad-spectrum antitumor agent that induces cell cycle arrest, apoptosis, endoplasmic reticulum stress and autophagy, *Cancer Sci 101*, 2644-2651.

266. Mizushima, N., and Yoshimori, T. (2007) How to interpret LC3 immunoblotting, *Autophagy 3*, 542-545.

267. Bjorkoy, G., Lamark, T., Pankiv, S., Overvatn, A., Brech, A., and Johansen, T. (2009) Monitoring autophagic degradation of p62/SQSTM1, *Methods Enzymol 452*, 181-197.

268. Pankiv, S., Clausen, T. H., Lamark, T., Brech, A., Bruun, J. A., Outzen, H., Overvatn, A., Bjorkoy, G., and Johansen, T. (2007) p62/SQSTM1 binds directly to Atg8/LC3 to facilitate degradation of ubiquitinated protein aggregates by autophagy, *J Biol Chem 282*, 24131-24145.

269. Avivar-Valderas, A., Salas, E., Bobrovnikova-Marjon, E., Diehl, J. A., Nagi, C., Debnath, J., and Aguirre-Ghiso, J. A. (2011) PERK Integrates Autophagy and Oxidative

Stress Responses To Promote Survival during Extracellular Matrix Detachment, *Mol Cell Biol 31*, 3616-3629.

270. Goldman, S., Zhang, Y., and Jin, S. (2010) Autophagy and adipogenesis: implications in obesity and type II diabetes, *Autophagy 6*, 179-181.

271. Ichimura, Y., and Komatsu, M. (2010) Selective degradation of p62 by autophagy, *Semin Immunopathol 32*, 431-436.

272. Larsen, K. B., Lamark, T., Overvatn, A., Harneshaug, I., Johansen, T., and Bjorkoy, G. (2010) A reporter cell system to monitor autophagy based on p62/SQSTM1, *Autophagy 6*, 784-793.

273. Christian, F., Anthony, D. F., Vadrevu, S., Riddell, T., Day, J. P., McLeod, R., Adams, D. R., Baillie, G. S., and Houslay, M. D. (2010) p62 (SQSTM1) and cyclic AMP phosphodiesterase-4A4 (PDE4A4) locate to a novel, reversible protein aggregate with links to autophagy and proteasome degradation pathways, *Cell Signal 22*, 1576-1596.

274. Myeku, N., and Figueiredo-Pereira, M. E. (2011) Dynamics of the degradation of ubiquitinated proteins by proteasomes and autophagy: association with sequestosome 1/p62, *J Biol Chem 286*, 22426-22440.

275. Rouschop, K. M., van den Beucken, T., Dubois, L., Niessen, H., Bussink, J., Savelkouls, K., Keulers, T., Mujcic, H., Landuyt, W., Voncken, J. W., Lambin, P., van der Kogel, A. J., Koritzinsky, M., and Wouters, B. G. (2010) The unfolded protein response protects human tumor cells during hypoxia through regulation of the autophagy genes MAP1LC3B and ATG5, *J Clin Invest 120*, 127-141.

276. Friis-Moller, N., Weber, R., Reiss, P., Thiebaut, R., Kirk, O., d'Arminio Monforte, A., Pradier, C., Morfeldt, L., Mateu, S., Law, M., El-Sadr, W., De Wit, S., Sabin, C. A.,

Phillips, A. N., and Lundgren, J. D. (2003) Cardiovascular disease risk factors in HIV patients--association with antiretroviral therapy. Results from the DAD study, *Aids 17*, 1179-1193.

277. Gentile, C. L., Frye, M. A., and Pagliassotti, M. J. (2011) Fatty acids and the endoplasmic reticulum in nonalcoholic fatty liver disease, *Biofactors 37*, 8-16.

278. Puri, P., Mirshahi, F., Cheung, O., Natarajan, R., Maher, J. W., Kellum, J. M., and Sanyal, A. J. (2008) Activation and dysregulation of the unfolded protein response in nonalcoholic fatty liver disease, *Gastroenterology 134*, 568-576.

279. Lei, X., Zhang, S., Barbour, S. E., Bohrer, A., Ford, E. L., Koizumi, A., Papa, F. R., and Ramanadham, S. (2010) Spontaneous development of endoplasmic reticulum stress that can lead to diabetes mellitus is associated with higher calcium-independent phospholipase A2 expression: a role for regulation by SREBP-1, *J Biol Chem 285*, 6693-6705.

280. Czaja, M. J. (2010) Autophagy in health and disease. 2. Regulation of lipid metabolism and storage by autophagy: pathophysiological implications, *Am J Physiol Cell Physiol 298*, C973-978.

281. Mizushima, N., Yoshimori, T., and Levine, B. (2010) Methods in mammalian autophagy research, *Cell 140*, 313-326.

282. Ni, H. M., Bockus, A., Wozniak, A. L., Jones, K., Weinman, S., Yin, X. M., and Ding, W. X. (2011) Dissecting the dynamic turnover of GFP-LC3 in the autolysosome, *Autophagy 7*, 188-204.

283. Moreno-Torres, A., Domingo, P., Pujol, J., Blanco-Vaca, F., Arroyo, J. A., and Sambeat, M. A. (2007) Liver triglyceride content in HIV-1-infected patients on combination antiretroviral therapy studied with 1H-MR spectroscopy, *Antivir Ther 12*, 195-203.

284. Amir, M., and Czaja, M. J. (2011) Autophagy in nonalcoholic steatohepatitis, *Expert Rev Gastroenterol Hepatol 5*, 159-166.

285. Yin, X. M., Ding, W. X., and Gao, W. (2008) Autophagy in the liver, *Hepatology 47*, 1773-1785.

286. Boyd, M. A., and Hill, A. M. (2010) Clinical management of treatment-experienced, HIV/AIDS patients in the combination antiretroviral therapy era, *Pharmacoeconomics 28 Suppl 1*, 17-34.

287. Ribera, E., and Curran, A. (2008) Double-boosted protease inhibitor antiretroviral regimens: what role?, *Drugs 68*, 2257-2267.

288. Gagnon, A., Angel, J. B., and Sorisky, A. (1998) Protease inhibitors and adipocyte differentiation in cell culture, *Lancet 352*, 1032.

289. Riddle, T. M., Kuhel, D. G., Woollett, L. A., Fichtenbaum, C. J., and Hui, D. Y. (2001) HIV protease inhibitor induces fatty acid and sterol biosynthesis in liver and adipose tissues due to the accumulation of activated sterol regulatory element-binding proteins in the nucleus, *J Biol Chem 276*, 37514-37519.

290. Vernochet, C., Azoulay, S., Duval, D., Guedj, R., Ailhaud, G., and Dani, C. (2003) Differential effect of HIV protease inhibitors on adipogenesis: intracellular ritonavir is not sufficient to inhibit differentiation, *Aids 17*, 2177-2180.

291. Molto, J., Valle, M., Back, D., Cedeno, S., Watson, V., Liptrott, N., Egan, D., Miranda, C., Barbanoj, M. J., and Clotet, B. (2011) Plasma and intracellular (peripheral blood

mononuclear cells) pharmacokinetics of once-daily raltegravir (800 milligrams) in HIV-infected patients, *Antimicrob Agents Chemother 55*, 72-75.

292. Ofotokun, I., Chuck, S. K., Binongo, J. N., Palau, M., Lennox, J. L., and Acosta, E. P. (2007) Lopinavir/Ritonavir pharmacokinetic profile: impact of sex and other covariates following a change from twice-daily to once-daily therapy, *J Clin Pharmacol 47*, 970-977.

293. Jackson, A., Hill, A., Puls, R., Else, L., Amin, J., Back, D., Lin, E., Khoo, S., Emery, S., Morley, R., Gazzard, B., and Boffito, M. (2010) Pharmacokinetics of plasma lopinavir/ritonavir following the administration of 400/100 mg, 200/150 mg and 200/50 mg twice daily in HIV-negative volunteers, *J Antimicrob Chemother 66*, 635-640.

294. Boyd, M. A., Aarnoutse, R. E., Ruxrungtham, K., Stek, M., Jr., van Heeswijk, R. P., Lange, J. M., Cooper, D. A., Phanuphak, P., and Burger, D. M. (2003) Pharmacokinetics of indinavir/ritonavir (800/100 mg) in combination with efavirenz (600 mg) in HIV-1-infected subjects, *J Acquir Immune Defic Syndr 34*, 134-139.

295. Dupin, N., Buffet, M., Marcelin, A. G., Lamotte, C., Gorin, I., Ait-Arkoub, Z., Treluyer, J. M., Bui, P., Calvez, V., and Peytavin, G. (2002) HIV and antiretroviral drug distribution in plasma and fat tissue of HIV-infected patients with lipodystrophy, *Aids 16*, 2419-2424.

296. Janneh, O., Hoggard, P. G., Tjia, J. F., Jones, S. P., Khoo, S. H., Maher, B., Back, D. J., and Pirmohamed, M. (2003) Intracellular disposition and metabolic effects of zidovudine, stavudine and four protease inhibitors in cultured adipocytes, *Antivir Ther 8*, 417-426.

297. Shirakawa, K., Maeda, S., Gotoh, T., Hayashi, M., Shinomiya, K., Ehata, S., Nishimura, R., Mori, M., Onozaki, K., Hayashi, H., Uematsu, S., Akira, S., Ogata, E., Miyazono, K.,

and Imamura, T. (2006) CCAAT/enhancer-binding protein homologous protein (CHOP) regulates osteoblast differentiation, *Mol Cell Biol 26*, 6105-6116.

298. Vankoningsloo, S., De Pauw, A., Houbion, A., Tejerina, S., Demazy, C., de Longueville, F., Bertholet, V., Renard, P., Remacle, J., Holvoet, P., Raes, M., and Arnould, T. (2006) CREB activation induced by mitochondrial dysfunction triggers triglyceride accumulation in 3T3-L1 preadipocytes, *J Cell Sci 119*, 1266-1282.

299. Brennan, C. M., and Steitz, J. A. (2001) HuR and mRNA stability, *Cell Mol Life Sci 58*, 266-277.

300. Raineri, I., Wegmueller, D., Gross, B., Certa, U., and Moroni, C. (2004) Roles of AUF1 isoforms, HuR and BRF1 in ARE-dependent mRNA turnover studied by RNA interference, *Nucleic Acids Res 32*, 1279-1288.

301. Timchenko, N. A., Welm, A. L., Lu, X., and Timchenko, L. T. (1999) CUG repeat binding protein (CUGBP1) interacts with the 5' region of C/EBPbeta mRNA and regulates translation of C/EBPbeta isoforms, *Nucleic Acids Res 27*, 4517-4525.

302. Poleev, A., Hartmann, A., and Stamm, S. (2000) A trans-acting factor, isolated by the three-hybrid system, that influences alternative splicing of the amyloid precursor protein minigene, *Eur J Biochem 267*, 4002-4010.

303. Karagiannides, I., Thomou, T., Tchkonia, T., Pirtskhalava, T., Kypreos, K. E., Cartwright, A., Dalagiorgou, G., Lash, T. L., Farmer, S. R., Timchenko, N. A., and Kirkland, J. L. (2006) Increased CUG triplet repeat-binding protein-1 predisposes to impaired adipogenesis with aging, *J Biol Chem 281*, 23025-23033.

304. Cherry, J., Jones, H., Karschner, V. A., and Pekala, P. H. (2008) Post-transcriptional control of CCAAT/enhancer-binding protein beta (C/EBPbeta) expression: formation of a

nuclear HuR-C/EBPbeta mRNA complex determines the amount of message reaching the cytosol, *J Biol Chem 283*, 30812-30820.

305. Jones, H., Carver, M., and Pekala, P. H. (2007) HuR binds to a single site on the C/EBPbeta mRNA of 3T3-L1 adipocytes, *Biochem Biophys Res Commun 355*, 217-220.

306. Iakova, P., Wang, G. L., Timchenko, L., Michalak, M., Pereira-Smith, O. M., Smith, J. R., and Timchenko, N. A. (2004) Competition of CUGBP1 and calreticulin for the regulation of p21 translation determines cell fate, *EMBO J 23*, 406-417.

307. Raulin, J. (2002) Human immunodeficiency virus and host cell lipids. Interesting pathways in research for a new HIV therapy, *Progress in lipid research 41*, 27-65.

308. Caron, M., Auclair, M., Vigouroux, C., Glorian, M., Forest, C., and Capeau, J. (2001) The HIV protease inhibitor indinavir impairs sterol regulatory element-binding protein-1 intranuclear localization, inhibits preadipocyte differentiation, and induces insulin resistance, *Diabetes 50*, 1378-1388.

309. von Schwarzenberg, K., Held, S. A., Schaub, A., Brauer, K. M., Bringmann, A., and Brossart, P. (2009) Proteasome inhibition overcomes the resistance of renal cell carcinoma cells against the PPARgamma ligand troglitazone, *Cell Mol Life Sci 66*, 1295-1308.

310. Liu, S. H., Yang, C. N., Pan, H. C., Sung, Y. J., Liao, K. K., Chen, W. B., Lin, W. Z., and Sheu, M. L. (2010) IL-13 downregulates PPAR-gamma/heme oxygenase-1 via ER stress-stimulated calpain activation: aggravation of activated microglia death, *Cell Mol Life Sci 67*, 1465-1476.

311. Park, S. H., Choi, H. J., Yang, H., Do, K. H., Kim, J., Lee, D. W., and Moon, Y. (2010) Endoplasmic reticulum stress-activated C/EBP homologous protein enhances nuclear

factor-kappaB signals via repression of peroxisome proliferator-activated receptor gamma, *J Biol Chem 285*, 35330-35339.

312. Tamama, K., Kawasaki, H., Kerpedjieva, S. S., Guan, J., Ganju, R. K., and Sen, C. K. (2011) Differential roles of hypoxia inducible factor subunits in multipotential stromal cells under hypoxic condition, *J Cell Biochem 112*, 804-817.

313. Caron, M., Auclair, M., Donadille, B., Bereziat, V., Guerci, B., Laville, M., Narbonne, H., Bodemer, C., Lascols, O., Capeau, J., and Vigouroux, C. (2007) Human lipodystrophies linked to mutations in A-type lamins and to HIV protease inhibitor therapy are both associated with prelamin A accumulation, oxidative stress and premature cellular senescence, *Cell Death Differ 14*, 1759-1767.

314. Coffinier, C., Hudon, S. E., Farber, E. A., Chang, S. Y., Hrycyna, C. A., Young, S. G., and Fong, L. G. (2007) HIV protease inhibitors block the zinc metalloproteinase ZMPSTE24 and lead to an accumulation of prelamin A in cells, *Proc Natl Acad Sci U S A 104*, 13432-13437.

315. Capanni, C., Mattioli, E., Columbaro, M., Lucarelli, E., Parnaik, V. K., Novelli, G., Wehnert, M., Cenni, V., Maraldi, N. M., Squarzoni, S., and Lattanzi, G. (2005) Altered pre-lamin A processing is a common mechanism leading to lipodystrophy, *Hum Mol Genet 14*, 1489-1502.

316. Lloyd, D. J., Trembath, R. C., and Shackleton, S. (2002) A novel interaction between lamin A and SREBP1: implications for partial lipodystrophy and other laminopathies, *Hum Mol Genet 11*, 769-777.

317. Thoen, L. F., Guimaraes, E. L., Dolle, L., Mannaerts, I., Najimi, M., Sokal, E., and van Grunsven, L. A. (2011) A role for autophagy during hepatic stellate cell activation, *J Hepatol*.

318. Kabeya, Y., Mizushima, N., Ueno, T., Yamamoto, A., Kirisako, T., Noda, T., Kominami, E., Ohsumi, Y., and Yoshimori, T. (2000) LC3, a mammalian homologue of yeast Apg8p, is localized in autophagosome membranes after processing, *The EMBO journal 19*, 5720-5728.

319. Kabeya, Y., Mizushima, N., Yamamoto, A., Oshitani-Okamoto, S., Ohsumi, Y., and Yoshimori, T. (2004) LC3, GABARAP and GATE16 localize to autophagosomal membrane depending on form-II formation, *J Cell Sci 117*, 2805-2812.

320. Tanida, I., Sou, Y. S., Ezaki, J., Minematsu-Ikeguchi, N., Ueno, T., and Kominami, E. (2004) HsAtg4B/HsApg4B/autophagin-1 cleaves the carboxyl termini of three human Atg8 homologues and delipidates microtubule-associated protein light chain 3- and GABAA receptor-associated protein-phospholipid conjugates, *J Biol Chem 279*, 36268-36276.

321. Hosokawa, N., Hara, Y., and Mizushima, N. (2007) Generation of cell lines with tetracycline-regulated autophagy and a role for autophagy in controlling cell size, *FEBS Lett 581*, 2623-2629.

322. Kirkin, V., Lamark, T., Sou, Y. S., Bjorkoy, G., Nunn, J. L., Bruun, J. A., Shvets, E., McEwan, D. G., Clausen, T. H., Wild, P., Bilusic, I., Theurillat, J. P., Overvatn, A., Ishii, T., Elazar, Z., Komatsu, M., Dikic, I., and Johansen, T. (2009) A role for NBR1 in autophagosomal degradation of ubiquitinated substrates, *Mol Cell 33*, 505-516.

323. Liang, J. S., Distler, O., Cooper, D. A., Jamil, H., Deckelbaum, R. J., Ginsberg, H. N., and Sturley, S. L. (2001) HIV protease inhibitors protect apolipoprotein B from degradation by the proteasome: a potential mechanism for protease inhibitor-induced hyperlipidemia, *Nat Med 7*, 1327-1331.

324. Piccinini, M., Rinaudo, M. T., Chiapello, N., Ricotti, E., Baldovino, S., Mostert, M., and Tovo, P. A. (2002) The human 26S proteasome is a target of antiretroviral agents, *Aids 16*, 693-700.

325. Piccinini, M., Rinaudo, M. T., Anselmino, A., Buccinna, B., Ramondetti, C., Dematteis, A., Ricotti, E., Palmisano, L., Mostert, M., and Tovo, P. A. (2005) The HIV protease inhibitors nelfinavir and saquinavir, but not a variety of HIV reverse transcriptase inhibitors, adversely affect human proteasome function, *Antivir Ther 10*, 215-223.

326. Bauvy, C., Meijer, A. J., and Codogno, P. (2009) Assaying of autophagic protein degradation, *Methods Enzymol 452*, 47-61.

327. Cheong, H., and Klionsky, D. J. (2008) Biochemical methods to monitor autophagy-related processes in yeast, *Methods Enzymol 451*, 1-26.

328. Nakatogawa, H., Ichimura, Y., and Ohsumi, Y. (2007) Atg8, a ubiquitin-like protein required for autophagosome formation, mediates membrane tethering and hemifusion, *Cell 130*, 165-178.

329. Scheuner, D., Song, B., McEwen, E., Liu, C., Laybutt, R., Gillespie, P., Saunders, T., Bonner-Weir, S., and Kaufman, R. J. (2001) Translational control is required for the unfolded protein response and in vivo glucose homeostasis, *Mol Cell 7*, 1165-1176.

330. Shen, X., Zhang, K., and Kaufman, R. J. (2004) The unfolded protein response--a stress signaling pathway of the endoplasmic reticulum, *J Chem Neuroanat 28*, 79-92.

331. Tu, B. P., and Weissman, J. S. (2004) Oxidative protein folding in eukaryotes: mechanisms and consequences, *J Cell Biol 164*, 341-346.

332. Zhu, C., Xu, F., Wang, X., Shibata, M., Uchiyama, Y., Blomgren, K., and Hagberg, H. (2006) Different apoptotic mechanisms are activated in male and female brains after neonatal hypoxia-ischaemia, *J Neurochem 96*, 1016-1027.

333. Samokhvalov, V., Scott, B. A., and Crowder, C. M. (2008) Autophagy protects against hypoxic injury in C. elegans, *Autophagy 4*, 1034-1041.

334. Lugea, A., Waldron, R. T., French, S. W., and Pandol, S. J. (2011) Drinking and driving pancreatitis: links between endoplasmic reticulum stress and autophagy, *Autophagy 7*, 783-785.

335. Rzymski, T., Milani, M., Singleton, D. C., and Harris, A. L. (2009) Role of ATF4 in regulation of autophagy and resistance to drugs and hypoxia, *Cell Cycle 8*, 3838-3847.

336. Ludtke, A., Buettner, J., Schmidt, H. H., and Worman, H. J. (2007) New PPARG mutation leads to lipodystrophy and loss of protein function that is partially restored by a synthetic ligand, *J Med Genet 44*, e88.

337. Fischer, P., Moller, P., Bindl, L., Melzner, I., Tornqvist, H., Debatin, K. M., and Wabitsch, M. (2002) Induction of adipocyte differentiation by a thiazolidinedione in cultured, subepidermal, fibroblast-like cells of an infant with congenital generalized lipodystrophy, *J Clin Endocrinol Metab 87*, 2384-2390.

338. Carr, A., Workman, C., Carey, D., Rogers, G., Martin, A., Baker, D., Wand, H., Law, M., Samaras, K., Emery, S., and Cooper, D. A. (2004) No effect of rosiglitazone for treatment of HIV-1 lipoatrophy: randomised, double-blind, placebo-controlled trial, *Lancet 363*, 429-438.

339. Hadigan, C., Yawetz, S., Thomas, A., Havers, F., Sax, P. E., and Grinspoon, S. (2004) Metabolic effects of rosiglitazone in HIV lipodystrophy: a randomized, controlled trial, *Ann Intern Med 140*, 786-794.

340. Sekhar, R. V., Patel, S. G., D'Amico, S., Shi, J., Balasubramanyam, A., Rehman, K., Jahoor, F., and Visnegarwala, F. (2010) Effects of rosiglitazone on abnormal lipid kinetics in HIV-associated dyslipidemic lipodystrophy: a stable isotope study, *Metabolism 60*, 754-760.

341. Nguyen, A., Calmy, A., Delhumeau, C., Mercier, I., Cavassini, M., Mello, A. F., Elzi, L., Rauch, A., Bernasconi, E., Schmid, P., and Hirschel, B. (2011) A randomized cross-over study to compare raltegravir and efavirenz (SWITCH-ER study), *Aids 25*, 1481-1487.

342. Teppler, H., Brown, D. D., Leavitt, R. Y., Sklar, P., Wan, H., Xu, X., Lievano, F., Lehman, H. P., Mast, T. C., and Nguyen, B. Y. (2011) Long-term safety from the raltegravir clinical development program, *Curr HIV Res 9*, 40-53.

343. Cocohoba, J. (2009) The SWITCHMRK studies: substitution of lopinavir/ritonavir with raltegravir in HIV-positive individuals, *Expert Rev Anti Infect Ther 7*, 1159-1163.

344. Eron, J. J., Young, B., Cooper, D. A., Youle, M., Dejesus, E., Andrade-Villanueva, J., Workman, C., Zajdenverg, R., Fatkenheuer, G., Berger, D. S., Kumar, P. N., Rodgers, A. J., Shaughnessy, M. A., Walker, M. L., Barnard, R. J., Miller, M. D., Dinubile, M. J., Nguyen, B. Y., Leavitt, R., Xu, X., and Sklar, P. (2010) Switch to a raltegravir-based regimen versus continuation of a lopinavir-ritonavir-based regimen in stable HIV-infected patients with suppressed viraemia (SWITCHMRK 1 and 2): two multicentre, double-blind, randomised controlled trials, *Lancet 375*, 396-407.

345. Perez-Matute, P., Perez-Martinez, L., Blanco, J. R., and Oteo, J. A. (2011) Neutral actions of Raltegravir on adipogenesis, glucose metabolism and lipolysis in 3T3-L1 adipocytes, *Curr HIV Res 9*, 174-179.

Vita

Personal Summary:

Beth Shoshana Zha was raised in the tiny village of Hume, Virginia. Although focused on the performing arts for most of her childhood, she internally aspired to become a physician. She began her higher education in this pursuit at The College of William and Mary, majoring in Neuroscience and graduating *sum cum laude* in 2006. That same year, she began the MD/PhD program and Virginia Commonwealth University/Medical College of Virginia. Besides focusing on her studies, two more passions emerged – volunteering for the local Mattaponi health clinic and running. In 2008, Shoshana began working in the laboratory of Dr. Huiping Zhou where she not only studied the intricacies of basic science research, but also met her husband.

Education:

September 2011	Ph.D. Defense, Virginia Commonwealth University, Richmond, VA Dissertation title:"HIV protease inhibitors trigger lipid metabolism dysregulation through endoplasmic reticulum stress and autophagy." GPA: 3.917
May 2006	Bachelors of Science, The College of William and Mary Major: Neuroscience Minor: Biochemistry GPA: 3.81

Awards:

May 2011	Forbes Day Finalist, *Virginia Commonwealth Universiy*
April 2011	Oral Presentation Award, Graduate Association, *Viriginia Commonwealth*
April 2011	Oral Presentation, *American Physician Scientist Annual Meeting*
April 2011	Travel Award, Graduate Association, *Virginia Commonwealth University*
April 2011	Travel Award, *American Physician Scientist Association*
April 2011	Travel Award, Midwest Trainee, *Central Society for Clinical Research*
March 2011	Mary P. Coleman Award, *Microbiology/Immunology, VCU*
May 2010	Charles C. Clayton Fellowship, *Microbiology/Immunology, VCU*
November 2011	Phi Kappa Phi Inductee, *Virginia Commonwealth University*
May 2011	Who's Who Among Graduate Students
October 2009	Ruth L. Kirschstein National Research Service Award for Individual Predoctoral MD/Ph.D (F30) - NIDDK
May 2009	Graduate Travel Fellowship, *American Society for Biochemistry and Molecular Biology*
April 2008	Highest Honors, Behavioral Science II, *VCU/MCV*
May 2006	M.D./Ph.D. Full Scholarship, *Virginia Commonwealth University*
May 2006	Honors and *suma cum laude, The College of William and Mary*
April 2006	Travel Award, Howard Hughes Medical Institute, *The College of William and Mary*
May 2005	Summer Fellowship, Howard Hughes, *The College of William and Mary*
September 2003	Golden Key International Honor Society Inductee
September 2003	National Collegiate Honor Society Inductee

Societies:

American Physician Scientist Association
International Society of Infectious Diseases
American Medical Association
Physicians for Human Rights

Abstracts and Publications:

HIV Protease Inhibitors Disrupt Lipid Metaoblism by Activating Endoplasmic Reticulum Stress and Autophagy in Adipocytes. **Zha B.S.**, Zha W., Zhou J., Zhao R., Wang X., Hylemon P.B., and Zhou H. *Submitted September 2011*

ER Stress and Lipid Metabolism in Adipocytes. **Zha B.S.** and Zhou H. *Submitted September 2011*

Highly Active Antiretroviral Therapy (HAART) and Metabolic Complications. **Zha, B.S.**, Studer E., Zha W., Hylemon P.B., Pandak W., and Zhou H. (2011) *HIV Infection/Book 3.* ISBN 979-953-307-189-2. *In Press*

A Link Between HIV Protease Inhibitor-Induced ER Stress and Autophagy in Adipocytes and Hepatocytes. **Zha B.S.,** Liang M., Holt S.E., Hylemon P.B., Zhou H. Presented at the Association of American Physicians, American Society for Clinical Investigation, and VCU Graduate Student Symposium, April 2011

Cellular Pharmacokinetic Mechanisms of Adriamycin Resistance and its Modulation by 20(S)-Ginsenoside Rh2 in MCF-7/Adr Cells. Zhang J., Zhou F., Wu X., Zhang X., Chen Y., **Zha B.S.**, Niu F., Lu M., Hao G., Sun Y., Sun J., Peng Y., Wang G. Br J Pharmacology, 2011. PMID 21615726

Metabonomic Approach to Evaluating Pharmacodynamics of Ginkgo biloba Extract on the Perturbed Metabolism. Zha W.B., AJ Y., Wang G.J., Zhu X.X., Gu S.H., Cao B., Yan B., **Zha B.S.**, Hao H.P., Huang Q., Liu L.S., Shi J., Sun J.G. Chinese J of Natural Med, 2011. 9 (3), 232-240.

HIV Protease Inhibitors Differentially Regulate PPARγ Expression in Adipocytes. **Pecora B.S.**, Zha W., Hylemon P.B., Wabitsch M., Zhou H. Presented at Experimental Biology: American Society for Biochemistry and Molecular Biology, April 2010

HIV Protease Inhibitors Activate the ER Stress Response and Disrupt Lipid Metabolism in 3T3-L1 Adipocytes. **Pecora B.S.**, Gurley E., Zhou H. Presented at Experimental Biology: American Society for Biochemistry and Molecular Biology, April 2009

Thermoregulatory Projections to the Dorsomedial Hypothalamus. **Pecora B.S.**, Straub A., Griffin J.D. Presented at Experimental Biology: Physiology - Thermoregulation, April 2006